

**School Of Civil and Mechanical Engineering  
Department of Civil Engineering**

***Numerical modelling for flexible pavement materials applying advanced finite element approach to develop Mechanistic-Empirical design procedure***

**Behzad Ghadimi**

**This thesis is presented for the Degree of  
Doctor of Philosophy  
of  
Curtin University**

**January 2015**



## **DECLARATION**

This thesis contains no material which has been accepted for the award of any other degree or diploma in any university.

To the best of my knowledge and belief this thesis contains no material previously published by any other person except where due acknowledgment has been made.

The following publications have resulted from the work carried out for this degree.

### **Journal Articles:**

1. Ghadimi, B., H. Nikraz, C. Leek, and A. Nega. 2013. A Comparison Between Austroads Pavement Structural Design and AASHTO Design in Flexible Pavement. *Advanced Materials Research* 723: 3-11.
2. Ghadimi, B., H. Nikraz, C. Leek, and A. Nega. 2013. A Comparison Between Effects of Linear and Non-Linear Mechanistic Behaviour of Materials on the Layered Flexible Pavement Response. *Advanced Materials Research* 723: 12-21.
3. Nega, A., H. Nikraz, C. Leek, and B. Ghadimi. 2013. Evaluation and Validation of Characterization Methods for Fatigue Performance of Asphalt Mixes for Western Australia. *Advanced Materials Research* 723: 75-85.
4. Nega, A., H. Nikraz, C. Leek, and B. Ghadimi. 2013. Pavement Materials Characterization of Hot-Mix Asphalt Mixes in Western Australia. *Advanced Materials Research* 723: 434-443.
5. Ghadimi, B., H. Nikraz, and C. Leek. 2014. A Comparison of Different Approaches in Numerical Modeling of Pavement Granular Material. *Journal of Civil Engineering and Architecture* 8 (4): 446-455.
6. Ghadimi, B., A. Nega, and H. Nikraz. Simulation of Shakedown Behavior in Pavement's Granular Layer. *International Journal of Engineering and Technology* (accepted in 2014).
7. Chegenizadeh, A., B. Ghadimi, H. Nikraz, and M. Simsek. A Novel Two-Dimensional Approach to Modelling Functionally Graded Beams Resting on

- a Soil Medium. *Structural Engineering and Mechanics, An International Journal* (accepted in 2014).
8. Chegenizadeh, A., B. Ghadimi, and H. Nikraz. Investigation on Ship Collision into Floating Pier Structures. *Interaction and Multiscale Mechanics: An International Journal* (accepted in 2014).
  9. Nega, A., H. Nikraz, S. Herath, and B. Ghadimi. Distress Identification, Cost Analysis and Pavement Temperature Prediction for the Long-Term Pavement Performance for Western Australia. *International Journal of Engineering and Technology* (accepted in 2014).
  10. Nega, A., B. Ghadimi, H. Nikraz. Development and Predicting Dynamic Modulus of Polymer Modified Hot-Mix Asphalt Mixtures. *International Journal of Engineering and Technology* (accepted in 2014).
  11. Ghadimi, B., and U. Hasan. Review of Finite Element Simulation of Granular Materials. *Applied Mechanics and Materials*.(accepted in 2014)

#### **Conference Papers:**

1. Ghadimi B., H. Asadi, and H. Nikraz. 2012. Effect of Stage Construction on Numerical Modelling of Layered Flexible Pavement System. *ASEA-SEC-1 the First Australasia and South-East Asia Structural Engineering and Construction Conference, Perth, Western Australia, 28 November-2 December 2012*.
2. Asadi, H., A. Asadi, B. Ghadimi, and H. Nikraz. Drainage Design for a Freeway to Counter Water Infiltration Effects. *ASEA-SEC-1 the First Australasia and South-East Asia Structural Engineering and Construction Conference, Perth, Western Australia, 28 November-2 December 2012*.
3. Asadi, H., B. Ghadimi, and H. Nikraz. An Operational Solution to Overcome the Very Poor Subgrade Soil Condition of the Azadegan Freeway. *ASEA-SEC-1 the First Australasia and South-East Asia Structural Engineering and Construction Conference, Perth, Western Australia, 28 November-2 December 2012*.
4. Haeri, S., B. Ghadimi, and H. Nikraz. "Scattering of Rayleigh Waves by a Trapezoidal Canyon. *ASEA-SEC-1 the First Australasia and South-East Asia Structural Engineering and Construction Conference, Perth, Western Australia, 28 November-2 December 2012*.

5. Ghadimi, B., H. Asadi, H. Nikraz, and Colin Leek. 2013. Effects of Geometrical Parameters on Numerical Modeling of Pavement Granular Material. *2013 Airfield and Highway Pavement Conference: Sustainable and Efficient Pavements, Los Angeles, 9-12 June 2013.*

Signature: .....

Date: ..... 05-05-2015 .....

## ABSTRACT

A layered structure with asphalt as a surface pavement is one of the usual pavement systems used in road and transportation. This structure is a combination of surface asphalt concrete and good quality granular materials called the base and subbase. Through these layers, the traffic load is transferred to the existing ground beneath, which is called the subgrade.

Since each layer is constructed of different types of materials with specific behaviours, the system is complex. The contribution of layers to the total strength of this structure is also complicated and difficult to define. The total function of the layered system is mainly defined by the combined response of the layers to the dynamic loading from the traffic. Therefore, the traits of the materials in each layer should be accurately accounted for.

A mechanistic-empirical (ME) design procedure has been developed to answer the demand for a design procedure that addresses these complications. In this approach, constitutive models are implemented to calculate the mechanical response of pavement structure in terms of stress, strain and displacement. These values are entered to sit in an empirical formula (called the transfer function) which connects them to pavement performance.

Following the introduction, this dissertation presents an inclusive review of published research and design methods. Various design codes are investigated and their differences are discussed. The concept of modelling in flexible pavement engineering is categorized into three types: analytical, experimental and numerical modelling. Each of these approaches is discussed and explained. Since this research concentrates on the finite element simulation of unbound granular materials (UGM) in layered flexible pavement, there is a more detailed review of the literature regarding finite element modelling of flexible pavement.

The finite element method was selected as a mathematical tool to solve differential equations which are used for the simulation of flexible pavement structure. The main objective of this thesis is to introduce an advanced method for the numerical

modelling of flexible pavement. Therefore the details of constitutive models are presented to accurately model the simulation of flexible pavement.

The results of static modelling along with model construction are discussed. Especial attention is given to the effects of various constitutive models when applied to granular layers, specifically base and subgrade. Constitutive models investigated in this chapter include linear elastic, nonlinear elastic, linear elastoplastic and nonlinear elastoplastic constitutive models. The results for each model are compared to the others and discussed. Other factors are also investigated, including the effects of asphalt thickness, loading axles and material strength. It was found that nonlinearity and three dimensional modelling would have a great effect on the calculated results.

Finally 6 the results of the dynamic simulation of flexible pavement subjected to a moving load are presented. The main focus was on the effect of the shakedown model introduced in this thesis on the long-term response of the pavement. In addition, the effects of soil-asphalt interaction are studied in this chapter. Simulations include simple Mohr-Coulomb nonlinear elasto-plastic materials, Mohr-Coulomb nonlinear elasto-plastic materials considering shakedown effects and Mohr-Coulomb nonlinear elasto-plastic materials considering shakedown effects.

The results of all of the simulations conducted in this thesis are compared. The relationship of the results with other published research and codes is mentioned. It was found that considering the shakedown and soil-asphalt interaction can result in more optimistic design of flexible pavement.

## **ACKNOWLEDGEMENTS**

This thesis conducted as part of a research project on pavement modelling at Curtin University. Author acknowledges the Australian Research Council (ARC) financial support to this research under the ARC Scheme (LP110100634), conducted at the Department of Civil Engineering, Curtin University. Author also acknowledges financial contribution of Australian Asphalt Pavement Association and Canning City Council in this research.

The focus of the thesis was on numerical simulation (using ABAQUS software) of granular materials used as base layer in pavement, considering shakedown effects and soil-asphalt interaction. During this research, several organizations and individuals provided support and help. Although it is not possible to name all of them, I would like to point out some of the most important contributors, while implicitly expressing my thanks to and appreciation of all those I could not directly mention here.

First of all I would like to acknowledge and express my gratitude for the contribution, guidance and strong support of my supervisor Professor Hamid Nikraz. I would also like to thank Mr. Colin Leek, Dr. Amin Chegenezadeh, Dr. Peerapong Jitsangiamand and Dr. Komsun Siripun, each of whom helped me during my project. I also would like to acknowledge the valuable comments of Professor Cyrille Chazallon and Professor Erol Tutumluer, which they provided through personal communication.

I also would like to thank all of my colleagues and friends at Curtin University for their kindness and honest friendship.

Last but not least, I deeply appreciate the emotional support of my beloved wife, Farzaneh, my parents, and all of my family members who kindly supported me during my thesis.

## Nomenclature

- A Area
- B** Matrix of derivatives of shape functions
- C** Constitutive matrix
- c Cohesion
- D Required accuracy
- $d_p$  Damping ratio for pressure waves
- $d_s$  Damping ratio for shear waves
- E Elastic modulus
- F External force
- f Function
- G Shear modulus
- g Function
- h Thickness
- i Counter indices ( $i=1,2,3,\dots$ )
- $I_1$  First invariant of stress tensor
- $J_2$  Second invariant of stress tensor
- K** Stiffness matrix
- $K_1$  Material constant
- $k_2$  Material constant
- $k_3$  Material constant
- L Length
- M Mass
- $M_r$  Resilient Modulus
- N Number of repetition
- $N_i$  Shape function
- p Pressure
- $P_0$  Atmospheric pressure
- $P_1$  Unite pressure
- Q Horizontal pressure
- R Resultant force
- r Radius
- $R_f$  Material constant

S	Surface
$S_u$	Undrained shear strength
T	Temperature
$t$	Tractional force
$\tau$	Time
U	Deformation
V	Volume
$V_i$	Volumetric force
$X_i$	Direction
z	Depth
$\alpha$	Damping coefficient
$\beta$	Damping coefficient
$\gamma$	Shear strain
$\varepsilon$	Strain
$\varepsilon_r$	Recoverable strain
$\varepsilon^p$	Plastic strain
$\theta$	Bulk stress
$\theta_l$	Load angle
$\lambda$	Lame's constant
$\nu$	Poisson's ratio
$\varrho$	Self-satisfied residual field
$\rho$	Density
$\sigma$	Stress
$\sigma_d$	Deviator stress
$\tau$	Shear stress
$\tau_{oct}$	Octahedral shear stress
$\Phi$	Unknown field
$\phi$	Angle of internal friction
$\psi$	Dilation angle

## Table of Contents

<b>DECLARATION</b>	I
<b>ABSTRACT</b>	IV
<b>ACKNOWLEDGEMENTS</b>	VI
<b>Nomenclature</b>	VII
<b>Table of Contents</b>	IX
<b>List of Figures</b>	XII
<b>List of Tables</b>	XVI
1. 1: INTRODUCTION	1
1.1 Introduction	1
1.2 Aims and scope	2
1.3 Background	4
1.4 Significance and innovation	7
1.5 Methodology	7
1.6 Thesis outline	10
2. 2: LITERATURE REVIEW	13
2.1 Introduction	13
2.2 A Review Pavement Design	15
2.2.1 Basic Concepts in Pavement Design	16
2.2.2 Empirical Methods	18
2.2.3 Mechanistic Empirical Design	19
2.3 Modelling of Flexible Pavement Layers	29
2.3.1 Analytical Models	29
2.3.2 Experimental Models	32
2.3.3 Numerical Models	42
2.4 Application of Finite Element Method in Numerical Modelling of Flexible Pavement System	49
2.4.1 Numerical Simulation of Layered Flexible Pavement System	50
2.4.2 Numerical Simulation of Granular Materials	65
2.4.3 Numerical Simulation of Load	87

2.5 Summary of Chapter	98
3. 3: CONSTITUTIVE MODELS IN FINITE ELEMENT METHOD	101
3.1 Basics of the Finite Elements Method (FEM)	101
3.2 Types of Numerical Analyses	112
3.2.1 Static Analysis	113
3.2.2 Dynamic Analysis	117
3.3 Constitutive Models	122
3.3.1 Application of Constitutive Models in FEM	123
3.3.2 Geotechnical Constitutive Models	128
3.3.3 Constitutive Models for Pavement Materials	133
3.4 Summary of Chapter	144
4. 4: A REVIEW OF PROPOSED SIMULATION	146
4.1 Introduction	146
4.2 Methodology	147
4.3 Modelling of layered system	149
4.3.1 Plane strain, Axisymmetric and Three Dimensional Analysis	150
4.3.2 Interface Element	152
4.4 Modelling of Load and Boundary Conditions	154
4.4.1 Pressure Distribution	155
4.4.2 Static and Dynamic Loading	157
4.4.3 Boundary Conditions	159
4.5 Modelling of Materials	160
4.5.1 Linear and Nonlinear Elastic	161
4.5.2 Linear and Nonlinear Elastoplastic	164
4.5.3 Shakedown Model	166
4.6 Summary of the Chapter	168
5. 5: STATIC SIMULATION OF LAYERED FLEXIBLE PAVEMENT	169
5.1 Introduction	169
5.2 Static Analysis	170
5.2.1 Linear Elastic Analysis	170

5.2.2 Nonlinear Elastic Analysis	187
5.2.3 Linear Elastoplastic Analysis	204
5.2.4 Nonlinear Elastoplastic Analysis	211
5.3 Remarks	217
<b>6. 6: DYNAMIC SIMULATION OF LAYERED FLEXIBLE PAVEMENT</b>	<b>221</b>
6.1 Introduction	221
6.2 Dynamic Analysis	222
6.2.1 Model Construction	223
6.2.2 Nonlinear Elastoplastic assuming Mohr-Coulomb Plasticity	231
6.2.3 Nonlinear Elastoplastic assuming Mohr-Coulomb Plasticity considering Shakedown Effects	244
6.2.4 Final Dynamic Analysis Considering Mohr-Coulomb Plasticity, Shakedown effects and Base-Asphalt Interaction	260
6.3 Remarks	271
<b>7. 7: COMPARISON, REMARKS AND DISCUSSION</b>	<b>277</b>
7.1 Introduction	277
7.2 Comparison of Results of Elastic Analysis	278
7.3 Comparison of Results of Elastoplastic Analysis	281
7.4 Effect of Dynamic Loading	283
7.5 Effect of Interaction of Soil-Asphalt layers	286
7.6 Discussion	286
<b>8. 8: Conclusion and Recommendation</b>	<b>290</b>
8.1 Conclusion of the research	290
8.2 Recommendation for Future Studies	293
<b>9. References</b>	<b>295</b>

## List of Figures

Figure 1.1. Research Method .....	9
Figure 2.1 - Structure of Literature Review .....	14
Figure 2.2 - Thickness Design Chart (from Figure 8.4, AUSTROADS 2004)....	19
Figure 2.3 – Fatigue Cracking.....	21
Figure 2.4 - Rut Failure (Nicholson Road WA, Picture is provided by Colin Leek) .....	23
Figure 2.5 - Induced Stress under Wheel Load.....	25
Figure 2.6 - Kelvin Model (a) and Maxwell Model (b) .....	27
Figure 2.7- Possible Responses of Structure to Cyclic Load.....	38
Figure 2.8 – Permanent Strain of UGM: (a) Shakedown Limit (b) Failure (from Figures 2.36 and 2.37 Siripun 2010).....	40
Figure 2.9 - Permanent Strain Equations (from Figure 5 Siripun et al. 2010)....	41
Figure 2.10 – GFEM Concept (from Figure 1 Ozer, Al-Qadi and Duarte 2011) .	44
Figure 2.11 - ANN Solver Concept (a) and ANN Layers (b) (from Figures 2 and 3 Saltan and Sezgin 2007).....	46
Figure 2.12- DEM Concept.....	47
Figure 2.13 - DEM Model to Simulate Shakedown of UGM (from Figure 5 Chazallon et al. 2011) .....	48
Figure 2.14 – Typical 3-D model of flexible pavement.....	57
Figure 2.15 – Typical Stress-Strain Curve.....	69
Figure 2.16 – Elastoplastic Stress-Strain Curve.....	76
Figure 2.17 - FEM Mesh Used by Zaghloul and White.....	78
Figure 2.18-Translation of Contact Area .....	96
Figure 3.1 - Stresses on an Element.....	102
Figure 3.2- Discretization of Medium.....	105
Figure 3.3-Flow Chart of FEM .....	109
Figure 3.4 - Element's Types: (a) Linear Rectangular (b) Parabolic Rectangular (c) Parabolic Rectangular reduced (d) Linear Triangular (e) Parabolic Triangular .....	111
Figure 3.5 - Iterations and Increments in FEM .....	115
Figure 3.6 - Tresca and von Mises Criteria.....	128
Figure 3.7 - Mohr-Coulomb and Drucker-Prager Criteria .....	131
Figure 3.8 - Return Mapping Technique.....	132
Figure 3.9 - Calculation of Shakedown Limit.....	137
Figure 3.10 - Development of Plastic strains (a) Simple Mohr-Coulomb .....	142
Figure 4.1 - Axisymmetric, Plane Strain and 3D Model .....	151
Figure 4.2 - Interface Elements.....	154
Figure 4.3 - Single Axle Dual Tyre Loading .....	156
Figure 4.4 - Distribution of Pressure in Time .....	158
Figure 4.5 - Boundary Conditioins of Static Analysis .....	159

Figure 4.6 - Infinite Element in ABAQUS Mesh .....	160
Figure 4.7 - Schematic Algorithm for Elastic Constitutive Model .....	162
Figure 4.8 – Schematic Algorithm of Nonlinear Constitutive Model.....	163
Figure 4.9 - Schematic Algorithm of Elastoplastic Model .....	165
Figure 4.10 - Schematic Algorithm of Shakedwon Model .....	167
Figure 5.1- Geometry Constructed Model in KENLAYER and CIRCLY .....	172
Figure 5.2- Geometry of The Axisymmetric Model .....	173
Figure 5.3-Mesh Distributions for The Models .....	174
Figure 5.4- Surface Deflection of Plane Strain Model.....	176
Figure 5.5- Surface Deflection of Axisymmetric Model .....	177
Figure 5.6-Surface Deflection of 3-D Model.....	177
Figure 5.7-Comparison of the Surface Deflections for Different Models .....	178
Figure 5.8 - Simulated Loads (a) Single Axle Dual Tyre (b) Tandem Axle Dual Tyre .....	183
Figure 5.9 - Constructed Models for (a) SADT and (b) TADT .....	184
Figure 5.10 - Vertical Deformation of SADT (left) and .....	185
Figure 5.11- Constructed Axisymmetric Model Used for Verification of Nonlinear Elasticity.....	189
Figure 5.12-Constructed Model for Second Stage of Nonlinear Analysis.....	191
Figure 5.13- Comparison of the normalised Critical Response- Case 1 .....	197
Figure 5.14-Increase of the Nonlinear Resilient Modulus - Case 1 .....	198
Figure 5.15-Distribution of Vertical Stress in Base Layer - Case 1 .....	199
Figure 5.16 - Vertical Deformation of NE-1-1-1 (Left) and NE-1-2-1 (Right) ..	202
Figure 5.17 - Vertical Deformation of LP-1-1-1 (Left) and LP-1-2-1 (Right) ...	205
Figure 5.18 - Developement of Plastic Strain in Base (Left) and Subgrade (Right) Linear Elastoplastic .....	207
Figure 5.19- Distribution of Horizontal Strain in Elastoplastic Analysis .....	208
Figure 5.20- Distribution of Vertical Strain in Elastoplastic Analysis .....	208
Figure 5.21 - Vertical Deformation of NP-1-1-1 (Left) and NP-1-2-1 (Right) ..	212
Figure 5.22 - Developement of Plastic Strain in Base (Left) and Subgrade (Right) Nonlinear Elastoplastic .....	213
Figure 5.23- Distribution of Horizontal Strain in Nonlinear Elastoplastic Analysis .....	214
Figure 5.24- Distribution of Vertical Strain in Nonlinear Elastoplastic Analysis .....	215
Figure 5.25 - Comparison of Surface Deflection in Static Analysis.....	218
Figure 5.26-Comparison of AC Tensile Strain in Static Analysis .....	219
Figure 5.27-Comparison of SG Compressive Strain in Static Analysis .....	219
Figure 5.28-Comparison of SG Compressive stress in Static Analysis .....	220
Figure 6.1- Constructed Mesh for Dynamic Analysis .....	224
Figure 6.2 - Loading in Dynamic Analysis.....	226
Figure 6.3- Amplitude of Loading in Dynamic Analysis .....	227

Figure 6.4 - Implementation of Infinite Elements in Dynamic Analysis .....	229
Figure 6.5 - Deformed Mesh in Dynamic Analysis (Model 1) .....	232
Figure 6.6 – Sequence of Dynamic Longitudinal Deformation: Loading (Model 1) .....	233
Figure 6.7 – Sequence of Dynamic Longitudinal Deformation: Unloading .....	233
Figure 6.8 – Sequence of Dynamic Transverse Deformation: Loading (Model 1) .....	235
Figure 6.9 – Sequence of Dynamic Transverse Deformation: Unloading (Model 1) .....	236
Figure 6.10 – Time History of Deformation under the Wheel (Model 1).....	237
Figure 6.11 – Development of Total Vertical Strain (Model 1) .....	238
Figure 6.12 – Development of Equivalent Plastic Strain (Model 1).....	238
Figure 6.13- Development of Equivalent Plastic Strain in Base (Model 1).....	240
Figure 6.14 – Hysteresis Loops of Initial Cycles (Model 1).....	241
Figure 6.15 – Hysteresis Loops of Final Cycles (Model 1) .....	242
Figure 6.16 - Constructed Mesh for Verification Purpose in Shakedown Simulation .....	245
Figure 6.17- Shakedown Code Verification (I).....	245
Figure 6.18-Shakedown Code Verification (II) .....	246
Figure 6.19-Deformed Mesh in Dynamic Analysis (Model 2) .....	248
Figure 6.20- Sequence of Dynamic Longitudinal Deformation: Loading (Model 1) .....	249
Figure 6.21 – Sequence of Dynamic Longitudinal Deformation: Unloading (Model 2).....	250
Figure 6.22 – Sequence of Dynamic Transverse Deformation: Loading (Model 2) .....	251
Figure 6.23 – Sequence of Dynamic Transverse Deformation: Unloading .....	251
Figure 6.24 – Time History of Deformation under the Wheel (Model 2).....	253
Figure 6.25 – Development of Total Vertical Strain (Model 2) .....	254
Figure 6.26 – Development of Equivalent Plastic Strain (Model2).....	254
Figure 6.27- Development of Equivalent Plastic Strain in Base (Model 2).....	256
Figure 6.28 – Hysteresis Loops of Initial Cycles (Model 2).....	258
Figure 6.29 – Hysteresis Loops of Final Cycles (Model 2) .....	258
Figure 6.30 - Deformed Mesh in Dynamic Analysis (Model 3) .....	261
Figure 6.31 – Sequence of Dynamic Longitudinal Deformation: Loading .....	261
Figure 6.32 – Sequence of Dynamic Longitudinal Deformation: Unloading .....	262
Figure 6.33 – Sequence of Dynamic Transverse Deformation: Loading (Model 3) .....	263
Figure 6.34 – Sequence of Dynamic Transverse Deformation: Unloading .....	264
Figure 6.35 – Time History of Deformation under the Wheel (Model 3).....	264
Figure 6.36 – Development of Total Vertical Strain (Model 3) .....	265
Figure 6.37 – Development of Equivalent Plastic Strain (Model 3).....	266

Figure 6.38- Development of Equivalent Plastic Strain in Base (Model 3).....	268
Figure 6.39 – Hysteresis Loops of Initial Cycles (Model 3).....	269
Figure 6.40 – Hysteresis Loops of Final Cycles (Model 3) .....	270
Figure 6.41-Comparison of Surface Deformation .....	272
Figure 6.42-Comparison of Vertical Total strain in Base .....	273
Figure 6.43-Comparison of Plastic Strain in Base .....	273
Figure 6.44-Comparison of Final Hysteresis Loops in Base .....	274
Figure 6.45-Comparison of Critical Values in First Cycle .....	275
Figure 6.46-Comparison of Critical Values in Final Cycle .....	275

## List of Tables

Table 2-1 - Comparison of AASHTO and AUSTRROADS .....	28
Table 3-1 - List of Nonlinear Equations For UGM.....	134
Table 5.1- Material Properties for KENLAYER and CIRCLY Programs.....	171
Table 5.2- Comparison of the Results for Different Models .....	179
Table 5.3-Effect of Layer Thickness on The Numerical Approximation .....	181
Table 5.4 -Layer's Composition .....	183
Table 5.5 - Results of 8 Cases of Simulation .....	185
Table 5.6- Material Properties Used for Verification of Nonlinear Elasticity ....	188
Table 5.7- Comparison of the Results of Axisymmetric Model .....	190
Table 5.8- Model Characteristic of Second Stage of Nonlinear Analysis .....	190
Table 5.9- Properties of Nonlinear Material Used in Second Stage of Nonlinear Analysis.....	193
Table 5.10- Critical Responses Calculated from Different Nonlinear Models...	194
Table 5.11- Material Properties Used in Final Stage of Nonlinear Analysis.....	201
Table 5.12 - Responses of 8 Cases of Nonlinear Simulation.....	202
Table 5.13- Material Properties for Linear Elastoplastic Analysis .....	205
Table 5.14 - Responses of 8 Cases of Linear Elastoplastic Simulation .....	210
Table 5.15- Material Properties for Nonlinear Elastoplastic Analysis .....	211
Table 5.16 - Responses of 8 Cases of Linear Elastoplastic Simulation .....	216
Table 6.1- Materials Properties in Dynamic Analysis Model 1 .....	231
Table 6.2 - Reponses of Flexible Layer in Dynamic Analysis (Model 1) .....	243
Table 6.3 - Reponses of Flexible Layer in Dynamic Analysis (Model 2) .....	259
Table 6.4 - Reponses of Flexible Layer in Dynamic Analysis (Model 3) .....	270

# **CHAPTER 1**

## **1: INTRODUCTION**

### **1.1 Introduction**

The history of pavement is almost as long as that of civilization itself. It is known that ancient civilizations such as the Persians and Romans manipulated their techniques in order to improve their pavement structures. In modern times, pavement engineering is heavily affected by the usage of materials such as asphalt and cement. One of the most common pavement structures is the layered flexible pavement system. This system typically consists of a few layers of asphalt concrete (AC) on the surface above layers of good quality granular materials called the base and subbase. The granular layers transfer the load to the existing ground, which is called the subgrade.

The layered nature of this system means that the system displays complex behaviour as a united structure. Each layer consists of a different type of material with different behaviour. The asphalt layer is the first layer and is expected to provide the greatest strength against the load. It is a viscous material and its behaviour is a function of various parameters including age, temperature, environmental conditions and rate of loading. The granular layers act as a foundation for the asphalt concrete and are constructed from good quality geomaterials (typically coarse grained unbound material). The strength of these layers is mainly due to the frictional behaviour of the granules. Finally, the load is transferred to the ground conditions present at the construction site, which could be made up of different types of geotechnical materials ranging from soft clay

with highly cohesive (even expansive) behaviour, to high quality shale stone with enough strength to behave in a linear elastic manner.

The final performance of such a layered system is essentially defined by the response of materials in each layer to the moving tyre, known as the traffic load. Therefore the characteristics of materials in each layer need to be properly understood. However, this is complicated by the fact that the overall response of the whole system is defined not only by the properties of the materials in each individual layer, but also by the interaction of the layers with each other. In this regard, the task of pavement design necessitates a comprehensive understanding of the combined material traits in the analysis of an interactive layered system.

Pavement designers have tried different approaches to perform this analysis. Starting with a purely empirical method which relied on the observed field performance of constructed flexible layered pavements, designers gradually employed their analytical knowledge to expand the applicability of design procedures to a wider range of conditions on construction sites. This led to the development of the mechanistic-empirical (ME) design procedure, which has attracted the interest of modern researchers. This procedure uses constitutive models to predict the mechanistic response of a layered pavement system, i.e. the stress, strain and deformation in the pavement structure. These results are then transferred to an empirical formula (called the transfer function) which correlates the mechanical values to actual pavement performance.

## **1.2 Aims and scope**

This dissertation aims to achieve a comprehensive and reliable numerical analysis of layered flexible pavements that can be integrated into an improved pavement

design. To obtain a more precise evaluation of pavement responses, the analysis should include appropriate constitutive models for pavement materials that can be used in a finite element analysis. Such an analysis could result in an improved substitution for inaccurate empirical formulae in current design methods. In this research, the energy concept is implemented through the shakedown theory. The research objectives are as follows:

- I. To provide the response of layered flexible pavement in terms of stress, strain and deflection for different types of materials used as granular layers (base and subgrade).
- II. To analyse development of permanent strain versus cycles of loading for different types of materials used as granular layers and find out their contribution to the general failure mechanism of layered flexible pavement.
- III. To investigate the energy dissipation behaviour of granular layers through the implementation of shakedown constitutive models.
- IV. To present a verification of newly developed material models compared to the response obtained from the laboratory samples.
- V. To compare different numerical simulations of the flexible pavement design and analyse the results for each model. Simulations include static and dynamic loading, plane strain, axisymmetric and three-dimensional modelling, and the implementation of different constitutive models for material behaviour including linear elastic, nonlinear elastic, elastoplastic and nonlinear elastoplastic, considering the shakedown effect.

VI. To investigate the effect of dynamic soil-asphalt interaction for nonlinear elastoplastic materials taking shakedown behaviour into account.

### **1.3 Background**

In the mechanistic part of the ME design approach, principles of continuum mechanics such as elasticity, plasticity and viscoelasticity are applied to form a governing equation of the modelled medium which is usually the mechanical equilibrium of the system. Once this equation is obtained, different techniques such as the finite element (FE) procedure are applied to solve it. In order to solve the equation, it is necessary to assume a constitutive model to predict the material behaviour. This constitutive model, then, has a significant role in the final solution of the system. This is why in recent decades it has been of interest of researchers to introduce new constitutive models which are capable of more accurately predicting material behaviour. These constitutive models include linear and nonlinear elastic, elasto-perfect-plastic (such as the Tresca or von Mises yield criterion), frictional elastoplastic (such as the Drucker-Prager or Mohr-Coulomb yield criterion) and hardening/softening elastoplastic behaviour (Desai and Whitenack 2001; Schofield and Wroth 1968; Vermeer 1982). In this stage, a load is usually broken down into increments and the whole system is solved for each of these loading increments under the assumption of a selected constitutive model for the materials. The solution in terms of stress, strain and deformation is transferred to the empirical formula to calculate pavement damage such as rutting or fatigue, pavement life endurance (in term of cycles of loading) and pavement environmental endurance (such as thermal cycles). A common trend is to use the values for critical responses to calculate pavement damage. These critical responses are usually deformation and stress exactly beneath the loading tyre,

tensile strain at the very bottom of the asphalt layer and vertical strain and vertical stress at the top of the subgrade (Huang 2004). An appropriate prediction of these critical responses is heavily dependent upon the quality and capability of the assumed constitutive model for the materials. It is obvious that each type of material used in construction necessitates a different constitutive model and in many cases, a new one.

In Western Australia, it is common practice to build a flexible pavement system consisting of thin asphalt concrete lying on unbound granular materials (UGM). While a decrease in asphalt thickness reduces the cost of the pavement, it simultaneously intensifies the significance of the UGM layers (i.e. base, subbase and subgrade) in the overall performance of the pavement system.

Failure of the granular materials used in pavement construction is formally known to be the cause of unacceptable surface deflection (rutting). The failure of granular materials is mainly governed by their shear strength and the state of stress. Therefore geotechnical constitutive models representing this type of behaviour are widely used to model granular layers (base, subbase and subgrade) in flexible pavement structures. It is also accepted that the characteristics of granular materials are subject to change as a function of loading cycles. This concept can be illustrated by the resilient modulus and shakedown theory. The shakedown theory is based on the different long term (large number of loading cycles) responses of sample granular materials in different stress states. Repeated cyclic triaxial tests are used to investigate the progressive accumulation of plastic strain and permanent deformation in material test samples. Depending on the stress state (confined pressure and deviator stress) three types of responses are defined:

- a) Purely elastic behaviour in which the material has no plastic deformation in any cycle;
- b) Elastic shakedown in which materials experience a few cycles of plastic behaviour and then tend towards elastic behaviour;
- c) Plastic shakedown in which the material's plastic behaviour is sustained during loading cycles and causes a final failure.

The shakedown theory is a well-known concept in the fatigue failure of metals, and was introduced in pavement engineering for the first time by Sharp and Booker (Sharp 1985; Sharp and Booker 1984). There has been growing interest among pavement researchers in investigating the application of this concept to pavement engineering (Collins and Boulbibane 1998b; Habiballah and Chazallon 2005 Yu and Hossain 1998b;).

It is generally accepted (even before failure) that the behaviour of granular material is not linear elastic. Laboratory experiments indicate that this type of material displays nonlinear, stress-dependent behaviour known as nonlinear elastic behaviour (Thompson and Elliott 1985). Pavement researchers indicate that there is a need for an advanced constitutive model to be implemented in a comprehensive finite element analysis (Hjelmstad and Taciroglu 2000).

This inclusive FE analysis can take into account static and dynamic loading assuming complex nonlinear elastoplastic behaviour for granular layers. It is also possible to closely investigate the effect of interaction between the layers and obtain an improved prediction of pavement response.

## **1.4 Significance and innovation**

While finite element programs (like ABAQUS and ANSYS) are capable of having built-in nonlinear constitutive models to account for nonlinear elastic behaviour, it should be noted that all of these constitutive models are based on a strain state. However, as stated in the background, the UGM used in pavement is known to behave according to a stress state. Therefore, a separate constitutive model should be coded in FE programs to account for this specific type of nonlinearity.

The significance of this research is to implement a nonlinear stress dependent elastic-plastic model considering the shakedown characteristics of granular layers according to the Mohr-Coulomb criterion. The effect of dynamic soil-asphalt interaction is also considered for the materials governed by the abovementioned properties.

These results will improve current pavement design procedure and result in a more accurate and realistic design.

## **1.5 Methodology**

The methodology used to deliver the aims of the research is illustrated in Figure 1.1

Literature review: The first step is a systematic review of the literature regarding UGM modelling. The review branches out into both experimental and numerical methods to provide a scientific basis for further investigation. Special

consideration has been given to the concept of nonlinear stress dependence and shakedown theory for granular pavement materials.

**UGM Characteristics:** Experimental models published in the literature are the source of the material parameters to be implemented in the FE model, and the results of these experiments are employed for the purpose of verification.

**Layered Analysis:** In this step, two well-known programs (CIRCLY and KENLAYER) are employed to conduct the initial simulation. The results of this analysis are already used in the Western Australia (WA) pavement design code. The results also provide a basis for mesh and geometry verification in FE models.

**Finite Element Analysis:** This stage investigates two different branches of analysis: static analysis and dynamic analysis. In static analysis, the simulation is conducted for UGM constitutive models including linear elastic, nonlinear elastic, linear elastoplastic and nonlinear elasto-plastic. In the dynamic analysis there are three different simulations. The first simulation considers the Mohr-Coulomb elastoplastic criterion for UGM layers. The second simulation includes the implementation of the shakedown concept in Mohr-Coulomb elastoplasticity. Finally, the third simulation investigates the effect of soil-asphalt interaction on elastoplastic materials, taking shakedown behaviour into consideration.

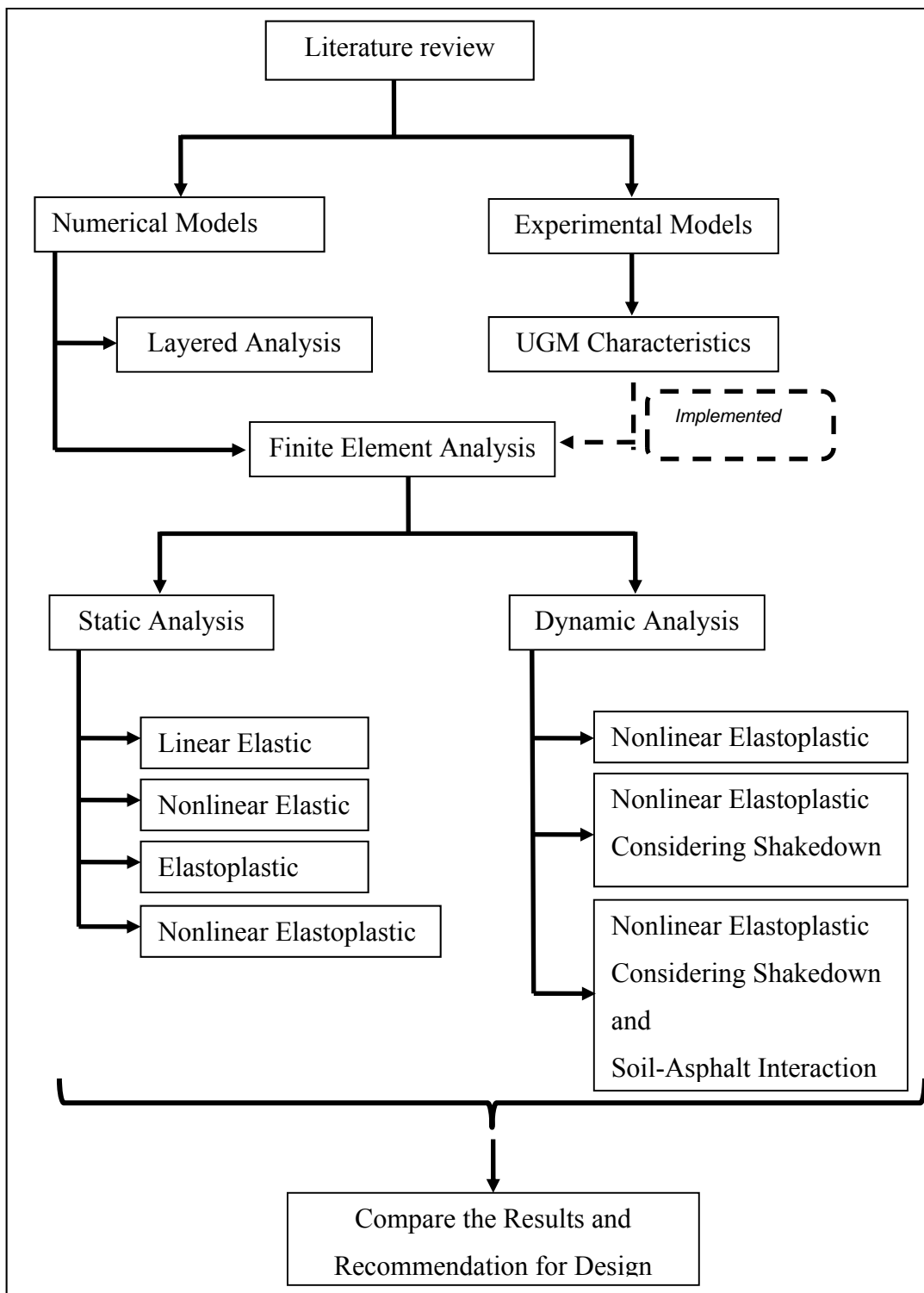


Figure 1.1. Research Method

Interpretation of Results and Design Recommendations: In the final step of this research an inclusive comparison among all numerical simulations considering different constitutive material models is presented. The results are discussed and interpretation of each simulation outcome is indicated. Then recommendation is provided to be applied in current pavement design code.

It should be mentioned that the Mohr-Coulomb behaviour for plasticity of granular materials can cause some limitation on calculated responses of the flexible pavement.

## **1.6 Thesis outline**

This dissertation includes eight chapters as follows:

Chapter 1 covers the background and significance of the study, introducing the scope of the research and setting the objectives. Moreover, the structure of the research is presented and the methodology is briefly reviewed.

Chapter 2 presents an analysis of the previous literature in the field of layered flexible pavement. The main focus is to state the mainstream approach to modelling UGM in flexible pavement. The review seeks to understand the concept of behaviour from experimental research and discusses the parameters to be included in numerical simulation. The review of numerical studies covers previous research with a critical perspective on comparing the different simulations. Finally, the gap in the previous research is identified, allowing for the place of the current study among the current research to be established.

Chapter 3 covers the basics of FEM, in particular introducing the constitutive model with a perspective on its application in FEM simulations. The chapter then explores the concept of the layered medium, including the interaction phenomenon and the influence of boundary conditions in two types of analysis (static and dynamic). Finally, the chapter presents the new constitutive model which includes nonlinear stress dependent elasticity along with the shakedown concept in the Mohr-Coulomb yield criterion.

Chapter 4 describes the simulation of different models used for the FEM analysis in this research. The mesh and boundary conditions are discussed in detail and the loading details for both the static and dynamic analysis is explained. After that, the material constitutive models used in this simulation are indicated.

Chapter 5 is a representation of the various static numerical simulations conducted in this research and the analytical graphs illustrating the effect of each approach on the calculated response of the whole layered system. This chapter includes the results of simulations consisting of static loading assuming linear elastic, nonlinear elastic, linear elastoplastic and nonlinear elastoplastic UGM behaviour.

Chapter 6 presents the results of the dynamic analyses allowing for nonlinear elastoplastic behaviour, nonlinear elastoplastic with shakedown, and nonlinear elastoplastic with shakedown and the interaction of asphalt and base layer. This is followed by a comprehensive discussion of the results.

The results of all the analyses and simulations are compared and remarks are made on each individual analysis in Chapter 7. Finally, the implication of the results and their contribution to the design chart is discussed.

The conclusions drawn from this research are presented in Chapter 8 along with the scope for future research in the field.

## **CHAPTER 2**

### **2: LITERATURE REVIEW**

#### **2.1 Introduction**

New researchers in the field of pavement engineering have devoted especial attention to the recently developed concept of mechanistic-empirical design. Before the introduction of this new concept, pavement design relied on experimental formulation. However, advancing computer technology along with an increasing demand for sustainable roads necessitated a more scientific process which could be widely trusted and more accurately predict pavement mechanical responses.

This chapter presents a comprehensive review with a critical perspective of the scientific literature. The structure of the review is illustrated in Figure 2.1. Following this introduction, section 2.2 contains a brief review of current pavement design methods. The main differences between two major codes (American Association of State Highway Officials (AASHTO) (2002) and Austroads (2004)) are discussed. Section 2.3 describes the concept of modelling in the field of layered flexible pavement engineering. Sub-section 2.3.1 presents the mathematical and analytical models for layered flexible pavement. Sub-section 2.3.2 discusses experimental field and laboratory models. Sub-section 2.3.3 reviews the numerical methods approach to pavement systems. Because the main focus of this research is on the finite element modelling of UGM in layered flexible pavement, section 2.4 presents an in-depth review of previously published FE models in this field.

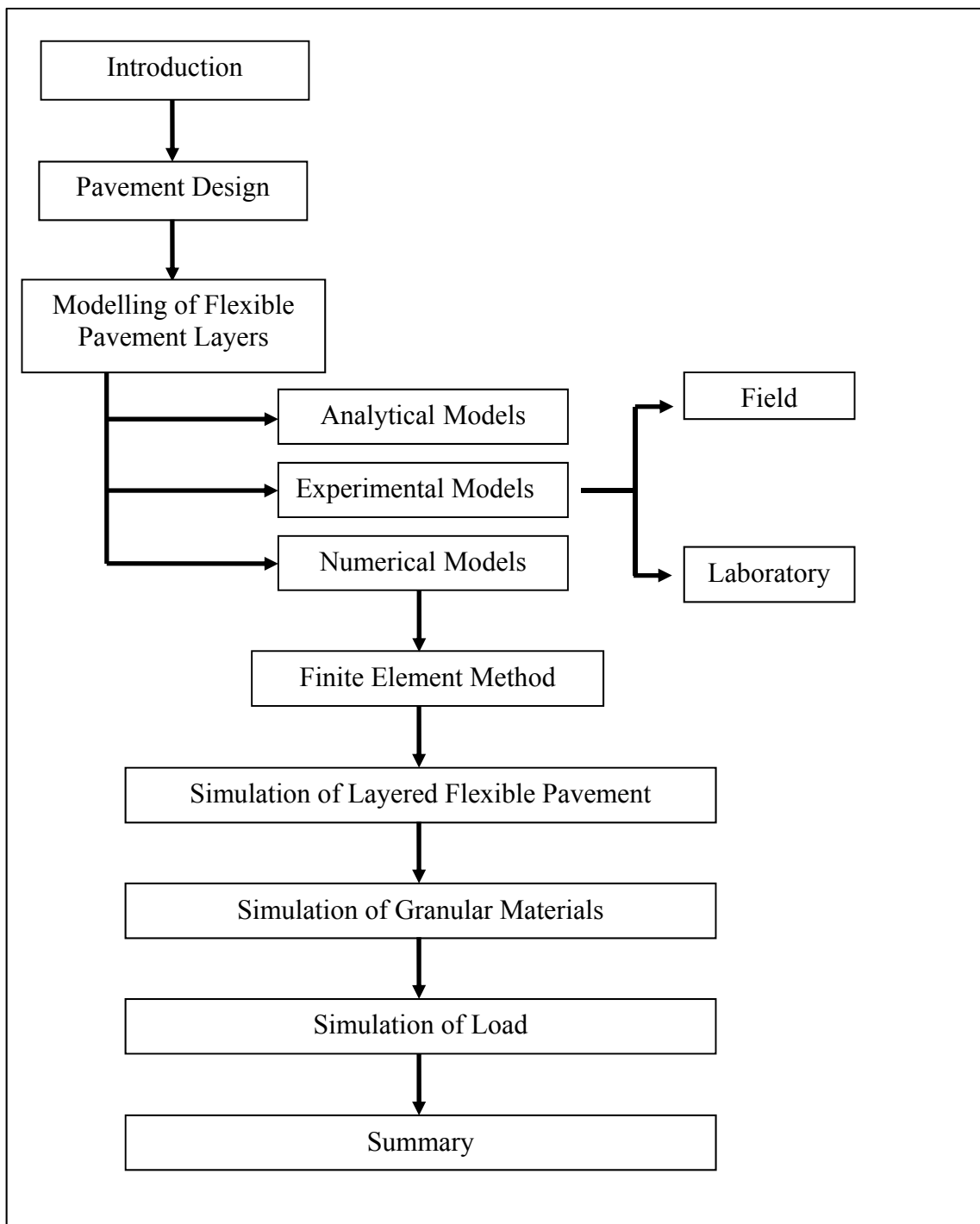


Figure 2.1 - Structure of Literature Review

The review of FE models is divided into three sub-sections, each of which deals with one major aspect of simulation. Sub-section 2.4.1 describes previous attempts to model layered systems and discusses the interaction of layers. Sub-section 2.4.2 contains an inclusive review of constitutive equations implemented to model UGM in layered flexible pavement. The loading conditions (either dynamic or static) are then investigated in sub-section 2.4.3. Finally, the chapter closes with a summary of the literature review.

## **2.2 A Review Pavement Design**

In early approaches to pavement design, empiricism made the main contribution to the field. Even in the recent era, there is an undeniable role for experiment and field observation. According to Huang (2004), prior to the 1920s pavement design was based only on experience and observation. The effect of subgrade soil on pavement thickness was ignored, as were many other important factors. The heavy vehicular load introduced after World War II resulted in the failure of existing pavement designed on an empirical basis. In 1961, the American Association of State Highway Officials (AASHTO) conducted a full scale test (Bodhinayake 2008). This famous test made a significant contribution to the development of a new generation of design codes. Moreover, increasing car usage, highway developments and advances in technology have led to significant improvements in design procedures. During the 20<sup>th</sup> century there were many different codes, each related to specific locations or conditions. For example, the AASHTO code was developed in the USA and has been accepted in some other parts of the world, while the Austroads code for pavement design is used across Australia.

### **2.2.1 Basic Concepts in Pavement Design**

Typically when the term ‘road pavement’ is used, it refers to a durable layer of construction materials laid down on other layers or the existing soil to provide a paved face for vehicular traffic load. It should be able to sustain this type of load for many cycles.

In most cases, the existing soil (the subgrade) in its virgin form cannot provide enough strength to withstand the load of traffic cycles. The solution to this problem is a specific type of structure called pavement in civil engineering, and as mentioned above, this consists of layers of construction materials in composition. The critical task of this integrated system is to resist the designated traffic load for a predicted time period at an optimized economic cost. In addition, the structure is usually expected to be serviceable for traffic loads under varying environmental conditions. Therefore, environmental loading of pavement also has to be considered, and this includes temperature and moisture conditions.

Different materials are used for pavement layers, including good quality granular materials, chemical additives such as cement or lime, recycled materials, bitumen, etc. Pavement is generally classified into two major categories: flexible and rigid pavement.

Rigid pavement is a combination of cement and granular which forms concrete materials. The usage of this type of pavement has been referred to since the late 19<sup>th</sup> century (Huang 2004). The strength provided by the concrete slab is sufficient enough to bear heavy loads as large as aeroplanes.

By contrast, flexible pavement is asphalt concrete which is a combination of bitumen as a cohesive material and granular grains as a skeleton. The first use of asphalt surfaced pavement in the USA was in 1876 on Pennsylvania Avenue in Washington, D.C. (Huang 2004).

The categorization of pavement types relates not only to the type of ingredients, but more importantly to the mechanical behaviour of each type. In a rigid pavement structure, the mechanical behaviour of the system is expected to be brittle which means a high initial strength and a sudden decrease in strength after the limit load is reached. This sudden failure could be undesirable in many cases. In flexible pavement, material failure is a consequence of gradual deformation. Although the final strength of flexible pavement may be less than that of rigid concrete pavement, the gradual failure mechanism which allows for repair and maintenance could be a significant advantage. This research is focussed on layered flexible pavement and the rest of this review is therefore about this pavement type.

Different criteria have been considered in the design of flexible pavement. These include but are not restricted to surface deformation of the asphalt layer, shear failure of the asphalt layer, shear failure of the granular layer and surface cracking of the asphalt layer. Surface cracking of the asphalt layer in particular has been investigated widely; with various types of cracks due to traffic loads or cyclic thermal loads being identified.

There are two major approaches to designing flexible pavement for roads. The first one is the empirical method which was developed earlier, and the second one is the mechanistic-empirical which is a more recent development.

Empirical methods of pavement design date back to 1929 when the concept of soil classification was established (Huang 2004). This concept was further developed and resulted in the group index method (currently known as the AASHTO method) for soil classification. In this classification, soils and mixtures of aggregate in granular subgrade are classified from a-1 to a-7, with each category having its own implications and applications in road construction.

The contribution of soil strength to pavement thickness was taken into account in the development of the California bearing ratio (CBR) test method. CBR is defined as the ratio of the resistance of a given subgrade to penetration in respect to the resistance of crushed rock to the same penetration.

### **2.2.2 Empirical Methods**

The empirical methods based on the CBR usually consist of the relationship between the required thickness for pavement according to the existing CBR and the predicted traffic loads as a number of equivalent standard axles (ESA). This relationship is presented in AASHTO (Bodhinayake 2008) where the number of ESA is defined as the ratio of single axle load over 80 kN raised to the power of four.

The same concept has been used in Austroads (2004) to develop a chart that a designer can use to evaluate pavement thickness based on equivalent standard axle (ESA) and CBR. Figure 2.2 illustrates such a chart.

Although the empirical design method has been used for many years, the shortcomings of this approach have recently become undeniable. The empirical method relies heavily on the investigation of the constructed field but does not

provide any comprehensive knowledge about pavement mechanical behaviour. Therefore, the extension of any formula based on this investigation can be doubtful. The application of the empirical method is also limited in significant aspects such as loading conditions, environmental conditions and material variations.

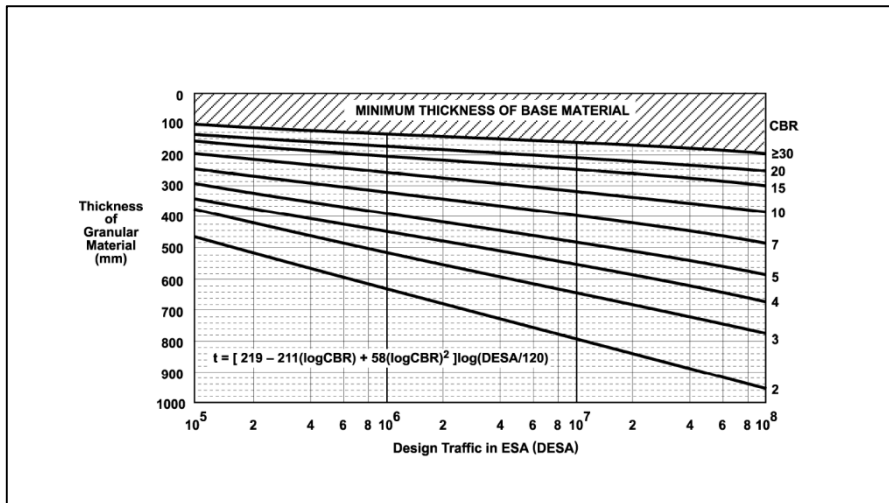


Figure 2.2 - Thickness Design Chart (from Figure 8.4, AUSTROADS 2004)

There is an increasing demand to use newly available knowledge and technology to develop a more scientific procedure for pavement design which relies not only on laboratory observation but also on analytical science. Such a design should provide a procedure that can be more easily applied to new situations in different environmental conditions.

### 2.2.3 Mechanistic Empirical Design

The mechanistic-empirical (ME) process is a recently developed pavement design method that combines mechanical science and empirical observation. In this

method, the primary response of the pavement in terms of stress, strain and displacement is calculated through the mechanical solution of the layered system. These critical values are then entered in an empirical formula which correlates them to actual pavement performance. The final goal is to produce a more sustainable pavement system.

This method applies a limited use of mechanical principles such as continuity, equilibrium and the virtual work principle to a layered system. Materials then are modelled according to elasticity, plasticity and viscoelasticity. The steps in ME design are as follows: Firstly, the layered pavement system is solved using a selected mechanistic model. The solution can be analytical (closed form) or numerical (like FE). Materials can be modelled in different ways including elastic, nonlinear elastic, resilient modulus or elastoplastic such as von Mises, Tresca, Drucker-Prager, Mohr-Coulomb, and hardening or continuous yielding (Desai and Whitenack 2001; Schofield and Wroth 1968; Vermeer 1982). In the second step, the critical values calculated from the mechanical models are entered in empirical formulas to predict rutting, damage, cracking under mechanical and thermal loads, and cycles to failure. Usually, uniaxial values such as the tensile strain at the bottom of the asphalt layer, vertical compressive strain at the top of the subgrade layer, vertical stress under the wheel load and surface deflection under the wheel load are employed for this final computation (Huang 1993).

In both the empirical and ME methods, the pavement should be designed in such a way that its layers are able to withstand a certain number of vehicle cycles and remain in a serviceable condition. The serviceability of pavements is defined by restriction of the pavement critical distress mode. Two of the major distress modes in flexible pavement are fatigue and rutting.

Fatigue cracking is a chain of connected cracks mainly due to fatigue failure in the asphalt layer. While there is some dispute on this subject, it is generally believed that cracking begins at the bottom of the asphalt layer, resulting from high tensile stress and strain in one spot. The crack is then propagated upward to the surface beneath the wheel, in the longitudinal direction of the road. Under repeating traffic loading, the cracks become connected and form polygons on the pavement surface. The shape is similar to alligator's skin, which is why fatigue cracking is also known as alligator cracking (Huang 2004). A typical example of fatigue failure is shown in Figure 2.3.



Figure 2.3 – Fatigue Cracking  
(Nicholson Road WA, Picture is provided by Colin Leek)

Rao Tangella et al. (1990) reviewed various fatigue test methods and made recommendations on the proper procedure to determine fatigue in the asphalt layer of flexible pavement. The repeated flexure test yielded the best score. In order to examine the fatigue, different equipment was employed to apply the simple

flexure principle. A well-known example is the four-point bending (4PB) frame (Tayebali, Rowe and Sousa 1992; Pelgröm 2000).

It should be mentioned that fatigue failure from testing is defined as the final number of cycles after which the sample fails. This can yield different results and the number is dependent on test parameters such as loading mode (Al-Khateeb and Shenoy 2004). Some researchers have suggested that the complete fracture of the sample is the final failure in stress-controlled tests (Pell and Cooper 1975; Tayebali, Rowe and Sousa 1992). However, Rowe (1993) recommended a particular failure criterion in order to protect the instrument itself. In his recommendation, the failure is defined by a 90% reduction in initial stiffness at the point where the largest crack occurs in the specimen. This led to a modified concept of failure which depends on the crack initiation instead of the total failure of the whole specimen. The accepted way to define the fatigue from different tests remains a topic of dispute. Among recently proposed concepts, the approach of Ghuzlan and Carpenter (2000) is worth mentioning, where failure is based on the change in dissipated energy ( $\Delta DE$ ) between two consecutive cycles. In 2013, Nega et al. (2013a) investigated characterization methods for fatigue performance in WA (Nega et al. 2013a).

Another type of major distress in flexible pavement is rutting which is defined as surface depression in the wheel paths (Figure 2.4). There may be uplift along the sides of the rutting. It is believed that rutting happens due to permanent deformation of different pavement layers or subgrade.

The subgrade is more sensitive to applied traffic load and permanent deformation occurs in this layer due to consolidation, shear failure or any other type of movement. Plastic deformation of asphalt can also cause rutting deformation,

especially where compaction has been insufficient or where asphalt is subjected to hot weather. High rutting can lead to unserviceable conditions in the whole pavement (Huang 2004).



Figure 2.4 - Rut Failure (Nicholson Road WA, Picture is provided by Colin Leek)

It is generally accepted that the subgrade makes a significant contribution to the rutting failure of pavement. Accelerated pavement tests have been used by researchers to indicate the contribution of granular layers to surface rutting (Arnold, Alabaster and Steven 2001; Little 1993; Pidwerbesky 1996; Korkiala-Tanttu, Laaksonen and Törnqvist 2003), and it is stated that granular layers are responsible for 30% to 70% of rutting deformation at the pavement surface. Therefore permanent displacement in the granular layers could have an important role in pavement failure occurring as rutting at the surface. This is where efforts to understand UGM behaviour in response to traffic loading are valuable.

As mentioned before, the ME method requires the solution of the given geometry under vehicle loads in terms of stress and strain. Consider an element in Figure 2.5. It is illustrated that, due to the pressure load from the tyre at the

surface, stress is induced on each surface of the cubic element. For this element to be in an equilibrium state, the opposite faces of the cube should sustain stress of equal value and in opposite directions. Stresses are divided into two types, normal and shear stresses, shown as  $\sigma$  and  $\tau$  in Figure 2.5 respectively.

These stresses produce deformation and therefore strain in the same direction as the stress in the element. Strain, similarly, can also be divided into two types, normal and shear strain, symbolized as  $\epsilon$  and  $\gamma$  respectively.

In continuum mechanics there is a relationship between stress and strain which is defined by material behaviour. A simple example of this relationship is when a linear elasticity is assumed for the materials and the stress-strain relationship is defined by Equation 2-1 and Equation 2-12:

$$\sigma = E\epsilon \quad \text{Equation 2-1}$$

$$\tau = G\gamma \quad \text{Equation 2-2}$$

Where E and G are Young and shear modulus, respectively.

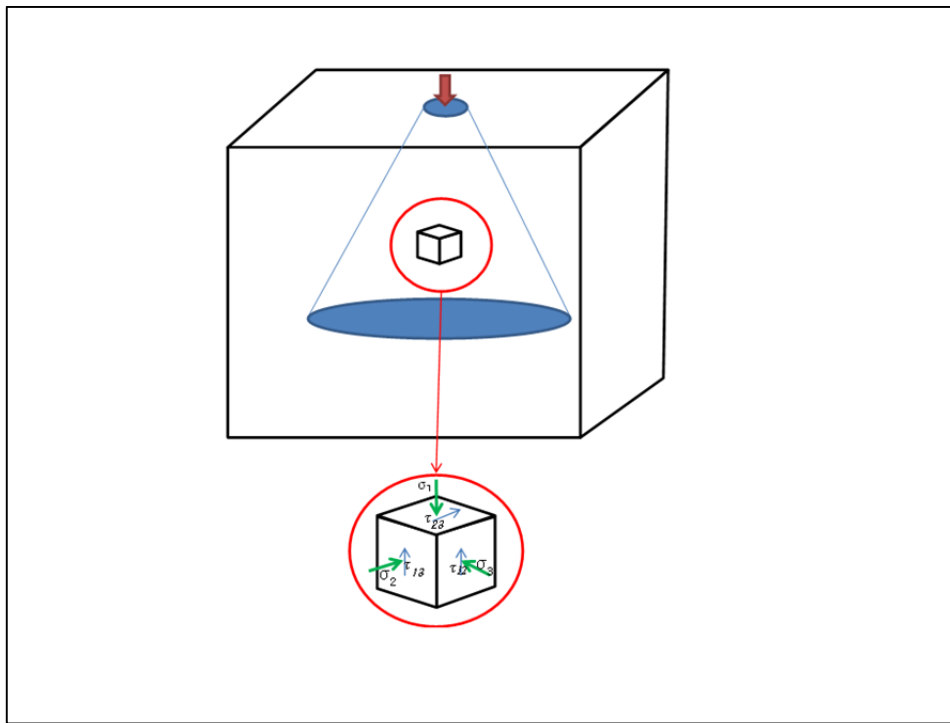


Figure 2.5 - Induced Stress under Wheel Load

An easy way to analyze the response of flexible pavement to tyre pressure is to consider the system as a homogeneous half-space. The half-space here is a space which is restricted by a surface plane (the plane upon which the tyre load is applied) and is infinite in other directions (here this means the horizontal direction and downward vertical direction).

In this problem, the theory of Boussinesq (1885) can be applied where stresses and strains are calculated under a concentrated load on the surface of an elastic half-space. This solution can be integrated to form a circular area representing the tyre loading area. For a better analysis, Burmister et al. (1943) developed a solution for the layered system in which the half-space consists of some layers on the surface attached to a semi-infinite space at the bottom. These two are

considered to be an initial analytical solution to calculate the mechanistic response of layered flexible pavement.

Based on the abovementioned points, it is important to investigate material models for the different layers of flexible pavement. Selecting the material model has a direct effect on the calculated mechanistic response.

The asphalt layer, which is the first and strongest layer withstanding the load, has usually been modelled as one of three types: elastic, viscoelastic or viscoelastoplastic. The elastic model follows Equation 2-1 and correlates stress and strain similarly. In viscoelastic behaviour, the material can show viscous behaviour in which the strain changes over time while the stress remains constant. There are different models of such viscous behaviour (Huang 2004). The Kelvin and Maxwell models are two of the most well-known models used to account for viscoelasticity (Figure 2.6). In more advanced modelling, an assumption is made of the viscoelastoplacticity of asphalt layers (Starovoitov and Nağıyev 2012). The material characteristics of hot mix asphalt used in flexible pavement in WA have been investigated (Nega et al. 2013b) and its specific traits reported.

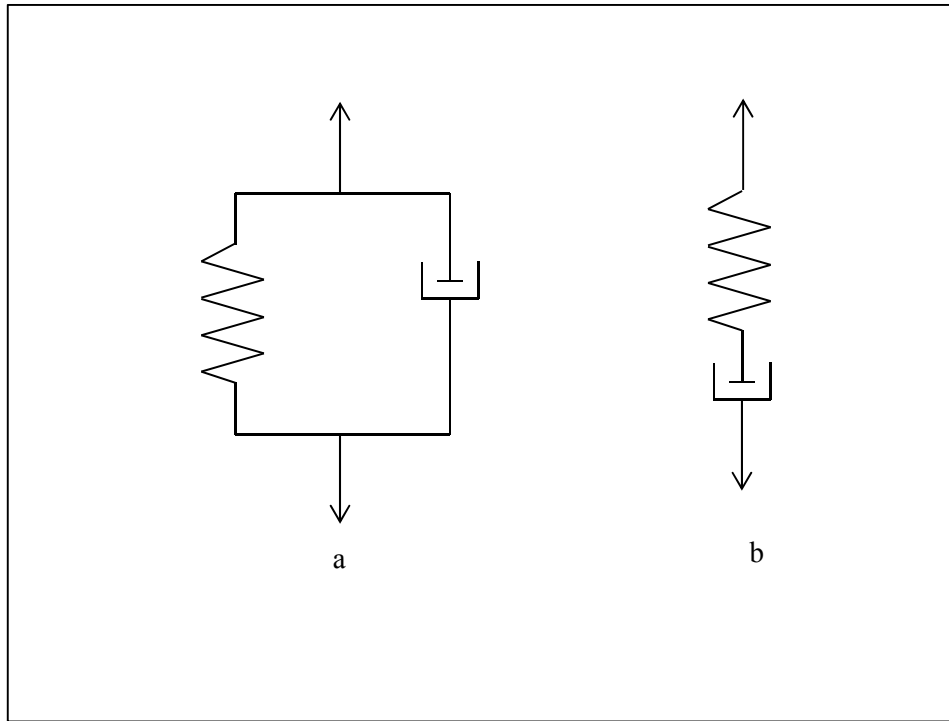


Figure 2.6 - Kelvin Model (a) and Maxwell Model (b)

The base layer and subgrade are usually modelled as a linear elastic model (such as in Wardle (1977)), nonlinear elastic model (such as in Kim and Tutumluer (2006)) or linear elastoplastic model (such as in Saad, Mitri, and Poorooshahab (2005)). Among nonlinear elastic models, a well-known stress dependent model is the universal octahedral shear stress model (Witczak and Uzan 1988), which accounts for the nonlinearity of UGM in a three-dimensional space. The plasticity of UGM has been modelled under the classical plasticity criteria such as Drucker-Prager, Mohr-Coulomb or Cam-Clay (Yu 2006)

However, UGM shows a complicated behaviour when subjected to cyclic loading, demonstrating different behaviour at different periods of cyclic loading. Such behaviour is currently under investigation in the area of pavement engineering. Different concepts such as resilient modulus and shakedown theory have been

developed to cover this aspect of UGM. A detailed review of this characteristic is covered in a following sub-section of this chapter.

Table 2-1 - Comparison of AASHTO and AUSTROADS  
(from Table 1 Ghadimi et al. 2013)

Pavement Layer	Austroad Assumptions	AASHTO Assumptions
Subgrade	elastic and cross-anisotropic modelled by five parameters: two elastic moduli, two Poisson ratios and one shear modulus	Non-Linear stress dependent elastic modelled by two parameters: Resilient modulus and Poisson ratio
Subbase/Base (UGM)	Non-Linear stress dependent elastic modelled by two parameters: Elastic modulus and Poisson ratio	Non-Linear elastoplastic depended to number of repetitions of traffic loads and elastic material properties
Asphalt layer (Rutting)	Ignored	Viscoelastic behaviour of asphalt depended to temperature and number of loading and dynamic modulus
Asphalt layer (Fatigue)	Elastic behaviour modelled by two parameters : Bitumen viscosity and stiffness	Elastic behaviour modelled by one parameter : Elastic modulus

Based on what has been stated previously, ME design codes have been developed worldwide. Two of the major codes are Austroads (2004) and AASHTO (2002). A comparison of these two design codes is presented by Ghadimi et al.(2013a). In their study, the fundamental assumptions of each code on the materials in different layers are reviewed and compared. Table 2-1 summarizes the

comparison of these two codes. It is necessary to develop advanced knowledge of material behaviour in order to improve the current design methods.

Since this dissertation is about modelling UGM in flexible pavement, the coming sections will review the previous scientific attempts to model these materials.

### **2.3 Modelling of Flexible Pavement Layers**

Modelling is used in pavement engineering to evaluate the behaviour of a layered structure in response to a given traffic load. The modelling approach in essence is to simplify a complex matter in order to arrive at a possible solution. The same approach is used in flexible pavement engineering. Simplification can apply to the layer geometry, load or material characteristics. The goal of modelling is to provide a close simulation of the actual problem. This can be achieved by improving the simplification of previous models. This section reviews previous scientific attempts to model layered flexible pavement structures.

Sub-section 2.3.1 reviews analytical closed form solutions, sub-section 2.3.2 covers laboratory and field experiments and measurement, and sub-section 2.3.3 reviews different approaches to numerical modelling.

#### **2.3.1 Analytical Models**

Attempts to model the different behaviours of pavement layers have been made mainly in the 20<sup>th</sup> century. However, the theory of Boussinesq (1885) was the one of the foundations for all of the solutions developed thereafter. Boussinesq (1885) dealt with a semi-infinite homogeneous medium assuming linear elastic materials. A concentrated load is applied on an axisymmetric coordinate and the solution is presented through the manipulation of static equilibrium and constitutive and

kinematic equations. This solution, however, cannot be used directly in the field of pavement engineering since in an actual pavement system there are different layers with different elastic properties.

In the solution devised by Boussinesq (1885), the load was a concentrated load. To better evaluate a tyre loading, Foster and Ahlvin (1958) extended the solution for a circular area of loading through the integration of Boussinesq's solution. They then presented the response of the medium in terms of horizontal and vertical stress and strain in charts.

To account for multilayer conditions in pavement, Burmister et al.(1943) investigated the solutions for two and three layer elastic half-space which significantly affects pavement engineering. The solution also provided the opportunity to collect the responses of multilayered systems. In this study, layers are assumed to be homogeneous, isotropic and linear elastic; the weight of the layers is not considered; loading is applied over a circular area as a uniform pressure and the layer interface is continuous.

Huang (2004) has attempted to apply previous studies to multilayered systems. This book summarizes previously published papers that present different charts for the responses of layered systems.

These types of analytical solution are the basis of multilayer programs such as KENLAYER (Huang 1993) and CYRCLY (Wardle 1977) and will be described in detail in Chapter 3.

While the abovementioned studies consider the layers as linear elastic materials under static loading, other researchers have investigated the effects of dynamic

loading on materials and on UGM behaviour. Pavement engineers know that UGM subjected to cyclic loads behave differently according to the loading cycles. The most obvious reason for this is the compaction effect of loading cycles on UGM which results in stiffer behaviour for a greater number of cycles. To account for this kind of complex behaviour, researchers recently tried to apply the concept of shakedown to UGM. The shakedown concept was developed in the early 20<sup>th</sup> century and was mainly employed in material engineering, especially to account for behaviour of metal in fatigue failure (Melan 1938; Koiter 1960; Zarka and Casier 1979). In Chapter 3 a detailed description of the shakedown theory is provided.

Yu (2006) has summarized his previous attempts to apply the shakedown theory in analysis of layered pavement systems. He presented an analytical solution for the shakedown of rolling and sliding lines and point contacts separately. Then he attempted to propose a new method by which a shakedown solution could be considered in a FE analysis.

There have also been investigations to extend the Zarka shakedown theory (Zarka and Casier 1979) for Drucker-Prager plastic criteria (Chazallon, Hornych and Mouhoubi 2006; Chazallon, Koval and Mouhoubi 2011; Habiballah and Chazallon 2005; Allou, Chazallon and Hornych 2007; Allou et al. 2009). However, in this research, the analysis is static and neglects the inertial forces caused by mass and damping of materials.

The concept of shakedown has attracted the attention of researchers because it can model one of the most important and simultaneously complicated behaviours of UGM. This dissertation presents a new method in which shakedown behaviour based on Mohr-Coulomb criteria can be taken into account in a dynamic FEM.

### **2.3.2 Experimental Models**

This section briefly reviews the scientific attempts to model the behaviour of UGM in flexible pavement layers through laboratory experiments or field observations.

While there are a vast range of UGM properties that can be modelled, this section focuses on the mechanical behaviour of UGM. More specifically, studies on elastic (linear and nonlinear) and plastic (including shakedown) behaviour are reviewed. The purpose of this is to provide an initial insight into the final numerical simulation of layered systems.

The process of modelling is an interaction between experimental observation and analytical abstraction. Firstly, a phenomenon (let say a failure mode in pavement layers) is observed in the field. Then an experimental sample is made to simulate the same phenomenon under controlled conditions in the laboratory (which provides scientific data). In the final stage, an analytical abstraction is made based on the laboratory data, in order to enable the researcher to obtain a mechanical concept governing the phenomenon (here the mechanical behaviour of pavement materials). This understanding makes it possible to predict the phenomenon in the future.

Therefore, a review of the experimental models provides the initial stage for the analytical models that are developed in this dissertation. Moreover, some of these data are also used for the purpose of verifying the numerical simulation.

Cyclic behaviour of UGM is not elastic and there is some plastic deformation in each cycle. The induced strain in each cycle is composed of elastic strain and a

plastic strain. The elastic part of the strain is recoverable when unloading, while the plastic part is permanent. The resilient modulus is defined through the elastic strain in Equation 2-3.

$$M_R = \frac{\sigma_d}{\varepsilon_r} \quad \text{Equation 2-3}$$

where

$M_R$  = Resilient modulus

$\sigma_d$  = Deviator stress

$\varepsilon_r$  = Axial strain for recoverable strain under repeated load

The resilient modulus is usually determined through the repeated load unconfined compression test and the repeated load triaxial compression test. Austroads (2004) suggests Equation 2-4 to evaluate the resilient modulus of subgrade according to existing CBR. This evaluation can be used for relatively soft subgrade with an  $M_R$  lower than 150 MPa.

$$M_R (MPa) = 10 CBR \quad \text{Equation 2-4}$$

The influence of various factors on  $M_R$  have been studied through experimental investigations (Seed, Chan and Lee 1962; Ahmed and Larew 1962; Hicks and Monismith 1971). In these studies, triaxial apparatus was used to determine the relationship between  $M_R$  and material properties.

A study by Selig (1987) indicated that there was a large lateral plastic strain in UGM during the first cycle of loading, while in the following cycles the UGM

tended towards elastic behaviour. It was inferred that the tensile stress at the bottom of the UGM was induced in the first few cycles and cancelled by induced plastic strain in further cycles.

In the study carried out by Brown and Pell (1974), the relationships between recoverable strain (elastic strain) and stress cycles, as well as permanent strain and stress cycles were investigated. The same study found that resilient strain was correlated to deviator stress.

One of the first studies to find that the nonlinearity of UGM is related to the state of stress was conducted by Boyce, Brown, and Pell (1976). In this experiment, the effects of aggregate size on anisotropic behaviour of UGM was investigated and it was concluded that the larger the aggregate, the more anisotropic behaviour in UGM is expected.

The relation between material resilient modulus and stress state is known to pavement engineers. The resilient modulus of UGM increases due to an increase in confining pressure and these results in the nonlinear elastic behaviour of UGM. One of the first nonlinear models is called K-θ, where  $M_R$  is depended on bulk stress, as shown by Equation 2-5:

$$M_R = K \left( \frac{\theta}{P_1} \right)^n \quad \text{Equation 2-5}$$

Here K and n are the material properties determined in laboratory, θ is the bulk stress and P1 is the unit pressure to make the θ a dimensionless value. Seed et al. (1962) used this to investigate the response of UGM under repeated loading. Following Seed et al., other researchers also became interested in employing this

concept (Hicks and Monismith 1971). However, this model does not include the effect of deviator stress on UGM.

This deviator stress has been considered in the model presented by Uzan (1985). In this model  $M_R$  is a function of bulk and deviator stress together:

$$M_R = K_1 \left( \frac{\theta}{P_1} \right)^{k_2} \left( \frac{\sigma_d}{P_1} \right)^{k_3} \quad \text{Equation 2-6}$$

Here  $\sigma_d$  is the deviator stress and  $P_1$  is the unit pressure.  $K_1$ ,  $k_2$  and  $k_3$  are the material properties. This model is appropriate for axisymmetric conditions. Uzan and Witczak (1988) further expanded it to three-dimensional conditions:

$$M_R = K_1 P_0 \left( \frac{I_1}{P_0} \right)^{k_2} \left( \frac{\tau_{oct}}{P_0} \right)^{k_3} \quad \text{Equation 2-7}$$

$$\tau_{oct} = 1/3 \sqrt{(\sigma_1 - \sigma_2)^2 + (\sigma_2 - \sigma_3)^2 + (\sigma_3 - \sigma_1)^2} \quad \text{Equation 2-8}$$

Here  $I_1$  is the first invariants of stress tensors,  $\tau_{oct}$  is octahedral shear stress,  $P_0$  indicates the atmospheric pressure and  $K_1$ ,  $k_2$  and  $k_3$  are the material properties.

In an attempt to introduce an analytical base model which accounts for this nonlinearity, Lade and Nelson (1987) derived an equation which correlated the  $M_R$  to mean normal stress and deviator stress. They used the concept of elastic energy and virtual work and indicated that the stiffness of the material should be a function of the first invariant of the stress tensor and the deviator stress as in Equation 2-9:

$$M_R = K_1 \left[ \left( \frac{I_1}{P_1} \right)^2 + R \left( \frac{\tau_{oct}}{P_1} \right)^2 \right]^{k_2} \quad \text{Equation 2-9}$$

$$\text{Where } R = 6 \frac{1+v}{1-2v} \quad \text{Equation 2-10}$$

All parameters are as stated for Equation 2-7, and v is Poisson's ratio.

Research is still going on to propose new models to account for the nonlinearity of UGM. A relatively recent approach was introduced by Hjelmstad and Taciroglu (2000), where  $M_R$  depended on both first and second invariants of the strain tensor instead of the stress tensor.

In the study carried out by Fahey and Carter (1993), an experimental nonlinear equation was introduced in which the shear modulus of sand was connected to induced shear stress. To examine the accuracy of nonlinear models in the prediction of mechanical responses of UGM, Gonzalez, Saleh, and Ali (2007) carried out a series of simulations and field measurements. The conclusion confirms the validity of nonlinear models. In 2009, Lee, Kim, and Kang (2009) presented a new nonlinear model which was based on an experimental method. This model linked the resilient modulus to induced stresses and the time history of the stresses.

The difference between various proposed nonlinear models was investigated by Attia and Abdelrahman (2011) through experimental tests. Nine different constitutive models were investigated, among them Uzan (2-D and 3-D), Witczak (5 parameters) and K-θ.

Recently Araya et al. (2011) and Araya et al. (2012) studied triaxial tests and carried out an ABAQUS simulation. They introduced a new test, termed RL-CBR, and established a correlation between the California Bearing Ratio (CBR) and the stress-dependent  $M_R$ .

The effect of aggregate shape and characteristics on  $M_R$  was studied by Mishra and Tutumluer (2012). In this research, different nonlinear models were used, and experimental results were generated and compared against field data.

While the experimental investigations reviewed above provide researchers with input data, it is necessary to use this data in a full numerical simulation. The purpose of any constitutive model presented either experimentally or analytically is to be used for a numerical simulation. In this way, a constitutive model can contribute to the final design of a pavement system.

The abovementioned experimental studies relate to the nonlinear elastic behaviour of UGM. However, another important part of UGM behaviour occurs when the load exceeds the plastic limit of UGM. A unique response is observed when UGM undergoes cyclic traffic loading in which material behaviour changes with increasing cycles of loading. The phenomenon can be understood through the shakedown theory.

The concept of shakedown has been developed in order to model the responses of different engineering materials under cyclic loads. One of the initial applications of shakedown theory was to provide a solution for metallic elements under repeated loads (Zarka and Casier 1979).

The application of the shakedown concept for UGM used in flexible pavement layers was initially investigated by Sharp and Booker (Sharp 1985; Sharp and Booker 1984). In these studies, the shakedown theory was employed to describe the behaviour of UGM based on the published data of the AASHTO experiment (AASHTO 1986). After that, the limit analysis approach was used to determine lower and upper bound shakedown for UGM. Two of the major studies worth mentioning are the upper bound solution by Collins and Boulbibane (1998) and the lower bound solution by Yu and Hossain (1998). In a study, Lekarp, Isacsson, and Dawson (2000) reviewed the major published studies on the contribution of material properties to the plastic strain of UGM.

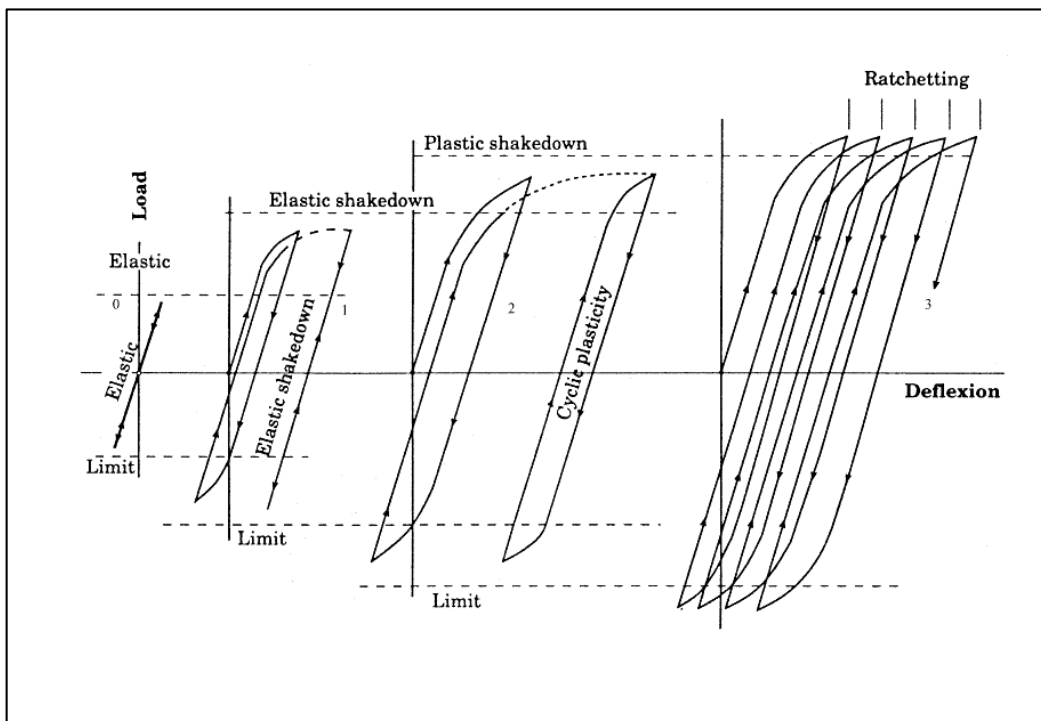


Figure 2.7- Possible Responses of Structure to Cyclic Load

(from Figure 1 Collins and Boulbibane 2000)

According to Collins and Boulbibane (2000), there are four potential responses for an elastic-plastic structure, as illustrated in Figure 2.7.

1. When the amplitude of the load is small, the response of the structure remains elastic and there is no induced plastic strain. In this case, any point of a structure returns to its origin during each loading and unloading cycle.
2. In the second case, the load amplitude is greater than the elastic limit but within the shakedown limit. In this case, after a few cycle of plastic deformation, material properties change in such a way that responses to further cycles are purely elastic. Collins and Boulbibane point out that: ‘In a pavement this could mean that some rutting, subsurface deformation, or cracking occurs but that after a certain time this deterioration ceases and no further structural damage occurs’ (Collins and Boulbibane 2000, 51)
3. In the third case, the load is large enough to produce constant plastic deformation in each loop of loading-unloading. This loop is a closed loop and the condition is known as ‘plastic shakedown’.
4. If the load still exceeds the plastic shakedown limit, the accumulation of plastic deformation in each cycle moves toward infinity. In this case an incremental failure will occur and the condition is known as ‘ratchetting’.

The first three cases are acceptable in the design of flexible pavement layers.

When UGM is subjected to a cyclic load and the shakedown occurs, the shape of accumulated residual strain versus cycle can be illustrated as seen in Figure 2.8 (Siripun 2010). There has been growing interest among researchers in providing a

relationship which can cover the UGM permanent strain as a function of cycle number.

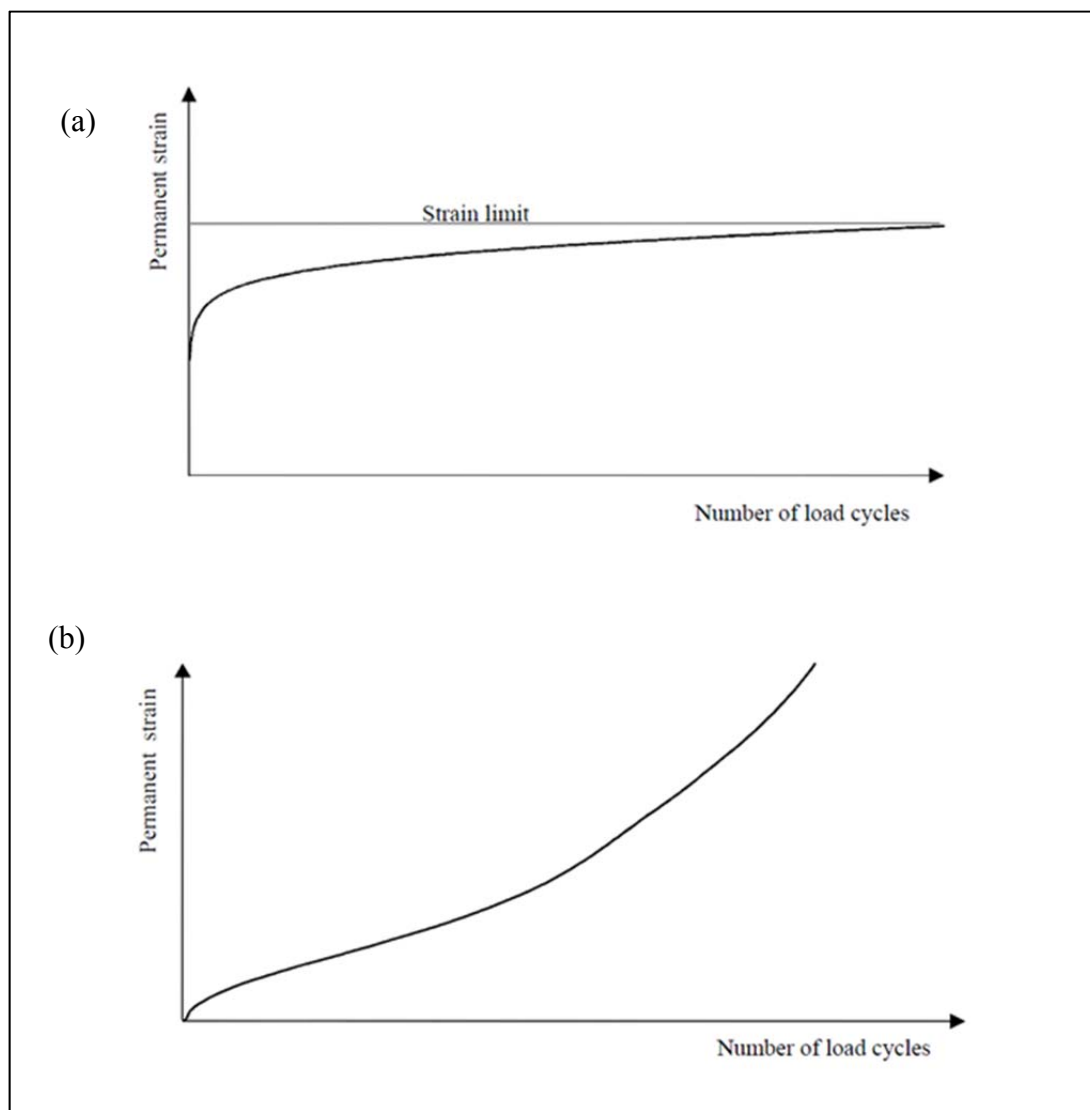


Figure 2.8 – Permanent Strain of UGM: (a) Shakedown Limit (b) Failure (from Figures 2.36 and 2.37 Siripun 2010)

Some of the major equations are logarithmic function(Barksdale 1972; Sweere 1990), hyperbolic towards a given final deformation (Wolff and Visser 1994; Paute, Hornych and Benaben 1996) and the log-log equation introduced by Huerman (Huerman 1997).

In 2004, Werkmeister, Dawson, and Wellner conducted repeated load triaxial tests on a crushed rock aggregate. The experiment used various stress levels on the samples and the shakedown was investigated. The materials were selected from the types used in Germany.

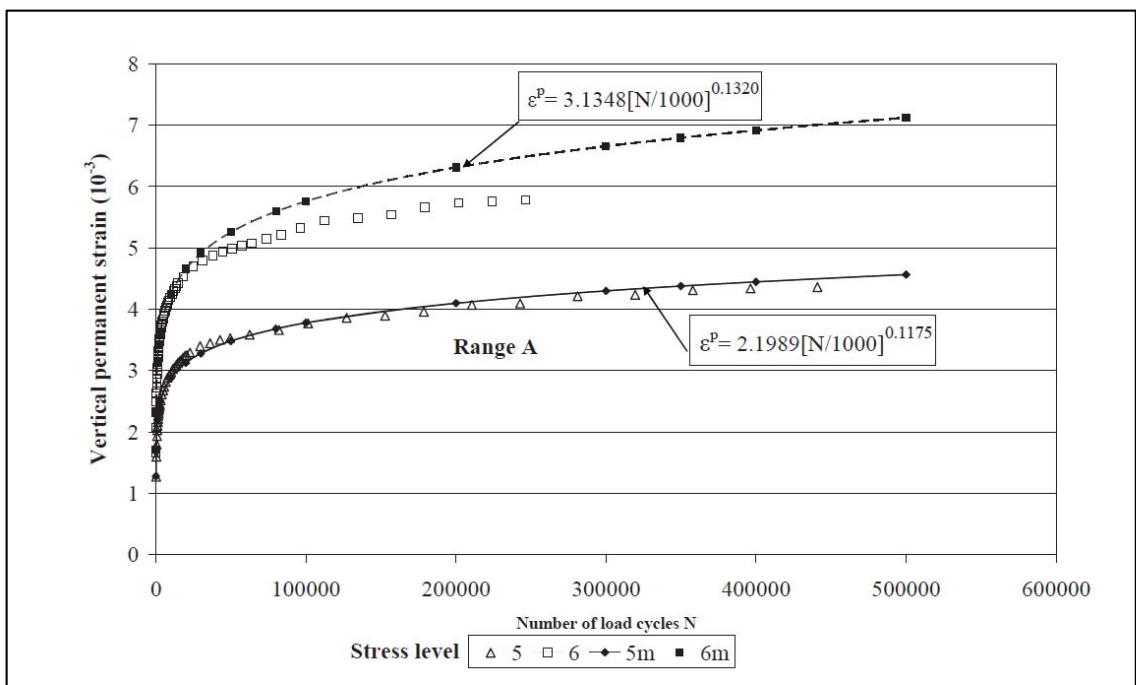


Figure 2.9 - Permanent Strain Equations (from Figure 5 Siripun et al. 2010)

Brown (2008) presented the results of experiments from two laboratory wheel tracking devices, producing a lower bound theory for the shakedown limits based on the Mohr-Coulomb criterion and comparing the predictions of the analytical model with the experimental data.

Siripun, Jitsangiam, and Nikraz (2010) investigated the behaviour of crushed rock base UGM used in WA flexible pavement and derived a shakedown equation for this type of material. In this study, an exponential relationship was suggested between accumulated plastic strain and number of cycles divided by 1000 (see Figure 2.9).

One of the most recent studies is the work of Cerni et al. (2012), where the shakedown properties of granular mixture were investigated and a new equation was presented where the plastic strain rate (variation of plastic strain to time) was also considered in the formula.

These equations resulting from experimentation can form the basis of a constitutive model which accounts for the particular type of elastoplasticity known as shakedown behaviour. The resulting constitutive model then can be implemented in a numerical analysis to simulate an overall complex behaviour of UGM under cyclic loading. Such a procedure has been conducted in this research.

### **2.3.3 Numerical Models**

Advancements in computer technology have increased the interest of pavement researchers in the numerical modelling of physical problems. These types of models can be easily made and adjusted to address various problems.

This section presents a general review of the numerical modelling of flexible pavement. The numerical modelling can be investigated from various aspects, including the type of analysis, which can be static or dynamic, from the

geometrical characteristics of the model including the model dimensions (axisymmetric, plane-strain or three dimensional), and finally from the techniques it employs to solve the problem.

As well as FEM, there have been other approaches used to simulate pavement structure. These approaches include generalized finite element, discrete element methods and artificial intelligence (Chen, Pan and Huang 2011; Liu, You and Zhao 2012; Mashrei, Seracino and Rahman 2013; Saltan and Sezgin 2007; Ozer, Al-Qadi and Duarte 2011).

Section 2.4 of this chapter makes a complete review of the application of FEM in the simulation of pavement layers. Some of the major publications investigating approaches other than FEM are reviewed in this section.

Ozer, Al-Qadi, and Duarte (2011) used the generalized finite element method (GFEM) to investigate near-surface cracking. GFEM has the potential to provide computational capacity for crack modelling in the same frame as FEM. In GFEM an enrichment function is used to provide more capacity for the shape-function of elements. Figure 2.10 illustrates the concept of this enriched shape function.

The enrichment function strengthens the ordinary shape function of FEM with the capacity to estimate displacement on irregularities. These irregularities may be discontinuous points, kink points or singular points. Although the GFEM provides the FEM with the capacity to simulate cracks, a disadvantage is the increase in computation costs. It is difficult to integrate this method with FEM in dynamic loading due to the interaction between surfaces.

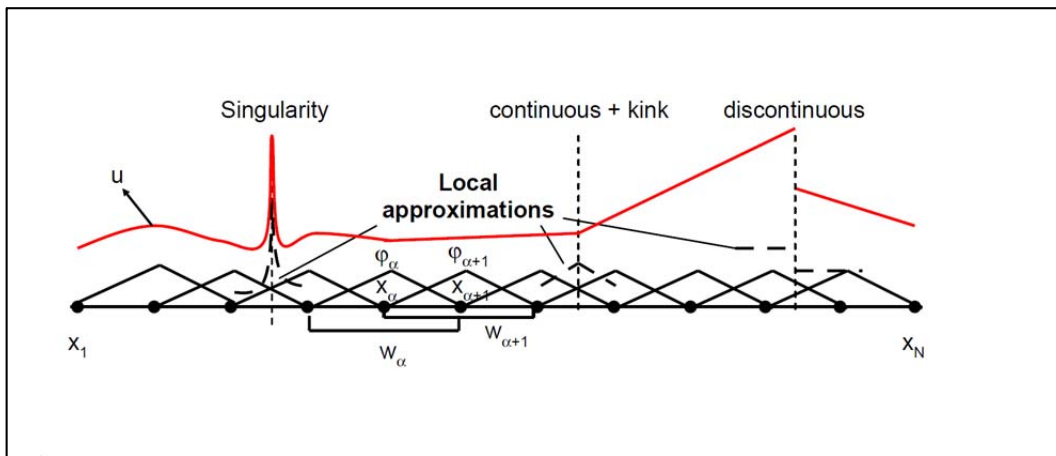


Figure 2.10 – GFEM Concept (from Figure 1 Ozer, Al-Qadi and Duarte 2011)

Saltan and Sezgin (2007) tried to combine the neural network concept and FEM. In this study, an artificial neural network (ANN) was employed to model the behaviour of UGM used for subbase. The ANN was trained through experimental data, and the FEM was then applied as a back calculation tool.

Figure 2.11 illustrates the concept of an ANN. In this concept, a solver consisting of several nodes in different layers is trained through the available pack of data. The data pack is fed to the input nodes. ANN tries to predict the outputs and these outputs are then checked with the available actual outputs. The weight of the layers is then modified accordingly. The process is repeated until the ANN achieves sufficient accuracy.

The predicted values then can be combined in a FEM which can back calculate the data. Such a method has the advantage of linking to an experimental package and therefore a greater possibility of validation. However, if a complex analysis (such as dynamic analysis) is considered, the provision of experimental data may present difficulties.

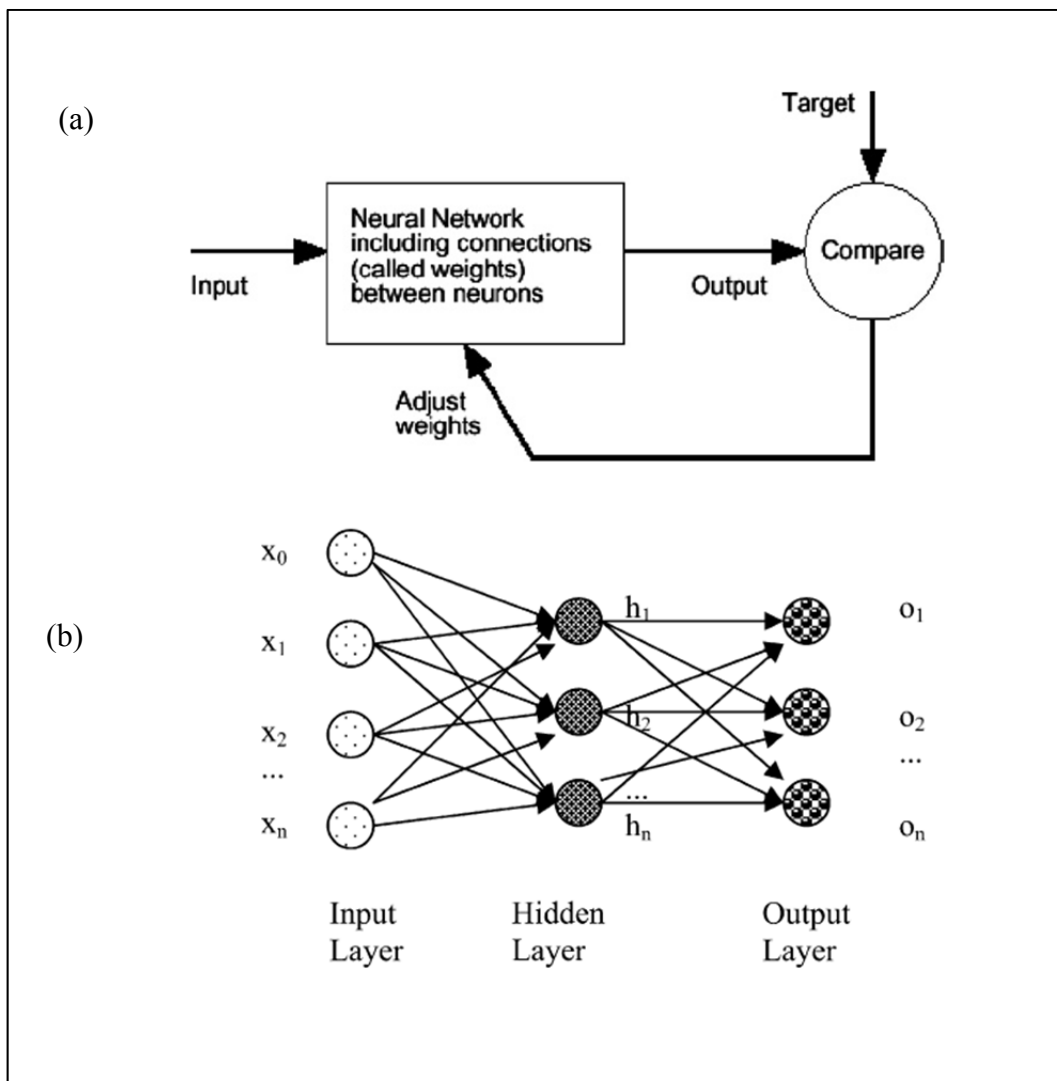


Figure 2.11 - ANN Solver Concept (a) and ANN Layers (b) (from Figures 2 and 3  
Saltan and Sezgin 2007)

Another numerical approach which is used mostly to cover the cracks and discontinuity in pavement layers is called the discrete element method (DEM). In this method, element size is decreased to the grains or particle size, and the interaction between particles is modelled through spring, dashpot-spring

(Figure 2.6), slider or a combination of these. Figure 2.12 illustrates the concept of DEM.

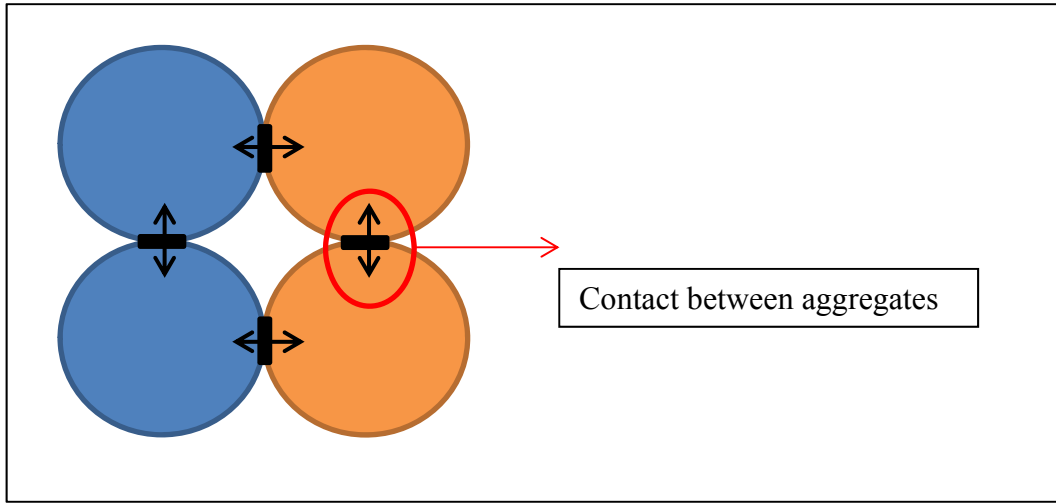


Figure 2.12- DEM Concept

DEM was used to simulate asphalt aggregates and their interaction (Liu, You and Zhao 2012). In this research, four numerical samples were modelled through DEM, and then the effect of element size was examined. The researchers concluded that the effect of element size on the simulation of creep stiffness for asphalt concrete (AC) is insignificant, but the calculation of permanent deformation and cracks needs a fine element size.

Chazallon, Koval, and Mouhoubi (2011) applied DEM to a model shakedown concept in granular layers of flexible pavement structure. The shakedown limit was solved according to the Zarka method (Zarka and Casier 1979) and two yield surfaces (von Mises and Drucker-Prager) were employed and compared with each

other. Figure 2.13 presents the DEM model made in this research. The researchers concluded that DEM was capable of predicting the plastic hardening behaviour of UGM. However, the expansion of DEM to three dimensions induced critical problems, among which was the long computation time and the complicated formulation.

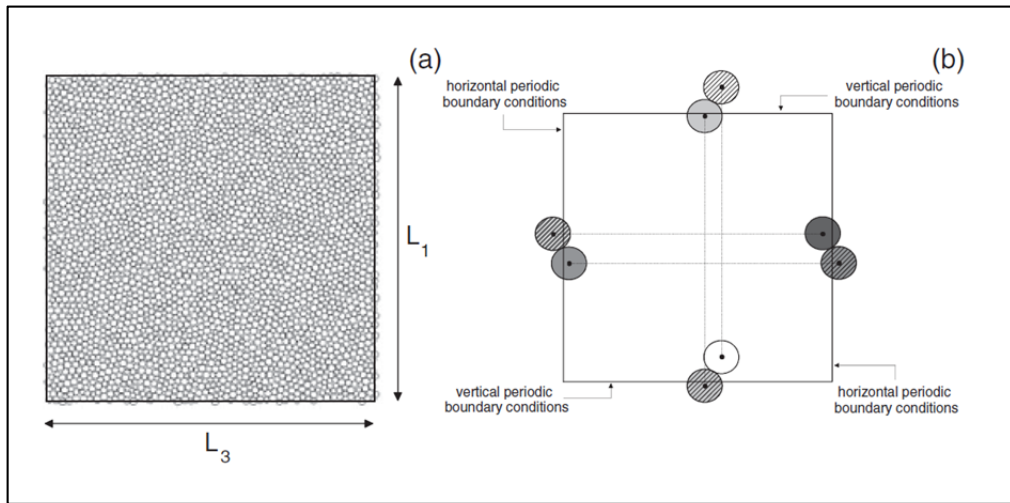


Figure 2.13 - DEM Model to Simulate Shakedown of UGM (from Figure 5 Chazallon et al. 2011)

All of the abovementioned methods are either based on FEM or work in close conjunction with FEM. FEM simulation is one of the most accepted methods for numerical simulation because it provides the ability for complex analysis (such as a dynamically interactive layered system) along with complex material properties

(such as shakedown behaviour). Therefore, FEM was selected as the main approach to achieve the objectives of this research. The next section presents an in-depth review of the numerical simulation of layered flexible pavement using FEM.

## **2.4 Application of Finite Element Method in Numerical Modelling of Flexible Pavement System**

FEM is a new engineering method based on computer technology to solve complicated problems in engineering. Mathematically, it is a numerical approach to finding estimated solutions to a set of differential equations with defined boundary values. FEM employs variational calculus procedures to minimize a defined error function. In this approach, a medium of physical problem is discretized to a smaller domain (called an element) and the partial differential equation (such as an equilibrium equation) is solved in each of these elements. The connectivity of the elements should satisfy certain conditions (usually continuity) and the solution should be compatible with defined loading and boundary conditions. Having solved the problem in the element, a general solution for the whole domain may be predicted.

In pavement engineering, FEM has recently been used on a large scale to simulate pavement structure. This section reviews the application of FEM to the simulation of flexible pavement.

#### **2.4.1 Numerical Simulation of Layered Flexible Pavement System**

Section 2.3.1 provided a review of the initial ideas on calculating the response of layered materials assuming linear elasticity. A numerical simulation was developed based on analytical solutions. The analytical solutions (Boussinesq 1885; Burmister 1945) were used as a basis for different pavement software. One of these programs was BISIAR (De Jong, Peatz and Korswagen 1973). According to Kim (2007), this program was developed by Shell researchers to predict the behaviour of layered systems assuming linear elasticity. It employs Burmister's theory and is capable of solving multi-axle loading.

In 1977, CIRCLY (Wardle 1977) was introduced for use in pavement design. This program applies linear elastic theory for a layered semi-infinite half-space. CIRCLY assumes that the stress-strain curve is linear elastic and the modelled medium is limitless in a horizontal direction. The vertical dimension is restricted by a horizontal stress-free surface at the top and an infinite depth in the downward direction. The software is capable of accounting for the anisotropy of UGM. This is implemented through the capacity to define a half elastic modulus in the

horizontal direction. However, the ratio of anisotropy is constant to 0.5 and cannot be modified and the Poisson ratio in all directions is the same. Tyre pressure is modelled as a uniform distributed load on a circular contact surface. Since the materials are assumed to behave linear elastically, the superposition principle is valid in all steps of the analysis.

According to Bodhinayake (2008), the software was first developed for use as a geomechanical tool in the Division of Applied Geomechanics at the Commonwealth Scientific and Industrial Research Organization (CSIRO) in Australia. Later, in 1987, the National Association of Australian State Road Authorities (NAASRA) integrated CIRCLY into the ‘Guide to Structural Design of Pavements’. Part 2 of the Austroads (formerly NAASRA) design code called ‘Guide to Structural Design of Pavements’ was developed in 1992 and 2004 based on the same idea. The platform of CIRCLY 5.0 (recent version) is FORTRAN IV.

Another software widely used by pavement engineers is KENLAYER (Huang 1993, 2004). KENLAYER works under the same assumptions as CIRCLY and the linear elastic theory is used to calculate pavement responses in different layers. KENLAYER cannot model anisotropy, but there is a possibility to model nonlinearity through iterative calculation.

These linear elastic-based programs provide the grounds for comparison for pavement researchers. It is widely accepted among finite element modellers that the model can be evaluated assuming linear elastic material with the results from the abovementioned programs. In this way, the effect of mesh size on the results can be estimated. There is also an opportunity to compare the results of different material behaviour to linear elastic behaviour and study the effect of this behaviour on the final design of the layers.

Hadi and Symons (1996) used the same approach to study the number of allowable repetitions on a sample layered flexible pavement. In this study, the upper layer material was modelled as an isotropic material, while the under layer material used for the subgrade was modelled as orthotropic. MSC/NASTRAN and STRAND programs were used for the FEM model and the results of simulation were compared with CIRCLY. The allowable number of repetitions then was evaluated based on the guide provided by Austroads. It was concluded that the number of allowable repetitions calculated using CIRCLY was lower than from the FEM model.

Another interesting comparison of this kind of simulation was presented by Ullidtz (2002). This investigation compared the field data measurement and calculated responses of different pavement programs: BISAR, CAPA3D,

CIRCLY, KENLAYER, MICHPAVE, NOAH, SYSTUS and VEROAD. The field data was obtained from full scale pavement projects by CEDEX in Spain, DTU in Denmark and LAVOC in Switzerland. The study concluded that accuracy of prediction of linear elastic theory from behaviour of UGM in pavement is an important question.

Wardle, Youdale, and Rodway (2003) reviewed mechanistic pavement design, using CIRCLY to evaluate the vertical strain in sample layered pavement under four and 20 ton wheels. A method was introduced for a more accurate estimation of the response of UGM layers. In this method, the UGM layer should be divided into sublayers, which can simulate the nonlinearity of UGM.

Tutumluer, Little, and Kim (2003) studied the cross anisotropic properties of materials, using the finite element program GT-PAVE and linear elastic program CIRCLY for modelling purposes. In later studies (Kim and Tutumluer 2006; Kim, Tutumluer and Kwon 2009), KENLAYER and CIRCLY were used to evaluate the results of a linear elastic FEM model constructed in ABAQUS.

KENLAYER and HDM-4 programs were compared in a study by Gedafa (2006). The programs were used to predict flexible pavement performance, and according

to the results, KENLAYER was the best for performance analysis, while HDM-4 was the most appropriate tool for strategic analysis.

Ghadimi, Asadi, et al. (2013) investigated the effects of geometrical parameters in the numerical modelling of flexible pavement systems. In the first step of this study, a sample layered flexible pavement was modelled through CIRCLY, KENLAYER and ABAQUS (Dassault Systemes Simulia Corp. 2010). Then the results were compared to reveal that the predicted results calculated from FEM (ABAQUS programs) showed a stiffer behaviour of the layered system, and the surface deflection calculated by CIRCLY and KENLAYER was greater than that calculated by FEM.

Ghadimi et al. (2013b) introduced a new method for calculating the nonlinearity of granular layers. The method was inspired by the work of Wardle (Wardle, Youdale and Rodway 2003); however, instead of dividing the layers into sublayers, in this study the analysis was divided into sub-stages, and in each stage of the analysis the materials were assumed to be linear elastic. In this study, the granular materials used for the base were assumed to behave according to Uzan (1985), and subgrade materials were modelled according to Thompson and Robnett (1979). The results of the analysis were then compared to the calculated results from CIRCLY and KENLAYER.

When modelling flexible pavement layers through FEM, the first subject is the geometrical dimension. So far, three types of geometry are considered for the purpose of FEM modelling: two-dimensional plane-strain, reduced three-dimensional axisymmetric, and full three-dimensional modelling. It is important to remember that the dimensions of the model have a huge impact, especially on the computation time. Considering elastic theory in a three-dimensional medium, the relationship between stress and strain is stated as follows in Equation 2-11 to Equation 2-13 (Yu 2006):

$$\varepsilon_{xx} = \frac{1}{E} [\sigma_{xx} - \nu(\sigma_{yy} + \sigma_{zz})] \quad \text{Equation 2-11}$$

$$\varepsilon_{yy} = \frac{1}{E} [\sigma_{yy} - \nu(\sigma_{xx} + \sigma_{zz})] \quad \text{Equation 2-12}$$

$$\varepsilon_{zz} = \frac{1}{E} [\sigma_{zz} - \nu(\sigma_{xx} + \sigma_{yy})] \quad \text{Equation 2-13}$$

where:

$\sigma$  = normal stress

$\varepsilon$  = normal strain

$E$  = elastic modulus of the materials.

$\nu$  = Poisson's ratio

The definitions of the abovementioned symbols are applicable for all equations in this dissertation unless otherwise indicated.

Although 3-D (three-dimensional) modelling is known to be the most inclusive simulation of an actual problem, there is a disadvantage in the huge amount of computation time required for this type of simulation. This results in modelling just a limited area close to tyre contact in 3-D. This causes another disadvantage when considering the real dimensions of a road. Actual road pavement has a large longitudinal dimension and width in comparison with the loading area of a single tyre. The part selected for simulation has to be confined by boundary conditions (roller, fixed etc.), and these boundary conditions may apply some extra restrictions, thus unintentionally affecting the results. Figure 2.14 illustrates a typical 3-D FEM mesh used for pavement simulation.

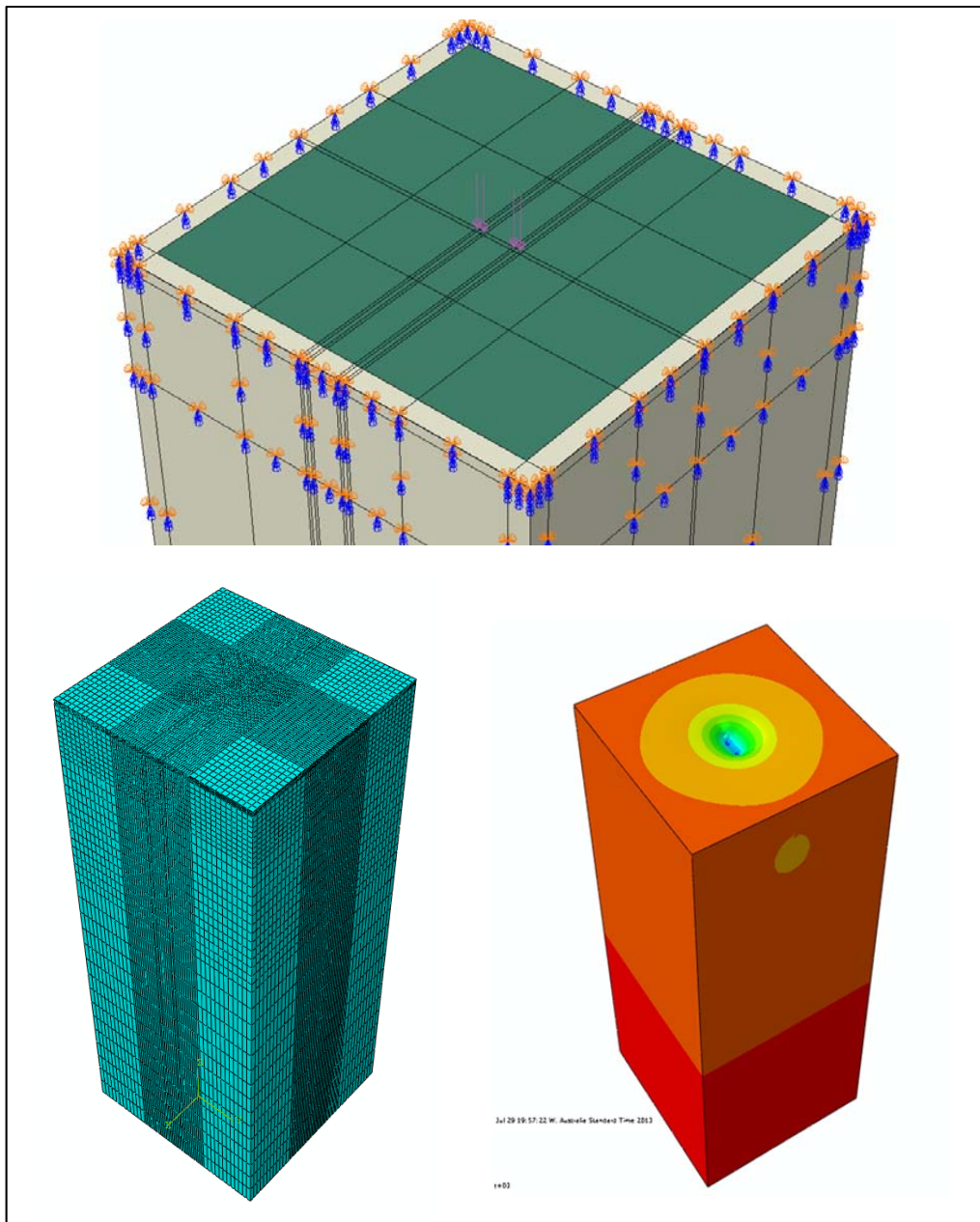


Figure 2.14 – Typical 3-D model of flexible pavement  
(from Figure 4 Ghadimi, Nikraz, and Leek (2013))

The geometrical conditions of a road can be modelled under the plane strain assumption which is a common simplification in geomechanics. In plane strain modelling, it is assumed that one of the strain components (say  $\varepsilon_{zz}$ ) is zero due to the long dimension of the model in that axis (i.e. z). This significantly reduces the complication of the system of equations for the modelled problem. However, the major restriction of this 2-D plane strain modelling is that the loading tyre is assumed to be a continuous strip pressure on the surface of the pavement, which is obviously not accurate where the true loading area is an elliptical area (Cho, McCullough and Weissmann 1996). The stress-strain relationship is indicated in Equation 2-14 to Equation 2-16 for the condition of plane strain (Yu 2006):

$$\sigma_{xx} = \frac{(1-\nu)E}{(1+\nu)(1-\nu^2)} \left( \varepsilon_{xx} + \frac{\nu}{1-\nu} \varepsilon_{yy} \right) \quad \text{Equation 2-14}$$

$$\sigma_{yy} = \frac{(1-\nu)E}{(1+\nu)(1-\nu^2)} \left( \varepsilon_{yy} + \frac{\nu}{1-\nu} \varepsilon_{xx} \right) \quad \text{Equation 2-15}$$

$$\sigma_{zz} = \frac{E}{(1+\nu)} \varepsilon_{xy} \quad \text{Equation 2-16}$$

The third typical geometry used for pavement simulation is known as the axisymmetric formulation. In the axisymmetric formulation, it is assumed that the model is symmetrical along a vertical axis in the cylindrical coordinates. An axisymmetric model simulates a 3-D model in a 2-D formulation. Equation 2-17 and 2-18 show the stress-strain relationship in the cylindrical coordinates.

$$\varepsilon_r = \frac{1}{E} (\sigma_r - \nu \sigma_z) \quad \text{Equation 2-17}$$

$$\varepsilon_z = \frac{1}{E} (\sigma_z - \nu \sigma_r) \quad \text{Equation 2-18}$$

The computational time consumption is in the same order as for a 2-D plane strain. The main disadvantage in the field of pavement modelling is that just one tyre can be modelled and the contact area should be circular. Therefore, the simulation of dual tyre or multiple axles is impossible in this formulation. Moreover, the interface shear, cracks and shoulder conditions are ignored (Cho, McCullough and Weissmann 1996).

One of the first major studies on the effect of the geometrical size of an FEM model for pavement simulation was conducted by Duncan, Monismith, and Wilson (1968). In this study, the range of boundary conditions for the axisymmetric problems was investigated. The material was assumed to be nonlinear. The researchers tried to find out the proper domain through comparison of the results of FEM with linear elastic layered solutions. It was concluded that a boundary condition as far as 12 times the loading radius in the horizontal and 18 times the loading radius in depth could provide acceptable results. However a 50-times R (loading radius) was recommended in order to achieve more accurate results.

The initial investigation of the effects of the dimensions of modelling was carried out by Cho, McCullough, and Wiseman (1996). They studied the effect of different geometrical parameters such as aspect ratio, size of element and model dimensions. Three types of 2-D plane strain, 2-D axisymmetric and a 3-D simulation were constructed and BISAR was used to obtain layered elastic results. It was revealed that the 3-D and axisymmetric FEM models yielded similar results and were capable of modelling traffic loading.

Myers, Roque, and Birgisson (2001) investigated the effects of the geometrical dimensions of FEM models in 3-D, axisymmetric and two-dimensional analysis. While it was found that a 3-D formulation could lead to more accurate results, the computation time was significantly increased. The researchers introduced a modification to the 2-D analysis which could enhance the accuracy of the results to an acceptable level.

Holanda et al. (2006) investigated a new proposed technique using objective-oriented programming. The technique was implemented in both axisymmetric and three-dimensional models. Comparing the results of the available analytical solution, the authors concluded that the location of the boundaries of the model had a significant effect on deformation. However, the problem vanished when sufficiently distant boundaries were selected.

A series of studies used the ABAQUS FEM program to construct axisymmetric and 3-D models (Kim 2007; Kim and Tutumluer 2006; Kim, Tutumluer and Kwon 2009). Different nonlinear models were implemented and the results were compared. The differences were noticeable according to their conclusion.

Ghadimi et al. (2013) investigated different models assuming plane strain, axisymmetric and 3-D formulations. The effect of each formulation on the results was reported and the results were compared with linear elastic programs CIRCLY and KENLAYER. According to their conclusions, the axisymmetric and 3-D models yielded an acceptable agreement with the analytical solution; however, the difference between the plane strain results was not within the accepted range.

Three major factors regarding the geometry of models are the formulation of the medium (2-D plane strain, 2-D axisymmetric or 3-D), the dimensions of the modelled area, and the mesh density. The abovementioned literature considers the problem of medium formulation. It is also important for a modeller to correctly select the dimensions of the model. The dimensions of modelled area can depend on the type of analysis (static or dynamic) and the focussed subject of the study (whether it is strains, stresses or deformation).

In a study carried out by Uddin and Pan (1995), a numerical simulation was carried out to model discontinuities and cracks in pavement. The model was constructed in a 3-D FEM formulation for a dynamic analysis and the results were checked against the results of falling weight deflectometer FWD. The pavement model assumed a block shape with the boundary conditions (BC) with rollers on the sides and fixed at the bottom. In this study, one axis of symmetry was assumed through the loading centre and therefore half of the actual experimental area was numerically modelled. The model had dimensions of 26.6 m in X direction, 9.15 m in Y direction and a thickness of 12.2 m for the subgrade layer at Z (depth), where the other layer thicknesses were added.

Another study by Mallela and George (1994) carried out a numerical simulation of FWD load on pavement. In this model, only a quarter of the actual experimental geometry was modelled. Since the FWD contact area on the pavement was assumed to be a circle, there could be two perpendicular axes of symmetry. Assuming X and Y as these two axes, the Z axis was the one towards the depth of the pavement. In this study, the dimensions were set to be 12.2 m in X and Y directions. Subgrade thickness was assumed to be 12.2 m and this was added to the thickness of other layers.

A number of studies (Kim 2007; Kim and Tutumluer 2006; Kim, Tutumluer and Kwon 2009) used the dimension of 20-R (loading radius) in the horizontal axisymmetric model and 140-R in the vertical direction (3 m x 21 m). Ghadimi, Nikraz, and Leek (2014) used 55-R (5 m) in the horizontal and 167-R (15 m) in the vertical direction in the axisymmetric model.

The values can be compared to the dimensions recommended by Duncan, Monismith, and Wilson (1968), where it is stated that 50-R in the vertical and 12-R in the horizontal direction is sufficient. It can be seen that the overall sizes used by recent studies (Cho, McCullough and Weissmann 1996; Ghadimi, Asadi, et al. 2013; Kim 2007; Kim and Tutumluer 2006; Kim, Tutumluer and Kwon 2009; Mallela and George 1994; Uddin and Pan 1995) are larger than those used in previous FEM simulations (Duncan, Monismith and Wilson 1968; Huang 1969; Harichandran, Yeh and Baladi 1990).

The large size of the models necessitates a larger number of elements and more computational capacity. Coarse mesh (large element size and less element numbers) leads to less accurate results and fine mesh (smaller element size and larger number of elements) leads to accuracy but at the cost of computational time. Here, the final geometrical aspects of a numerical model, which are mesh size and element type, have their effects.

Elements can be first order elements or second order elements. In the first order elements, liner interpolation is applied to estimate the values between Gauss points while in quadratic (second order) elements the interpolation has a higher polynomial order. Cho, McCullough, and Weissmann (1996) investigated the effect of interpolation order and indicated that the higher order element results in a more accurate outcome. However, the computation time for quadratic elements was also greater.

The effect of element interpolation was also investigated by Ghadimi, Asadi, et al. (2013), who proved that the computation time for higher order elements (eight-node axisymmetric elements or 20-node brick elements) was longer than for linear elements. However, to reach the same accuracy using linear elements necessitates finer mesh and a larger element number, which in turn increases the computation time. As a conclusion, using a higher order element is more efficient than a finer mesh of linear elements if the computation time is acceptable.

The ABAQUS program (Hibbit and Sorenson Inc. 2010), which was used in this research as the FEM software, provides a variety of elements for the modeller. This capability enables the simulation to be simultaneously accurate and time efficient.

## **2.4.2 Numerical Simulation of Granular Materials**

The behaviour of granular materials in relation to static and dynamic loading in a layered flexible pavement structure is one of the most challenging subjects in the field of pavement engineering. Difficulties arise due to the behaviour of UGM being dependent on various parameters including loading magnitude, environmental conditions, particle characteristics and loading cycles. The other essential difficulties come from the nature of FEM. The formulation of FEM is such that it should be able to model a ‘continuum’ medium, while this is not the exact case regarding UGM. The main problem is that UGM has little or no tension capacity and it will fail in tension quickly. Modelling this condition in a continuum domain where the elements are joined to each other may produce critical differences to what actually happens in the physical medium.

As described in section 2.3.3 researchers have tried to apply different numerical methods (e.g. DEM) to overcome the FEM problem regarding UGM. However, these methods have their own critical disadvantages in other aspects of modelling (see section 2.3.3).

Researchers in the field of pavement engineering have tried to develop new formulations for UGM in order to overcome the problem of the complex

behaviour of the materials. This section reviews the previous research and the current position of this process.

The first concept used to simulate UGM behaviour is linear elasticity, in which the stress-strain relationship is assumed to be according to Equation 2-11. This concept has been used by different researchers (Gedafa 2006; Ghadimi et al. 2013; Hadi and Symons 1996; Huang 1993; Ullidtz 2002). The concept has the advantage of simplicity in calculation and formulation; however, it cannot account for the stress-dependent and time-dependent behaviour of materials which may cause inaccuracy, especially if a dynamic analysis is necessary.

Linear elastic formulation is one of the most studied formulations and it is especially useful for the purposes of comparison. Such a comparison provides knowledge about the degree of difference between UGM and perfectly elastic materials.

Another aspect of UGM which should be mentioned here is the anisotropy of materials. UGM is known for its directional-dependent responses. This particular behaviour can be related to the microstructural features of the material. In the isotropic model, the response of materials is direction free and therefore the effect of the oriented behaviours of UGM is neglected (Sadd 2009).

The types of anisotropic behaviours are categorized according to the type of available symmetrical responses from the materials (Sadd 2009). One anisotropic behaviour usually associated with UGM is known as cross-anisotropic behaviour. This is a weak form of orthotropic anisotropy in which the material behaviour is not the same in two (three if complete orthotropic) perpendicular axes.

UGM is known to have stiffer behaviour in the direction of the applied load (Adu-Osei, Little and Lytton 2001; Rowshanzamir 1997; Seyhan and Tutumluer 2000). The effect of cross-anisotropy is considered in the linear elastic program CIRCLY (Wardle 1977), where the horizontal elastic modulus is assumed to be half of the vertical elastic modulus (direction of loading). This is also in accordance with the Austroads design method (AUSTROADS 2004).

Using an experimental and analytical method, Rowshanzamir (1997) investigated the anisotropic traits of UGM. Of the different experimental methods, the simplified approach of Graham-Houlsby was found to be the proper method for use in the determination of resilient moduli of UGM considering cross-anisotropy.

Adu-Osei, Little, and Lytton (2001) proposed a laboratory testing protocol based on elasticity to identify the mechanical anisotropic characteristics of UGM. The

cross-anisotropic properties of four different materials were determined, and these properties were then implemented in an FEM model, and it was reported that considering cross-anisotropy diminished the tension zone, which was induced if isotropic properties were assumed.

The effect of cross-anisotropy of UGM was also considered by Seyhan and Tutumluer (2000). In this study, advanced triaxial tests were performed to investigate the effect of stress-induced anisotropy in UGM. In this research, the modular ratio of UGM was picked to categorize the properness of UGM where the ‘good quality’ materials had a lower modular ratio.

As well as the directional behaviours of UGM, in the elastic range materials can be assumed to be linear elastic or nonlinear elastic. If in Equation 2-11 the value of E (elastic moduli) is assumed to be constant, then the stress-strain path would be a line with the inclination of E. In this case, the materials are known to behave linearly elastic. However, in UGM it is generally accepted that the modulus of materials depends on the state of induced stress. Therefore, the E is not a constant number and stress-strain forms a curve. A tangent line at any point on this curve is indicated by E (Figure 2.15).

Some of the major equations that researchers have developed for UGM based on experimental or analytical investigation are reviewed in section 2.3.2. Equation 2-5 to Equation 2-9 are those implemented in FEM simulations to represent the nonlinearity of UGM.

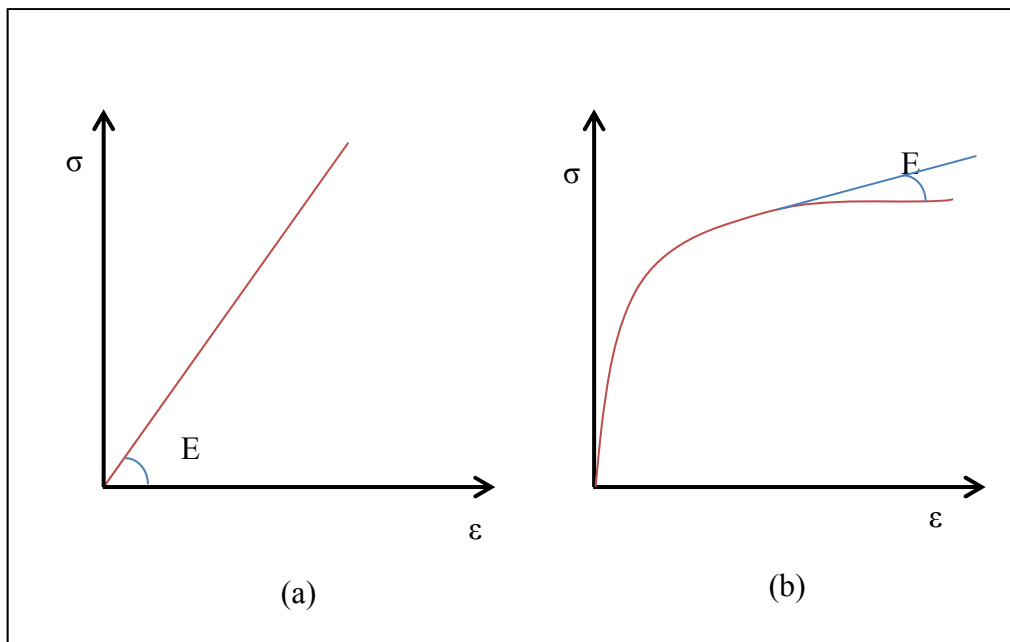


Figure 2.15 – Typical Stress-Strain Curve  
(a- Linear Elastic; b- Nonlinear Elastic)

From the initial attempts to consider this nonlinear behaviour, the work of Cho, McCullough, and Weissmann (1996) should be mentioned in which various aspects of the geometrical modelling of FEM and the nonlinearity of UGM are considered.

Helwany, Dyer, and Leidy (1998) have applied FEM to simulate different types of material behaviour used in pavement engineering. In this study they proved the usefulness of FEM in simulating a three layered pavement structure subjected to different types of assumed loading. Different axle load configurations and different magnitudes of tyre pressure ranging from 550 kPa to 830 kPa were examined in the FEM DACSAR program. Two different geometries (axisymmetric and 3-D) were used for the simulation. The material constitutive models used in the numerical simulation included linear elastic, nonlinear elastic and viscoelastic. The results of the linear elastic analysis were compared to the analytical solution provided by Boussinesq (1885). In nonlinear analysis they used a modified Duncan and Chang model (1970) where the strain-stress behaviour of the granular materials was assumed to be in a hyperbolic relationship, according to Equation 2-19:

$$E_t = E_i \left[ 1 - \frac{R_f(1 - \sin\varphi)(\sigma_1 - \sigma_3)}{2c \cos\varphi + 2\sigma_3 \sin\varphi} \right]^2 \quad \text{Equation 2-19}$$

Where:

$E$  = the elastic modulus in each increment

$R_f$  = material parameters

$c$  = soil cohesion (the entire of this dissertation unless otherwise is indicated)

$\varphi$  = internal friction of granular materials (in all of this dissertation unless otherwise is indicated)

The constitutive model of Duncan and Chang is further discussed in Chapter 3 of this dissertation. Finally in this research, the asphalt concrete layer (AC) was considered viscoelastic according to the shear modulus relaxation concept. The researchers finally concluded that the use of FEM in pavement design can be hugely efficient since it can save the cost of full scale modelling. It is suggested that for validation purposes, the primary response parameter be compared with the measured field data.

The study by Hjelmstad and Taciroglu (2000), which is mentioned in section 2.3.2, presented the resilient modulus for UGM as a function of the first and second invariants of the strain tensor rather than the stress tensor. This is especially useful for the implementation of this equation in ABAQUS software to account for material nonlinearity. A simulation was carried out for a numerically modelled triaxial sample and then the results were compared with the experimental data.

In a development of the previous work, Taciroglu and Hjelmstad (2002) presented a constitutive model for nonlinear elastic UGM in which the shear and normal properties of materials were in a stiffness matrix as a hyperelastic model. In this study, an analytical approach was employed to propose a new energy function density. This function was manipulated to generate a new stress-strain relationship for the granular materials.

Both of these studies tried to simulate the nonlinear behaviour of materials through strain tensors. Although this approach may have more numerical feasibility, the physical behaviour of UGM is stress dependent.

Fahey and Carter (1993) also used their experimentally developed nonlinear model in a FEM simulation. This model correlates the shear modulus of sand to produced shear stress. Here it should be noted that the dependency of the resilient modulus of UGM is more likely a function of confined pressure developed in the base layer.

The predicted behaviour of UGM through numerical simulation is dependent on the constitutive equation which is used. This has been confirmed by Gonzalez, Saleh, and Ali (2007), who conducted a series of simulations and field measurements to estimate the accuracy of nonlinear models in the prediction of

pavement responses. According to this research, nonlinear models were capable of estimating pavement responses. However, there was a difference among the responses calculated from the implementation of different models.

The proposed experimental model by Lee, Kim, and Kang (2009) was also applied in the FEM simulation. As indicated in section 2.3.2, this model included the stress path in the equation for the resilient modulus. This approach more comprehensively accounts for the behaviour of UGM, but it needs specific laboratory data providing different parameters to those used in this model. Such data may not be readily available for all types of UGM.

The research conducted by Araya et al (2011) and Araya et al. (2012) is reviewed from the experimental point of view in section 2.3.2. In these studies, the ABAQUS FEM simulation of triaxial samples was compared with the proposed experimental model for the prediction of resilient modulus.

A series of major studies investigated the implementation of different nonlinear models in FEM simulations of base and subgrade layers (Kim and Tutumluer 2006; Kim 2007; Kim, Tutumluer and Kwon 2009; Kim and Tutumluer 2010; Kim and Lee 2011). The 3-D Witczak and Uzan(1988) model was selected to represent the nonlinear modulus of the base, and the Thompson and Robnett

(1979) bilinear modulus was implemented for the subgrade. The simulation was carried out in axisymmetric and 3-D models. The result was then compared with the calculated results from linear elastic programs and in some cases significant differences were reported.

In a simulation carried out by Kim and Lee (2011) a 3-D ABAQUS model was constructed in which the Witczak and Uzan (1988) equation was used for the nonlinearity of the base and the Thompson and Robnett (1979) bilinear equation was used for the nonlinearity of the subgrade.

Among recent work, the study by Cortes, Shin, and Santamarina (2012) employed a nonlinear elastic model in the FEM analysis of an inverted pavement system.

In a study by Wang and Al-Qadi (2012), ABAQUS was employed in an FEM simulation to investigate the dynamic behaviour of anisotropic nonlinear UGM. Nonlinearity was modelled using the Uzan-Witzack equation and cross-anisotropic properties were used to simulate the anisotropy of UGM. The results were compared with data from field observations and linear elastic solutions.

Ghadimi et al. (2013b) introduced a simpler approach to include the nonlinearity of UGM in the numerical analysis. In this study, the same model that had been

analyzed by Kim and Tutumluer (2006) was used for the purpose of validating the results. In this new method, the stress dependency of UGM was modelled by defining several incremental linear steps. In each step, the stress was incorporated into the new resilient modulus. The difference between the results of the nonlinear and linear simulations was found to be as much as 33%.

Aside from the aspect of nonlinearity in the elastic domain, UGM shows plastic behaviour if sufficient load is applied. The magnitude of the load under which the UGM starts to behave elastically depends upon the constitutive model used.

Figure 2.16 illustrates the concept of elastoplasticity for UGM. Compared to Figure 2.15, it can be observed that the behaviour of elastoplastic materials is different when unloading is taken into account.

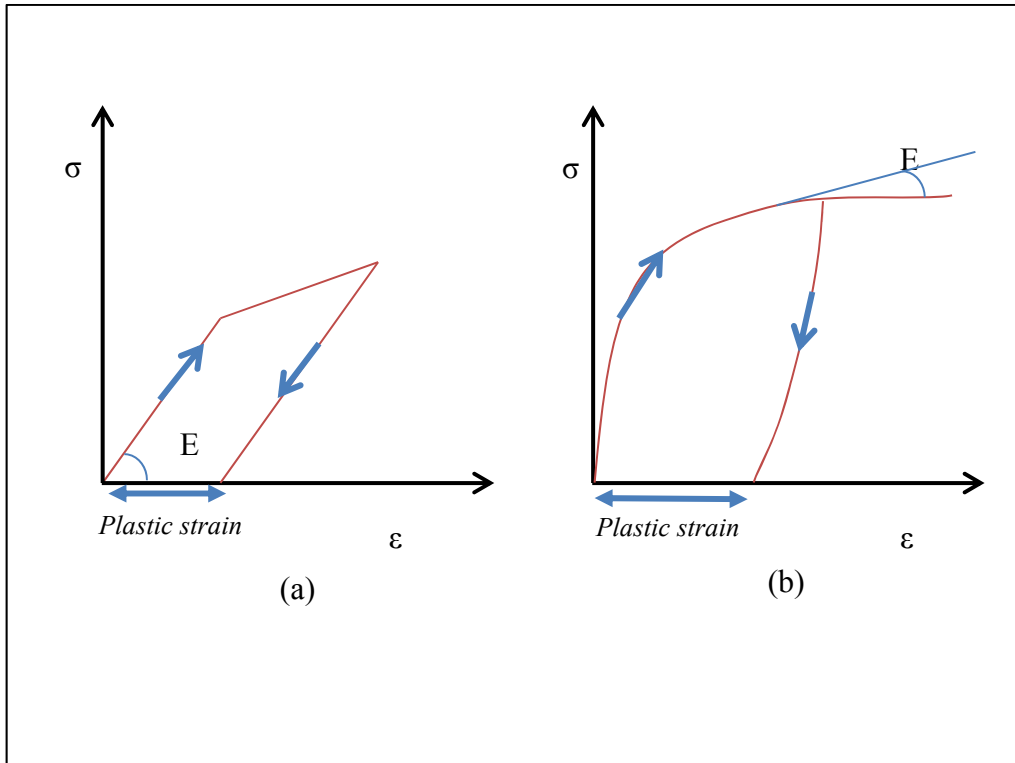


Figure 2.16 – Elastoplastic Stress-Strain Curve  
(a- Linear Elastoplastic b- Nonlinear Elastoplastic)

In the case of elastic materials (linear or nonlinear) there is no difference between the loading and unloading path and therefore there is no residual strain. However, in elastoplastic materials the loading path exceeds the plastic limit capacity of the materials and this induces a residual strain also known as plastic strain. Elastoplastic behaviour can be linear or nonlinear and the difference is about the behaviour of the stress-strain curvature during loading (Figure 2.16).

The plastic limit of materials is defined according to the constitutive model assumed for the behaviour of materials. Two constitutive models commonly used to simulate UGM behaviour in pavement engineering are the Drucker-Prager criterion and Mohr-Coulomb criterion (Yu 2006).

Equation 2-20 and Equation 2-21 indicate the mathematical representation of the plastic limit defined by the Mohr-Coulomb and Drucker-Prager criteria respectively, where  $I_1$  and  $J_2$  are the first and second invariants of stress tensors respectively. Chapter 3 gives a detailed description of these models.

$$\sigma_1 - \sigma_3 - (\sigma_1 + \sigma_3) \sin\varphi - 2c \cos\varphi = 0 \quad \text{Equation 2-20}$$

$$\sqrt{J_2} - \frac{2 \sin\varphi}{\sqrt{3} (3 - \sin\varphi)} I_1 - \frac{6c \cos\varphi}{\sqrt{3} (3 - \sin\varphi)} = 0 \quad \text{Equation 2-21}$$

In a significant study by Zaghloul and White (1993), the ABAQUS software was employed to dynamically analyze a layered flexible pavement. A 3-D dimensional model with 10.97 m (36 ft) in the transverse direction and 15.24 m (600 inches) in the longitudinal direction was constructed as illustrated in Figure 2.17.

In this simulation AC was modelled as viscoelastic materials. Viscoelasticity was considered through the shear modulus relaxation concept. The UGM used for the

base course was modelled according to the Drucker-Prager criterion and the material model for the subgrade (SG) layer according to the Cam-Clay model. The results were validated by data from the field. This study reported various effects including the effect of the deep foundation type, shoulder width, pavement-shoulder joint, asphalt mixture properties and loading speed. The researchers reported a high degree of confidence for the prediction capacity of dynamic FEM analysis when the proper material is used.

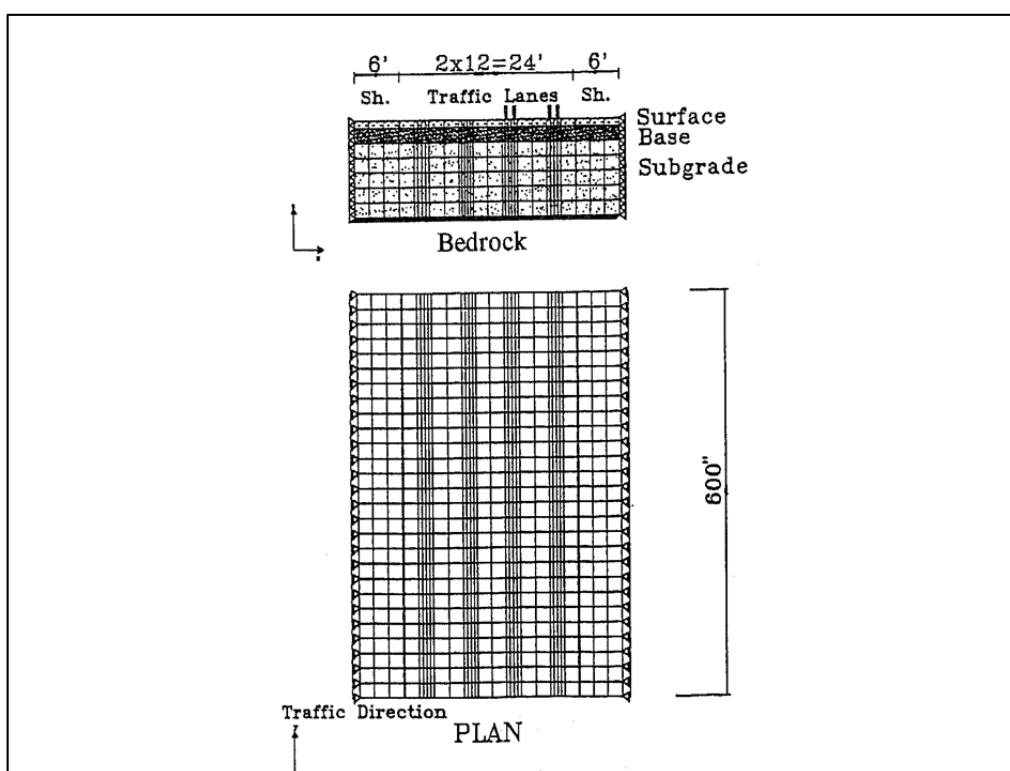


Figure 2.17 - FEM Mesh Used by Zaghloul and White  
(from Figure 1 Zaghloul and White 1993)

In 1994 Wolff. and Visser (1994) incorporated the Mohr-Coulomb plastic criterion to predict the UGM behaviour in pavement layers. The MICHPAVE program was used for the FEM simulation. In this simulation, the materials were modelled as nonlinear elastoplastic. Nonlinearity was defined by K- $\theta$  (Equation 2-5) and plastic criterion according to Mohr-Coulomb (Equation 2-20). The research proved that the nonlinear elastoplastic behaviour of materials was a significant characteristic of UGM which cannot be neglected. The researchers then used nonlinear elastoplastic behaviour to predict the behaviour of materials in cyclic repeated loading and a predictive formula was reported.

Shen and Kirkner (2001) studied the effect of the elastoplastic behaviour of UGM on rutting performance of flexible pavement structures. In this study, an iterative method using an infinite element was employed to study the residual displacement and minimize the effect of boundary conditions. The linear elastoplasticity was considered using the Drucker-Prager (Equation 2-21) model. The researchers concluded that the new method could more accurately predict the residual displacement of flexible layered pavement.

Ling and Liu (2003) observed the behaviour of reinforced AC under two-dimensional plane strain conditions where a monotonic load was applied. The

FEM model was constructed in the PLAXIS program where UGM was assumed to behave elastoplastically according to the Mohr-Coulomb criterion (Equation 2-20). The reinforcement was assumed to behave linear elastically. The results of the simulation were then compared to laboratory model tests. The implementation of the associated and non-associated flow rule was investigated with a minor difference between the results being reported.

The Drucker-Prager model was also employed to investigate the failure mechanism under moving loads of aircraft (Sukumaran, Willis and Chamala 2004). In this simulation, the ABAQUS FEM program was used to construct a 3-D model of airport pavement. The results were then verified against field data from the National Airport Pavement Test Facility (NAPTF) at the Federal Aviation Administration based in Atlantic City. The mesh distribution and model dimensions were then investigated to recommend a time efficient dimension for the model.

Saad, Mitri, and Poorooshashb (2005) tried to predict pavement design criteria by using FEM simulation. The strain at the bottom of the AC layer was selected as the fatigue criterion and the strain at the top of the SG was selected as the rutting criterion. The elastoplasticity of materials was modelled by Drucker-Prager (Equation 2-21) and a 3-D dynamic analysis was conducted using ADINA

software. In this simulation the UGM was considered to be cross-anisotropic in the linear elastic domain. It was concluded that the effect of cross anisotropy on the prediction of rutting was more significant than its effect on fatigue. Another major outcome was the much larger (by as much as five times) rutting depth prediction when an elastoplastic model was implemented in the base and SG.

Howard and Warren (2009) applied the Mohr-Coulomb criterion (Equation 2-20) to a FEM simulation of sample pavement. The results of the simulation were compared to data from the field. In this simulation, an axisymmetric model was constructed and the materials were assumed to be nonlinear elastoplastic. The nonlinearity of materials in the elastic domain was according to the Duncan-Change model (Equation 2-19) and the result was an acceptable agreement between the results of the numerical model and the field data.

Ghadimi, Nikraz, and Leek (2013) investigated the effect of AC thickness on the results of an elastoplastic dynamic simulation of a flexible pavement system. The elastoplasticity was modelled according to the Mohr-Coulomb criterion (Equation 2-20 and Equation 2-21) and the model was constructed in 3-D. It was found that the mechanical response of the layered system shifted when the thickness of asphalt was increased from 2 cm to 10 cm. In a very thin AC layer,

the failure tended to punch through the AC layer, while in a thicker AC layer the failure was more likely to be due to induced plastic strain in the UGM layers.

The nonlinearity and elastoplasticity of UGM used in pavement layers as reviewed so far are two major characteristics of UGM which cannot be analyzed through linear elasticity. However, there is one more significant aspect of UGM, which is the variation in its properties due to the application of loading cycles.

There are different approaches to modelling such a behaviour (Desai 2007; Desai and Whitenack 2001), and an interesting one is the use of the shakedown theory to model this specific type of response.

The concept of shakedown is explained in section 2.3.2. The theory of shakedown was introduced by Melan (1938) and is used to study the elastoplastic behaviour of structures under cyclic loading. Zarka and Casier (1979) used this theory in their study of fatigue failure of metals under cyclic loading (mechanical or thermal loading). As mentioned in section 2.3.2, the first application of shakedown theory in pavement engineering was by Sharp and Booker (1984) where they studied the effect of cyclic loading on UGM and tried to express the concept based on results of the AASHTO test.

Chapter 3 will contain the mathematical formulation and a detailed description of the theory. This section reviews the scientific efforts to apply the shakedown theory in the FEM modelling of UGM used in flexible pavement layers.

A study by Yu and Hossain (1998) presented a linear programming to solve the shakedown limit from the lower bound. In this study, a discontinuous stress field was manipulated into the FEM analysis. It was assumed that the residual stress was linearly distributed among three nodes of triangular elements in a way that the equilibrium of forces was satisfied. The formulation was presented in a 2-D medium. This formulation was then used to find out the shakedown limit for a plane strain modelling of flexible pavement layers.

Werkmeister, Dawson, and Wellner (2004) tried to include the shakedown concept in a FEM analysis of flexible pavement layers. Their research conducted a series of triaxial tests on crushed rock aggregate and equations relating permanent deformation to cycle number were developed. These tests were performed at different stress levels. After estimating the shakedown limit, the equations were implemented in an axisymmetric FEM analysis and the results were then compared with an empirical German design method.

Habiballah and Chazallon (2005) explored a lower bound solution integrating the Drucker-Prager criterion into shakedown theory. The study was based on the Zarka approach (Zarka and Casier 1979) and presented a method that could be implemented in an FEM simulation. According to the Zarka method, the shakedown limit can be evaluated through the stress conditions at a static elastic domain. Having the shakedown state in hand, a series of repeated triaxial loading was conducted to indicate the residual strain as a function of loading cycles. This function was then applied in the constitutive model to represent the shakedown behaviour of the materials.

Chazallon, Hornych, and Mouhoubi (2006) presented an elastoplastic model involving isotropic conditions and kinematic hardening. The modified Boyce model (Boyce, Brown and Pell 1976) was employed to represent sand behaviour in which the influence of void ratio and mean stress were taken into account. An FEM simulation then was carried out in which the triaxial samples were modelled and the results of the simulation based on the developed constitutive model were validated against the experimental data.

A nonlinear programming method to calculate the kinematic shakedown limit for materials with frictional behaviour was investigated by Li and Yu (2006). This analysis included frictional yield function in general form. Nonlinear

programming was used to find out the minimum so-called multiplier in which shakedown inequality was satisfied. FEM was manipulated to enforce the boundary conditions for a specific problem and calculate the rate of displacement used in plastic dissipation power. The proposed method was then used to calculate the shakedown limit of a plane strain model of flexible pavement layers subjected to a rolling load.

Allou, Chazallon, and Hornych (2007) implemented the constitutive model developed by Habiballah and Chazallon (2005) to conduct FEM analysis of a low volume traffic road. The Drucker-Prager based model was used to describe the shakedown behaviour of the materials. The elastic behaviour of granular material was assumed to be nonlinear according to the K- $\theta$  model stated in Equation 2-5. The results of the simulation were firstly verified against the triaxial test and the rut depth predicted by the analysis was then compared to measured field values. This simulation was carried out using CAST3M FEM software. Both axisymmetric and 3-D simulations were carried out, but the effect of dynamic loading was ignored. The equation relating the permanent strain to the number of cycles driven from the laboratory was integrated in the constitutive model to represent the behaviour of UGM at different times.

Later in 2009, Chazallon et al. (2009) integrated the previous studies (Allou, Chazallon and Hornych 2007; Chazallon, Hornych and Mouhoubi 2006) to conduct a FEM simulation considering the Boyce model (Boyce, Brown and Pell 1976) into the shakedown analysis of UGM used in flexible pavement layers. Different types of materials were selected for experimental data and the model parameters included frictional parameter, cohesion, nonlinear elastic parameter and shakedown plastic strain function. The FEM simulation was carried out for a quarter of the loading under tyre and the rut depth results were compared to the measured results of the LCPC facility.

Quite similarly to the concept of pavement engineering, Francois et al. (2010) studied the effect of accumulation of permanent deformation in soils due to repeated loading of small amplitude. In this study the effect of increased traffic loading on the settlement of soil under a constructed structure was investigated. Triaxial tests were carried out to identify the shakedown behaviour of soil and the equation was applied in a 3-D FEM analysis.

As can be observed from the literature reviewed in this section, there are three important parts to consider with regard to the behaviour of UGM used in pavement layers. First of all, a proper model should be selected to represent the elastic behaviour of these materials. The elastic behaviour is known to be

nonlinear stress dependent and there are different constitutive models representing this nonlinearity. Secondly, the plastic criterion has to be chosen, which in the case of UGM should be able to represent both the frictional and cohesive behaviour of these materials. Finally, the third important aspect of the model needs to take into account the change in material behaviour due to cycles of loading. One of the most interesting models presented here is the shakedown concept. In this research, the three abovementioned parts will be incorporated into a constitutive model to represent UGM behaviour.

The next section reviews the modelling of loads and boundary conditions in different types of FEM simulations of flexible pavement.

#### **2.4.3 Numerical Simulation of Load**

The final aspect of modelling reviewed in this dissertation is the loading and boundary conditions in flexible pavement simulation. Three major aspects are involved in simulating loads and boundary conditions. Firstly, the loading can be modelled dynamically or statically. Static loading can lead to a more simple analysis, therefore reducing computation time, however, pavement loading is by nature dynamic. The second factor is the effect of the interaction between boundary conditions and layers. Layers can be assumed to be fully attached or the interaction between layers can be considered. The third important factor in

modelling is the tyre pressure on the asphalt surface. The geometry of the tyre print which is used to apply pressure along with the pressure distribution on the tyre can influence the modelling results.

A number of multilayer programs introduced for pavement engineering purposes use static loading conditions (Bmmister et al. (1943), including BISAR (De Jong, Peatz, and Korswagen 1973), CIRCLY (Wardle 1977) and KENLAYER. Static loading cannot take account of the time dependency of materials and inertial forces. The major advantage of static loading is simplicity and reduction in computation time. Static loading ignores the force induced by mass and material damping. This type of loading is especially beneficial for investigations into geometry or elastic materials, because the loading and unloading path is exactly the same for elastic materials.

Early studies by Duncan, Monismith, and Wilson (1968), Raad and Figueroa (1980) and Harichandran, Yeh, and Baladi (1990) applied static loading as a uniformly distributed pressure on AC surface.

Static loading has also been used by researchers to investigate other aspects of FEM (Cho, McCullough and Weissmann 1996; Holanda et al. 2006; Myers, Roque and Birgisson 2001).

When static loading is applied, the simulation results can be used in existing design codes, while dynamic loading leads to direct calculation of the deformation induced in pavement. Static loading is therefore still of interest of researchers (Kim 2007; Kim and Tutumluer 2006; Kim, Tutumluer and Kwon 2009; Kim, Lee and Little 1997; Tutumluer, Little and Kim 2003).

There are also studies that investigated the dynamic behaviour of materials but did not include dynamic analysis (Allou, Chazallon and Hornych 2007; Allou et al. 2009; Chazallon et al. 2009; Chazallon, Hornych and Mouhoubi 2006; Chazallon, Koval and Mouhoubi 2011; Habiballah and Chazallon 2005). These studies considered the change in material properties during the dynamic loading through experimentation, and then applied the results in a constitutive model. However, the effect of mass and damping force was not considered in the final analysis.

The first study to model dynamic loading in the ABAQUS FEM program was conducted by Zaghloul and White (1993). This research was reviewed in section 2.4.2 with regard to material modelling. Here the dynamic analysis in this

research is of interest. A moving load was modelled as uniformly distributed pressure varies as a trapezoidal shape in time. A function correlating the loading speed to loading cycle was then used and an analysis was conducted for different speeds. According to this study, increasing the speed of loading resulted in a decrease in surface deflection. Most interestingly, it was found that static loading led to more deflection than dynamic loading.

In a study conducted by Uddin and Pan (1995), FWD loads were modelled dynamically in an FEM simulation. This study also reported less deflection in the dynamically modelled load.

Desai and Whitenack (2001) carried out a dynamic analysis of layered flexible pavement, and this work was further developed by Desai (2007). These studies presented the new constitutive model known as the ‘distributed state concept’ to model the distress induced in pavement during dynamic loading. As mentioned in section 2.4.2, the effect of material changes due to cycles of loading was considered through the stored strain energy. In this concept, there is a reduced dissipation of energy in each cycle, leading to stiffer material behaviour in each subsequent cycle.

Saad, Mitri, and Poorooshasb (2005) have also reported results on a dynamic analysis of flexible pavement. The dynamic loading was assumed to be a triangular pulse in a 0.1 s period. The researchers explained that the results of surface deflection may be expected to be less than 50% of the value calculated from static loading. This was attributed to the absorption of energy introduced to the whole pavement system through the damping and mass inertia which are not present in the case of static loading.

Bodhinayake (Bodhinayake 2008) conducted a study on the nonlinear dynamic simulation of flexible pavement. In this study, the loading was assumed to be a triangular pulse according to Barksdale's recommendation (Barksdale 1971), and the results of the dynamic analysis were verified against previously published data.

Al-Qadi, Wang, and Tutumluer (2010) studied the effect of a thin AC layer on nonlinear anisotropic UGM layers. In this study, the nonlinearity of granular materials integrated with anisotropic properties. Coding in ABAQUS used for the simulation and three dimensional Uzan model employed.

Beskou and Theodorakopoulos (2011) made an inclusive review of the previous approaches to the simulation of dynamic loading, where the dynamic analysis was categorized according to representative models for AC foundations.

Ghadimi et al. (2013) conducted a dynamic analysis of flexible pavement layers with AC layers of different thicknesses. The study found that static loading resulted in a smaller amount of surface deflection.

In the abovementioned research, the interaction between soil and asphalt has not been completely addressed. In the field of pavement engineering there are few studies into the effect of the interaction between soil and asphalt.

One of the very first studies on this effect was conducted by Pan, Okada, and Atluri (1994). This research carried out a nonlinear analysis of moving loads. The effect of the soil-pavement interaction was taken into account using the coupled boundary element method (BEM) and FEM. They presented a convolution integral of the interactive force transferred between layers. The iterative method was then used to calculate the stress and strain in each step. In the coupled FEM-BEM analysis, pavement layers were modelled through the FEM formulation and the whole soil body was modelled through BEM. The dynamic elastic and dynamic elastoplastic solutions were then compared and the results discussed.

Two major conclusions were that the dynamic analysis resulted in less deflection (as described in studies mentioned earlier), and the elastic soil medium led to less deflection than the elastoplastic soil medium. Although the general method of calculating the effect was introduced in this paper, the method can easily be extended to consider different material behaviour including nonlinear elastoplasticity with shakedown.

Advancements in FEM software enable the modelling of layer interactions through the use of the interface element. Baek et al. (2010) used this capability to study the interaction effect in pavement layers composed of hot mix asphalt (HMA) laid over joint concrete pavement (JCP). In their study, the interface constitutive model was Mohr-Coulomb frictional behaviour. The main purpose of this study was to investigate crack development in asphalt and concrete layers and the effects of different interface parameters were studied with regard to the developed cracks. The soil was not modelled elastoplastically and the main focus was on the structural layers (HMA and JCP).

The same frictional behaviour of interface elements was used by Ozer et al. (2012) to study the effect of the interaction between soil and the AC layer. They used the ABAQUS program in a FEM simulation of dynamic loading. In this study, the AC layers lay on a Portland cement concrete (PCC) layer. The study

investigated the influence of the different properties of the interface elements on the strain induced in pavement layers, and reported a significant difference in the final results.

It is well-known that boundary conditions influence the results of FEM simulations. It should be mentioned that the effect of boundary conditions for static analysis is different from dynamic analysis. In static analysis, setting boundary conditions (BC) as rollers in the sides and encastré at the bottom can be accepted. If far enough from the loading area, the error produced can be negligible. Researchers have proposed different criteria for the BC and this is reviewed in section 2.4.1. In dynamic analysis, the rollers and encastré BCs may produce reflective waves which can induce another type of error (resonance phenomenon) which is not vanished easily by setting distant BC. One of the possible solutions for this problem is the use of infinite elements. This method has been used by researchers to avoid the effect of reflected waves on FEM simulations (Kouroussis, Verlinden and Conti 2009, 2010; Motamed et al. 2009; Pan and Selby 2002). This approach is especially used in railway simulations (Kouroussis, Verlinden and Conti 2009, 2010) and to simulate a soil body faced by vibrating or impact loads (Motamed et al. 2009; Pan and Selby 2002).

The final aspect of FEM regarding load simulation is the modelling approach to loading pressure and tyre contact area.

Barksdale (1971) investigated the dynamic loading of traffic on a layered pavement structure. This study investigated the form and duration of stresses in different layers. An axisymmetric FEM model using linear elastic material properties was then analyzed. Barksdale reported that the stress pulses near the surface of the pavement were close to half-sinusoidal form, and close to triangular form in the subgrade layer. The speed of the moving load was then related to the duration of stress pulses and the results were presented.

The idea of simulating of tyre loading on pavement through repeated periodic pressure is supported by researchers (Barksdale 1971; Elliott and Moavenzadeh 1971; Perloff and Moavenzadeh 1967). In FEM analysis, the pressure of a tyre is transferred to the pavement layers through distributed pressure on the contact area between the tyre and pavement. Several shapes can be assumed for this purpose. The first one is a circular area, which was frequently used by early researchers (Burmister et al. 1943; Duncan and Chang 1970; Harichandran, Yeh and Baladi 1990; Raad and Figueroa 1980; Shook et al. 1982; Wardle 1977). This is also the shape which is used in the Austroads (2004) code for flexible pavement design. Huang (Huang 1993, 2004) described a method to translate the circular shape of a

loading area into a rectangular shape. A rectangular shape has an advantage in 3-D FEM modelling because brick elements are used in mesh generation. Using a circular area in full 3-D modelling may cause some mesh generation difficulties especially when brick elements are used. Figure 2.18 shows the relationship between rectangular and circular shapes according to Huang (Huang 1993, 2004).

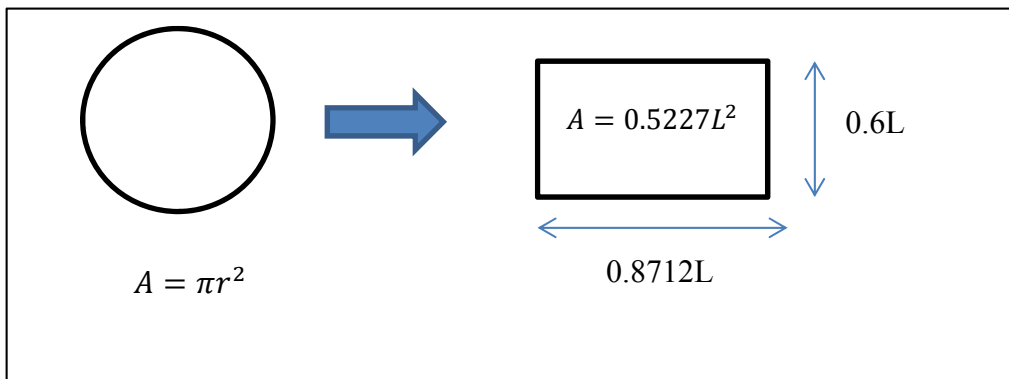


Figure 2.18-Translation of Contact Area

Al-Qadi et al. (2004) conducted a study on tyre pressure and the contact area in flexible pavement structure. In this investigation, a 3-D FEM model was constructed using the ABAQUS program. The results were verified against laboratory and field data. The anisotropic behaviour of the AC layer was found to have a significant effect on the results. In this study, the contact surface was modelled using rectangular strips with various distributed pressures.

The study by Fang et al. (2004) also modelled tyre loading using strips, with the pressure distribution being variable according to time.

An investigation conducted by Vale (2008) studied the effect of different loading assumptions on the FEM analysis of flexible pavement layers. The numerical simulation was carried out using the DIANA program. A rectangular contact area was assumed and two configurations of pressure were considered: time independent and various with time. It was found that time dependent pressure resulted in decreased deformation at points near to where the pressure was applied, in comparison with the results of a uniform distribution of load.

Hadi and Bodhinayake (2003) conducted a dynamic FEM analysis to investigate the effect of nonlinear properties of SG layers on the final results of a numerical simulation. A rectangular contact area was used in a 3-D FEM model constructed in ABAQUS. Both static loading and cyclic loading conditions were considered. Cyclic loading was assumed to be triangular periodic function under Barksdale's (1971) assumption. The study revealed that the nonlinear material assumption under cyclic loading yielded results that were closer to data measured in the field.

Ghadimi, Nikraz, and Leek (2013) modelled the tyre contact area as a rectangular shape with time dependent variation of distributed stress. The pressure variation

was a triangular periodic function according to Barksdale's (Barksdale 1971) assumption.

According to the abovementioned literature it can be concluded that a circular area can be used as a representative contact area if axisymmetric modelling is used, and in the case of 3-D FEM, a rectangular area can be without significant error.

## **2.5 Summary of Chapter**

This chapter presented a complete review of approaches to numerical modelling and its application in the field of flexible pavement design. Two major design methods were reviewed, one based on experience and experimental equations and the other based on mechanistic analysis. Current trends in the development of more accurate modelling in the mechanistic design of flexible pavement were also addressed.

Modelling as a scientific tool for mechanistic analysis is categorized into three major groups: analytical, experimental and numerical. These groups are not completely separate and they interact with each other. The analytical approach tries to develop mathematical differential equations governing the geometry of pavement structures; experimental modelling tries to produce equations

representing material behaviour, and numerical simulation integrates the developed experimental models into differential equations for the whole problem.

One of the widely used methods of numerical simulation is FEM, which is the approach selected for this dissertation. The application of this method in the analysis of flexible pavement layers was reviewed. Three major concerns with regard to modelling through FEM are the geometrical representation of the problem, simulation of the materials and simulation of dynamic loading.

The problem can be modelled plane-strain, axisymmetric or 3-D. The material modelling can be linear elastic, nonlinear elastic, nonlinear elastoplastic or more advanced material modelling to take into account the effect of shakedown behaviours. Finally, the simulation of the loading tyre can be static, dynamic or can consider the dynamic interaction between the soil and the AC layer.

Through the literature review, there is a gap for complete three dimensional modelling which consider nonlinear elastoplastic material behaviour under dynamic loading. Especially the effects of shakedown for granular materials and soil-asphalt interaction should be addressed.

The next chapter provides details on the FEM used in the simulation, along with the mathematical equations regarding constitutive models.

## **CHAPTER 3**

### **3: CONSTITUTIVE MODELS IN FINITE ELEMENT METHOD**

#### **3.1 Basics of the Finite Elements Method (FEM)**

Mechanical problems in the field of pavement engineering can be abstracted to a differential equation representing the governing equation of the medium. As explained in the previous chapter, this differential equation can then be solved through various analytical, experimental or numerical approaches. The purpose of this chapter is to shed light on one of the numerical methods (the finite element method, or FEM) which is used for the simulation of flexible pavement structure in this dissertation.

The finite element method (FEM) is a numerical method developed in mathematics to provide an approximate solution for a given differential equation (usually partial differential equations without a closed form solution), under specific boundary conditions (BC). This method employs a variational procedure (presented in calculus) to optimize a defined error function.

Clearly, FEM can be used in a wide range of physical or mathematical problems. The method is applied in the mechanical analysis of pavement layers to find out the stress/strain field of a given geometry under certain type of loading. To solve the problem it is necessary to define relationship connecting kinetic quantities to kinematic quantities. The relationship usually takes the form of a mathematical equation called the constitutive equation (or constitutive model).

There are certain types of constitutive models which have been widely used in pavement engineering. This chapter presents a description of these models.

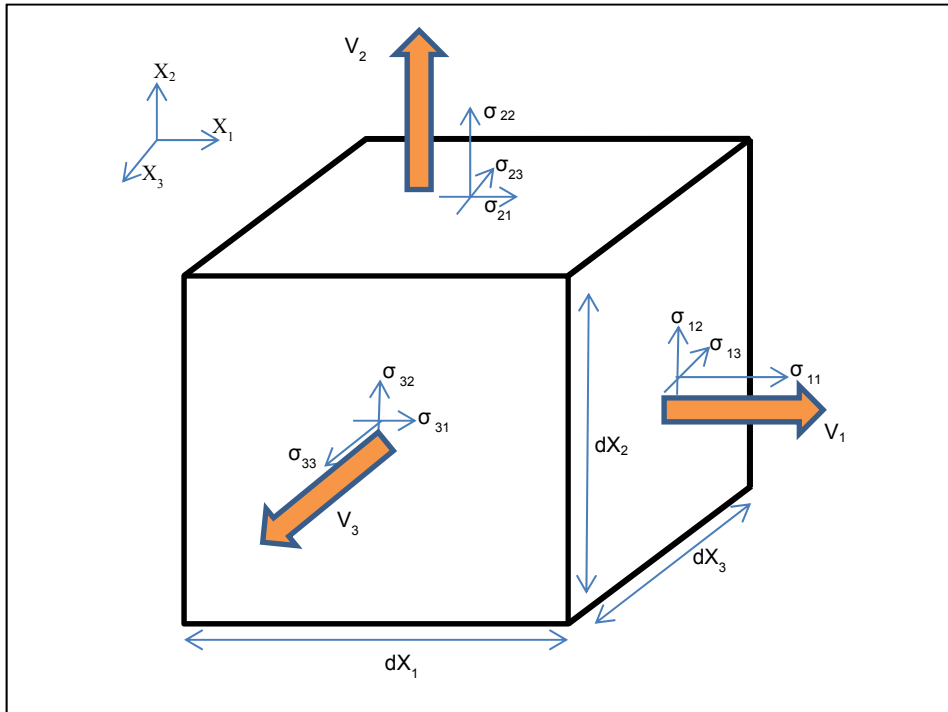


Figure 3.1 - Stresses on an Element

Figure 3.1 illustrates the stress components in a cubic element in a Cartesian coordination. In this figure,  $V_i$  ( $i = 1, 2$  and  $3$ ) are the volumetric forces acting on the cubic element.

For this element the equilibrium of the forces can be written as Equation 3-1. Dividing both sides of Equation 3-1 and expanding it for the other two dimensions ( $X_2$  and  $X_3$ ) leads to Equation 3-2, Equation 3-3 and Equation 3-4. Now considering the index notation and the presence of external force ( $F$ ) on the element, the general differential equation of the equilibrium state in a static condition can be written as Equation 3-5.

$$\begin{aligned}
\sum F_{X_1} = 0 \rightarrow & \left( \sigma_{11} + \frac{\partial \sigma_{11}}{\partial X_1} dX_1 \right) dX_2 dX_3 \\
& - \sigma_{11} dX_2 dX_3 \\
& + \left( \sigma_{21} + \frac{\partial \sigma_{21}}{\partial X_2} dX_2 \right) dX_1 dX_3 \\
& - \sigma_{21} dX_1 dX_3 \\
& + \left( \sigma_{31} + \frac{\partial \sigma_{31}}{\partial X_3} dX_3 \right) dX_1 dX_2 \\
& - \sigma_{31} dX_1 dX_2 - V_1 dX_1 dX_2 dX_3 = 0
\end{aligned} \tag{Equation 3-1}$$

$$\sum F_{X_1} = 0 \rightarrow \frac{\partial \sigma_{11}}{\partial X_1} + \frac{\partial \sigma_{21}}{\partial X_2} + \frac{\partial \sigma_{31}}{\partial X_3} + V_1 = 0 \tag{Equation 3-2}$$

$$\sum F_{X_2} = 0 \rightarrow \frac{\partial \sigma_{21}}{\partial X_1} + \frac{\partial \sigma_{22}}{\partial X_2} + \frac{\partial \sigma_{32}}{\partial X_3} + V_2 = 0 \tag{Equation 3-3}$$

$$\sum F_{X_3} = 0 \rightarrow \frac{\partial \sigma_{13}}{\partial X_1} + \frac{\partial \sigma_{23}}{\partial X_2} + \frac{\partial \sigma_{33}}{\partial X_3} + V_3 = 0 \tag{Equation 3-4}$$

$$\sigma_{ji,j} + V_i = F_i \text{ where } i, j = 1, 2 \text{ and } 3 \tag{Equation 3-5}$$

Other sets of equations can be derived from the geometrical relationship between strains and deformations. Assuming  $u$ ,  $v$  and  $w$  are the deformations in the direction of  $X_1$ ,  $X_2$  and  $X_3$  respectively, Equation 3-6 can present these relationships.

It can be seen that Equation 3-5 is the physical equation between stress derivatives and external forces. By contrast, Equation 3-6 to 3-11 represents the relationship between the derivatives of strains and deformations. To solve the

problem completely it is necessary to establish a relationship between the stress and strain tensor. This relationship is called a constitutive model.

$$\varepsilon_{11} = \frac{\partial u}{\partial X_1} \quad \text{Equation 3-6}$$

$$\varepsilon_{22} = \frac{\partial v}{\partial X_2} \quad \text{Equation 3-7}$$

$$\varepsilon_{33} = \frac{\partial w}{\partial X_3} \quad \text{Equation 3-8}$$

$$\varepsilon_{12} = \frac{1}{2} \left( \frac{\partial u}{\partial X_2} + \frac{\partial v}{\partial X_1} \right) \quad \text{Equation 3-9}$$

$$\varepsilon_{13} = \frac{1}{2} \left( \frac{\partial u}{\partial X_3} + \frac{\partial w}{\partial X_1} \right) \quad \text{Equation 3-10}$$

$$\varepsilon_{23} = \frac{1}{2} \left( \frac{\partial v}{\partial X_3} + \frac{\partial w}{\partial X_2} \right) \quad \text{Equation 3-11}$$

Employing the symmetric Cauchy stress tensor and the tensor notation, Equation 3-12 presents the general form of the constitutive model in relation to the six components of stress and strain.

$$\begin{pmatrix} \sigma_{11} \\ \sigma_{22} \\ \sigma_{33} \\ \sigma_{12} \\ \sigma_{23} \\ \sigma_{31} \end{pmatrix} = [C_{6 \times 6}] \begin{pmatrix} \varepsilon_{11} \\ \varepsilon_{22} \\ \varepsilon_{33} \\ \varepsilon_{12} \\ \varepsilon_{23} \\ \varepsilon_{31} \end{pmatrix} \quad \text{Equation 3-12}$$

In this equation, the components of tensor **C** indicate the constitutive model of material behaviour.

So far, the differential equation of equilibrium (Equation 3-5) has been translated into a system of algebraic equations for a given geometry and specific materials (Equation 3-12).

The finite element method uses the variational method to minimize the error function. Therefore, Equation 3-5 should be represented in an integral formation. To achieve this, the principle of virtual work will be applied to the equilibrium equation. After the mathematical steps, the final form of this equation can be written as follows:

$$\int_{V1}^{V2} (\sigma_{ij} \delta \varepsilon_{ij}) dV = \int_{S1}^{S2} (t_i \delta u_i) ds + \int_{V1}^{V2} (F_i \delta u_i) dV \quad \text{Equation 3-13}$$

In Equation 3-13, V is the volume of the total body of the element,  $t_i$  is the tractional force acting on the surface (S) of the element, and  $F_i$  are all external forces acting on the element volume.  $u_i$  represents the allowable deformation (identified by boundary conditions) in direction i. This integration representation of the equilibrium differential equation also is known as the *weak form*.

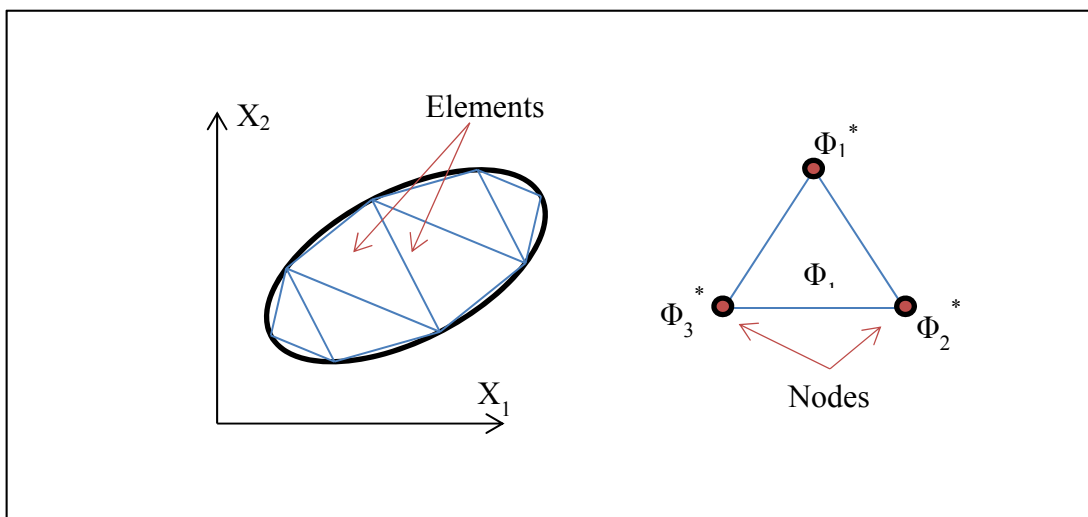


Figure 3.2- Discretization of Medium

To solve Equation 3-13, the whole continuum medium is discretized to *elements* as shown in Figure 3.2. The elements are connected to each other through *nodes*. The unknown values of the equations (such as deformations) are first calculated on the nodes then through interpolation techniques, and the unknown value is estimated on the whole element.

Referring to Figure 3.2, if the value of a requested unknown,  $\Phi$ , is known to be  $\Phi_1^*$  on node 1, then this value is calculated on any point inside the element through interpolation. Mathematically this can be represented as Equation 3-14.

$$\Phi = \sum_{i=1}^n N_i \Phi_i^* = N_1 \Phi_1^* + N_2 \Phi_2^* + \cdots + N_n \Phi_n^* \quad \text{Equation 3-14}$$

In this equation,  $n$  is total number of nodes and  $N_i$  is called the *shape function*. Shape functions define the contribution weight of the requested unknown from each node to a specific point inside the element.

If it is assumed that  $\Phi$  is deformation then Equation 3-15 can be written:

$$\{\varepsilon\} = [B]\{U^*\} \quad \text{Equation 3-15}$$

In this equation  $U^*$  are the deformations on the nodes and  $\varepsilon$  is the strain vector on any required point inside the element. The components of matrix B are the derivatives of shape function with respect to axes.

Referring to Equation 3-13 now we can write:

$$\int_{V1}^{V2} \langle \varepsilon^* \rangle \{\sigma\} dV = \langle U^* \rangle \{F\} \quad \text{Equation 3-16}$$

Equation 3-16 indicates the principle of the virtual work written for the nodes of the element. It states that the internal work of strain and stress on the whole volume of the element should be equal to the work of the external force acting on the element.

Applying Equation 3-12 and Equation 3-15 into Equation 3-16 gives the final form of the integral equation as follows:

$$\{F\} = \int_{V1}^{V2} [B]^T [C] [B] \{U\} dV + \int_{V1}^{V2} [B]^T \{\sigma_0\} dV - \int_{V1}^{V2} [B]^T [C] \{\epsilon_0\} dV \quad \text{Equation 3-17}$$

In this equation, the two terms of the integral which include  $\epsilon_0$  and  $\sigma_0$  respond to the initial strain and stress at the beginning step of the solution.

Based on Equation 3-17, two more nominations are taken into account in order to obtain a better understanding of the procedure so far:

$$\{R\} = \{F\} - \int_{V1}^{V2} [B]^T \{\sigma_0\} dV + \int_{V1}^{V2} [B]^T [C] \{\epsilon_0\} dV$$

$$[K] = \int_{V1}^{V2} [B]^T [C] [B] dV \quad \text{Equation 3-18}$$

In this nomination,  $\{R\}$  represents the vector of all forces acting on the elements. This includes forces, initial deformations, initial stresses and initial strains. By contrast,  $[K]$  is the stiffness matrix and numerically represents the resistance of the element against induced deformation. As can be seen from Equation 3-18, the stiffness of an element is a function of the material and geometrical properties of that element. It is worth mentioning here that while the material properties truly contribute to the stiffness of the element, the geometrical properties (represented

through derivatives of shape functions) produce additional stiffness which is not a part of the realistic behaviour of the materials. This is a source of in-built error in the FEM method. Given the theoretical background of FEM, a general solution for any FE problem should follow the procedure illustrated in Figure 3.3 (AASHTO 2002).

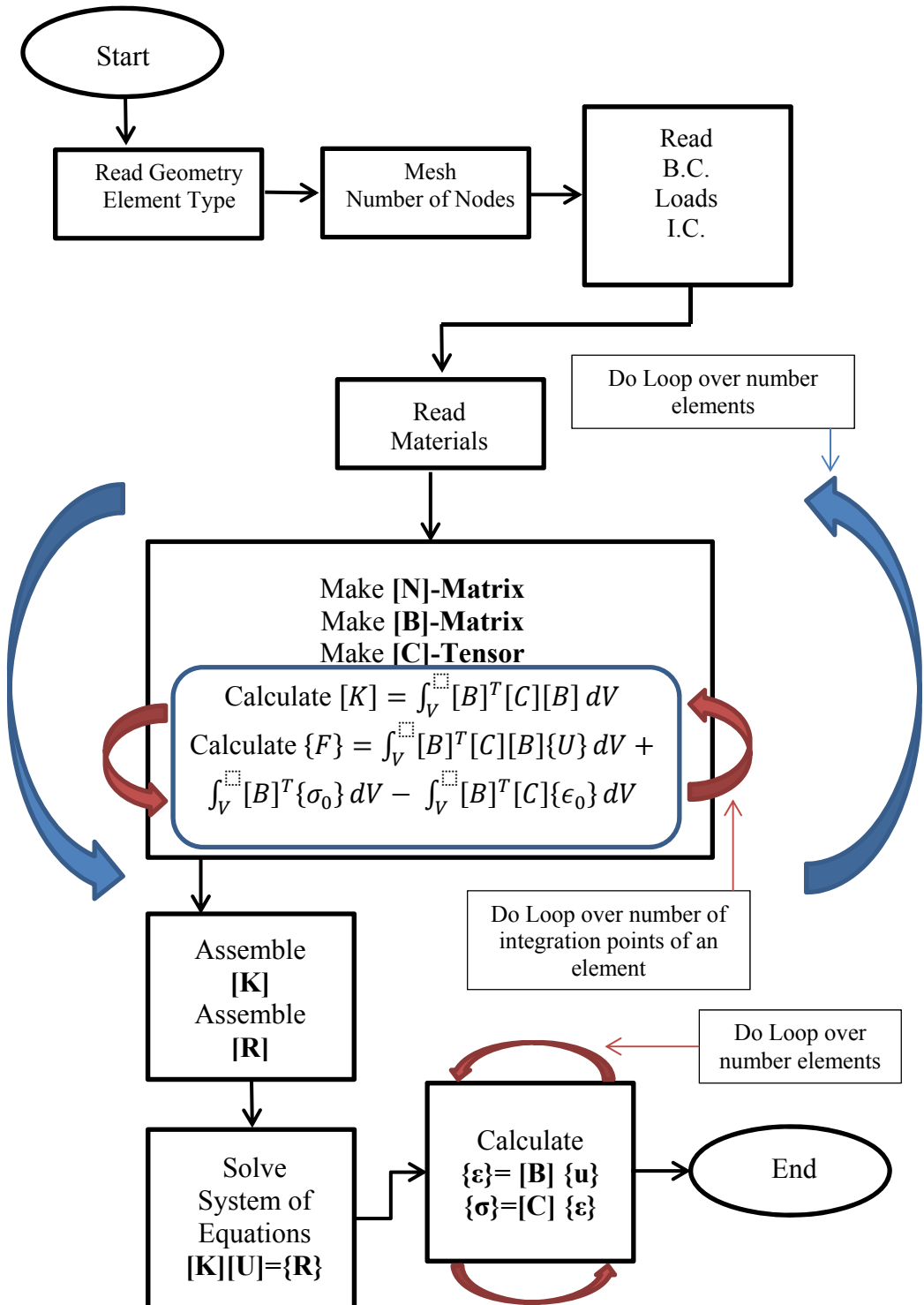


Figure 3.3-Flow Chart of FEM

So far, the finite element method has been explained. It is necessary to mention some details regarding elements in order to complete this section.

As discussed earlier, the values for the whole element are calculated by the interpolation of those values on the nodes of the elements. Interpolation functions are usually in the shape of algebraic polynomials. There are two types of interpolation order which have been used in FEM simulation. The first one is linear polynomial or the first order polynomial. In linear polynomial interpolation, the values for stress, strain, deformation and so on are assumed to be linearly distributed between two conjunctive nodes. The other interpolation is called quadratic interpolation, which employs second order polynomial function to estimate values between the nodes of an element. It is obvious that quadratic interpolation provides more accuracy, but it also requires more computational effort.

Elements in different dimensions serve different analyses. In ABAQUS, elements can be one-dimensional (beam element, linkage element, etc.), two-dimensional (shell element, surface elements, etc.) or three-dimensional (such as solid elements).

The other factor regarding elements is their shape. In ABAQUS, 3-D elements can take the form of a brick (six-sided element), wedge (five-sided element) or prism (four-sided element). The most stable element in 3-D analysis is a solid brick element and usage of other types of element depends on the requirements of the geometrical difficulties of the problem.

A final aspect of elements which needs explanation is the number of nodes on elements. Figure 3.4 shows the element nodes for two different shapes of element.

It is known that elements with a higher number of nodes provide less geometrical stiffness and therefore yield more accurate results. However, they also increase the computational effort required.

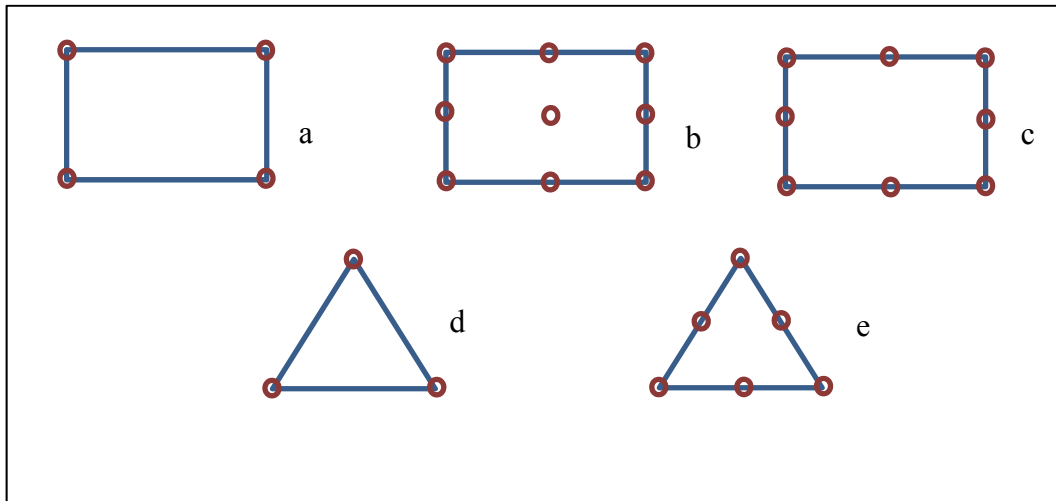


Figure 3.4 - Element's Types: (a) Linear Rectangular (b) Parabolic Rectangular  
(c) Parabolic Rectangular reduced (d) Linear Triangular (e) Parabolic Triangular

So far the basics of FEM, assembly the matrices of load and stiffness matrices and the theoretical background of the method have been presented, along with a detailed discussion of the element (dimensions, shape and nodes) and shape functions.

Section 3.2 explains the FEM approach to modelling loads (static and dynamic loads) and BC, and describes numerical integration, and incremental and iterative methods in time and space.

Finally, section 3.3 is devoted to the constitutive modelling of geomaterials, paying more specific attention to those constitutive models developed for pavement materials.

### 3.2 Types of Numerical Analyses

As mentioned in the previous section, FEM is an approach to solving differential equations (ordinary or partial). Therefore, FEM can be employed in geotechnical modelling to solve the main differential equations in this field. Some of these equations are shown below:

$$\text{Static Equilibrium} \quad Ku + F = 0 \quad \text{Equation 3-19}$$

$$\text{Dynamic Equilibrium} \quad M \frac{\partial^2 u}{\partial t^2} + C \frac{\partial u}{\partial t} + Ku + F = 0 \quad \text{Equation 3-20}$$

$$\text{Seepage} \quad K_x \frac{\partial^2 h}{\partial x^2} + K_y \frac{\partial^2 h}{\partial y^2} = 0 \quad \text{Equation 3-21}$$

$$\text{Consolidation} \quad C_v \frac{\partial^2 h}{\partial x^2} = \frac{\partial h}{\partial t} \quad \text{Equation 3-22}$$

$$\text{Heat Transfer} \quad K \frac{\partial^2 \theta}{\partial x^2} = \rho C \frac{\partial \theta}{\partial t} \quad \text{Equation 3-23}$$

$$\text{Solute Transfer} \quad D_x \frac{\partial^2 C}{\partial x^2} + K(t) = \frac{\partial C}{\partial t} + u_x \frac{\partial C}{\partial x} \quad \text{Equation 3-24}$$

The analysis to be taken into consideration depends on which equation is chosen to represent the physical problem. In this dissertation, two types of equations are investigated with respect to mechanical equilibrium (which are Equation 3-19 and Equation 3-20).

In FEM, any differential equation is firstly converted to an integral equation, and then this new form of equation is reduced to a system of algebraic equations over the elements.

The following sub-sections describe the method of numerical integration used by the ABAQUS program (Hibbit 2010) and provide descriptions of static analysis, geostatic analysis and dynamic analysis. The boundary conditions and infinite elements used in the static and dynamic analyses are also discussed.

The influence of damping and inertial force on dynamic analysis is explained. Time domain and frequency domain are also described and the method of analysis for each is briefly reviewed.

Finally, the basics of the dynamic interaction between layers and the methods for undertaking such an analysis are clarified.

### **3.2.1 Static Analysis**

Static analysis is an attempt to find out the stress-strain solution for a defined problem where the effects of inertia are ignored. In this case, static analysis is applicable for any stable (or slow enough) simulation and is applicable for both the linear or nonlinear behaviour of materials. In this regard it should be noted that static analysis cannot consider time-dependent material behaviours (such as viscoelasticity, swelling or creep), while rate-dependent plasticity and hysteretic characteristics of hyperelastic model can be included (Hibbit 2010).

When the analysis includes either geometric or material nonlinearity, FEM tries to divide the problem into several steps. In each step a small part of the load is

applied to the whole model. These small steps of loading are called increments, and during each increment FEM assumes that the materials and geometry of the problem remain linear. When finalizing an increment, FEM updates all necessary changes (either in geometry or material properties) and passes the final results of the increment (as field of stress and strain) to the subsequent increment. It is common to assign a virtual time to the load and then divide this time into several time-steps representing the increments of loading. This assigned time, clearly, does not have any physical interpretation and is added due to the numerical requirements of FEM.

Two general methods for the solution are available: implicit and explicit. These two are also applicable to dynamic analysis. In explicit FEM, the material stiffness matrix and geometrical change are applied at the end of the incremental process. The accuracy of the explicit procedure relies heavily on the small size of each increment.

By contrast, the implicit procedure is generally same as the explicit procedure with an additional computation step. In this extra step, FEM uses an iteration method (Newton-Raphson in the ABAQUS program) to satisfy the equilibrium condition in which the internal force of the model is equal to the external forces. The implicit method is more stable in its accuracy due to the extra computational effort.

In the Newton-Raphson method, the iterative process is employed to solve nonlinear problems. In each iteration, the stiffness matrix needs to be reconstructed and this requires more computational effort. To overcome this disadvantage, a modified Newton-Raphson method has been developed in which

the stiffness matrix is not completely reconstructed in each iteration but is partially updated (Bodhinayake 2008).

In the ABAQUS program the Newton-Raphson (or modified Newton-Raphson) method is available to be applied to nonlinear problems.

The Newton-Raphson method employs the principle of virtual work. In each increment, components of force and components of displacement are generated in each iteration. The iterations and increments in FEM are schematically demonstrated in Figure 3.5.

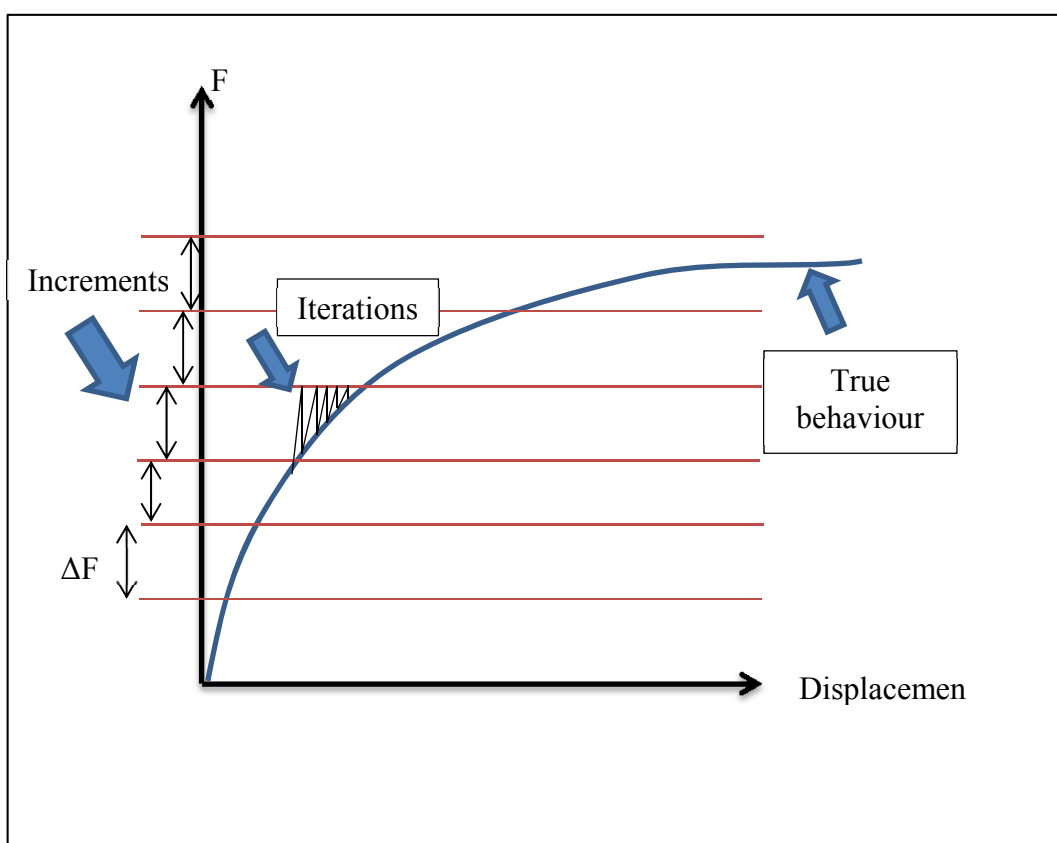


Figure 3.5 - Iterations and Increments in FEM

The ABAQUS program enables the user to select the increment size and choose the iteration procedure. In each of these iterations, the stiffness matrix of the materials, which consists of partial derivatives of the force respecting displacement, is constructed (Newton-Raphson) or updated (modified Newton-Raphson). According to this new stiffness matrix (called the material Jacobian matrix), the program then tries to solve the equilibrium of external and internal forces. If after sufficient tries the solution has not been converged with the required accuracy, the user is asked to change either the increment size or the iteration method. In some severe cases, total modification of the generated mesh domain and the geometrical definition of the problem are also necessary.

There is a specific type of static analysis which should be used in all simulations involving soil as a foundation. In ABAQUS it is called the geostatic analysis. A geostatic analysis is conducted to ensure that the necessary ‘at rest pressure’ is distributed in the soil mass. This usually is the first step before any further mechanical analysis. In geostatic analysis, gravity is applied to all of the elements and the stress distribution is calculated assuming elastic behaviour for the soil. Then if equilibrium is established, all displacement is set to zero. This is the way that the existing pressure in the soil body is produced without any unwanted displacement at the beginning of the simulation (Hibbit 2010).

It should be mentioned that the strength of the soil mass is not only a function of its granular properties (such as internal friction or cohesion) but also depends on the existing pressure inside the soil. In other words, having a great confining pressure increases the strength of the soil significantly. Therefore, the geostatic step is performed before the static or dynamic analysis in order to ensure that the soil has its actual strength. Without distribution of the actual stress in the soil body, it behaves much looser than its real state.

It is worth pointing out that dynamic analysis can be understood as an expansion of the static analysis in time. The next section explains dynamic analysis in detail.

### 3.2.2 Dynamic Analysis

The final stage of this research is to investigate effect of dynamic loading on the structure of layered flexible pavement. Therefore a detail explanation about the FEM application to conduct dynamic analysis is discussed in this section.

As it can be recalled from Equation 3-19(b) the differential equation of mechanical equilibrium in dynamic analysis takes the form as follow:

$$M\ddot{U} + C\dot{U} + KU = R(t) \quad \text{Equation 3-25}$$

In this equation, the dot sign “” denotes the derivation in respect to time. M is the mass matrix representing inertial force, C (separated from C as the matrix of the constitutive model) is the matrix of damping, and K is the stiffness matrix. R represents all external forces and boundary conditions which can be a function of time. R can therefore also take the form of displacement, velocity or acceleration. The latter is more applicable in earthquake analysis.

There are two common ways of using FEM to solve dynamic problems: direct integration and mode superposition. The method described here is the first one, direct integration.

In the direct integration method, the partial differential equation of dynamic equilibrium is solved directly through a step-by-step process. The unknown (for

example deformation) is calculated in each step and then passed on to the next step of the calculation. In this regard, dynamic analysis can be thought of as a series of static analyses, each one conducted in a small increment of time (separate from increments of loading). Various methods can be used to calculate the derivatives of U in Equation 3-25. One of the more stable methods is the central difference method. In this method, the following numerical approximation is applied:

$${}^t\dot{U} = \frac{{}^{t+\Delta t}U - {}^{t-\Delta t}U}{2\Delta t} \quad \text{Equation 3-26}$$

$${}^t\dot{U} = \frac{{}^{t+\Delta t}U - 2{}^tU + {}^{t-\Delta t}U}{\Delta t^2} \quad \text{Equation 3-27}$$

In this equation the differentiation of U (deformation) in terms of time is translated to subtraction terms. Equation 3-26 is substituted into Equation 3-25 and after an algebraic operation, Equation 3-28 can be written:

$$\begin{aligned} & \left( \frac{1}{\Delta t^2} M + \frac{1}{2\Delta t} C \right) {}^{t+\Delta t}U \\ &= {}^tR - \left( k - \frac{2}{\Delta t^2} M \right) {}^tU \\ & \quad - \left( \frac{1}{\Delta t^2} M - \frac{1}{2\Delta t} C \right) {}^{t-\Delta t}U \end{aligned} \quad \text{Equation 3-28}$$

In Equation 3-28 the right hand side of the equation is determined in the completed step and the only unknown is the left hand side (deformation in the step of  $t+\Delta t$ ). It can be deduced that this formation of the dynamic equation is very similar to the static equation of equilibrium (Equation 3-19).

In Equation 3-28 the coefficient of  $U$  on the left hand side is the effective stiffness matrix and the right hand side of Equation 3-28 is the effective load vector. It should also be mentioned that  $\Delta t$  should be small enough to assure the numerical stability of the problem.

So far, the central difference method has been described. There are various methods of translating the derivative terms of deformation to subtraction terms (such as the Houbolt Method, Wilson  $-\theta$  Method and Newmark Method). However, the ultimate aim of these methods is similar to that of the central difference method. In other words, all of these methods produce equations in the form of Equation 3-28.

Remembering the incremental method used for nonlinear static analysis, it can be seen that the basis of dynamic analysis and incremental nonlinear analysis are quite similar. The difference is that in nonlinear analysis a series of ‘virtual’ time steps is assumed to divide the applied load into increments, while in dynamic analysis the time step does have a physical meaning.

In the ABAQUS program, the direct integration technique is used to study linear and nonlinear simulation. In dynamic analysis, the implicit scheme of time integration is employed to evaluate the transient dynamic response of the model. The technique can be manipulated to suit a wide range of problems including varying the numerical damping required for convergence and selecting the time incrementing algorithm used by the program.

The two main differences between static and dynamic analysis are the effects of mass and damping. In Equation 3-28 these two are termed the  $M$  and  $C$  matrix.

In this research the mass of materials is applied through the assignment of proper density to the materials in each layer. The effect of mass is on geostatic calculation and more importantly the calculation of inertial forces in dynamic analysis.

The concept of damping is not as easy as the mass. In order to explain this it needs to be mentioned that the concept of mass and damping should be written in the form of Equation 3-29 and Equation 3-30 to be included in the FEM method.

$$M = \int_{V1}^{V2} N^T \rho N dV \quad \text{Equation 3-29}$$

$$C = \int_{V1}^{V2} N^T \kappa N dV \quad \text{Equation 3-30}$$

In Equation 3-29,  $N$  represents the shape function of the elements,  $V$  is the volume of the elements, superscript  $T$  indicates the transposition of a matrix and  $\rho$  is the density of materials in the elements. Now to include the damping matrix as an element dependent quantity it should be a physical quantity like  $\kappa$  which is defined in the whole of the element and can be integrated according to volume. However, in all of the simulations that include soil mass, such a definition is not practical. This is because damping in the soil body is not just dependent on the material properties but also on the variety of properties of a specific problem (some of them are purely geometrical), which results in the final dissipation of the total energy of the system in a specific time step. This dissipation can be induced by the yielding of materials, friction between granules and/or the viscous properties of materials. Therefore, in the FEM simulation of a soil body, instead of concentrating on the concept of damping, a general concept of the ‘total dissipated energy’ of the system should be considered.

In the ABAQUS program there are various ways to include damping, however, the most usual method of including the damping of a soil body is the Rayleigh damping method. In this method, the damping matrix is constructed as a combination of the mass and stiffness matrix. Equation 3-31 represents the general form of the Rayleigh damping matrix in FEM.

$$[C] = \alpha[M] + \beta[K] \quad \text{Equation 3-31}$$

In this equation, C, M and K represent the damping, mass and stiffness matrix respectively. The parameters  $\alpha$  and  $\beta$  are nominal parameters indicating the contribution of the mass and stiffness matrix to the final damping matrix. Users therefore have control over the damping of the model. Parameter  $\alpha$  damps the resonance effect caused by the mass of the model. On the other hand,  $\beta$  produces a damping effect that resists the resonance produced by materials or layers that are too stiff.

The final aspect of dynamic analysis reviewed in this section is the dynamic interaction between layers. The interaction of layers has been considered through the implementation of the interface element.

Contact pressure distribution is defined in relation to the existing (virtual) distance between surfaces. Equation 3-32 describes the mathematical representation of pressure distribution.

$$\begin{cases} P = 0 \text{ if } h < 0 \text{ (open)} \\ h = 0 \text{ if } p > 0 \text{ (closed)} \end{cases} \quad \delta\Pi = \delta pdh + dp\delta h \quad \text{Equation 3-32}$$

Where  $\Pi$  is the virtual work on the element,  $h$  is the distance between surfaces and  $p$  (as a function of  $h$ ) is the distributed pressure between surfaces. This definition is called the ‘hard contact’ condition and is used in this simulation.

In dynamic analysis the boundary conditions are represented by infinite elements to prevent wave reflection from the boundary. Infinite elements assume a damping inside element which prevents wave reflection towards the simulated medium. The boundary conditions enforced by infinite elements are as in Equation 3-33:

$$\begin{cases} \sigma_{xx} = -d_p \dot{u}_x \\ \sigma_{xy} = -d_s \dot{u}_y \\ \sigma_{xz} = -d_s \dot{u}_z \end{cases} \quad \text{Equation 3-33}$$

Where  $d_p$  and  $d_s$  denote the damping ratio for pressure and shear waves respectively.

Having reviewed the solver procedure, the next section is devoted to constitutive modelling in FEM.

### 3.3 Constitutive Models

In Equation 3-12 the relationship between stresses and strains is defined in a matrix called  $C$ . This matrix represents the behaviour of materials regarding induced stress and is called the constitutive model. The constitutive model should be a means of accurately demonstrating the behaviour of materials. Considering the geomaterials used in pavement engineering, it can be understood that the

constitutive model should be capable of modelling complex behaviour. Some of this complexity is reviewed in Chapter 2.

Numerical implementation of constitutive models consists of integrating the material response in the actual or virtual time increment on integration points. ABAQUS works in a time-implicit scheme, therefore accurate constitutive models (which define the material stiffness matrix) should be provided in the process of implementation.

A range of mechanical constitutive models are available in ABAQUS which cover elastic and inelastic behaviour. Inelastic behaviour is mainly considered through plastic constitutive models. It should be noted that the combination of elastic and plastic models commonly assumes that material characteristics in each of the processes are independent from each other. Therefore, exceeding the yield criterion does not affect the elastic characteristics of the materials. However, it should be noted that during the dynamic loading of UGM in pavement layers, the actual characteristics of materials are also modified. ABAQUS enables the user to code an individual constitutive model that can cover particular aspects of material behaviour. Such a technique is available by coding UMAT in FORTRAN and integrating this code to the general FEM solver. In this dissertation, such a technique is employed to cover the complex behaviour of UGM during FEM simulation.

The following subsection presents the mathematical formulation of constitutive equations used in the field of geomechanics and pavement engineering.

### **3.3.1 Application of Constitutive Models in FEM**

This section reviews some well-known constitutive models and their implementation in FEM, including the linear elastic model, and the Tresca and von Mises plastic models. The significance of these three models is that they are the basic models upon which other geotechnical constitutive models (such as the Mohr-Coulomb, Uzan-Witczak, Duncan-Chang and Drucker-Prager models) have been developed.

The linear elastic material is considered first, as it is the simplest model. In this model, Hook's law is applied where the stresses are linearly related to strains. Considering tensor notation, the relationship can be written as follows in Equation 3-34:

$$\boldsymbol{\sigma} = 2G\boldsymbol{\varepsilon}^e + \lambda\mathbf{I}\boldsymbol{\varepsilon}^e \quad \text{Equation 3-34}$$

In this equation  $G$  and  $\lambda$  are the Lame constants and  $\mathbf{I}$  is the identity tensor. Super script  $e$  denotes the elastic part of the strain. The bold letters indicate the tensor quantities.

Considering the incremental sequence used by FEM (section 3.2.1), the material stiffness matrix (also known as material Jacobian) can be represented as follows:

$$\begin{aligned}
C^e = \frac{\partial \Delta \sigma}{\partial \Delta \varepsilon} &= \begin{bmatrix} \frac{\partial \Delta \sigma_{11}}{\partial \Delta \varepsilon_{11}} & \frac{\partial \Delta \sigma_{11}}{\partial \Delta \varepsilon_{22}} & \frac{\partial \Delta \sigma_{11}}{\partial \Delta \varepsilon_{33}} & \frac{\partial \Delta \sigma_{11}}{\partial \Delta \gamma_{12}} \\ \frac{\partial \Delta \sigma_{22}}{\partial \Delta \varepsilon_{11}} & \frac{\partial \Delta \sigma_{22}}{\partial \Delta \varepsilon_{22}} & \frac{\partial \Delta \sigma_{22}}{\partial \Delta \varepsilon_{33}} & \frac{\partial \Delta \sigma_{11}}{\partial \Delta \sigma_{11}} \\ \frac{\partial \Delta \sigma_{33}}{\partial \Delta \varepsilon_{11}} & \frac{\partial \Delta \sigma_{33}}{\partial \Delta \varepsilon_{22}} & \frac{\partial \Delta \sigma_{33}}{\partial \Delta \varepsilon_{33}} & \frac{\partial \Delta \sigma_{33}}{\partial \Delta \gamma_{12}} \\ \frac{\partial \Delta \varepsilon_{11}}{\partial \Delta \varepsilon_{11}} & \frac{\partial \Delta \varepsilon_{22}}{\partial \Delta \varepsilon_{22}} & \frac{\partial \Delta \varepsilon_{33}}{\partial \Delta \varepsilon_{33}} & \frac{\partial \Delta \gamma_{12}}{\partial \Delta \varepsilon_{11}} \\ \frac{\partial \Delta \sigma_{12}}{\partial \Delta \varepsilon_{11}} & \frac{\partial \Delta \sigma_{12}}{\partial \Delta \varepsilon_{22}} & \frac{\partial \Delta \sigma_{12}}{\partial \Delta \varepsilon_{33}} & \frac{\partial \Delta \sigma_{12}}{\partial \Delta \gamma_{12}} \end{bmatrix} \\
&= \begin{pmatrix} 2G + \lambda & \lambda & \lambda & 0 & 0 & 0 \\ 2G + \lambda & 2G + \lambda & \lambda & 0 & 0 & 0 \\ & & 2G + \lambda & 0 & 0 & 0 \\ & & & G & 0 & 0 \\ Sym. & & & & G & 0 \\ & & & & & G \end{pmatrix}
\end{aligned} \tag{Equation 3-35}$$

Equation 3-35 represents the implementation of isotropic linear elastic constitutive models in FEM (Dunne and Petrinic 2005).

The linear elastic model is the one used by CIRCLY and KENLAYER. The model is also the basis of the other nonlinear elastic models which will be described in following sections.

In linear elastic behaviour there is no cap for the ultimate material strength. This means that materials never yield under applied loads. Such a lack can be resolved by defining a yield criterion after which material behaviour is plastic and some permanent deformation (plastic strain) in the material exists.

One of the simplest plastic models is the Tresca yield criterion (named after Henri Tresca October 12, 1814–June 21, 1885). Equation 3-36 presents the Tresca yield criterion:

$$f = \sigma_1 - \sigma_3 - 2S_u = \sqrt{J_2} \cos \theta_l - S_u = 0 \quad \text{Equation 3-36}$$

In this equation  $S_u$  is undrained shear strength,  $J_2$  is the second principal invariant of the deviator part of the Cauchy stress and  $\theta_l$  is Lode's angle (Yu 2006) .

Based on Equation 3-36, the components of the material Jacobian can be written as Equation 3-37:

$$C_{ijkl}^{ep} = C_{ijkl}^e - \frac{1}{H} C_{ijmn}^e \frac{\partial g}{\partial \sigma_{mn}} \frac{\partial f}{\partial \sigma_{pq}} C_{pqkl}^e \quad \text{Equation 3-37}$$

And

$$H = \frac{\partial f}{\partial \sigma_{ij}} C_{ijkl}^e \frac{\partial g}{\partial \sigma_{kl}} \quad \text{Equation 3-38}$$

Where

$$\frac{\partial f}{\partial \sigma_{ij}} = \frac{\cos \theta_l}{2\sqrt{J_2}} \frac{\partial J_2}{\partial \sigma_{ij}} - \sqrt{J_2} \sin \theta_l \frac{\partial \theta_l}{\partial \sigma_{ij}} \quad \text{Equation 3-39}$$

And

$$\frac{\partial g}{\partial \sigma_{ij}} = \frac{\cos \theta_l}{2\sqrt{J_2}} \frac{\partial J_2}{\partial \sigma_{ij}} - \sqrt{J_2} \sin \theta_l \frac{\partial \theta_l}{\partial \sigma_{ij}} \quad \text{Equation 3-40}$$

Small letter subscripts indicate indices,  $\mathbf{C}^{ep}$  is the elastoplastic constitutive tensor (Yu 2006).

The problem with the Tresca criterion is that at specific points it is indifferentiable. This problem is then solved through the introduction of the von Mises criterion (named after Richard Edler von Mises 19 April 1883 – 14 July 1953).

The von Mises criterion can be written as Equation 3-41:

$$f = \sqrt{J_2} - \frac{S_u}{\cos \theta_l} = 0 \quad \text{Equation 3-41}$$

Components of  $\mathbf{C}^{ep}$  can be determined by Equation 3-37 if the following modification is applied (Yu 2006):

$$\frac{\partial f}{\partial \sigma_{ij}} = \frac{1}{2\sqrt{J_2}} \frac{\partial J_2}{\partial \sigma_{ij}} \quad \text{Equation 3-42}$$

And

$$\frac{\partial g}{\partial \sigma_{ij}} = \frac{1}{2\sqrt{J_2}} \frac{\partial J_2}{\partial \sigma_{ij}} \quad \text{Equation 3-43}$$

The graphical representation of the Tresca and von Mises criteria together clarifies the relationship between these two constitutive models (Figure 3.6).

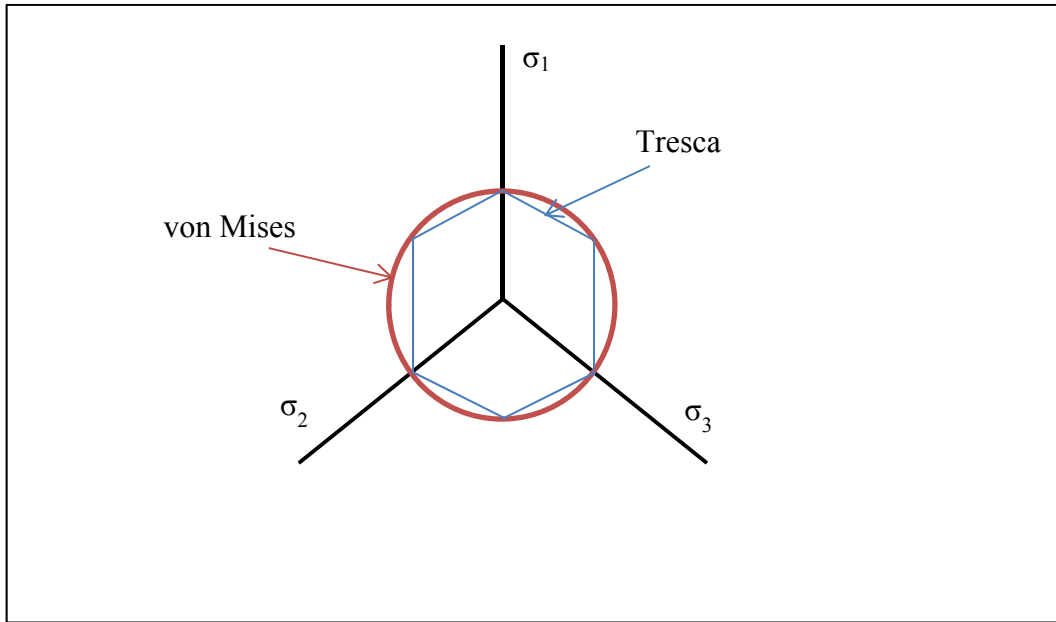


Figure 3.6 - Tresca and von Mises Criteria

### 3.3.2 Geotechnical Constitutive Models

In the previously mentioned elastoplastic models (Tresca and von Mises), it can be observed that failure of the materials is solely defined by the state of stress and one characteristic parameter representing material strength. In this way there is no difference between the strength of materials in tension or compression.

With respect to actual geomaterials, it is a generally accepted idea that the materials show frictional behaviour in which their strength is a function of existing pressure. In fact, the strength of geomaterials increases due to the increase in confining pressure.

To account for such behaviour a group of specific purpose constitutive models have been developed. One of the first constitutive models accounting for frictional

behaviour was introduced by Coulomb (1773) and is called the Mohr-Coulomb model (after Charles-Augustin de Coulomb and Christian Otto Mohr). According to this model the shear strength developed in soil is a function of internal friction, cohesion and applied stress. Equation 3-44 indicates the mathematical representation of the Mohr-Coulomb model:

$$\tau = c + \sigma_n \tan \varphi \quad \text{Equation 3-44}$$

Here  $c$  is cohesion of the soil materials,  $\varphi$  is the angle of internal friction and  $\sigma_n$  is normal stress on the failure surface.

Equation 3-44 can be rewritten in terms of stress invariants and Lode's angle as follows:

$$f = \sqrt{J_2} - \frac{m(\theta_l, \varphi)}{3} I_1 - m(\theta_l, \varphi) c \cos \varphi = 0 \quad \text{Equation 3-45}$$

Where

$$m(\theta_l, \varphi) = \frac{\sqrt{3}}{(\sqrt{3} \cos \theta_l + \sin \theta_l \sin \varphi)} \quad \text{Equation 3-46}$$

And

$$g = \sqrt{J_2} - \frac{m(\theta_l, \psi)}{3} I_1 - m(\theta_l, \psi) c \cos \psi = 0 \quad \text{Equation 3-47}$$

Where

$$m(\theta_l, \psi) = \frac{\sqrt{3}}{(\sqrt{3} \cos \theta_l + \sin \theta_l \sin \psi)} \quad \text{Equation 3-48}$$

Where  $\psi$  is dilation angle.

According to Yu (2006), the material stiffness matrix when combination of stress meet a single yield surface can be written as Equation 3-49.

Equation 3-49

$$C^{ep} = C_2 \begin{pmatrix} \left(K + \frac{G}{3}\right)(1+s)(1+n) & \left(K - \frac{2G}{3}\right)(1+s) & \left(K + \frac{G}{3}\right)(1+s)(1-n) \\ \left(K - \frac{2G}{3}\right)(1+n) & K(1+3sn) + \frac{4G}{3} & \left(K - \frac{2G}{3}\right)(1-n) \\ \left(K + \frac{G}{3}\right)(1-s)(1+n) & \left(K - \frac{2G}{3}\right)(1-s) & \left(K + \frac{G}{3}\right)(1-s)(1-n) \end{pmatrix}$$

Where

$$C_2 = \frac{G}{G + \left(K + \frac{G}{3}\right)sn} \quad \text{Equation 3-50}$$

In this equation,  $s = \sin \varphi$ ,  $n = \sin \psi$ ,  $K$  is bulk moduli and  $G$  is shear moduli. It can be understood that the case of Tresca yield criterion is a specific case of Mohr-Coulomb criterion in which  $\varphi=\psi=0$ . In other word, Mohr-Coulomb is a yield criterion developed based on Tresca which consider the frictional behaviour of materials.

The Mohr-Coulomb has a disadvantage of indifferentiable vertices inherited from Tresca yield criterion. This disadvantage is cover through introduction of Drucker-Prager (after Daniel Charles Drucker and William Prager) constitutive model. Here the yield criterion can be defined as Equation 3-51.

$$f = \sqrt{J_2} - \alpha I_1 - k = 0 \quad \text{Equation 3-51}$$

Where

$$\alpha = \frac{2 \sin \varphi}{\sqrt{3}(3 - \sin \varphi)} \quad \text{Equation 3-52}$$

And

$$k = \frac{6c \cos \varphi}{\sqrt{3}(3 - \sin \varphi)} \quad \text{Equation 3-53}$$

The Mohr-Coulomb criterion and Drucker-Prager criterion can be related to each other in a similar way to the relationship between the Tresca and von Mises criteria. This relationship is schematically illustrated in Figure 3.7.

In this dissertation, the Mohr-Coulomb criterion is selected as the initial yield criterion and other modifications with regard to nonlinear elasticity and the shakedown concept are developed based on that.

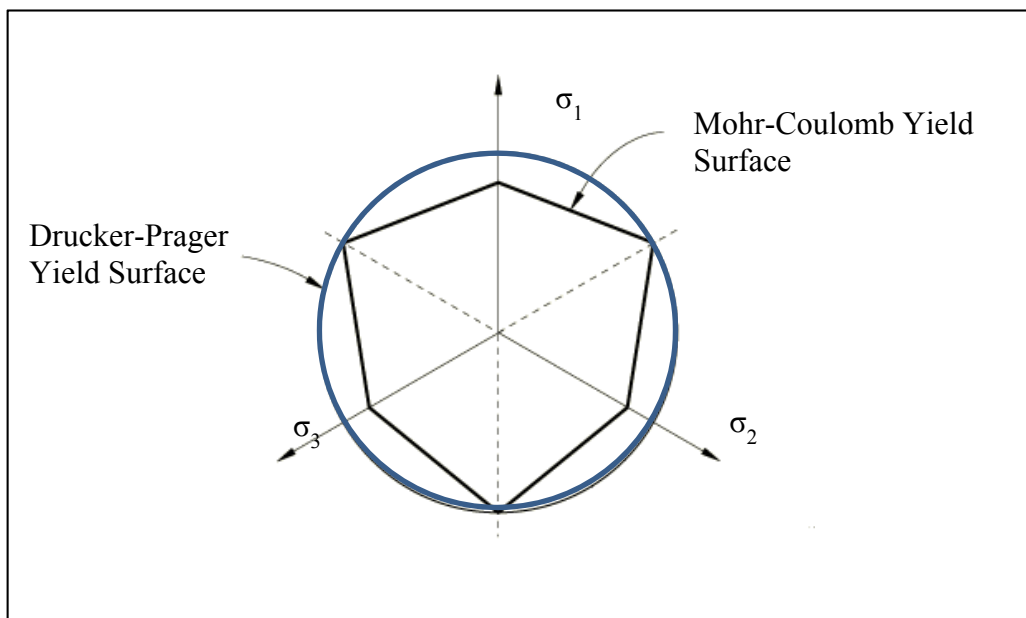


Figure 3.7 - Mohr-Coulomb and Drucker-Prager Criteria

In this regard the method introduced by Clausen, Damkilde, and Andersen (2007) is employed. This method applies an efficient return algorithm for stress update in the numerical simulation of plastic materials. The method requires a linear yield criterion in a principal stress space composed of any number of yield surfaces. Such a condition is well expressed by the Mohr-Coulomb criterion (Figure 3.7). The formulation of the constitutive matrix is expressed in principal stress space and the singularity problem at the intersection of planes is dealt with by a geometrical operation (it is based on the implementation of piecewise functions). Then the method was used for Mohr-Coulomb criteria and several basic problems were solved.

In the return mapping scheme, firstly the stresses are predicted by the elastic constitutive tensor, and then these stresses are updated according to the plastic constitutive model. Figure 3.8 illustrates this concept.

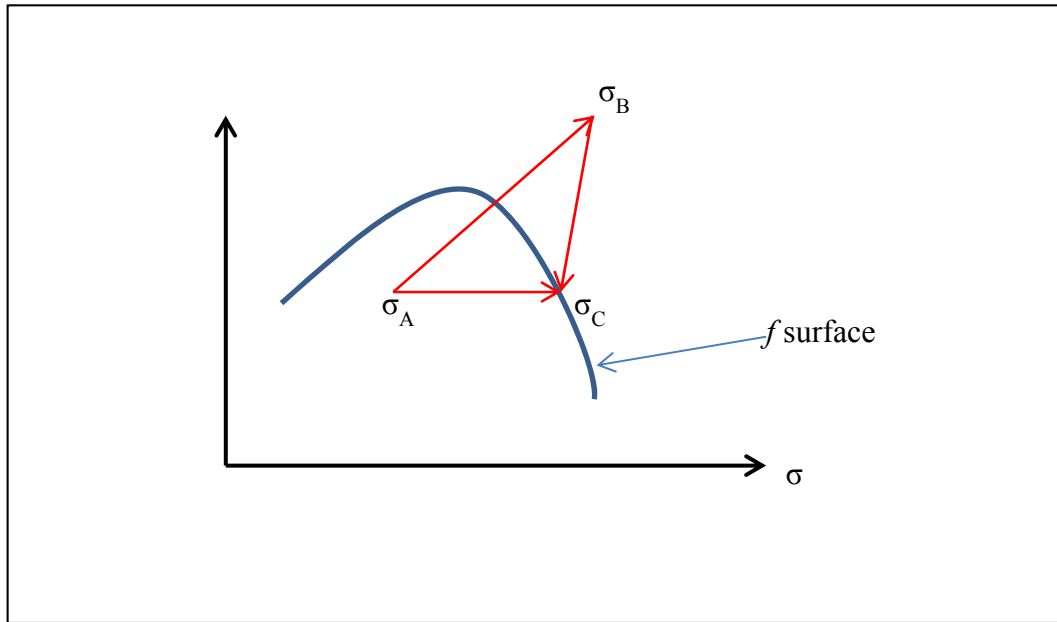


Figure 3.8 - Return Mapping Technique

Starting from  $\sigma_A$ , the method predicts the  $\sigma_B$  through the elastic constitutive matrix multiplied by strain. Then the allowable stress on the yield surface is calculated, and finally the initially calculated  $\sigma_B$  will be updated to achieve  $\sigma_C$ . The method is described in detail by Clausen, Damkilde, and Andersen (2007).

So far the constitutive models which are capable of modelling UGM and their implementation in FEM have been reviewed. In the next section, the attention will mainly be focussed on those constitutive models which are developed specifically for the simulation of pavement materials.

### **3.3.3 Constitutive Models for Pavement Materials**

Geomaterials used in pavement engineering have two distinguishing attributes which a proper constitutive model should cover. First of all, the materials used for base, subbase and subgrade layers do not behave linearly in an elastic domain. Researchers have therefore developed different nonlinear elastic models to predict the behaviour of UGM more accurately. Some of the major models were reviewed in sections 2.3.2 and 2.4.2. The challenge here is that the accepted models for UGM are usually stress dependent, which is basically how the materials are assumed to behave. Difficulty arises when it is considered that FEM software (such as ABAQUS) considers nonlinearity through strain dependency using concepts like hyperelasticity. Therefore, new coding is required to implement the stress dependent nonlinear elastic constitutive equation into the FEM simulation.

Another important characteristic of UGM in pavement layers is the change in material properties due to cyclic loading. This concept is known as the damage concept, where material characteristics actually differ if the loading surpasses the

yield criterion. Some of the proposed theories regarding this have been reviewed in sections 2.3.2 and 2.4.2. The concept of shakedown behaviour is one of the models accounting for the change of material properties in respect to loading cycles.

Now consider the nonlinear behaviour of materials in the elastic domain. Some of the widely accepted equations correlating the resilient moduli of UGM to the stress state existing in the layer were reviewed in section 2.3.2. These equations are listed here again in Table 3-1.

Table 3-1 - List of Nonlinear Equations For UGM

Equation Name	Formula	Equation Number
K-θ	$M_R = K \left( \frac{\theta}{P_1} \right)^n$	Equation 2-4
Uzan-Witczak axisymmetric	$M_R = K_1 \left( \frac{\theta}{P_1} \right)^{k_2} \left( \frac{\sigma_d}{P_1} \right)^{k_3}$	Equation 2-5
Uzan-Witczak 3D	$M_R = K_1 P_0 \left( \frac{I_1}{P_0} \right)^{k_2} \left( \frac{\tau_{oct}}{P_0} \right)^{k_3}$	Equation 2-6
Lade-Nelson	$M_R = K_1 \left[ \left( \frac{I_1}{P_1} \right)^2 + R \left( \frac{\tau_{oct}}{P_1} \right)^2 \right]^{k_2}$	Equation 2-7
Duncan-Chang	$E_t$ $= E_i \left[ 1 - \frac{R_f (1 - \sin\varphi) (\sigma_1 - \sigma_3)}{2c \cos\varphi + 2\sigma_3 \sin\varphi} \right]^2$	Equation 2-11

In Equation 3-35 the constitutive matrix of linear elastic materials is stated in terms of Lame constant. Definition of Lame constant is stated in Equation 3-54

$$\lambda = \frac{E \nu}{(1 + \nu)(1 - 2\nu)} \quad \text{Equation 3-54}$$

$$G = \frac{E}{2(1 + \nu)} \quad \text{Equation 3-55}$$

Where  $\lambda$  and  $G$  are the Lame constant defined in terms of the Poisson ratio and elastic moduli.

Equation 3-56 can be deduced by substituting Equation 3-54 into Equation 3-35 and performing an algebraic operation.

Equation 3-56

$$\mathbf{C}^e = \frac{E}{(1 + \nu)(1 - 2\nu)} \begin{pmatrix} 1-\nu & \nu & \nu & 0 & 0 & 0 \\ \nu & 1-\nu & \nu & 0 & 0 & 0 \\ \nu & \nu & 1-\nu & 0 & 0 & 0 \\ 0 & 0 & 0 & 1-2\nu & 0 & 0 \\ 0 & 0 & 0 & 0 & 1-2\nu & 0 \\ 0 & 0 & 0 & 0 & 0 & 1-2\nu \end{pmatrix}$$

To simulate the nonlinear elastic moduli which is a function of the stress state, the elastic moduli,  $E$ , should be replaced by resilient moduli  $M_R$ . This  $M_R$  is a function of the stress state according to one of the equations represented in Table 3-1. Therefore, in each increment of the nonlinear analysis, the resilient moduli are

modified according to calculated stresses (stress invariants) and the updated modulus is then implemented in the material constitutive matrix (Equation 3-56). This is the same method used by Kim (Kim 2007) to simulate nonlinearity in UGM using the ABAQUS program.

By implementing the abovementioned procedure with the procedure to calculate the plastic yield strength of UGM (described in section 3.2.2), the final behaviour can be modelled as nonlinear elastoplastic (Figure 2.16 b).

However, so far there is no difference in material characteristics in the different cycles in dynamic analysis. In other words, the material strength and behaviour remains constant during each cycle and the only difference produced in the model is due to the accumulation of plastic strain and permanent deformation (restricted by geometrical constraints such as the small strain assumption).

To consider the variation of materials as a function of the applied loading cycle, the shakedown theory is considered here. Chapter 2 reviewed previous studies on the application of shakedown theory in pavement layers. Here the mathematical background is described in detail.

According to Yu (2006), the preliminary development of the shakedown theory considered a very simple situation where the load sign was consistent and the geometry of the medium was a homogenous isotropic half space. When it comes to pavement engineering though, the simulation must consider more complicated problems. To resolve the basic problem, the idea of limit analysis (used in plastic collapse) is employed. Therefore the shakedown problem is divided to find an upper bound and lower bound limit for the shakedown load in a given problem.

Avoiding the actual mathematical representation of the method due to its complexity, its application to a simple case has been presented here. Figure 3.9 presents a case of the plane strain condition of an applied load whose pressure is distributed as a semicircular pressure over the contact area.

Assume that the surface tractions are vertically indicated by P and horizontally by Q. According to Yu (2006), normal and tangential stress in elastic materials can be represented by Equation 3-57:

$$\sigma_{zz} = -\frac{2P}{\pi a^2} \sqrt{(a^2 - x^2)} \quad \text{Equation 3-57}$$

$$\sigma_{xz} = -\frac{2\mu P}{\pi a^2} \sqrt{(a^2 - x^2)} \quad \text{Equation 3-58}$$

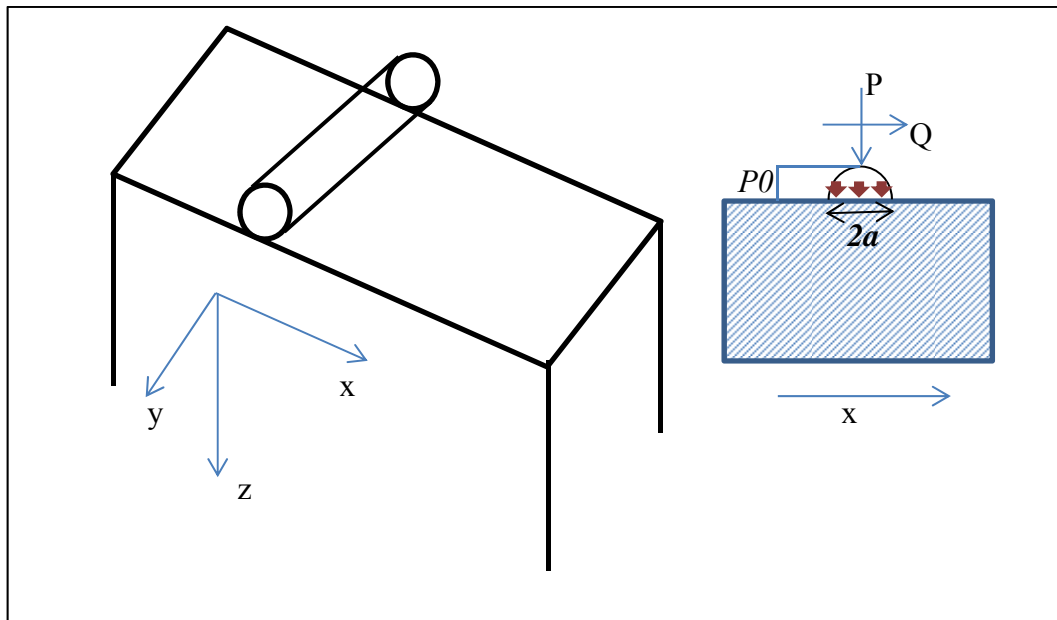


Figure 3.9 - Calculation of Shakedown Limit

Where  $\mu$  is the surface traction coefficient defined by the ratio of Q to P. In this case, the maximum pressure induced by normal load P can be written as Equation 3-59:

$$P_0 = \sqrt{\frac{PE}{\pi R}} \quad \text{Equation 3-59}$$

where

$$P_0 = \frac{2P}{\pi a} \quad \text{Equation 3-60}$$

In this equation, E and R represent material properties. Assuming the load does not exceed the elastic limit, we can obtain stress in all coordinates as follows:

$$\sigma_{xx} = -\frac{P_0}{a} \left\{ m \left( 1 + \frac{z^2 + n^2}{m^2 + n^2} \right) - 2z \right\} \quad \text{Equation 3-61}$$

$$\sigma_{xz} = -\frac{P_0}{a} \left\{ n \left( \frac{m^2 - z^2}{m^2 + n^2} \right) \right\} \quad \text{Equation 3-62}$$

$$\sigma_{zz} = -\frac{P_0}{a} \left\{ m \left( 1 - \frac{z^2 + n^2}{m^2 + n^2} \right) \right\} \quad \text{Equation 3-63}$$

Where m and n are functions of x, z and a.

According to lower bound shakedown theory the following condition should be satisfied:

$$f(\alpha \sigma_{ij}^e + \varrho_{ij}) \leq 0 \quad \text{Equation 3-64}$$

Where  $\sigma^e$  is the elastic stress field induced by applied pressure of  $P_0$  and  $f$  is any yield function.  $\varrho$  is the self-equilibrated residual field and  $\alpha$  is a dimensionless load multiplier scale.

If the simple Tresca yield criterion is assumed for the half-space medium in the presented plane-strain condition (Figure 3.9), applying Equation 3-64 and Equation 3-36 results in the following (Yu 2006):

$$\frac{1}{4}(\alpha\sigma_{xx}^e + \varrho_{xx} - \alpha\sigma_{zz}^e)^2 + (\alpha\sigma_{xz}^e)^2 \leq S_u \quad \text{Equation 3-65}$$

Then the lower bound solution would be to find out the load multiplier defined by Equation 3-66:

$$\alpha = \min \frac{S_u}{\sigma_{xz}^e(x, z)} = \frac{S_u}{\max(\sigma_{xz}^e(x, z))} \quad \text{Equation 3-66}$$

This equation is called the lower bound because it is not the direct solution for Equation 3-65, however, it is one of the limits that any stress field applied to a medium should clearly satisfy. In other words, the maximum shear stress induced in the field should not exceed the shear strength defined by  $S_u$ .

Now we simplify the problem assuming pure rolling conditions (where  $Q=0$ ). Considering Equation 3-61, the lower bound shakedown limit can be stated as follows:

$$\frac{\alpha P_0}{S_u} = \frac{1}{0.25} = 4 \quad \text{Equation 3-67}$$

So far it is stated that the lower bound shakedown should be as indicated by Equation 3-67. Now it is time to calculate the upper bound shakedown limit.

According to the upper bound shakedown theory, the following condition should be satisfied:

$$\alpha \leq \frac{\int_0^t \left( \iiint_V \sigma_{ij}^k \dot{\varepsilon}_{ij}^k dV \right) dt}{\int_0^t \left( \iint_S P_{0i} \dot{u}_i^k dS \right) dt} \quad \text{Equation 3-68}$$

This states that the structure will shakedown if the kinematically acceptable strain rate cycle ( $k$ ) and external load  $P_0$  can be found to satisfy equation Equation 3-68.

Now consider the example problem in which the Tresca yield criterion is applied to plane strain geometry. If a simple incremental collapse due to plastic shear in the direction of plane  $z=z_0=$  constant is considered, the incremental plastic deformation in  $x$ -direction produces work by the elastic stress field. In the meantime, internal dissipation due to the plastic yield is also produced. The value of this work and dissipation should satisfy the upper bound shakedown inequality as follows:

$$\alpha \leq \frac{\int_0^t \left( \iiint_V \sigma_{ij}^k \dot{\varepsilon}_{ij}^k dV \right) dt}{\int_0^t \left( \iint_S P_{0i} \dot{u}_i^k dS \right) dt} \leq \frac{S_u \times \Delta u_{xx}^{plastic}}{\sigma_{xz}^e \times \Delta u_{xx}^{plastic}} = \frac{S_u}{\sigma_{xz}^e} \quad \text{Equation 3-69}$$

A comparison of Equation 3-69 and Equation 3-49 indicates that the lower bound solution also satisfies the upper bound solution. Therefore, the lower bound solution is the exact solution for this specific problem (Yu 2006).

So far, the basics of shakedown theory and its application in calculating the shakedown limit of a given plane strain half space have been presented. However, in actual modelling the material properties and the geometry of the model (layered condition in 3-D analysis) is far more complicated than what has been expressed previously. Therefore, the FEM method (which is a lower bound approximation), is selected to solve the complicated problems. Section 2.3.2 reviewed the studies in which shakedown limits for specific materials used as UGM in pavement layers were determined. These studies usually provide us with load limits under which materials are inclined to elastic shakedown or incremental collapse, and for each of them an equation for the plastic strain developed in terms of loading cycles is also made available. Combining these ideas with the FEM approach used in this dissertation, the experimentally provided shakedown limits are coded to decide in any given stress field situation whether the materials fall within the shakedown limits or not. If the material behaviour is categorized as shakedown, the proper development of plastic strain with respect to the number of cycles is applied.

Based on the above, three different conditions exist for three specified stress fields as follow:

$$\begin{cases} f(\sigma_{ij}^k) > L_1 \rightarrow \varepsilon_{ij}^p(t) = f_1(N)\varepsilon_{ij}^p(0) \\ L_2 \leq f(\sigma_{ij}^k) \leq L_1 \rightarrow \varepsilon_{ij}^p(t) = f_2(N)\varepsilon_{ij}^p(0) \\ f(\sigma_{ij}^k) < L_2 \rightarrow \varepsilon_{ij}^p(t) = f_3(N)\varepsilon_{ij}^p(0) \end{cases} \quad \text{Equation 3-70}$$

Where N is the cycle number which can be comprehended as a function of time (t) and loading velocity.

If shakedown is not considered, then the plastic strain developed in each cycle will only be a function of the applied load. This means that if the magnitude of the load is constant during the cyclic analysis, there would be a constant amount of plastic strain developed in each cycle, and accumulated plastic strain increases linearly with time (or number of cycles). Figure 3.10 illustrates the difference between the behaviour of materials under shakedown or the simple Mohr-Coulomb yield criterion.

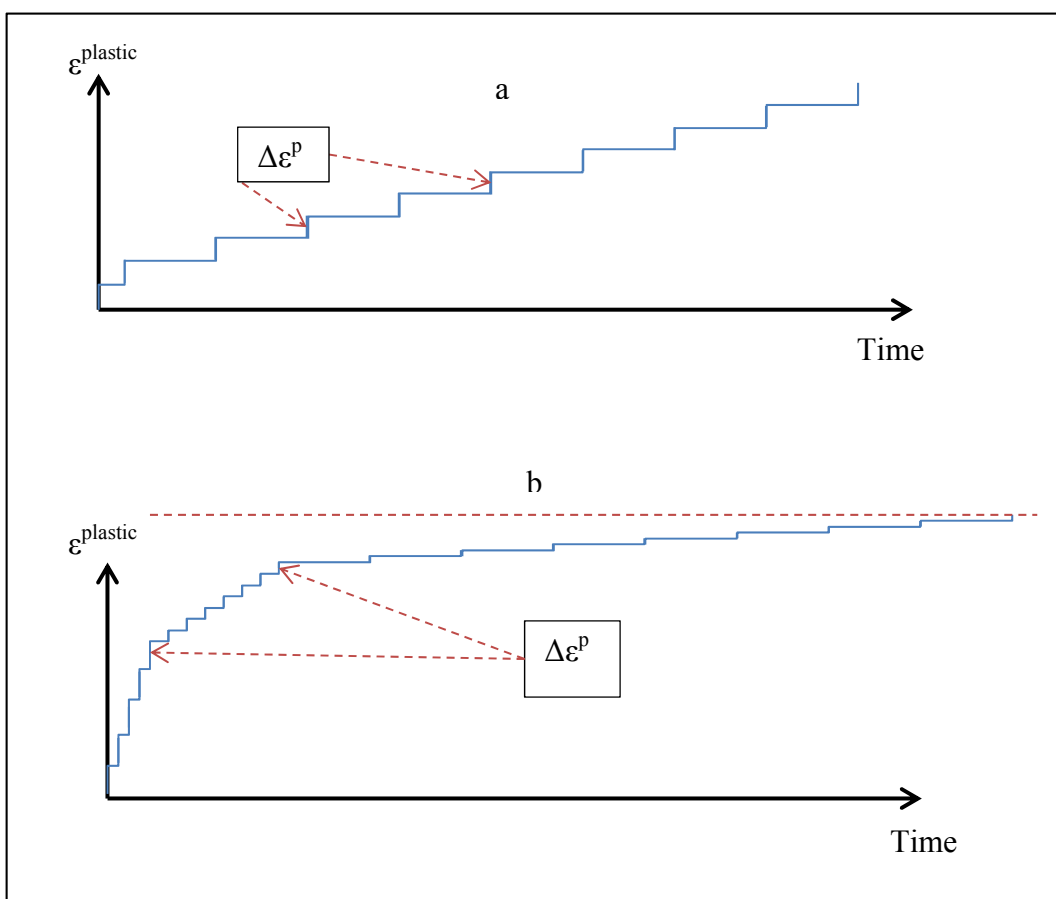


Figure 3.10 - Development of Plastic strains (a) Simple Mohr-Coulomb  
(b) Shakedown

If materials fall in the elastic domain (no plastic strain is developed), the constitutive model ( $\mathbf{C}^e$ ) is governed by Equation 3-56. In the case that the stress field passes the Mohr-Coulomb yield criterion, the constitutive model ( $\mathbf{C}^{ep}$ ) is indicated by Equation 3-49.

If the materials demonstrate shakedown behaviour, the initial plastic strains will be indicated by Equation 3-49, after which it will gradually evolve to purely elastic material with no plastic strain (Equation 3-56).

By combining Equation 3-12, Equation 3-49, Equation 3-56 and Equation 3-70, the current idea can be mathematically represented as Equation 3-71:

$$\begin{aligned}\sigma_{ij}^n &= C_{ijkl}^n \varepsilon_{kl}^n \\ \left\{ \begin{array}{l} \text{if } N = 1 \rightarrow \sigma_{ij}^n = (C_{ijkl}^n)^{ep} (\varepsilon_{kl}^n)^{ep} \\ \text{if } N \rightarrow \infty \rightarrow \sigma_{ij}^n = (C_{ijkl}^n)^e (\varepsilon_{kl}^n)^e \end{array} \right.\end{aligned}\quad \text{Equation 3-71}$$

Here the superscript n and letter N indicate the number of cycles.

However, based on Equation 3-70 the incremental plastic strain can be derived through differentiation in terms of N as follows:

$$\frac{\partial \varepsilon^p}{\partial t} = \frac{\partial f_i(N)}{\partial N} \varepsilon_0^p \quad \text{Equation 3-72}$$

Where

$$\left\{ \begin{array}{l} \text{if } N = 1 \rightarrow \frac{\partial f_i(1)}{\partial N} = 1 \\ \text{if } N \rightarrow \infty \rightarrow \frac{\partial f_i(N)}{\partial N} = 0 \end{array} \right.\quad \text{Equation 3-73}$$

The new developed constitutive model should now be able to change during loading cycles and depending on stress field conditions (whether or not it has exceeded the yield criterion).

The new constitutive model, therefore, can be written as Equation 3-74:

$$(C_{ijkl}^n)^s = \left( \frac{\partial f_i(N)}{\partial N} \right) (C_{ijkl}^n)^{ep} + \left( 1 - \frac{\partial f_i(N)}{\partial N} \right) (C_{ijkl}^n)^e \quad \text{Equation 3-74}$$

Equation 3-74 enables the gradual change of the constitutive model from elastoplastic to elastic as a function of loading cycle and stress field conditions.

The next chapter presents the schematic algorithm to implement this equation in the FEM procedure.

### **3.4 Summary of Chapter**

This chapter described the basic concept of using the finite element method to solve a partial differential equation with specific consideration of the equilibrium of a continuous medium. The method was detailed in mathematics formulations and computational procedures.

The two major categories of analysis used in this research, static and dynamic analysis, were specifically explained. The concept of space and time increments and their possible influence on the results were discussed. Moreover, the

contribution of body forces, including damping and density, to dynamic analysis was described and the mathematical formulation for these factors was provided.

Finally, this chapter detailed the concept of constitutive models and their contribution to FEM simulation. Geotechnical and pavement constitutive models were reviewed and explained, and a newly developed constitutive model corresponding to shakedown behaviour was mathematically presented.

The next chapter details the steps of the numerical simulation and the applied assumptions.

## **CHAPTER 4**

### **4: A REVIEW OF PROPOSED SIMULATION**

#### **4.1 Introduction**

Chapter 2 reviewed the main studies on modelling and analyzing pavement layers. It is obvious that there has so far not been much research into which UGM layers (base and subgrades) have been modelled as nonlinear layers together. Moreover, the effect of shakedown models is considered restrictively by numerical simulation of the layers (Allou, Chazallon and Hornych 2007; Allou et al. 2009; Chazallon et al. 2009; Chazallon, Hornych and Mouhoubi 2006; Chazallon, Koval and Mouhoubi 2011; Habiballah and Chazallon 2005), and these models do not consider dynamic loading or Mohr-Coulomb criteria.

Meanwhile, as described in Chapter 2, there is a significant difference in the response of materials if a different model is assumed (Kim 2007; Kim and Tutumluer 2006a; Kim, Tutumluer and Kwon 2009; Kim, Lee and Little 1997; Tutumluer, Little and Kim 2003; Ghadimi, Nikraz and Leek 2013; Ghadimi et al. 2013b). Therefore there is an actual need to study the effects of the implementation of different constitutive models and their integrated mechanical behaviours.

On the other hand, the actual distribution of loads between layers (AC and UGM) during different types of loading (static and dynamic) has been studied by a few researchers (Baek et al. 2010; Ozer et al. 2012; Pan, Okada and Atluri 1994), however a thorough study is certainly still needed.

Based on these points the main objectives of this dissertation are as follows:

- To identify the current pavement material models and improve it through advanced theoretical material modelling. This new, advanced model should in particular be able to provide a more precise prediction of the two most significant damage criteria in pavement, namely rutting and fatigue.
- To verify the results of simulations against previously published results under similar conditions in the laboratory or the field.
- To suggest future improvements to the current design methods based on the research findings.

In order to achieve these goals, newly developed constitutive models were used in a numerical study and the results of the simulation were analyzed. The next section describes the methodology used for this study.

## **4.2 Methodology**

The method used in this dissertation is a numerical simulation using FEM. Chapter 2 reviewed the application of FEM in modelling pavement layers and materials in detail. The modelling should be a way to represent the actual material behaviour in the field when subjected to static or dynamic loading.

As discussed in Chapter 2, UGM materials show complex behaviour which is not linear and also is dependent on loading cycle. To be able to simulate such

behaviour, a new constitutive model is developed based on the shakedown theory and the Mohr-Coulomb yield criterion as described in Chapter 3.

The research steps are selected to conduct a thorough numerical studies and indicate their influence on the results and finally their impact on the design.

The simulation is divided into two major categories: static loading and dynamic loading. In static loading, linear elastic material behaviour is considered first. Different models have been constructed in the ABAQUS, CIRCLY and KENLAYER programs. While ABAQUS is a general purpose FEM program, the other two work based on analytical solutions of elastic half-space. The preliminary effects of material strength on the results can be studied in this section. More importantly, decisions about the mesh size and the distance of the boundary conditions from the loading area can be made by comparing the results of the FEM and analytical methods. Finally, the results for the linear elastic materials can be verified in 2-D or 3-D simulation against the results for the analytical solution.

After completing the linear elastic analysis, the next step is the implementation of nonlinear elastic behaviour in the FEM simulation. Different models (as presented in Chapter 2 and Chapter 3) are used to investigate the influence of each model on the final results. The results of the analysis are verified by the results in previously published literature.

The final step in static loading is to study the effect of elastoplasticity. Linear elastoplastic and nonlinear elastoplastic materials based on the Mohr-Coulomb yield criterion are studied in this section.

The second analytical category deals with dynamic loading. Here, three different models and two types of material behaviour are investigated. The first behaviour is nonlinear elastoplastic behaviour based on the Mohr-Coulomb criterion and the second is nonlinear elastoplastic behaviour based on the Mohr-Coulomb criterion and taking the shakedown effect into consideration. The results of the analysis are verified against the previously published results of laboratory and field investigations.

In the third model, the final step of the dynamic analysis considers the effect of layer interactions between the AC layer and UGM layer. Finally, conclusions are drawn based on comparison of the results.

The following section describes the details of modelling techniques regarding layers, loading and materials.

### **4.3 Modelling of layered system**

The layered system of pavement structure consists of layers of asphalt at the surface supported by high quality granular materials. The granular layers transfer the tyre load to the subgrade materials.

In reality, asphalt materials illustrate complex viscoelastoplastic behaviour. In this research the focus of modelling is on the UGM. As AC layers always have far stiffer properties, it is not unrealistic to assume linear behaviour for this layer. In practice there may be several layers on the surface consisting of different asphalt materials, but in this modelling all of the asphalt layers are assumed to be a single structural layer whose behaviour is linear elastic. This simplification enables a clearer investigation of UGM behaviour.

The granular layer lies beneath the structural layer (AC) and transfers the tyre load to the existing layer (SG). It is usually made up of two layers of UGM called base and subbase. With respect to design and cost, the differences between these layers are meaningful, but for the purpose of analyzing their mechanical behaviour, the differences are negligible. Therefore, in this simulation all granular layers beneath the AC are assumed to have the same mechanical behaviour.

The final layer is the existing subgrade, which can vary from being strong bedrock to a very soft clay layer. Therefore, two extreme cases are considered for this layer.

#### **4.3.1 Plane strain, Axisymmetric and Three Dimensional Analysis**

Figure 4.1 demonstrates the difference between plane strain, axisymmetric and 3-D models.

As described in Chapter 2, the three major geometrical aspects of modelling are formulation, model dimension and mesh distribution.

As the results of analysis indicate (see Chapter 5) the simulation of pavement layers in plane strain leads to a considerably conservative design. Therefore, after a comparison of the three types of modelling, plane strain modelling was ignored for the rest of simulation.

The results of the axisymmetric and 3-D analysis were quite close, and with respect to the computational efficiency provided by axisymmetric formulation, this type of modelling is preferable. However, the main disadvantage of axisymmetric modelling is its restriction for modelling multiple axles and tyres.

For this reason, the axisymmetric model was used in verification modelling (simulating the results of a triaxial test) or the loading of a single circular tyre on the pavement. The main simulation undertaken in the current study was conducted using full 3-D modelling.

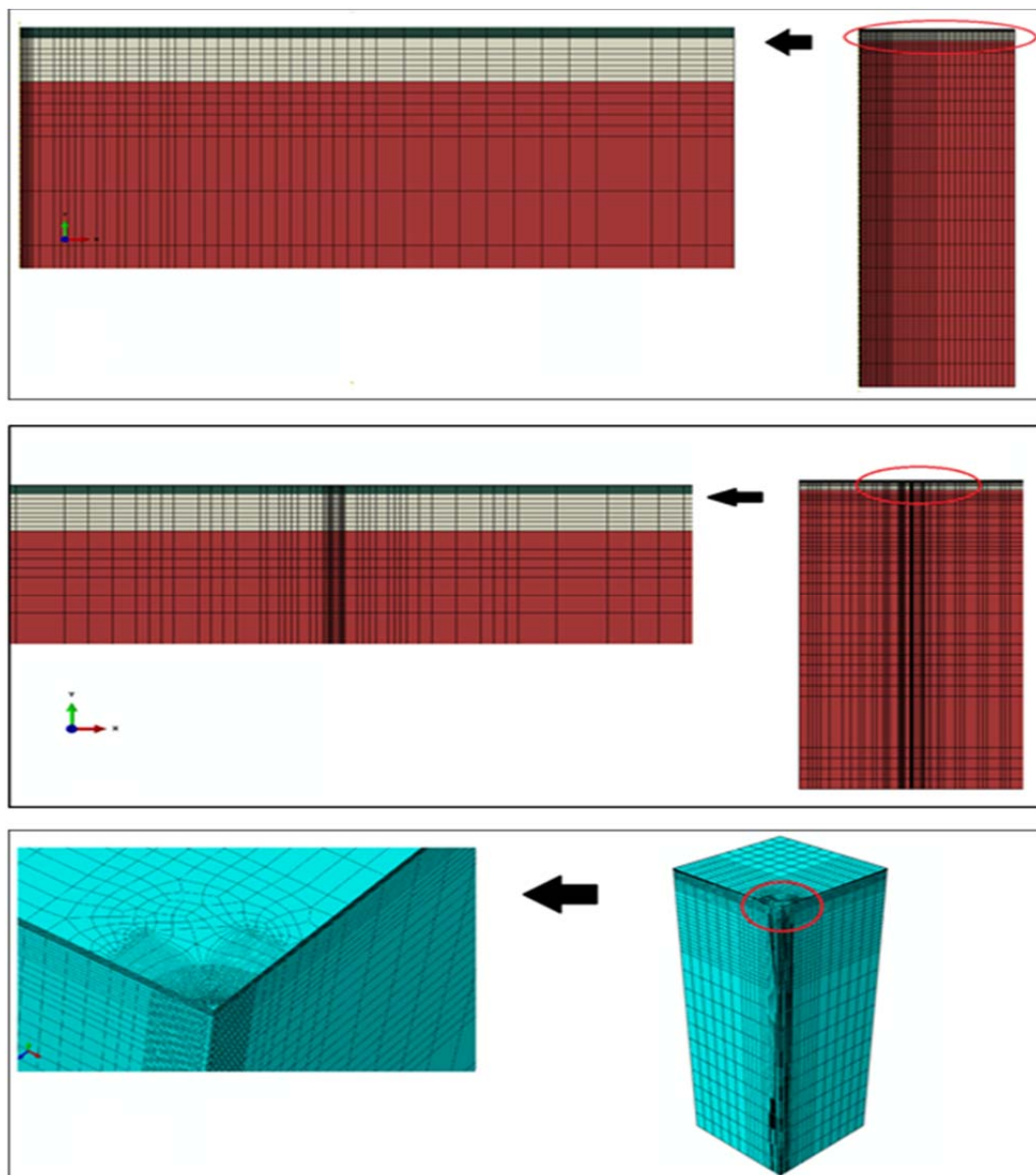


Figure 4.1 - Axisymmetric, Plane Strain and 3D Model

Regarding the model's dimensions, a series of analyses were conducted to investigate the influence of the model's limits and boundary conditions on the critical response of the pavement in the studied area. The results of the FEM were compared against the results calculated by the CIRCLY and KENLAYER programs which are based on analytical solutions. Proper model dimensions were then chosen for each case of axisymmetric and 3-D simulation.

For the dynamic analysis, a set of boundary elements (described in Chapter 3) was used to eliminate the wave reflection phenomenon in the simulated medium. However, to achieve greater accuracy, the limit of the models was set to be further than what was calculated in the static analysis.

While there are unlimited possibilities for layer composition, the general mechanical behaviour of pavement structure can be categorized as either thin asphalt layer or thick asphalt layer. The thickness of the UGM layer is then determined according to the thickness of the AC layer. In this regard, two typical thickness compositions were selected to study the different mechanical responses of pavement structure.

The first composition was a thin layer of asphalt concrete lying on a thicker layer of UGM supported by SG. The second model simulated a relatively thick layer of asphalt on a thinner layer of aggregates. Since the subgrade layer is supposed to be the final layer included in the simulation, sufficient depth is selected to eliminate the effects of boundary conditions.

#### **4.3.2 Interface Element**

Layer interaction can play a role when a dynamic analysis is considered. In dynamic analysis the difference between the responses of layers with different materials can produce inconsistencies in load translation between structural and granular layers.

The interface of layers with different material behaviour can have a meaningful effect on the final mechanical response of those layers. This effect is of interest to researchers and is called the ‘soil-structure interaction’ effect. The phenomenon has a greater effect if the materials’ mechanical properties are significantly different.

Where two different layers are assumed to stick together roughly, their deformation is the same in the shared area. However, in reality, the deformation of asphalt layer in respect to the granular layer depends on the mechanical behaviour of their interface. This interface may demonstrate a cohesive behaviour, a frictional behaviour or a roughly joined behaviour.

The AC-UGM interaction is induced for two main reasons. First of all, the stiffness of the layers (elastic modulus and Poisson ratio) is different. This difference leads to stress concentration on the interface layers. The second reason is the difference between the constitutive models used for AC and UGM. While the AC layer is assumed to be linear elastic, a different nonlinear elastoplastic behaviour is employed for the UGM layer.

To consider the effects of layer interaction in dynamic loading, frictional interface behaviour was assumed between the AC and UGM layers. The interaction between the UGM and SG layers was not considered because the mechanical

behaviour of the two is very similar and there is little difference between the material properties.

Figure 4.2 illustrates the interface elements used in this study.

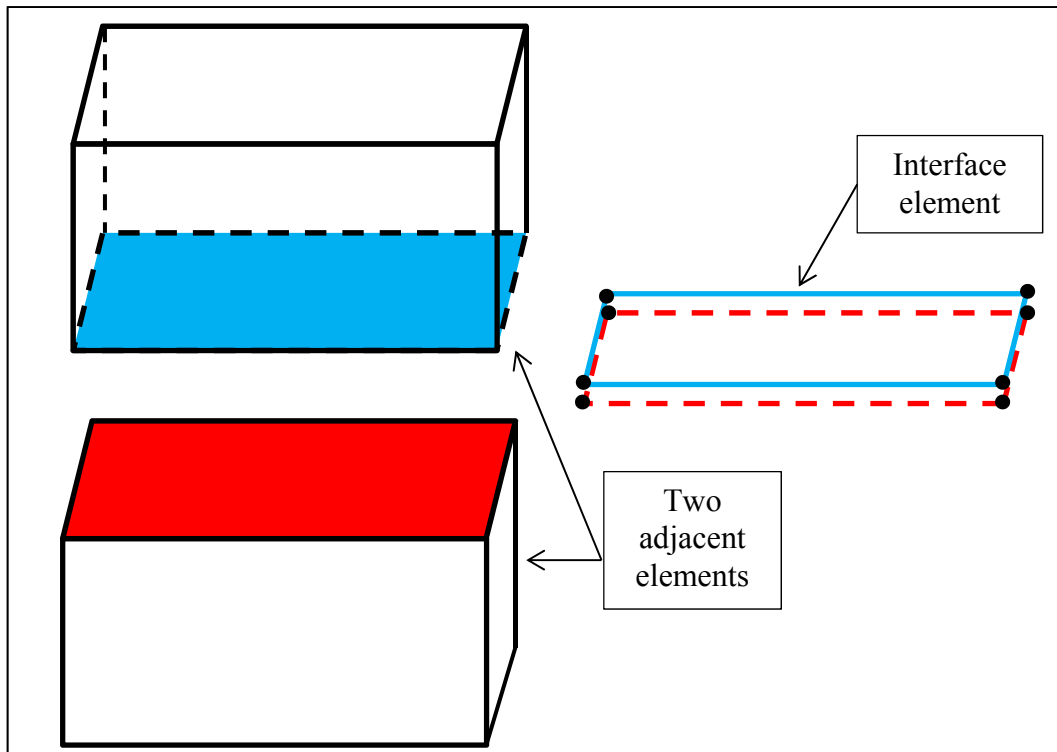


Figure 4.2 - Interface Elements

Interface elements are elements with virtual thickness. This means that while their physical thickness is zero, they can have two different sets of nodes in one place. Using this technique, variation between the deformation of two adjacent elements is possible. This variation induces interaction force which is transferred through the interface elements to both neighbour elements.

#### 4.4 Modelling of Load and Boundary Conditions

The other important factor whose influence should be considered is load. Loading should be simulated in a way that can truly represent the actual loading conditions in the field, however this is not completely achievable. Some simplification in the distributed pressure of tyres on the pavement surface is therefore assumed.

Regarding the applied load in the model, two aspects need consideration. The first is the load distribution in space (including pressure distribution and contact area), and the second is load distribution in time (including pressure distribution and speed).

By contrast, as described in Chapter 3, the boundary conditions for FEM are treated as an external force in the simulated models. Therefore they should also be consistent with the type of analysis (whether it is dynamic or static analysis).

The following sections present the details of assumptions regarding the distribution of pressure in space and time. Also the selection of boundary conditions for the static and dynamic analyses is discussed.

#### **4.4.1 Pressure Distribution**

Two contact areas for loads are considered in this modelling. The first is a circular area with a radius of 9.2 cm (in accordance with the Austroads (2004) guide). The other is an equivalent rectangular contact area (according to Huang (2004)).

The circular area of loading is mainly assumed during the axisymmetric analysis in order to be consistent with the assumed loading area in CIRCLY and KENLAYER.

Two different axles are simulated after the initial linear elastic analysis, as follows: Case 1 with 9 Tonnes on a single axle dual tyre and Case 2 with 17 Tonnes on a tandem axle dual tyre.

The analyses were conducted on the simulation of a single axle dual tyre and a tandem axle dual tyre (according to Austroads (2004)). Figure 4.3 gives a schematic representation of the loading axle and a sample of the FEM model used for the analysis.

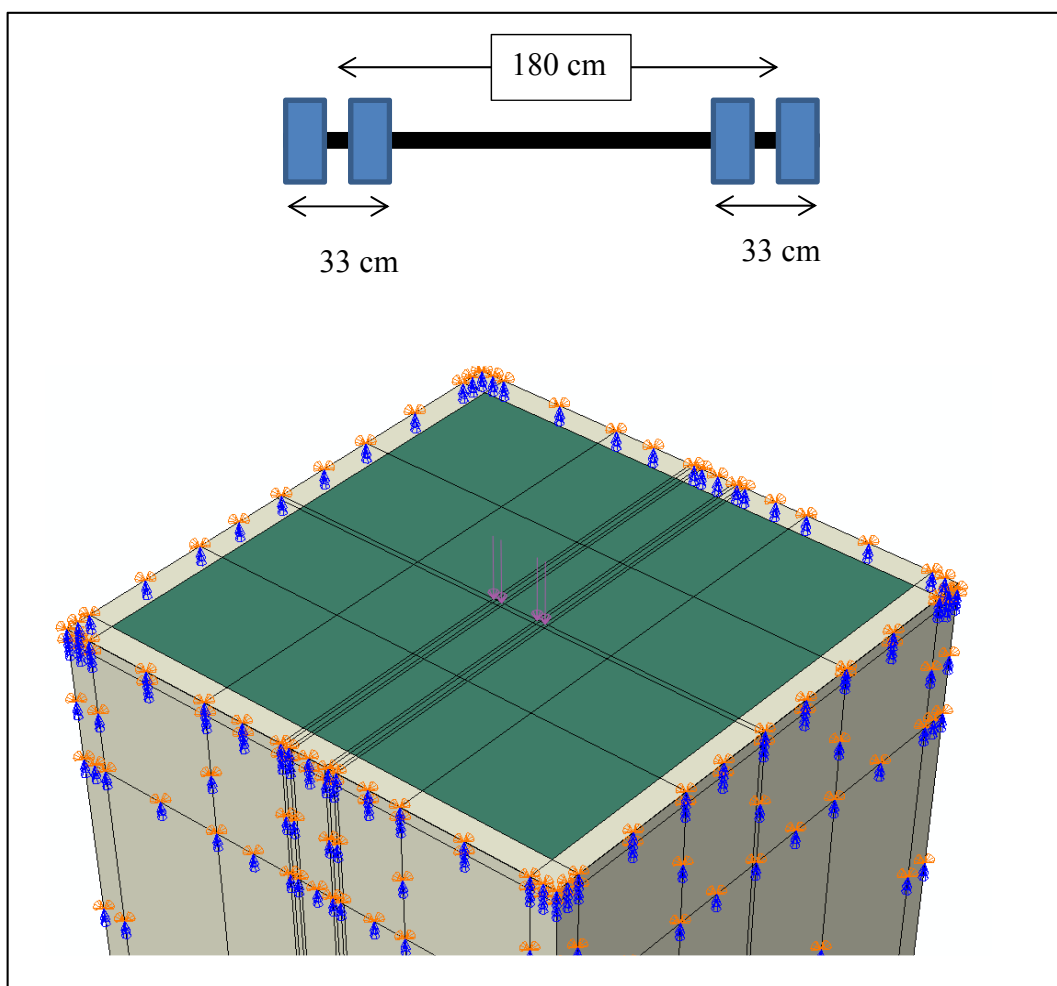


Figure 4.3 - Single Axle Dual Tyre Loading

Austroads (2004) assume a 750 kPa tyre pressure in their design guide. The pressure distribution can be uniform or in other forms such as a sinusoidal shape. However, in this thesis a uniform distribution of tyre pressure is assumed for the purpose of modelling.

#### **4.4.2 Static and Dynamic Loading**

In static analysis, the only effective pressure factor is its distribution over the contact area. However, in dynamic analysis another factor also contributes. When conducting dynamic analysis, the distribution of pressure in time should be taken into account. Different pressure distributions can be assumed, such as triangular, sinusoidal or haversine. Figure 4.4 illustrates the three forms of pressure wave in time.

In this research, haversine loading is used as it can properly represent the tyre loading cycle on the pavement surface. The pulse of the stress is not continuous in actual loading and there is a gap between each pulse. This effect is also taken into consideration and is described in detail in Chapter 6.

To correlate the actual speed of the vehicle to loading frequency, the study conducted by Barksdale (1971) is employed. The same source has been utilized by other numerical researchers as well (Bodhinayake 2008; Hadi and Bodhinayake 2003). The effects of vehicle speed can then be managed by changing the frequency of haversine pressure loading on the pavement.

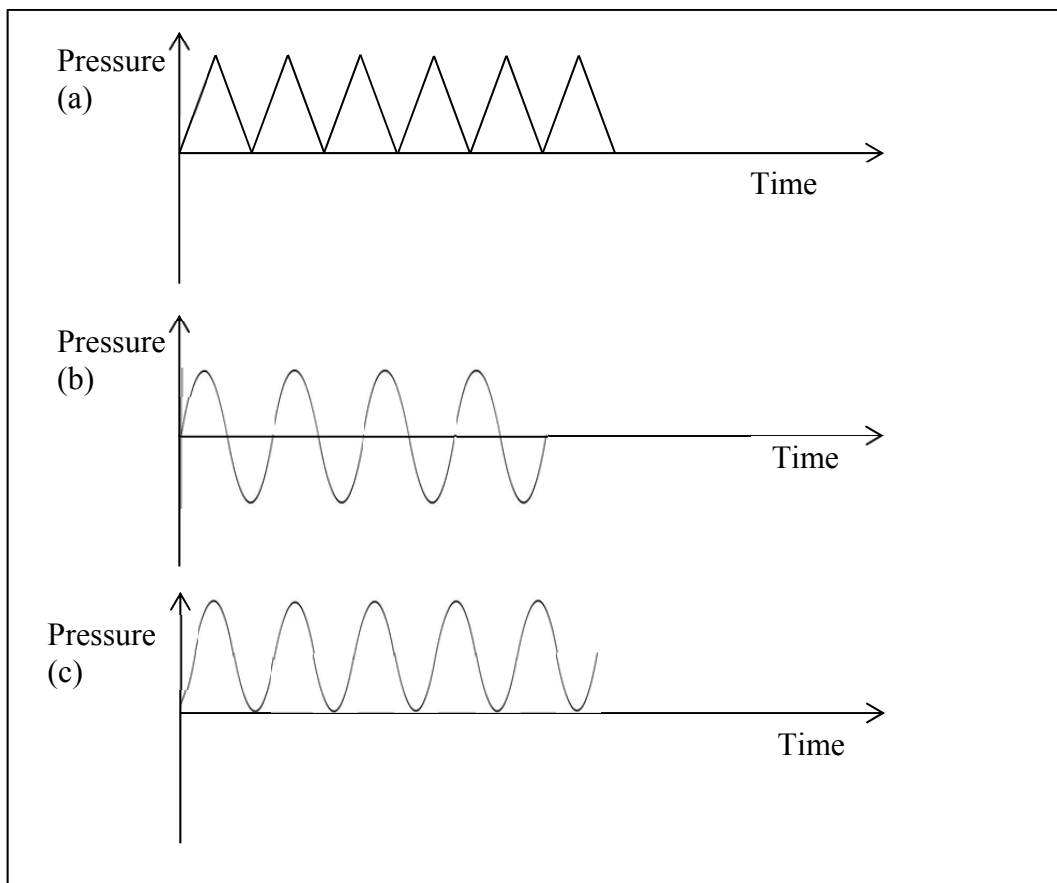


Figure 4.4 - Distribution of Pressure in Time  
 (a- Triangular b-Sinusoidal c- Haversine)

Based on what is stated in this section, two different magnitudes of loading (low and high) are selected for static analysis. While the effects of parameters have been studied in the static analysis, these were avoided in the dynamic analysis mainly because of the very long computation time required by dynamic analysis. Therefore, in the dynamic analysis the main focus was on the effects of material behaviour and the interactions between layers.

#### 4.4.3 Boundary Conditions

Chapter 2 discusses the proper dimensions of a modelled area required to avoid noticeable error. In static analysis, a set of roller conditions was applied on the sides of the model while an encastré condition was required for the bottom. Figure 4.5 represents the schematic boundary conditions used for the static analysis.

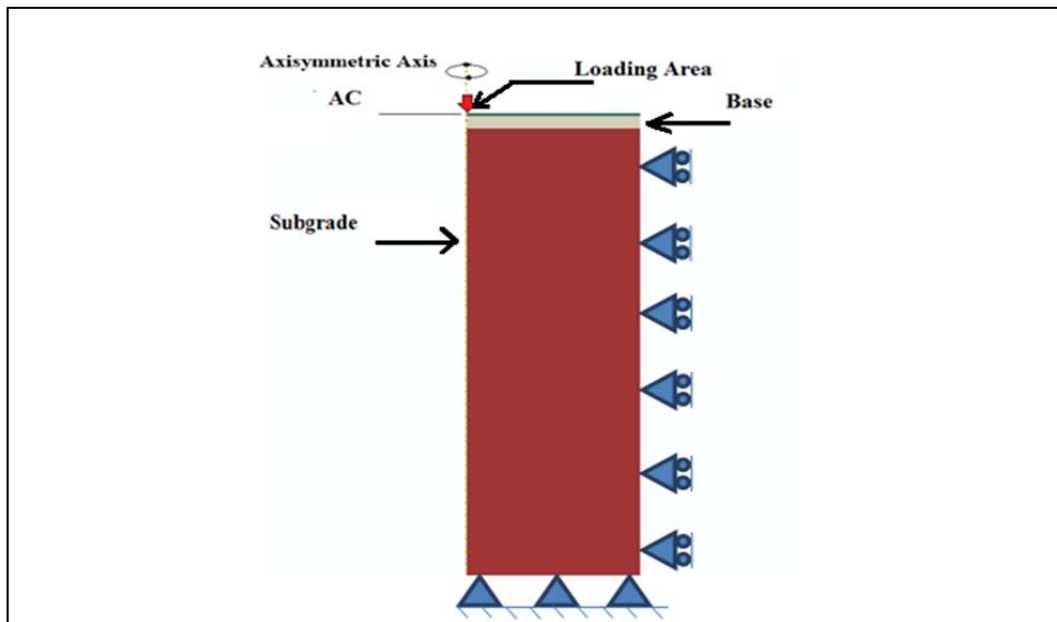


Figure 4.5 - Boundary Conditions of Static Analysis

The rollers on the sides ensure free displacement in a vertical direction while preventing horizontal displacement. The encastré condition at the bottom prevents all displacement, velocity, acceleration and rotation.

As described in Chapter 3, infinite elements are employed to prevent pressure wave reflection in the dynamic analysis. Figure 4.6 illustrates the usage of infinite elements in a sample model as a boundary condition in a dynamic simulation.

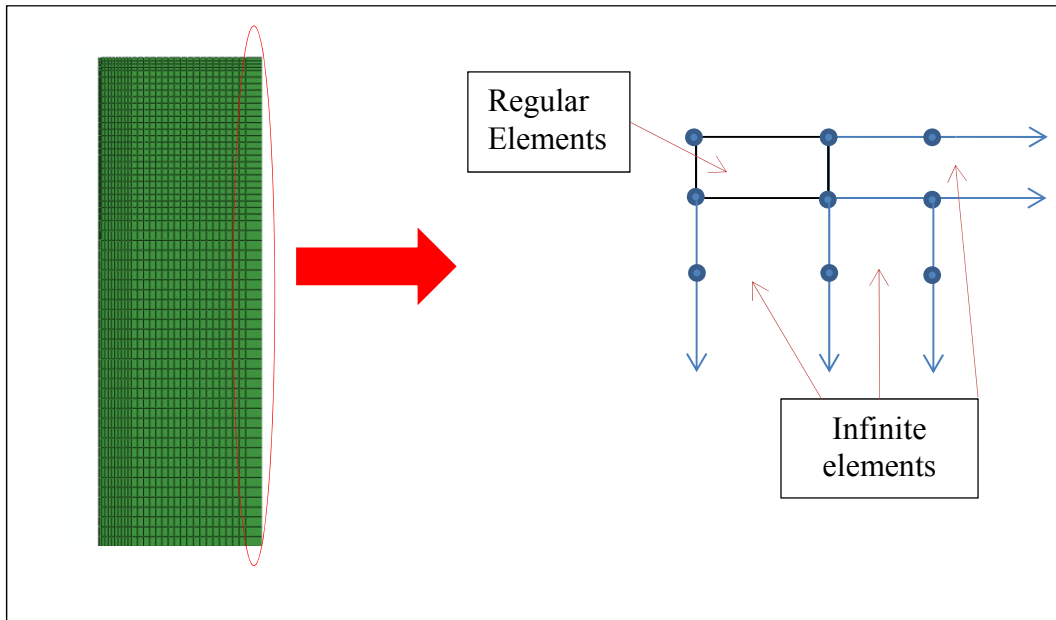


Figure 4.6 - Infinite Element in ABAQUS Mesh

Having specified the loading and boundary conditions for each analysis, the next section describes the details of the material constitutive models and coding algorithms used in this research.

#### 4.5 Modelling of Materials

This section describes the details of the material constitutive models and the implementation of those models in the numerical simulation. The material modelling generally includes five types of constitutive models: (a) linear elastic,

(b) nonlinear elastic, (c) linear elastoplastic, (d) nonlinear elastoplastic, and (e) nonlinear elastoplastic considering shakedown effects.

The details of the mathematical equations for each of these models were discussed in Chapter 3. This section presents a schematic algorithm for the implementation of each of these models.

Finally it should be pointed out that two different material compositions (weak and strong) were considered for the simulation.

#### **4.5.1 Linear and Nonlinear Elastic**

When linear or nonlinear elastic properties are assumed for material behaviour, the material characteristics are controlled only by a material stiffness matrix. The ABAQUS program has the ability to completely model the linear elastic behaviour of materials; however, there is no specific prepared materials model responding to stress dependent, nonlinear constitutive models.

Figure 4.7 represents the coding algorithm for implementing the linear and nonlinear elastic materials constitutive model in the FEM simulation. The matrix **C** in this figure is the constitutive matrix described in Chapter 3.

In linear elastic materials this matrix is merely determined according to the material characteristics. In the case of nonlinear elastic, however, the state of stress also contributes to the calculation of matrix **C**.

Figure 4.8 represents the calculation steps for **C** in the case of a stress dependent, nonlinear elastic material constitutive model. In this figure, **D** is the user-specified accuracy which controls the approximation of nonlinear matrix **C**.

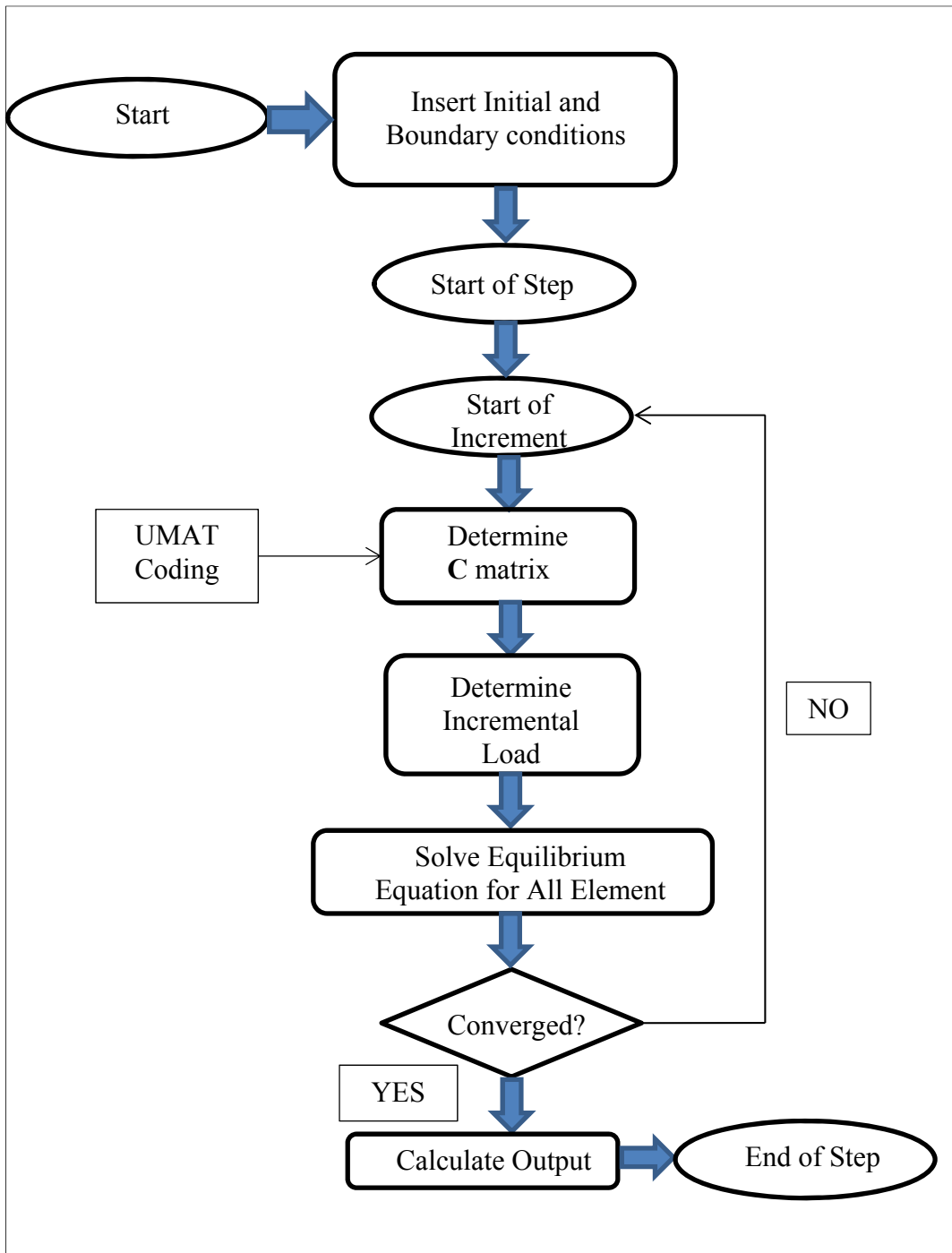


Figure 4.7 - Schematic Algorithm for Elastic Constitutive Model

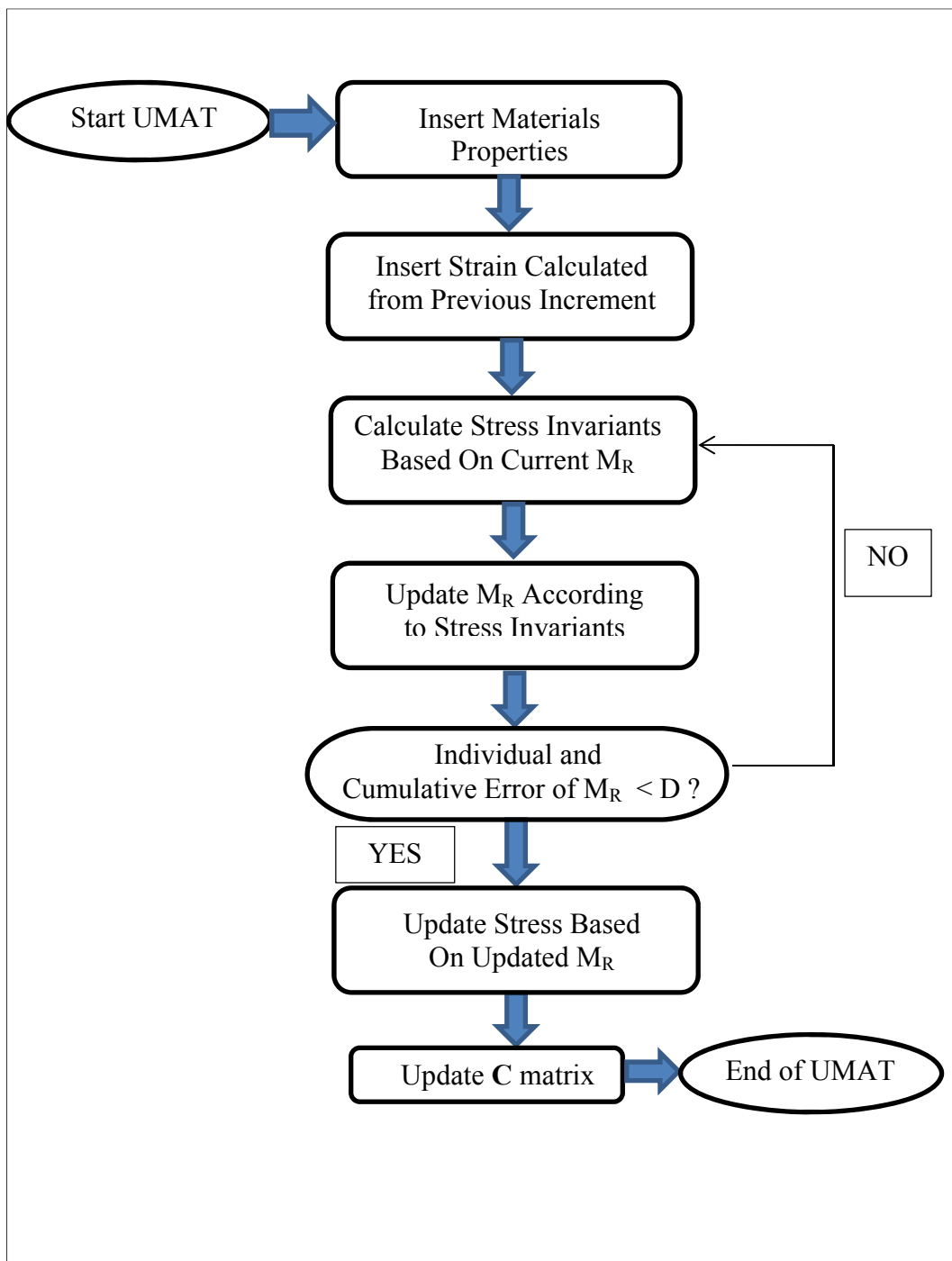


Figure 4.8 – Schematic Algorithm of Nonlinear Constitutive Model

Based on the algorithms presented in Figure 4.7 and Figure 4.8, linear and nonlinear elastic simulations were conducted. The next section presents the algorithm for including linear and nonlinear elastoplasticity.

#### **4.5.2 Linear and Nonlinear Elastoplastic**

Considering the plasticity of materials necessitates the application of a yield criterion. As stated earlier in this study, the Mohr-Coulomb yield criterion was chosen to represent the behaviour of materials after yield.

UGM behaviour was assumed to be elastic (either nonlinear or linear) till the stress state exceed the defined yield criterion. Then the stress, strain (including the elastic part and plastic part) and material Jacobian was modified according to the stress state and criterion.

Figure 4.9 demonstrates the schematic algorithm for taking the elastoplasticity of materials into account.

As stated in Chapter 3, the procedure for calculating the yield criterion is the return mapping technique (Clausen, Damkilde and Andersen 2007). In this technique the stresses are firstly predicted by the current elastic matrix, and are then compared to the allowable yield stress calculated from Mohr-Coulomb criterion. If the predicted stresses exceed the allowable yield stress, then the stresses are modified. In this modification, the amount of elastic stress which is below the yield remains, and the rest of the predicted stress is modified by substituting the exceeding elastic stress for plastic stress. It should be noted that the elastic part of stress can be calculated as linear elastic (Figure 4.7) or nonlinear elastic (Figure 4.8).

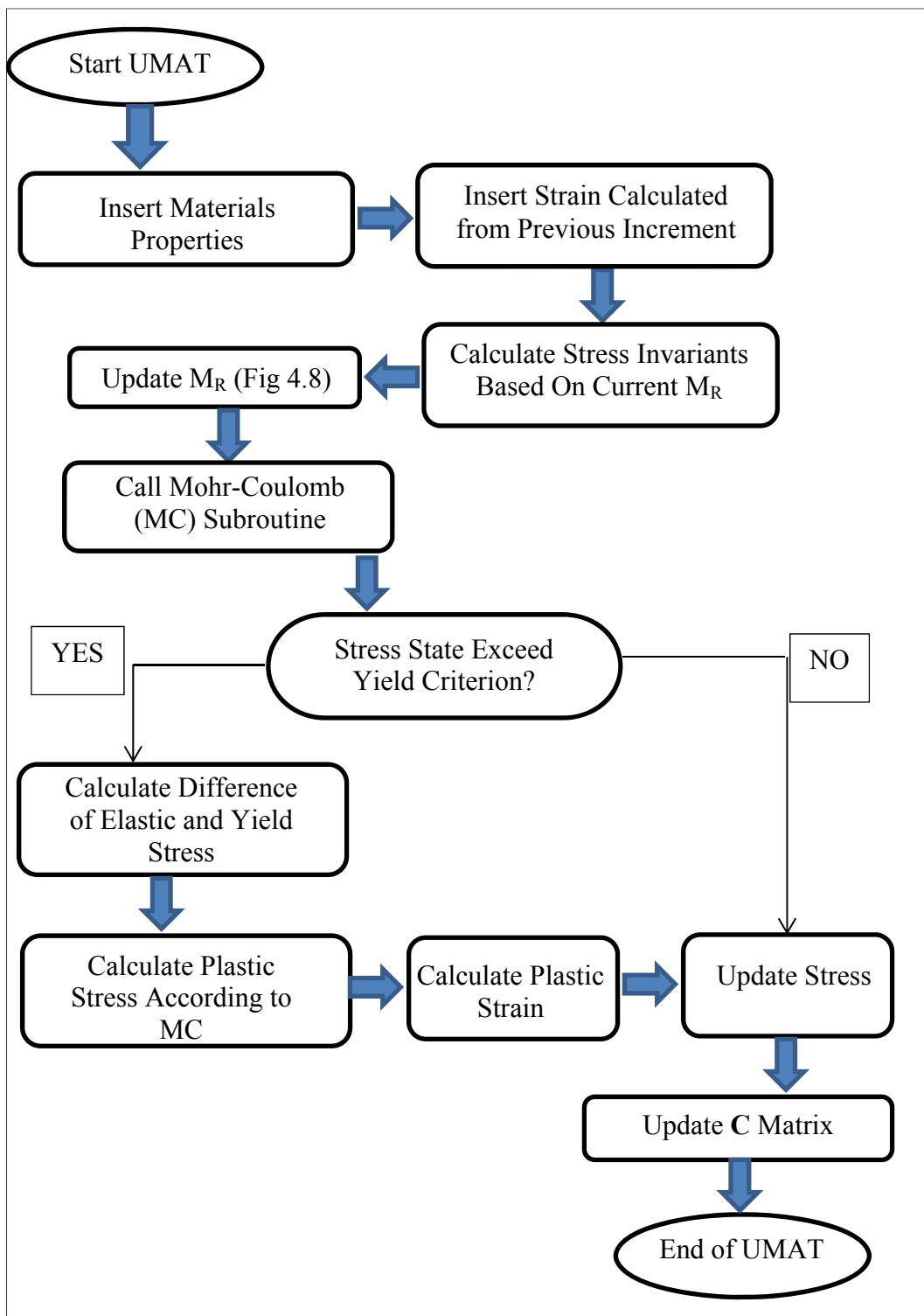


Figure 4.9 - Schematic Algorithm of Elastoplastic Model

### **4.5.3 Shakedown Model**

This section describes the material constitutive model developed to account for shakedown behaviour. In order to incorporate the shakedown effect into the analysis along with the Mohr-Coulomb yield criterion and nonlinear elasticity, a UMAT coding has been developed.

The method described in section 3.3 of Chapter 3 and the equations regarding shakedown are included in this section.

Figure 4.10 illustrates the schematic algorithm for elastoplastic materials taking shakedown effects into account. As can be seen, the first thing that needs to be determined is whether or not shakedown occurs according to the stress state at the initiation of the step. Then if shakedown occurs, the Mohr-Coulomb yield criterion can be modified based on the equations provided in Chapter 3. Moreover, the plastic stress and strain are subject to a decay function ( $f$  function described in Chapter 3) which is dependent on the number of cycles.

Finally it should be noted that the shakedown analysis can only be conducted in the dynamic analysis and its effects are not visible in the static analysis.

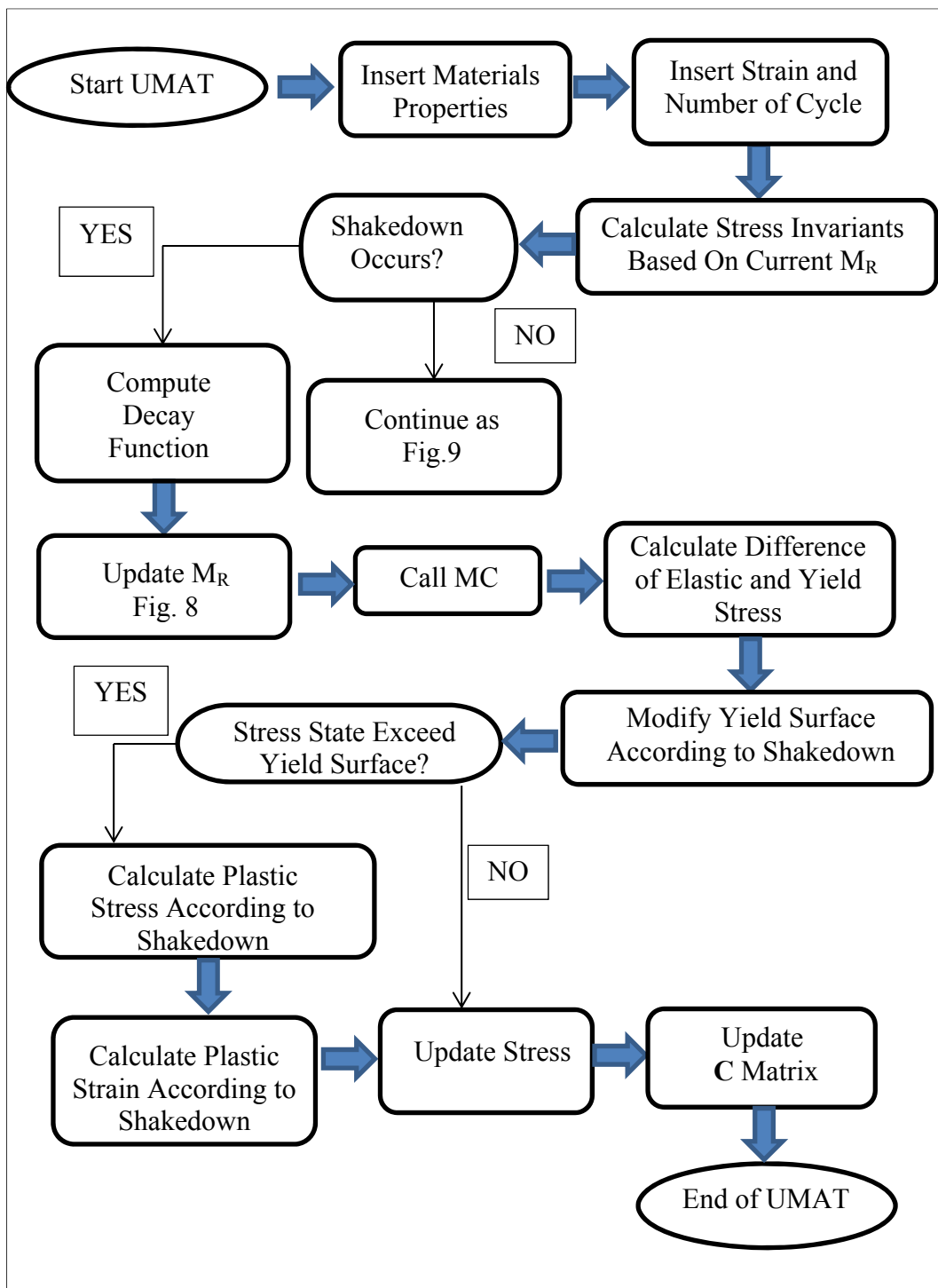


Figure 4.10 - Schematic Algorithm of Shakedwon Model

## **4.6 Summary of the Chapter**

This chapter described the aims and objectives of the simulation process and introduced the simulation process and the characteristics of the simulation. Specific details of the modelling boundary conditions in the static and dynamic simulations and concerns regarding their influence on the results were discussed. Aspects of modelling to be investigated and the reason for the investigation were also pointed out, and finally the approach selected for the simulation was introduced.

Separate sections described in detail the characteristics of the factors influencing the simulation such as layer interaction and geometries, load amplitudes and boundary conditions and material properties.

Since this research is mainly intended to make a contribution to developing a new material model for simulating granular behaviour of pavements under both static and dynamic loading, the chapter presented details of different constitutive models used in a series of analyses. Moreover, the algorithms for the implementation of this constitutive model in an FEM analysis were also presented in order to facilitate any future research along the same lines.

## **CHAPTER 5**

### **5: STATIC SIMULATION OF LAYERED FLEXIBLE PAVEMENT**

#### **5.1 Introduction**

This chapter discusses details of the model construction for the numerical simulation of layered flexible pavement under static loading. The main focus is on the effects of different constitutive models used to simulate granular layers, especially base and subgrade.

Another major focus of this chapter is the evaluation of the constitutive model, starting with the linear elastic simulation, and progressing to the nonlinear elastic, linear elastoplastic and finally nonlinear elastoplastic constitutive models and their effects on the results for simulated layered pavements.

Factors other than the constitutive models are also considered. The modelling includes two different types of layered geometry (thin and thick asphalt layer), two different types of loading (standard and heavy loading) and two different material characteristics (weak and strong).

Mesh sensitivity analysis and the effects of modelling dimension (2-D or 3-D) are investigated in the linear elastic part of the investigation. The results are also checked using linear elastic programs (CIRCLY and KENLAYER).

In the final section of this chapter, general remarks are made regarding the results of the simulation.

## **5.2 Static Analysis**

In this section, the results of the analyses are categorized according to the constitutive model used to simulate the responses of granular layers, resulting in four types of analysis.

The analyses in which all materials are assumed to behave linear elastically form the first type of simulation. In this class, mesh refinement and effects of boundary condition are investigated. The results can be compared with the other classes.

The second class of analysis consists of those with nonlinear elastic constitutive models. The different nonlinear elastic models previously reviewed in Chapter 2 are now implemented in the numerical simulation and the results are presented.

The third class of analysis considers the effect of using a plastic cap to simulate the failure of granular materials. This class of analysis, however, does not assume nonlinear behaviour while in the elastic domain.

The fourth class of analysis considers the nonlinearity of material in the elastic domain while the plastic cap is also used. Finally, the results from all four classes are compared and discussed.

### **5.2.1 Linear Elastic Analysis**

The first part of the linear elastic analysis studies the effects of mesh refinements and model dimensions and the results are compared using the linear elastic software. The main aim of this part of the study is to make decisions about further

simulations and determine the effects of simplification, if any. It should be mentioned that the results of this geometrical investigation were published in a paper by ASCE (Ghadimi et al. 2013), and the same results and explanations are reused here with permission from the publisher.

The sample section of layered pavement with the same material properties and loading characteristics are modelled in CIRCLY, KENLAYER and ABAQUS. Figure 5.1 illustrates the geometrical dimensions of the modelled pavement. The material properties are listed in Table 5.1. All layers are assumed to behave linear elastically under a 0.75 MPa pressure loading, which is applied over a circular area with a 90 mm radius. This is the standard representation of tyre pressure in Austroads (2004).

Figure 5.2 illustrates the geometry of the first constructed model in KENLAYER and CIRCLY. To investigate the effects of geometrical parameters on the analysis, the material properties are assumed to be consistent throughout the whole analysis.

Table 5.1- Material Properties for KENLAYER and CIRCLY Programs

Layer	Thickness (mm)	Elastic Modulus (MPa)	Poisson's Ratio
Asphalt (AC)	100 or 200	2800	0.4
Granular (Base/Subbase)	400 or 500	500	0.35
Subgrade	Infinite	62	0.4

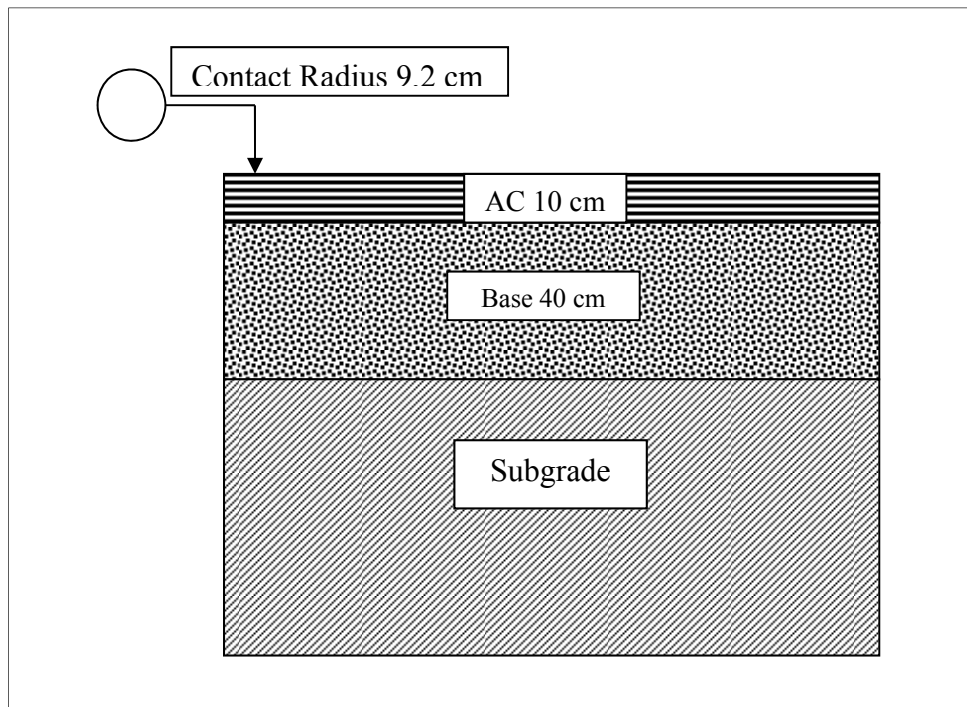


Figure 5.1- Geometry Constructed Model in KENLAYER and CIRCLY

Figure 5.2 illustrates the geometry of the FEM axisymmetric model. The geometry of the model in ABAQUS cannot be the same as in CIRCLY and KENLAYER, as the horizontal and vertical dimensions must be finite in the model. As discussed in Chapter 2, to overcome this problem Duncan, Monismith, and Wilson (1968) suggested a dimension of 50-times R (loading radius) in the vertical and 12-times R in the horizontal direction. Kim, Tutumluer, and Kwon (2009) found good agreement between the results of the FE analysis and KENLAYER when the model dimension was 140-times R in the vertical and 20-times R in the horizontal direction. In this study, the dimensions of the model have been selected as 55.55-times R in the horizontal direction and 166.70-times R in the vertical direction. The same ratio has been selected for the plane strain and three-dimensional models.

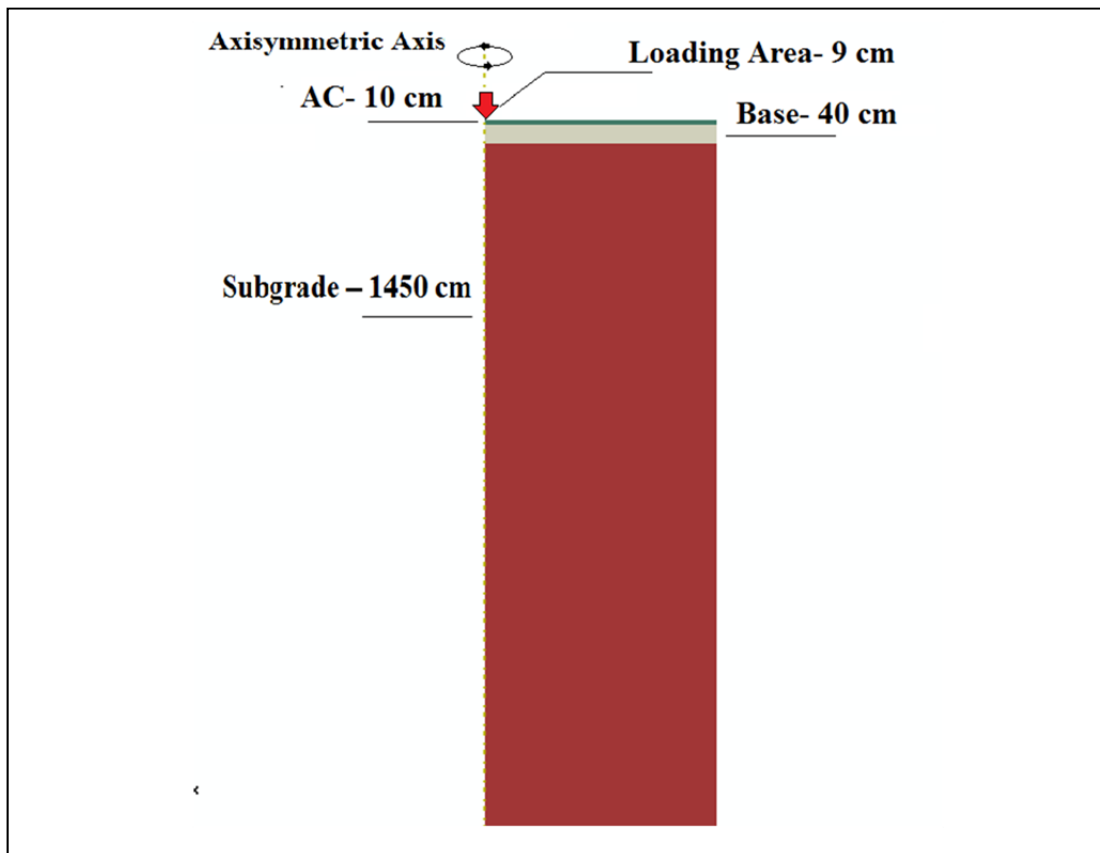


Figure 5.2- Geometry of The Axisymmetric Model

The next step is to investigate the mesh density and element type. Figure 5.3 illustrates the constructed FE meshes for the axisymmetric, plane strain and 3-D analyses.

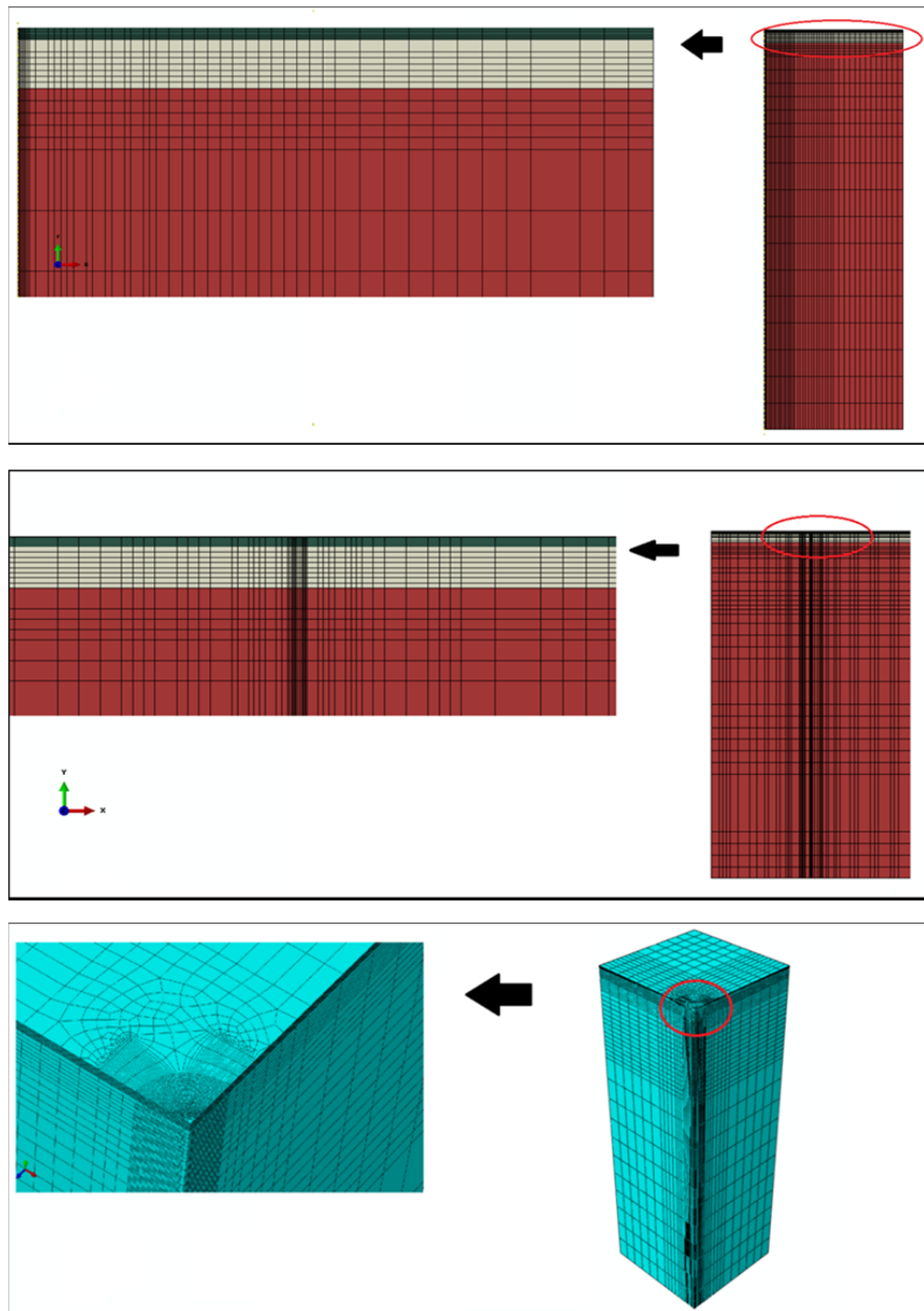


Figure 5.3-Mesh Distributions for The Models

The vertical boundaries of the finite element model are modelled using roller boundary conditions which permit displacement in the vertical direction but prohibit it in the horizontal direction. The lower boundary of the model is fixed in every direction (called encastré). For axisymmetric and 3-D models, two different types of element and two mesh densifications were modelled separately.

Three axisymmetric models were investigated: the dense axisymmetric model has 12,656 8-node biquadratic axisymmetric quadrilateral elements; a normal axisymmetric model with 2280 of the same elements; and for the same number of elements (2280) a model was constructed with 4-node bilinear axisymmetric quadrilateral elements.

The three-dimensional model was also investigated by varying the element types and mesh density. The first model had 86,730 20-node quadratic brick elements; the second model had 35,000 of the same elements and the third model had 35,000 8-node linear brick elements.

The effects of model dimensions is now investigated. The first step of this analysis is to compare the elastic solutions and FEM solutions in order to determine the range of induced errors in the approximation. In this comparison it was observed that while there was relative agreement among all constructed models, the plane strain results were out of range and not a reasonable representation of the situation.

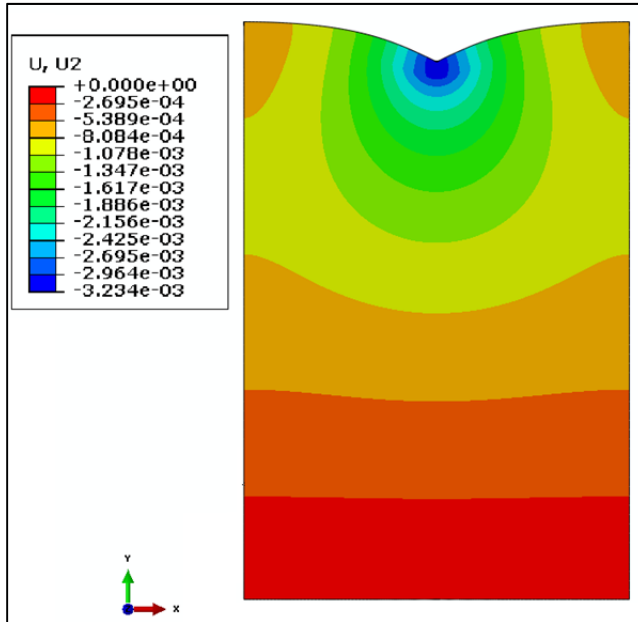


Figure 5.4- Surface Deflection of Plane Strain Model

Figure 5.4, Figure 5.5 and Figure 5.6 show the contours of surface deflection for the three types of model. It is clear from these figures that although the shape of the contours in plane strain analysis is acceptable, the values are significantly larger than those calculated from the three-dimensional and axisymmetric models.

Figure 5.7 illustrates the comparison between the models in terms of surface deflection. It can be seen that all of the FE models demonstrate the least surface deflection. This is not unusual for it is generally accepted that FEM is slightly stiffer than the actual analytical solution (Helwany 2006). More importantly, there is no meaningful difference between the models with dense or normal meshes. This implies mesh independency of the FE models.

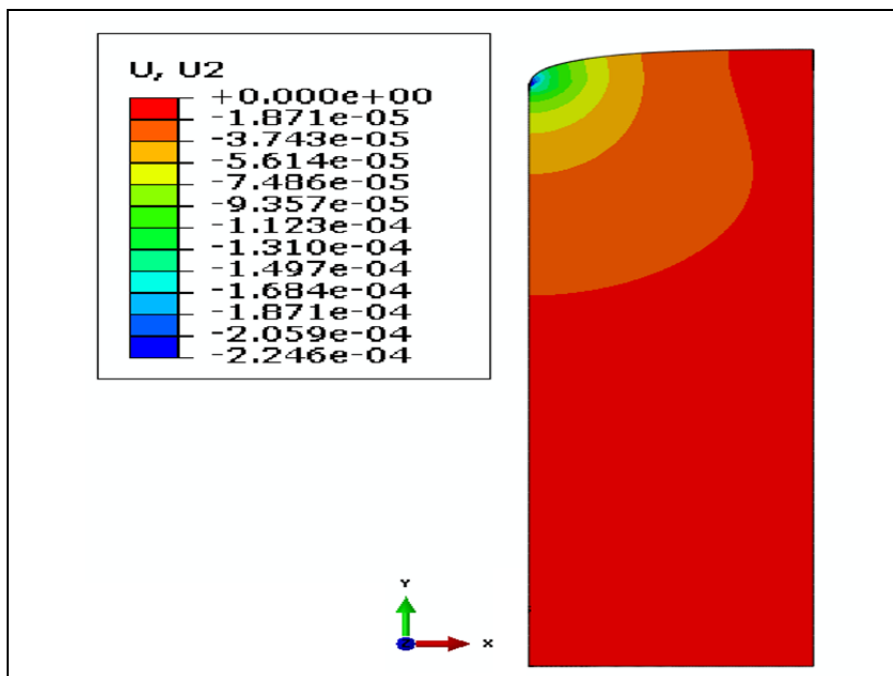


Figure 5.5- Surface Deflection of Axisymmetric Model

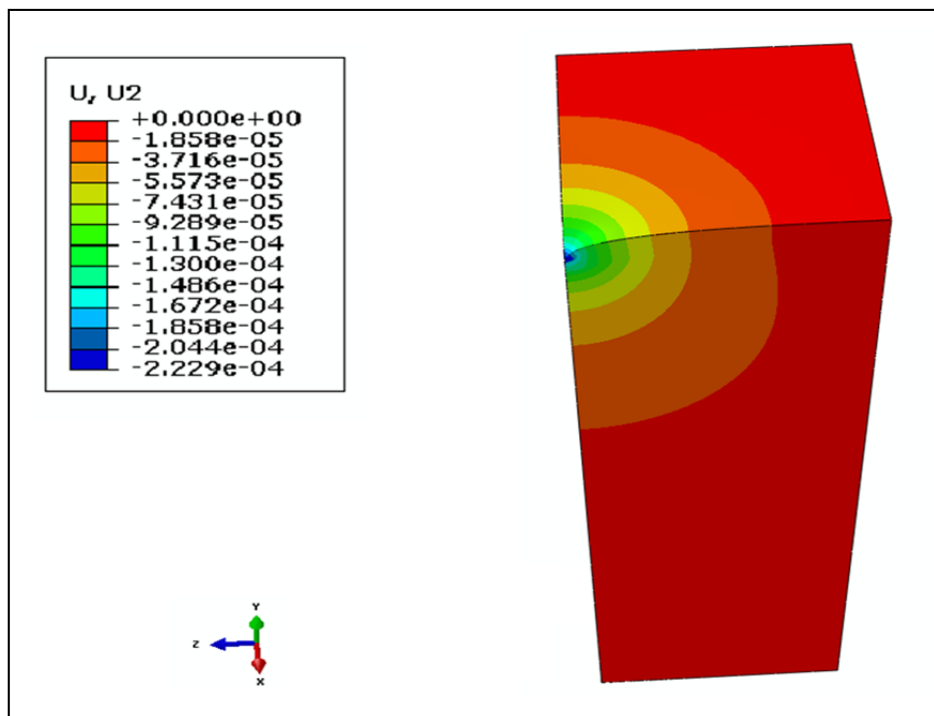


Figure 5.6-Surface Deflection of 3-D Model

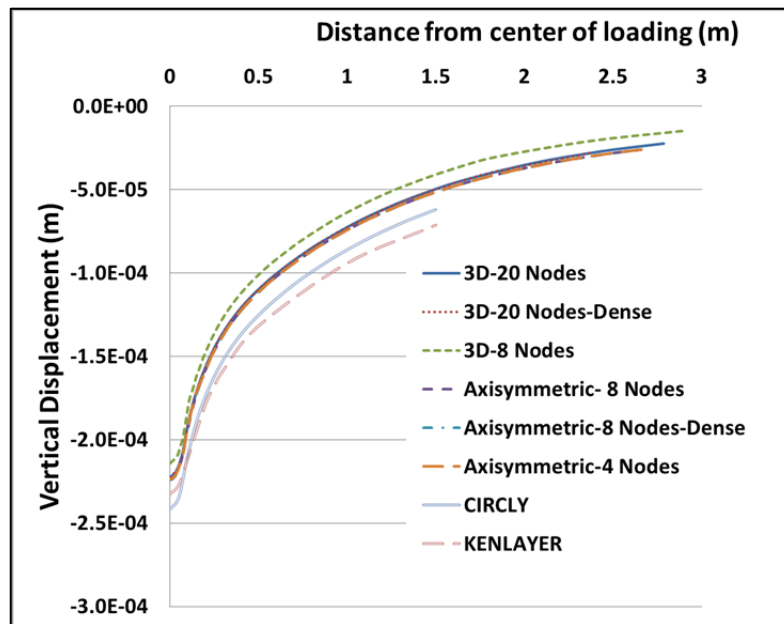


Figure 5.7-Comparison of the Surface Deflections for Different Models

There are four critical responses which play a vital role in flexible pavement design. These responses are surface deflection at the centre of loading, tensile strain at the bottom of the asphalt layer, vertical strain, and stress at the top of the subgrade layer. The values of these four responses for each model are presented in Table 5.2. The plane strain model yielded values considered extreme and not acceptable. For example, when the general surface deflection resulting from the other model was between 0.22 and 0.25 mm, the value calculated by plane strain was 3.228 mm which almost 13 times higher than 0.25 mm. This larger value is attributed to the effect of the loading condition, which was a strip of distributed pressure instead of a circular area as is the case in the 3-D, axisymmetric and analytical solutions. Therefore it can be said that the plane strain assumption will lead to an overestimation of pavement damage.

Table 5.2- Comparison of the Results for Different Models

Model	Vertical Deflection (Top of AC)	Tensile Strain (Bottom of AC)	Compressive Strain (Top of SG)	Compressive Stress (Top of SG)
CIRCLY	0.2417 mm	2.44E-04	9.44E-05	11110 Pa
KENLAYER	0.2327 mm	2.37E-04	9.46E-05	11120 Pa
ABAQUS	3D- Dense	0.2224 mm	2.69E-04	8.94E-05
	3D- 20 Nodes	0.2224 mm	2.60E-04	8.91E-05
	3D- 8 Nodes	0.2048 mm	2.24E-04	8.37E-05
	Axisymmetric-Dense	0.2240 mm	2.61E-04	9.04E-05
	Axisymmetric-8 Nodes	0.2240 mm	2.61E-04	8.91E-05
	Axisymmetric-4 Nodes	0.2238 mm	2.43E-04	8.48E-05
	Plain strain	3.2280 mm	2.95E-04	4.94E-04

The remaining models were in general agreement, however, the results for the 3-D model with 8-noded elements showed greater discrepancies. The error is especially large for the stress calculation in the subgrade layer (12200.4 Pa compared with 11110 Pa calculated in CIRCLY or 11120 Pa calculated in KENLAYER). This difference is due to the inner approximation of the element

(linear interpolation of calculated responses in nodes). Therefore a 4-noded brick should be used with finer mesh density to reach an acceptable approximation.

The second part of the analysis investigates the effect of variations in layer thickness and the influence they have on different models.

Here, three different pavement structures have been studied. The first structure is the same as Figure 5.1 with a 10 cm asphalt layer and a 40 cm base layer. The second structure has a 20 cm asphalt layer and a 40 cm base layer. The third has a 10 cm asphalt layer and a 60 cm base layer. Finite element modelling is in axisymmetric 8-noded element with normal mesh density.

Table 5.3 displays the results of four critical responses for three different pavement structures. There is acceptable agreement among the results, however, the calculated horizontal strain at the bottom of the asphalt layer was higher from ABAQUS than from KENLAYER and CIRCLY, but the difference is less than 10%.

It can be seen that the thickness of the layer does not produce a significant discrepancy in the FEM model, and there is general agreement among the numerical models with other programs.

Table 5.3-Effect of Layer Thickness on The Numerical Approximation

Model	Vertical Deflection (Top of AC)	Tensile Strain (Bottom of AC)	Compressive Strain (Top of SG)	Compressive Stress (Top of SG)
CIRCLY (10-cm AC)	0.2327 mm	2.37E-04	9.46E-05	11120 Pa
KENLAYER (10-cm AC)	0.2224 mm	2.69E-04	8.94E-05	10583 Pa
ABAQUS (10-cm AC)	0.2240 mm	2.61E-04	8.91E-05	10555 Pa
CIRCLY (20-cm AC)	0.1737 mm	9.45E-05	5.46E-05	6462 Pa
KENLAYER (20-cm AC)	0.1595 mm	1.01E-04	5.47E-05	6451 Pa
ABAQUS (20-cm AC)	0.1653 mm	1.10E-04	5.40E-05	6426 Pa
CIRCLY (60-cm Base)	0.2144 mm	2.37E-04	6.56E-05	7696 Pa
KENLAYER (60-cm Base)	0.2053 mm	2.31E-04	6.57E-05	7686 Pa
ABAQUS (60-cm Base)	0.2059 mm	2.60E-04	6.48E-05	7645 Pa

The following points summarize the results:

- (1) In comparison to the analytical solution, axisymmetric solution and 3-D model, the plane strain model results in an extremely severe response by the pavement system. Therefore, this simplification should be used only with extreme caution.
- (2) The 8-node brick elements lead to a stiffer medium and the results of the analysis has a range of 10% approximation. Therefore mesh refinement is necessary for proper approximation.
- (3) The 8-node axisymmetric elements or 20-node brick elements provide a close approximation to the currently used linear elastic solutions.

Based on this initial analysis, the next step of the linear elastic analysis deals with the two constructed models of layered flexible pavements with different materials and loading which are investigated in the following sections.

This part of the study investigates two different types of loading, two different layer thicknesses and two different material properties. Figure 5.8 demonstrates the simulated axles of loading. A single axle dual tyre loading is assumed to have a 9 ton allowable load capacity and a tandem axle dual tyre loading has a 17 ton allowable load capacity. The load is divided by the number of tyres which have a pressure of 0.75 MPa. Then, in accordance with Figure 2.18, the contact area between the tyre and asphalt is calculated in each case.

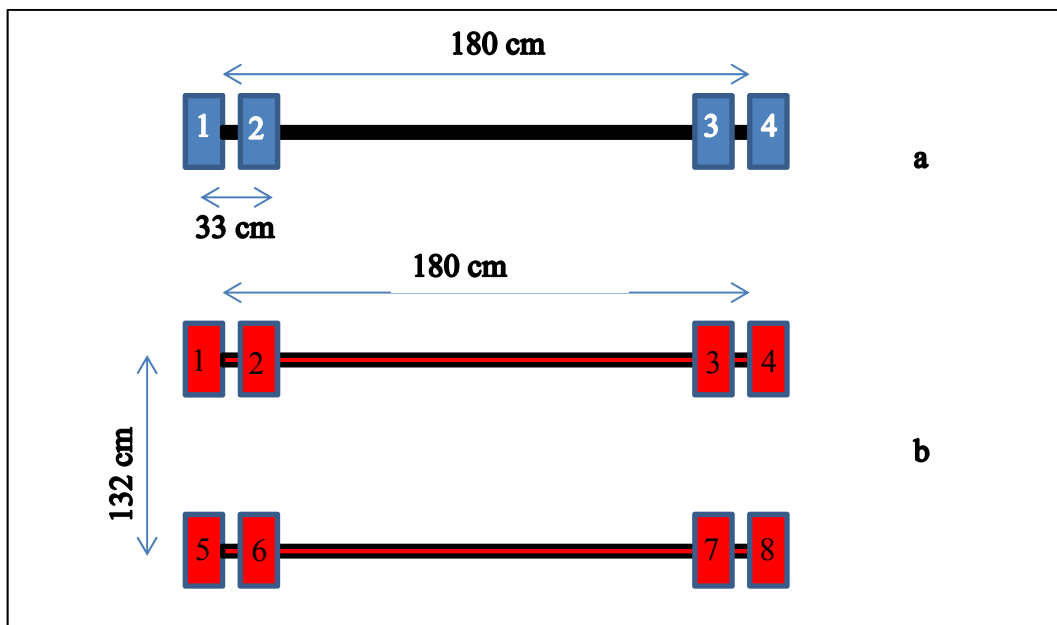


Figure 5.8 - Simulated Loads (a) Single Axle Dual Tyre (b) Tandem Axle Dual Tyre

Table 5.4 presents the two sets of geometries and two sets of material characteristics used for modelling. Eight sets of analyses were therefore conducted to consider the effects of axles, layers and material properties.

Figure 5.9 illustrates the constructed model for two cases of single axle dual tyre (SADT) and tandem axle dual tyre (TADT). The boundary conditions are same as before and the ratio of the boundary conditions in both cases exceeds the value calculated from the previous step. Here it is assumed that the axis parallel to the axle is X, the axis parallel to the travelling direction is Y, and the depth is parallel to the Z axis.

Table 5.4 -Layer's Composition

Layer	Thickness (mm)	Elastic Modulus (MPa)	Poisson's Ratio
-------	----------------	-----------------------	-----------------

	Geo. 1	Geo. 2	M1	M2	
Asphalt (AC)	100	250	2800	2800	0.35
Granular (Base/Subbase)	200	15	200	500	0.4
Subgrade	20000	20000	50	120	0.45

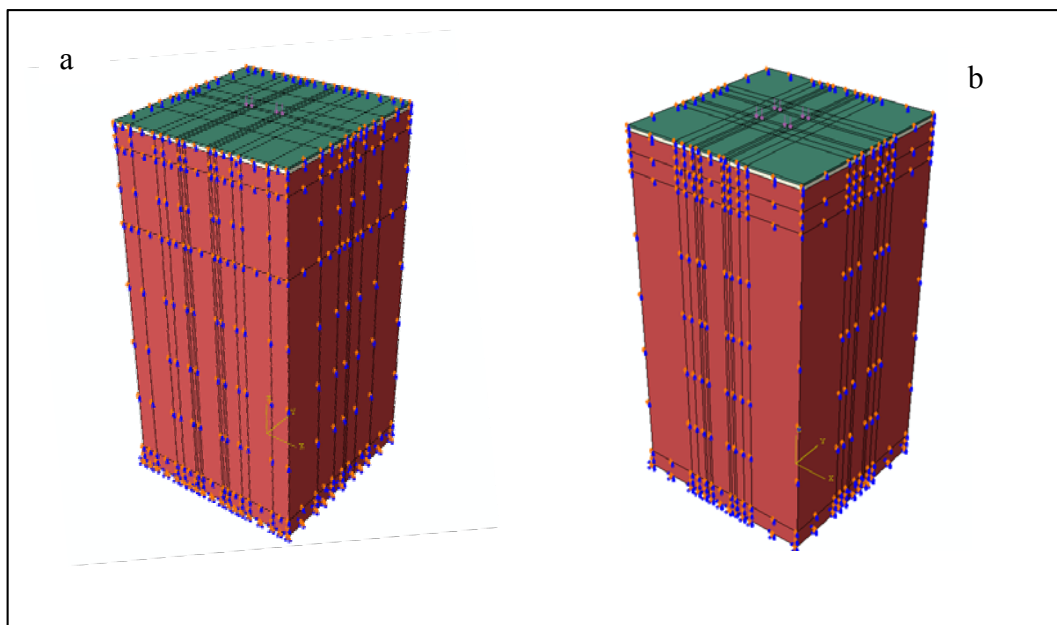


Figure 5.9 - Constructed Models for (a) SADT and (b) TADT

The results of the vertical deformation for geometry 1 and material 1 (Table 5.4) are presented in Figure 5.10. For SADT, the section selected was at the middle of model and parallel to the axle (X-Z-plan), while for TADT the section was at the middle of the model and perpendicular to the axle (parallel to the travelling direction: Y-Z plan).

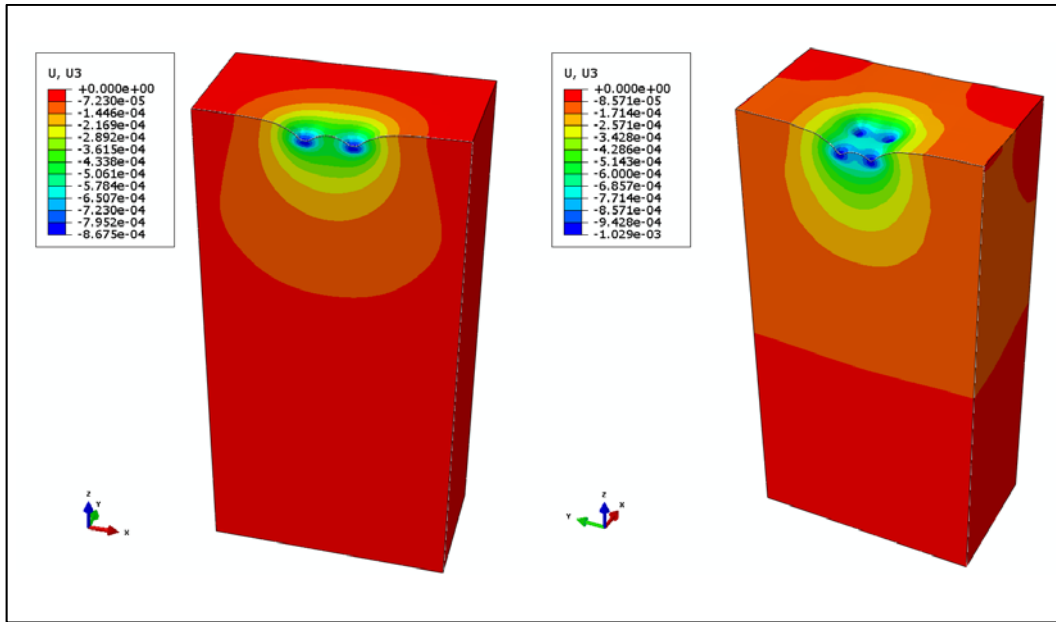


Figure 5.10 - Vertical Deformation of SADT (left) and TADT (right) for Geo1 M1

Finally in this section, the results of the four critical responses of pavement are presented in a table for all of the cases. The responses for both SADT and TADT are calculated along the Z-axis passing from the centre of tyre 2 (Figure 5.8). Table 5.5 lists the four critical responses for all cases. In this table, SADT is indicated by L1 and TADT is indicated by L2. Geometries 1 and 2 are indicated by G1 and G2 and the two materials are indicated by M1 and M2. The results are presented in Table 5.4.

Table 5.5 - Results of 8 Cases of Simulation

Case	Model	Vertical Deflection (Top of AC)	Horizontal Strain (X-Axis) (Bottom of AC)	Vertical Strain (Z-Axis) (Top of SG)	Vertical Stress (Top of SG)
1	<b>G1-L1-M1</b>	0.855 mm	-203E-06	-751E-06	-43658 Pa
2	<b>G1-L1-M2</b>	0.398 mm	-131E-06	-368E-06	-50854 Pa
3	<b>G1-L2-M1</b>	1.010 mm	-198E-06	-674E-06	-40984 Pa
4	<b>G1-L2-M2</b>	0.466 mm	-128E-06	-329E-06	-47313Pa
5	<b>G2-L1-M1</b>	0.555 mm	-60E-06	-310E-06	-19407Pa
6	<b>G2-L1-M2</b>	0.285mm	-41E-06	-187E-06	-26485Pa
7	<b>G2-L2-M1</b>	0.730 mm	-105E-06	-296E-06	-20401Pa
8	<b>G2-L2-M2</b>	0.361 mm	-63E-06	-171E-06	-26402Pa

As can be observed from this table, increasing the asphalt thickness generally reduced the surface deflection and the tensile strain at the bottom of the asphalt layer. For instance, a comparison between Case 1 and Case 5 shows a decrease in surface deflection from 0.855 mm for Case 1 to 0.555 for Case 5 (35% reduction). Here the tensile strain at the bottom of the asphalt layer is reduced from 203 micro-strain in Case 1 to 60 micro-strain in Case 5 (70% reduction).

It is also obvious that applying TADT loading increases the surface deflection and also strain at the asphalt layer and subgrade for thick layer asphalt. For example, comparing Case 5 and Case 7 indicates an increase in surface deflection from 0.555 to 0.73 (32% increase).

Finally, the effect of material characteristics can be seen. The results illustrate that stiffer materials (higher elastic modulus) cause less deflection and strain, but

higher stress. For instance, a comparison between Case 1 and Case 2 demonstrates a noticeable decrease in surface deflection from 0.855 to 0.398 (53% reduction).

The outcome can be interpreted clearer if the effect of material constitutive models is taken into account. This is covered in the following sections. In the next section, the effect of nonlinear elasticity for base materials is studied.

### 5.2.2 Nonlinear Elastic Analysis

This section investigates the effect of nonlinear elastic constitutive models for the UGM used in the base layer of flexible pavement. To achieve this, new subroutines were developed in ABAQUS UMAT to simulate nonlinearity (see Figure 4.8).

The analyses in this section are conducted in three stages. In stage one the verification of coding is examined. This is done by comparing the constructed models of this study with results published in the literature. In the second stage, a series of simulations are conducted to study the effects of implementing different nonlinear constitutive models on the numerical responses of the UGM layer. This study has been submitted as a paper to the journal *Road Materials and Pavement Design* and is reused in this thesis with permission from the publisher. In the final stage of this section, the same eight simulated models which were analyzed in section 5.1.1 are studied now under assumption of nonlinear elasticity of the base layer.

For the purposes of verification, the same material properties and the geometry of the layers used by Kim, Tutumluer and Kwon (2009) were reconstructed in CIRCLY, KENLAYER and ABAQUS. Table 5.6 presents the details of the model's characteristics:

Table 5.6- Material Properties Used for Verification of Nonlinear Elasticity

Layer	Thickness (mm)	Elastic Modulus (MPa)	Poisson Ratio
Asphalt (AC)	76	2759	0.35
Granular (Base/Subbase)	305	207	0.4
Subgrade	20000	41.4	0.45

To minimize the effects of the boundary conditions on the final results, the side is at a 3 m distance from the centre of the load and the bottom is situated 21 m below the loading. The loading is assumed to be a circular area (152 mm radius) and a pressure of 551 kPa is uniformly applied over this area. Therefore the boundary conditions are located as recommended by Kim, Tutumluer, and Kwon (2009). The geometry and deformation of the mesh is illustrated in Figure 5.11.

In this model, the nonlinear elasticity of materials is applied to the same geometry. The material properties are those used by Kim, Tutumluer, and Kwon (2009). Here, the nonlinear constitutive model used is Uzan -1985 for the axisymmetric geometry. The only nonlinear layer is the base layer and the properties of the other layers are the same as those stated in Table 5.1. The properties used for nonlinear materials regarding Uzan equation are  $K_1 = 4.1$  MPa,  $k_2 = 0.64$  and  $k_3 = 0.065$ .

Table 5.7 summarizes the results of this simulation in comparison to the results calculated by Kim, Tutumluer, and Kwon (2009).

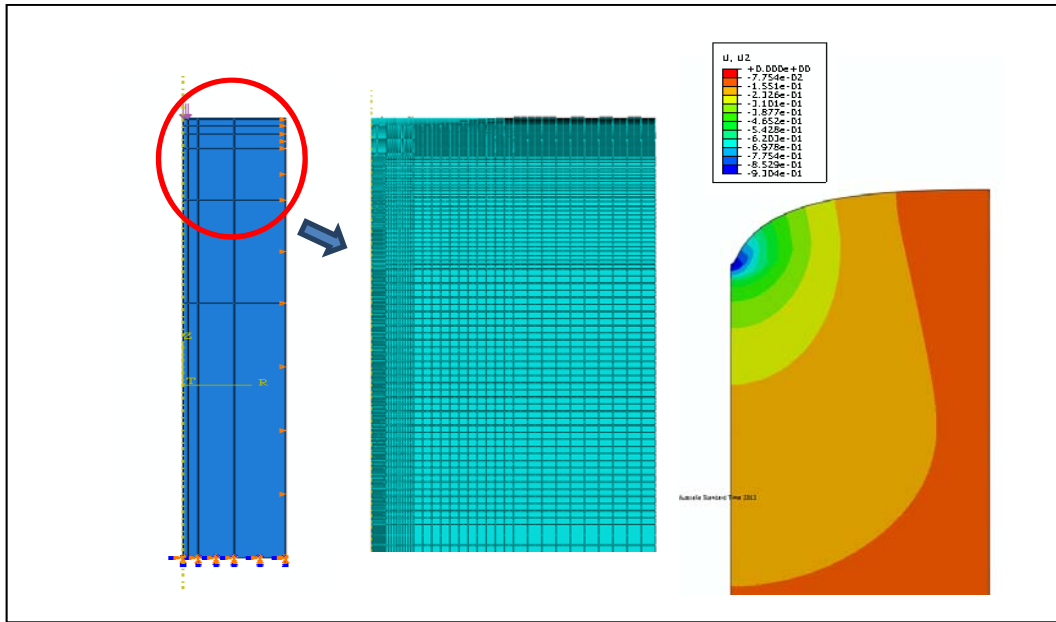


Figure 5.11- Constructed Axisymmetric Model Used for Verification of Nonlinear Elasticity

The same approach as described in the previous section was conducted to check the mesh sensitivity for this model. Comparison of the results of vertical deflection calculated in CIRCLY, KENLAYER and ABAQUS showed that the mesh refinement can deliver the required accuracy for the analysis.

Table 5.7 presents the results of the analysis compared against the published results of Kim, Tutumluer, and Kwon (2009), and a satisfactory agreement can be observed.

Table 5.7- Comparison of the Results of Axisymmetric Model

Critical Response	Current Research (Linear )	Kim-Tutumluer (Linear)	Current Research (Nonlinear)	Kim-Tutumluer (Nonlinear)
$\delta$ (mm) surface	-0.930	-0.930	-1.276	-1.240
$\epsilon_h$ (microstrains) bottom of AC	251	227	312	267
$\epsilon_v$ (microstrains) top of SG	-921	-933	-1170	-1203
$\sigma_v$ (MPa) top of SG	-0.040	-0.041	-0.054	Not Presented

Table 5.8- Model Characteristic of Second Stage of Nonlinear Analysis

Layer	Thickness (mm)	Elastic Modulus (MPa)	Poisson's Ratio
Asphalt (AC)	100	2800	0.35
Granular (Base/Subbase)	400	Variable	Variable

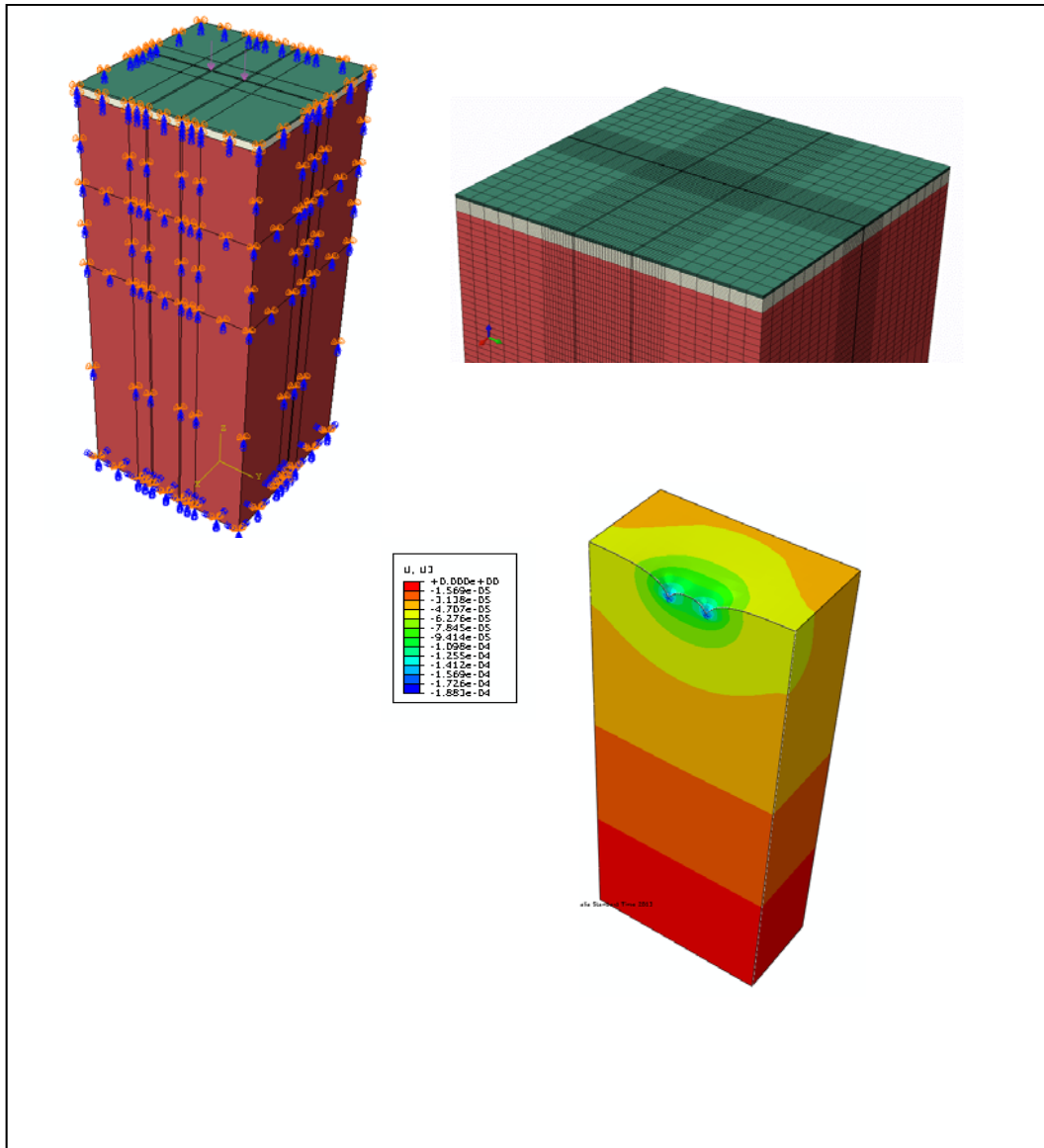


Figure 5.12-Constructed Model for Second Stage of Nonlinear Analysis

Having validated the method, in the second stage of the nonlinear analysis a sample three-layered flexible pavement was constructed using three-dimensional geometry. Figure 5.12 demonstrates the geometry of the model, mesh distribution and vertical deflection for the linear analysis. The characteristics of the model are described in Table 5-8.

The load was applied as a uniform pressure of 750 kPa over two rectangular areas (representing the contact surface of the tyres) of 10 cm by 10 cm. The tyres are assumed to be 1.8 m apart.

In this stage, the effect of different constitutive models on the critical response of layered flexible pavement was investigated. The main variables in this study were the constitutive materials used for the granular base layer. Four types of constitutive equations were implemented. The experimental data from the study conducted by Taciroglu and Hjelmstad (2002) was used for the parameters of the materials. Table 5.9 shows these material parameters for different cases.

The effect of the constitutive model's equation can be clarified if the results of the numerical analysis are compared via the range of material input parameters. From the experimental data made available by Taciroglu and Hjelmstad (2002), three different samples of materials (Cases 1 to 3) were selected for the numerical implementation. These three cases, in effect, represented a range of materials used in the base layer for flexible pavement. The results of the numerical implementation of the constitutive models for all three cases were compared in order to provide a better understanding of exactly how the constitutive models function with different types of materials. The material properties of Case 1 represented the normal average elastic modulus used for base materials. Case 2 represented hard and stiff materials and Case 3 looser materials.

The experimental samples were selected from a single type of material and the material parameters for each model were driven from its specific test. A complete explanation of the reliability of these parameters can be found in the work of Taciroglu and Hjelmstad (2002). As the samples are the same, any differences in

the results of the numerical model can be understood as the effects of specific equations of a constitutive model and the experiments assigned to it.

Table 5.9- Properties of Nonlinear Material Used in Second Stage of Nonlinear Analysis

Case Number	Constitutive model Equations	Material Parameters
Case 1 (Sample HD1)	Linear  K-θ : Eq. 2-4  Uzan-Witczak : Eq.2-6  Lade-Nelson: Eq.2-7	E = 240 (MPa), v = 0.34  K= 259 (MPa), v = 0.33, n= 0.05  K1= 459 (MPa), v = 0.33, k2 = 0.03, k3 = 0.27  K1= 242 (MPa), v = 0.33, k2=0.13
Case 2 (Sample HD3)	Linear  K-θ : Eq. 2-4  Uzan-Witczak : Eq.2-6  Lade-Nelson: Eq.2-7	E = 308 (MPa), v = 0.4  K= 352 (MPa), v = 0.4, n= 0.11  K1= 798 (MPa), v = 0.41, k2 = -0.14, k3 = 0.51  K1= 301 (MPa), v = 0.4, k2=0.20
Case 3 (Sample LD2)	Linear  K-θ : Eq. 2-4  Uzan-Witczak : Eq.2-6  Lade-Nelson: Eq.2-7	E = 179 (MPa), v = 0.36  K= 226 (MPa), v = 0.34, n= 0.16  K1= 504 (MPa), v = 0.35, k2 = 0.12, k3 = 0.37  K1= 202 (MPa), v = 0.36, k2=0.23

The four critical responses calculated from the numerical analysis are shown in Table 5.10. Excluding linear elastic results, the Lade-Nelson models gave the highest values for all four critical responses. The results from the Uzan-Witczak model were the lowest, and K-θ fell in between.

It can be observed that the value of the surface deflection under load is less variable in different materials. Linear elastic analysis resulted in measurements of 0.178 mm to 0.202 mm for three different cases of materials (0.024 mm difference). For K-θ the value went from 0.224 mm to 0.262 mm (0.038 mm difference), for Uzan-Witczak it changed from 0.156 mm to 0.214 mm (0.058 mm difference) and for the Lade-Nelson it changed from 0.294 mm to 0.325 mm (0.031 mm). It can be understood from this that the Uzan-Witczak method has a greater sensitivity to material parameters in terms of surface deflection results.

Table 5.10- Critical Responses Calculated from Different Nonlinear Models

Case 1				
	Linear	K-θ	Uzan-Witczak	Lade-Nelson
δ (mm) surface	-0.188	-0.224	-0.196	-0.294
ε <sub>h</sub> (microstrains) bottom of AC	89.256	104.321	82.869	139.473
ε <sub>v</sub> (microstrains) top of SG	-89.281	-96.711	-76.384	-122.194
σ <sub>v</sub> (kPa) top of SG	-4.176	-4.605	-3.678	-6.068

Table 1.10- Continue

Case 2				
	Linear	K-θ	Uzan-Witczak	Lade-Nelson
δ (mm) surface	-0. 178	-0. 225	-0. 156	-0. 325
ε <sub>h</sub> (microstrains) bottom of AC	82.172	105.145	53.319	152.726
ε <sub>v</sub> (microstrains) top of SG	-82.422	-101.615	-44.172	-133.539
σ <sub>v</sub> (kPa) top of SG	-3.867	-4.840	-2.237	-6.782
Case 3				
	Linear	K-θ	Uzan-Witczak	Lade-Nelson
δ (mm) surface	-0. 203	-0. 262	-0. 214	-0.294
ε <sub>h</sub> (microstrains) bottom of AC	100.284	126.307	94.177	139.473
ε <sub>v</sub> (microstrains) top of SG	-99.360	-115.904	-91.494	-122.194
σ <sub>v</sub> (kPa) top of SG	-4.645	-5.598	-3.678	-4.387

The tensile strain at the bottom of the asphalt and the vertical strain on the top of the subgrade are the key parameters in the calculation of fatigue repetition and rutting in the design of flexible pavement (AUSTROADS 2004) respectively. Here, looking at the range of differences in the different constitutive models regarding the changes in the material, it can be stated that the same trends of sensitivity for the constitutive models are observable. Uzan-Witczak shows the most variation and Lade-Nelson shows the least variation.

Figure 5.13 illustrates the normalized values of critical responses calculated from four constitutive models for Case 1 of material parameters. Here the results are divided by the values calculated from the linear analysis in order to obtain a more effective comparison in terms of the actual effect of each model.

Based on the results of Figure 5.13, the largest difference relates to the Lade-Nelson model. The surface deflection and horizontal strain calculated from this model is 56% greater than the linear elastic calculation. In the K- $\theta$  model, the highest difference is 19% for the calculated surface deflection and for Uzan-Witczak it is the vertical strain that shows a -14% difference. However it should be noted that the Uzan-Witczak values from the linear analysis are lower with the exception of the value for surface deflection.

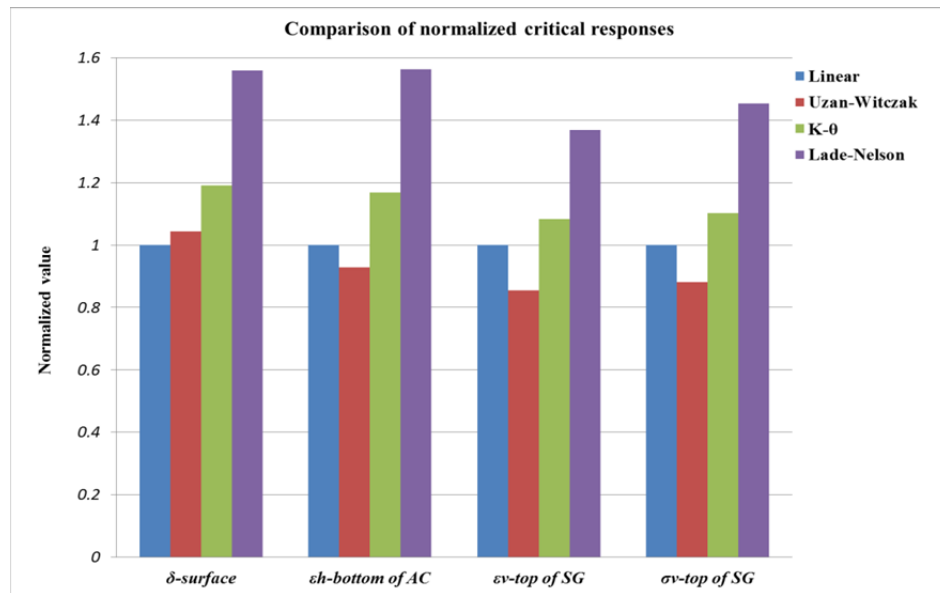


Figure 5.13- Comparison of the normalised Critical Response- Case 1

To investigate the mechanical behaviour of the granular layer with different constitutive models, it is of interest to consider comparisons regarding the increasing trend of the modulus during the incremental loading. Figure 5.14 represents these trends at top of the base layer in Case 1.

As mentioned previously, in the ABAQUS program the load is applied in increments. The resilient modulus in nonlinear constitutive models is a function of the stress state, and the modulus then varies in each increment for all of the elements of the base layer. However, the increasing trend of a point in the centre of the loading at the top of the base layer has been selected for representation here.

Figure 5.14 shows the increasing trends for the materials in Case 1. As can be observed, all of the nonlinear constitutive models have a final value which is less than the value of the linear model except for Uzan-Witczak. The Lade-Nelson

model shows the lowest trends and final values in this case, and the K-θ falls between that of Lade-Nelson and Uzan-Witczak.

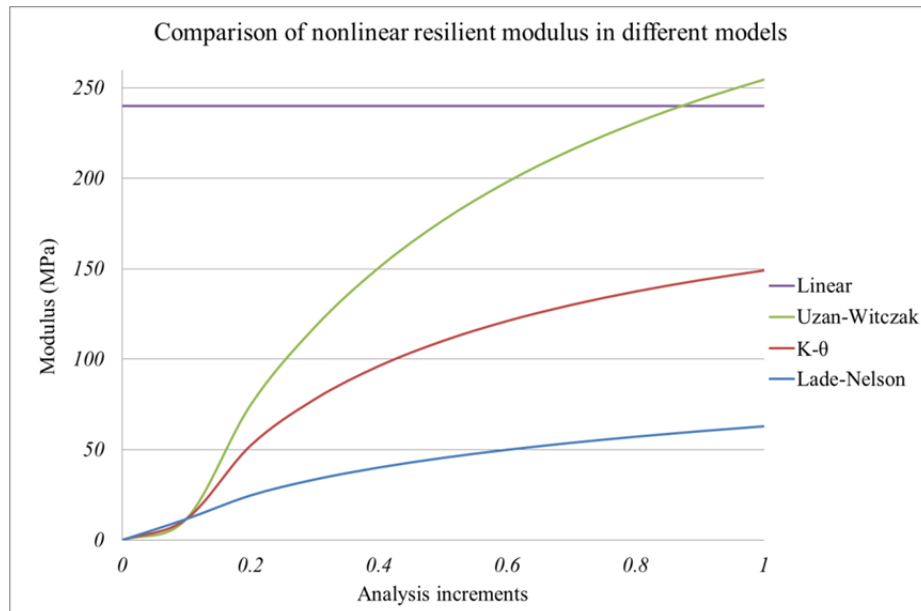


Figure 5.14-Increase of the Nonlinear Resilient Modulus - Case 1

It is worth mentioning that the Uzan-Witczak model shows the highest range of variation with respect to material change. This can be understood from the results presented in Table 5.10. It can also be concluded that the Uzan-Witczak model has a rapidly increasing trend due to increasing stresses. This is because of the nature of the exponential function of Uzan-Witczak. Comparing Equations 2–4, 2–6 and 2–7, it can be seen that K-θ is independent of deviatoric stress, Uzan-Witczak has two terms (depending on bulk and deviatoric stress simultaneously) which multiply and intensify each other, and Lade-Nelson has two terms (depending on bulk and deviatoric stress) but these terms do not multiply.

Increasing stiffness in the base layer also leads to an increase in calculated stress in the layer itself. In Figure 5.15, the distribution of vertical stress across the depth of the base layer is presented for Case 1.

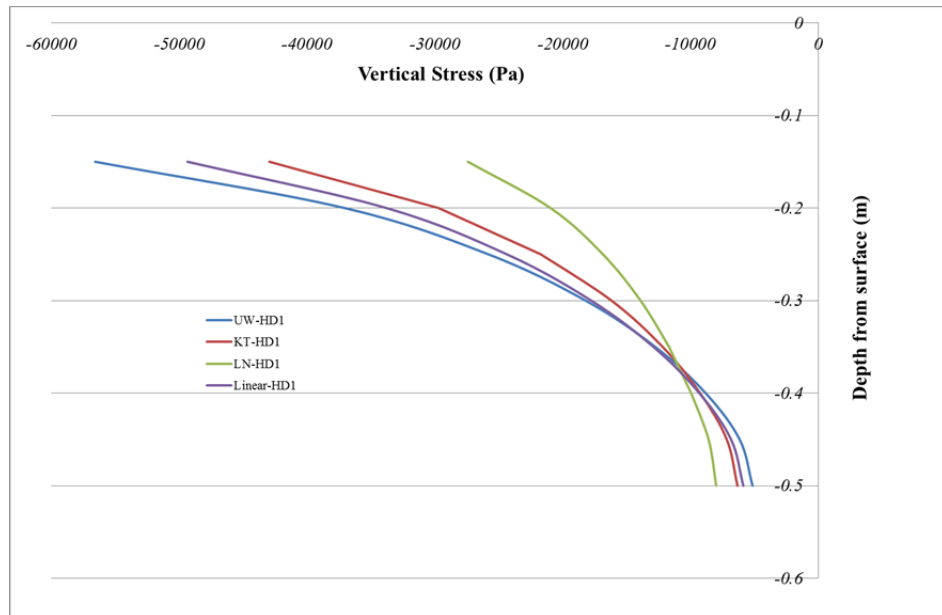


Figure 5.15-Distribution of Vertical Stress in Base Layer - Case 1

In material Case 1, the calculated stress distribution in depth for Uzan-Witczak, linear elastic and K- $\theta$  are roughly similar, while the Lade-Nelson model has less potential to bear vertical stresses. Here, with Uzan-Witczak, the stress varies from -56 kPa at the top of the base to -5 kPa at the bottom. The variation range for the linear model is from -49 kPa to -6 kPa. For K- $\theta$  this range is from -43 kPa to -6 kPa. It is clear that the variation in these three models demonstrates a relatively close relationship (-56 kPa to -43 kPa at top and -6 kPa to -5 kPa at the bottom). However, a considerable difference is presented in Lade-Nelson where the stress varies from -27 kPa to -8 kPa. Moreover, the stress distribution of Lade-Nelson is more uniform than in the other three models.

As an overall comparison, some of the major points can be further discussed. Firstly, the implementation of the Uzan-Witczak model resulted in a generally ‘stiffer’ behaviour than that of other constitutive models (including linear elastic). Here the word ‘stiff’ refers to less deformation (deflection and strain) against the applied pressure. In this regard, Lade-Nelson has the ‘softest’ behaviour. The stiffness can be related to trends in the development of the elastic modulus with respect to an increasing load increment and accordingly, stresses in the base layer. Here again the rate of increase in the elastic modulus of Uzan-Witczak is higher than in the other constitutive models. This is due to the dependency of the Uzan-Witczak constitutive equation on both bulk stress and deviator stress. Although the Lade-Nelson model is also dependent upon these two, the nature of the equation is different from that of Uzan-Witczak. In Lade-Nelson, the two terms are simply added to each other, while in Uzan-Witczak the two terms are multiplied and therefore greatly intensify the effect of the increasing stress. Another cause of the stiffer behaviour of Uzan-Witczak can be explained by investigating the development of stress in the base. Calculations show that having a higher elastic modulus in loading increments leads to higher stress in the same layer. Considering the dependency of the modulus on the stress values this itself results in a higher elastic modulus. This demonstrates another reason for the ‘stiffer’ behaviour in Uzan-Witczak.

Finally, it should be noted that although changes in the asphalt and subgrade properties (including thickness and material properties) will produce different results, the trend in mechanical behaviour is expected to be the same regarding the implementation of constitutive models. Therefore, stiffer responses (as mentioned before) can be expected from Uzan-Witczak, and more uniformly distributed responses can be expected from Lade-Nelson in any of the cases.

Based on the results of the analysis in stage 2, the Uzan-Witczak model is selected to represent the nonlinear elasticity of UGM in the base layer. Therefore, in the final stage of the nonlinear elastic analysis the same eight cases analyzed in the linear elastic section (Table 5.5) were selected for analysis under the Uzan-Witczak nonlinear elastic constitutive model (Equation 2–6). The first material properties (M1) were selected from the experimental data published by Hjelmstad and Taciroglu (2000), where the nonlinear properties of sample MD2 had equal linear properties to M1 in section 5.1.2. The second material property (M2) was arbitrarily constructed to provide the 500MPa elastic modulus on top of the base layer beneath the wheel. These material properties are listed in Table 5.11.

Figure 5.16 demonstrates the contours of deformation for the nonlinear elastic analysis in both cases of SADT and TADT for geometry 1 and materials 1 (NE-G1-(L1 and L2)-M1).

Table 5.11- Material Properties Used in Final Stage of Nonlinear Analysis

M1 (Sample MD2 from (Hjelmstad and Taciroglu 2000))	$K_1 = 332 \text{ (MPa)}$ , $\nu = 0.4$ , $k_2 = 0.08$ , $k_3 = 0.2$
M2	$K_1 = 850 \text{ (MPa)}$ , $\nu = 0.4$ , $k_2 = 0.15$ , $k_3 = 0.45$

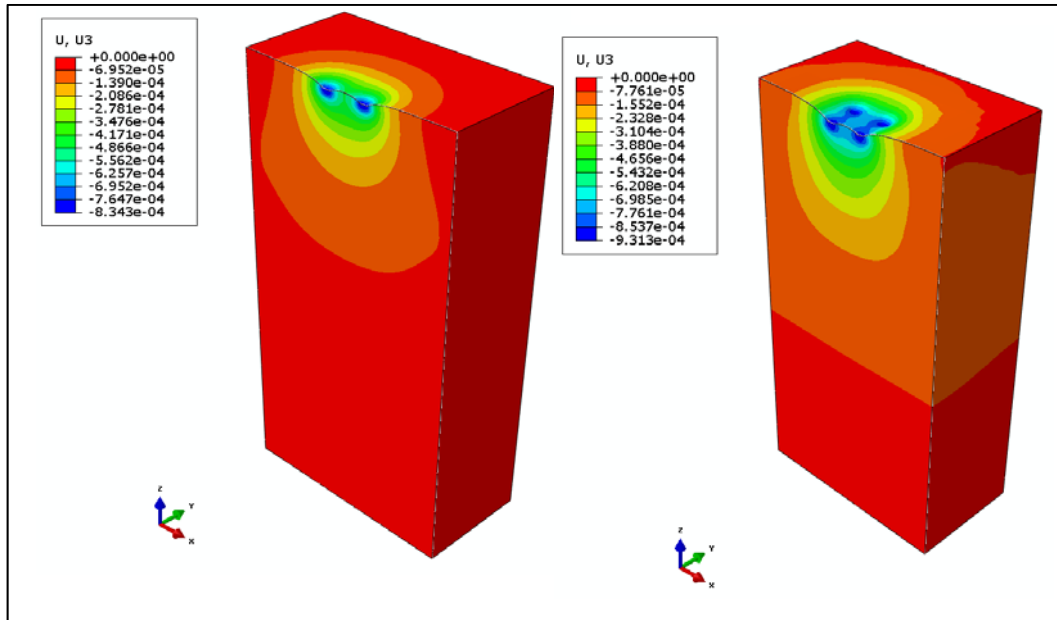


Figure 5.16 - Vertical Deformation of NE-1-1-1 (Left) and NE-1-2-1 (Right)

Finally, the results of the four critical responses for eight cases of nonlinear analyses are presented in Table 5.12.

Table 5.12 - Responses of 8 Cases of Nonlinear Simulation

Case	Nonlinear Model	Vertical Deflection (Top of AC)	Horizontal Strain (X-Axis) (Bottom of AC)	Vertical Strain (Z-Axis) (Top of SG)	Vertical Stress (Top of SG)
1	<b>G1-L1-M1</b>	0.830 mm	-180E-06	-705E-06	-41557 Pa
2	<b>G1-L1-M2</b>	0.412 mm	-128E-06	-202E-06	-26805 Pa
3	<b>G1-L2-M1</b>	0.920 mm	-133E-06	-528E-06	-34452 Pa
4	<b>G1-L2-M2</b>	0.478 mm	-125E-06	-341E-06	-48765 Pa
5	<b>G2-L1-M1</b>	0.553 mm	-59E-06	-305E-06	-19326 Pa

6	<b>G2-L1-M2</b>	0.293 mm	-45E-06	-191E-06	-27336 Pa
7	<b>G2-L2-M1</b>	0.749 mm	-103E-06	-294E-06	-20555 Pa
8	<b>G2-L2-M2</b>	0.374 mm	-65E-06	-176E-06	-27385 Pa

As can be seen from Table 5.12, increasing the asphalt thickness reduced the surface deflection and tensile strain at the bottom of the asphalt layer which is the same trend observed in the linear elastic analysis. For instance, a comparison between Case 1 and Case 5 indicates a decrease in surface deflection from 0.830 mm in Case 1 to 0.553 in Case 5 (33% reduction). The tensile strain at the bottom of the asphalt layer decreased from 180 micro-strain in Case 1 to 59 micro-strain in Case 5 (67% reduction).

TADT loading increases the surface deflection and strains at the asphalt and subgrade for a thick asphalt layer. For example, comparing Case 5 and Case 7 shows an increase in surface deflection of 0.553 mm to 0.749 mm (35% increase).

Finally, the effect of material properties can be induced. The stronger material (M2) caused less deflection and strain but higher stress. For instance, comparing Case 1 and Case 2 demonstrated a decrease in surface deflection from 0.830 mm to 0.412 mm (50% reduction).

Section 5.2 of this chapter presents a conclusive comparison of the effects of different material behaviour on the critical responses. In sections 5.1.1 and 5.1.2 the materials were assumed to behave in the elastic domain. In the next section, the plastic properties of materials are taken into account.

### 5.2.3 Linear Elasto-plastic Analysis

The effect of linear elasto-plastic behaviour for UGM layers (base and subgrade) of flexible pavement are studied in this section. To attain this objective, subroutines were developed in ABAQUS UMAT according to the procedure defined in section 4.5.2 (Figure 4.9). The Mohr-Coulomb constitutive model was implemented to represent frictional plastic hardening behaviour of materials (Equation 3-27). The procedure for the return mapping scheme described in section 4.5.2 was manipulated to calculate the yield surface of Mohr-Coulomb in principal stress space.

Since the resistance of the soil body in the Mohr-Coulomb model is a function of existing confining pressure, the static elasto-plastic analysis of UGM includes two steps. In the first step, the geostatic pressure of the medium due to the gravity of materials should be calculated to determine the initial stress in the soil body. In the second step, the tyre pressure is applied over the contact area and then the stresses, strains and deformation are computed. It should be noted that the asphalt layer is assumed to behave linear elastically in this dissertation.

The static linear elasto-plastic analysis was conducted for the same eight cases of simulation studied in the previous sections. The material properties for the elasto-plastic analysis are listed in Table 5-13. In this table,  $\varphi$  is the internal friction of UGM,  $c$  is cohesion and  $\psi$  is dilation angle.

Figure 5.17 represents the contours of vertical deformation for the linear elasto-plastic simulation of geometry 1 and material 1 in SADT and TADT loading (LP-1-1-1 and LP-1-2-1).

The main difference between elastoplastic simulations and elastic simulations is the development of plastic strain which is produced during incremental loading. Such progress can shed light on the mechanism of failure due to traffic loading.

Table 5.13- Material Properties for Linear Elastoplastic Analysis

Layer		Elastic Modulus (MPa)	Poisson's Ratio	$\varphi$ (degrees)	c (kPa)	$\psi$ (degrees)
M1	Asphalt (AC)	2800	0.35	NA	NA	NA
	Base	200	0.4	30	10	15
	Subgrade	50	0.45	20	10	10
M2	Asphalt (AC)	2800	0.35	NA	NA	NA
	Base	500	0.4	35	10	17
	Subgrade	120	0.45	25	10	15

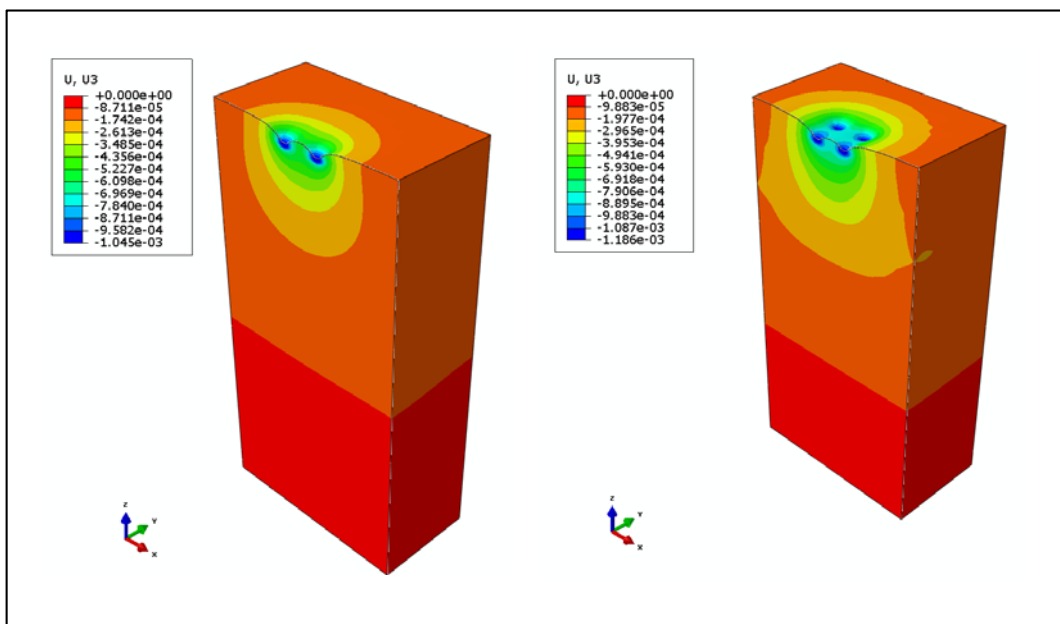


Figure 5.17 - Vertical Deformation of LP-1-1-1 (Left) and LP-1-2-1 (Right)

Figure 5.18 demonstrates the progressive development of equivalent plastic strain in three increments of loading in the simulation of Case 1 (LP-1-1-1). The increment 0 is at the end of geostatic and before the application of tyre loads; increment 1 is in the middle of the analysis where half of the tyre pressure is applied, and increment 2 is at the end of the analysis where complete tyre pressure is applied. The equivalent plastic strain is stored in variables named SDV4 for the base and PEEQ for the subgrade layer.

As can be observed from the results, the base layer reached its plastic limit sooner than the subgrade layers. This indicates that base provides a delay to the development of plastic strain for subgrade which is due to the higher resistance of the base layer. In other words, since the base layer has higher resistance to pressure, it bears more stress than the subgrade; therefore the stress level in the subgrade reaches its plastic limit after the plastic strain is developed in the base layer. The same trend was observed for all eight cases of simulation.

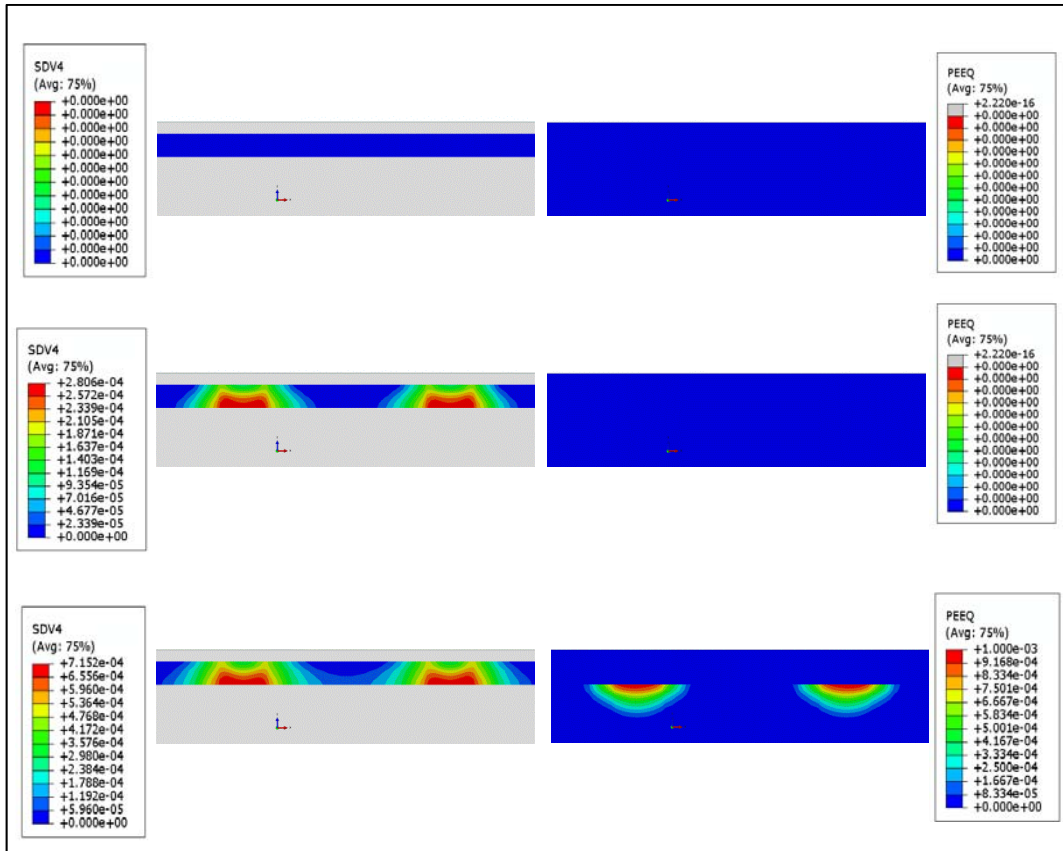


Figure 5.18 - Developement of Plastic Strain in Base (Left) and Subgrade (Right)  
Linear Elastoplastic

The overall concept of the mechanical behaviour of flexible pavement due to different loadings can be better understood if the distribution of strain in depth is considered. Figure 5.19 and Figure 5.20 demonstrate the distribution of horizontal and vertical strain in depth respectively. The strain is calculated beneath wheel number 2 (Figure 5.8). Travel direction is assumed to be Y-direction and depth is assumed to be in Z-direction.

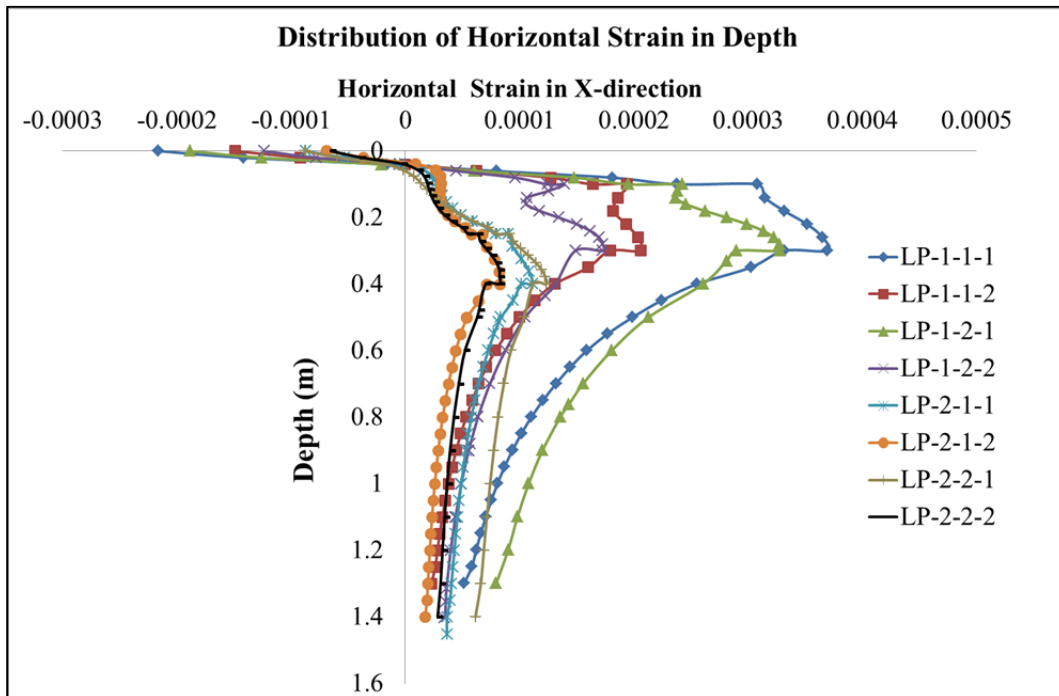


Figure 5.19- Distribution of Horizontal Strain in Elastoplastic Analysis

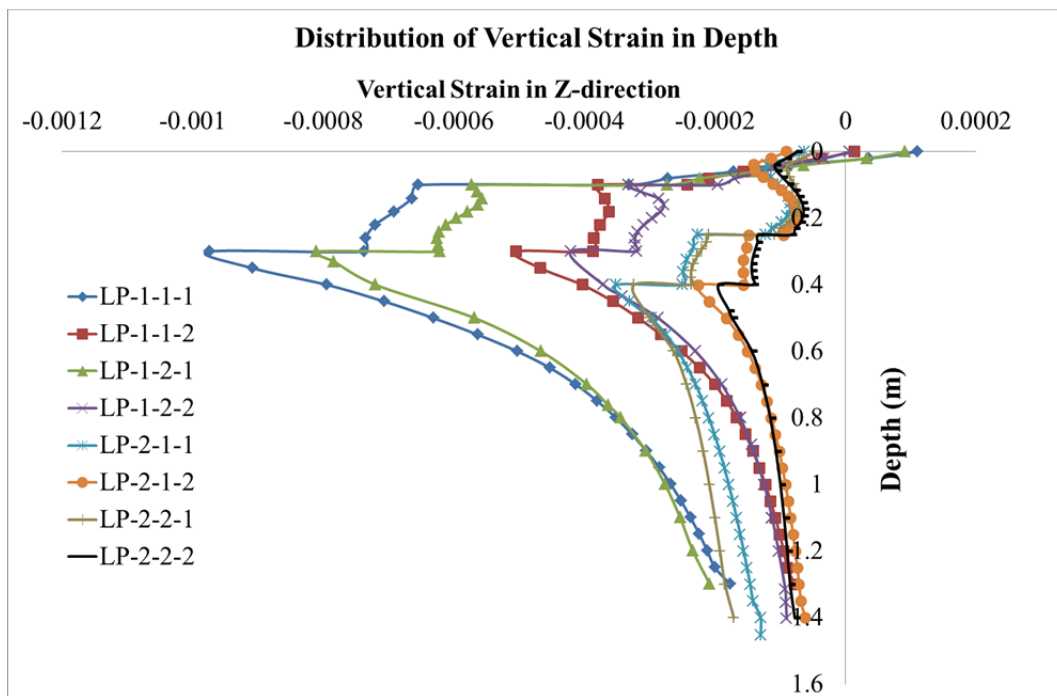


Figure 5.20- Distribution of Vertical Strain in Elastoplastic Analysis

In these figures, the positive numbers are tensile strain and negative numbers are compressive strain. A clear stepwise break can be seen in the distribution of strain at the intersection of the layers. This is at depths of 10 cm and 30 cm for geometry 1 and at depths of 25 cm and 40 cm for geometry 2.

It is observed that in Case 1, when an 10 cm AC layer is constructed on weak materials (M1), small amount of vertical tensile strain is computed exactly beneath the wheel load. This phenomenon is also observable if a linear elastic closed form solution is taken into account and this has been checked through CIRCLY and KENLAYER results. The reason for such an unusual expansion is the existence of a large amount of horizontal tensile stress and relatively large value for the Poisson ratio. The calculation of vertical elastic strain ( $\epsilon_{33}$ ) in linear elastic formulation is indicated in Equation 5-1.

$$\epsilon_{33} = \frac{1}{E} (\sigma_{33} - \nu \sigma_{11} - \nu \sigma_{22}) \quad \text{Equation 5-1}$$

According to this equation, the presence of a large value of tensile stress ( $\sigma_{11}$  and  $\sigma_{22}$ ) can nullify and even exceed the magnitude of compressive stress beneath the tyre ( $\sigma_{33}$ ). Such a combination of stress and Poisson ratio occurred in geometry 1 when the thickness of the AC layer was not enough to act as a uniform solid mat. While the material properties and/or thickness of the AC layer are improved, the effect vanishes.

The results of the critical responses calculated for all eight different cases of linear elastoplastic analysis are presented in Table 5.14. As can be seen from Table 5.15, increasing asphalt thickness decreased the surface deflection and tensile strain at the bottom of the asphalt layer, which is the same trend observed in previous analyses. A comparison between Case 1 and Case 5 indicates a decrease in surface

deflection from 1.026 mm for Case 1 to 0.754 mm for Case 5 (26% reduction). Tensile strain at the bottom of the asphalt layer in this comparison decreased from 236 micro-strain in Case 1 to 63 micro-strain in Case 5 (73% reduction).

Table 5.16 - Responses of 8 Cases of Linear Elastoplastic Simulation

Case	Nonlinear Model	Vertical Deflection (Top of AC)	Horizontal Strain (X-Axis) (Bottom of AC)	Vertical Strain (Z-Axis) (Top of SG)	Vertical Stress (Top of SG)
1	<b>G1-L1-M1</b>	1.029 mm	-236E-06	-951E-06	-51162 Pa
2	<b>G1-L1-M2</b>	0.490 mm	-167E-06	-493E-06	-62337 Pa
3	<b>G1-L2-M1</b>	1.171 mm	-226E-06	-803E-06	-49660 Pa
4	<b>G1-L2-M2</b>	0.543 mm	-157E-06	-422E-06	-59801 Pa
5	<b>G2-L1-M1</b>	0.754 mm	-63E-06	-345E-06	-27920 Pa
6	<b>G2-L1-M2</b>	0.374 mm	-46E-06	-220E-06	-35533 Pa
7	<b>G2-L2-M1</b>	0.953 mm	-120E-06	-319E-06	-29351 Pa
8	<b>G2-L2-M2</b>	0.450 mm	-82E-06	-192E-06	-35084 Pa

TADT loading increases surface deflection and also strain at the asphalt and subgrade for the thick asphalt layer. For example, comparing Case 5 and Case 7 indicates an increase in surface deflection from 0.754 mm to 0.953 mm (26% increase).

Finally, the effect of material properties can be investigated. The stronger materials (M2) cause less deflection and strain, but higher stress. For instance, a comparison of Case 1 and Case 2 demonstrates a decrease in surface deflection from 1.0290 mm to 0.490 mm ( 52% reduction).

Final discussion and remarks are presented in section 5.2 where the effects of the implementation of different constitutive models are analyzed.

#### **5.2.4 Nonlinear Elastoplastic Analysis**

The final stage of the static analysis considered in this dissertation studied the responses of nonlinear elastoplastic behaviour of UGM layers (base and subgrade) in a layered flexible pavement. The simulation was achieved through subroutines developed in ABAQUS UMAT based on procedures indicated in section 4.5.2 (Figure 4.9). Frictional plastic behaviour was modelled by the Mohr-Coulomb constitutive equation (Equation 3–27), and for linear elastoplastic, the return mapping scheme procedure (section 4.5.2) was applied.

The analysis consists of two steps of loading. The first step of the analysis is the geostatic pressure of the medium produced by the gravity of materials, and the second step is the introduction of tyre pressure over the contact area. Finally, the stresses, strains and deformation are computed. The behaviour of the asphalt layer is modelled as a linear elastic material.

The difference between linear elastoplastic and nonlinear elastoplastic behaviour is schematically illustrated in Figure 2.16. The static nonlinear elastoplastic was analyzed for the same eight cases of simulation studied in the previous sections. The material properties for the nonlinear elastoplastic analysis are listed in Table 5.17. The material properties are a combination of the properties stated for the nonlinear elastic (Table 5.11) and linear elastoplastic parts (Table 5.17).

Table 5.17- Material Properties for Nonlinear Elastoplastic Analysis

Layer		Elastic Modulus (MPa)	Poisson's Ratio	$\varphi$ (degrees)	c (kPa)	$\psi$ (degrees)
M1	Asphalt (AC)	2800	0.35	NA	NA	NA
	Base	K1= 332(MPa), v = 0.4, k2 = 0.08, k3 = 0.2		30	10	15
	Subgrade	50	0.45	20	10	10
M2	Asphalt (AC)	2800	0.35	NA	NA	NA
	Base	K1= 850 (MPa), v = 0.4, k2 = 0.15, k3 = 0.45		35	10	17
	Subgrade	120	0.45	25	10	15

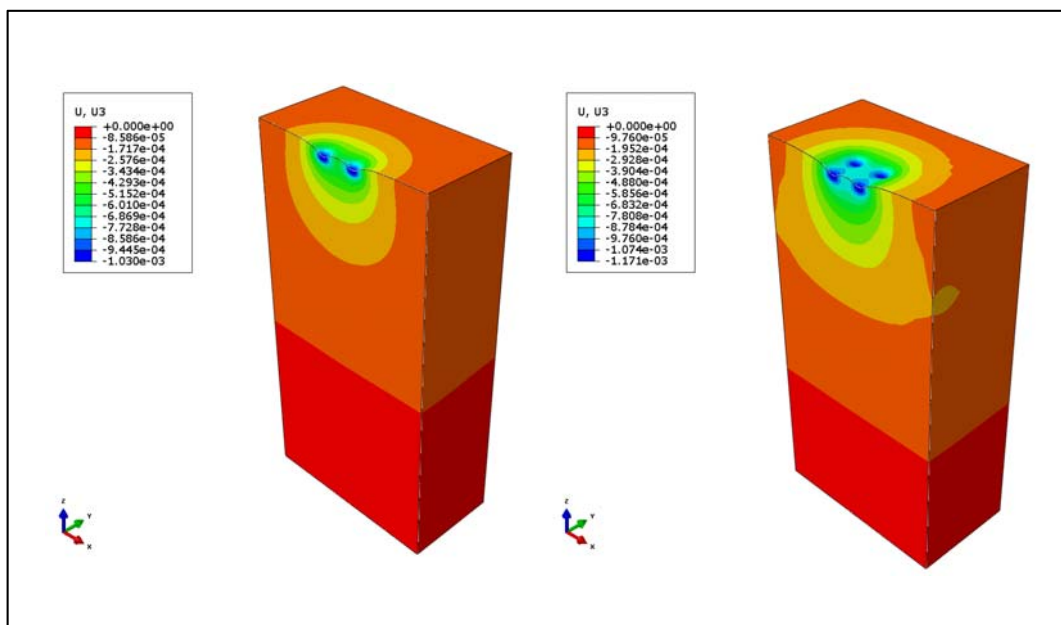


Figure 5.21 - Vertical Deformation of NP-1-1-1 (Left) and NP-1-2-1 (Right)

Figure 5.21 represents the contours of vertical deformation for the linear elastoplastic simulation of geometry 1 and material 1 in SADT and TADT loading (NP-1-1-1 and NP-1-2-1).

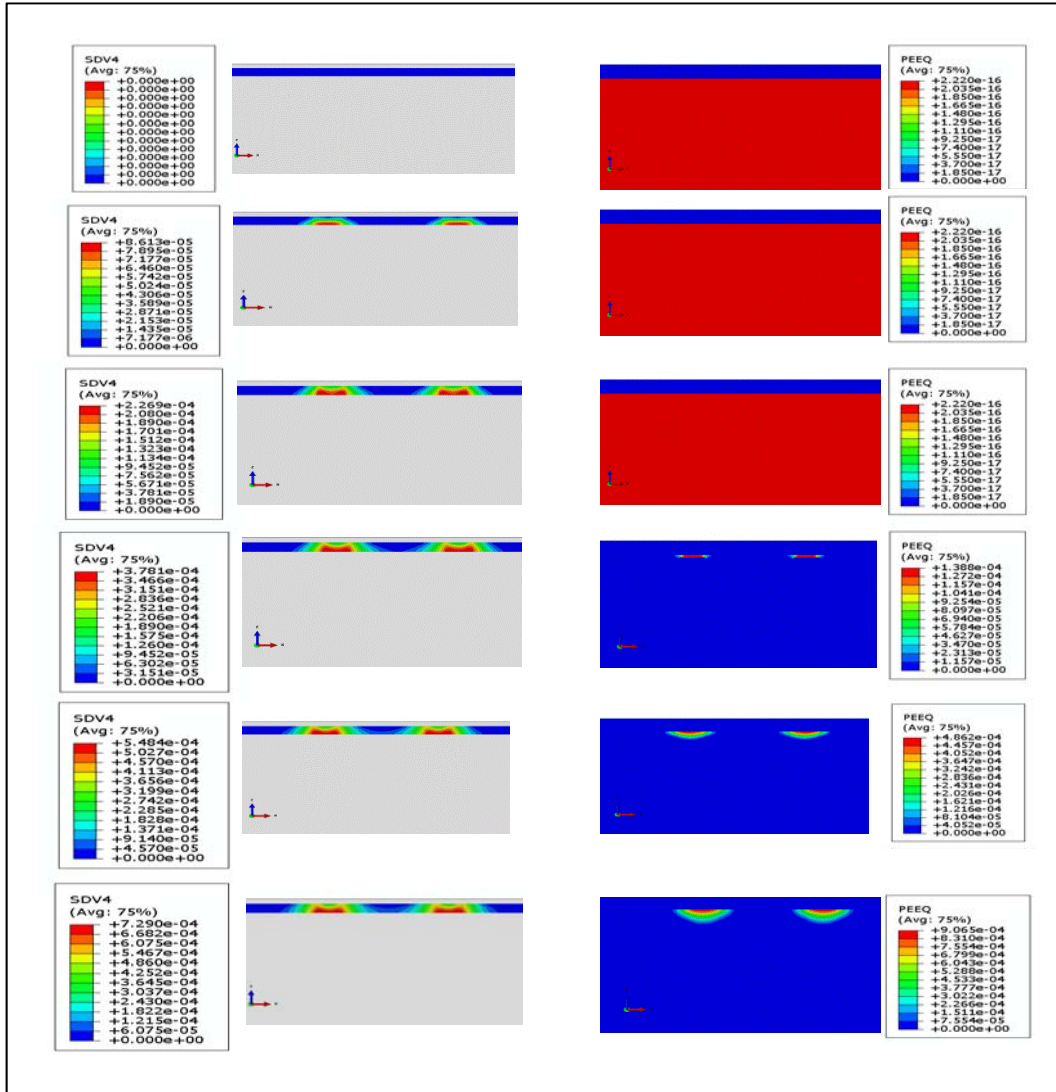


Figure 5.22 - Developement of Plastic Strain in Base (Left) and Subgrade (Right)  
Nonlinear Elastoplastic

The main difference between nonlinear elastoplastic simulations and linear elastoplastic simulations is the development of a stress-strain curve due to incremental loading. Such progress can help improve understanding of the mechanism of failure due to traffic loading. This progress is illustrated in Figure 5.22.

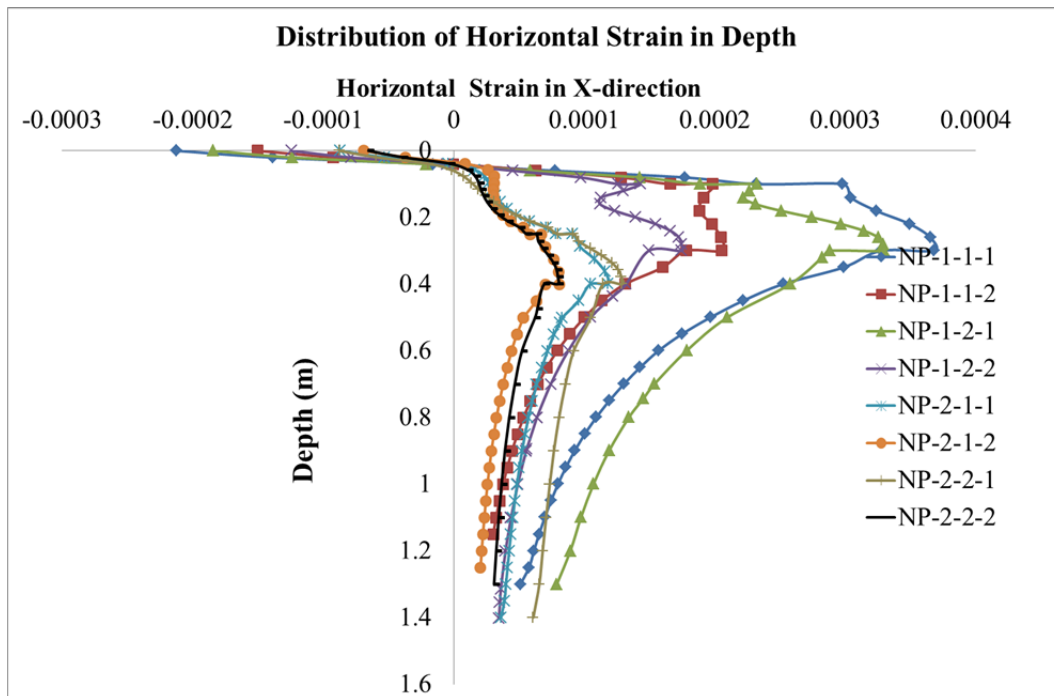


Figure 5.23- Distribution of Horizontal Strain in Nonlinear Elastoplastic Analysis

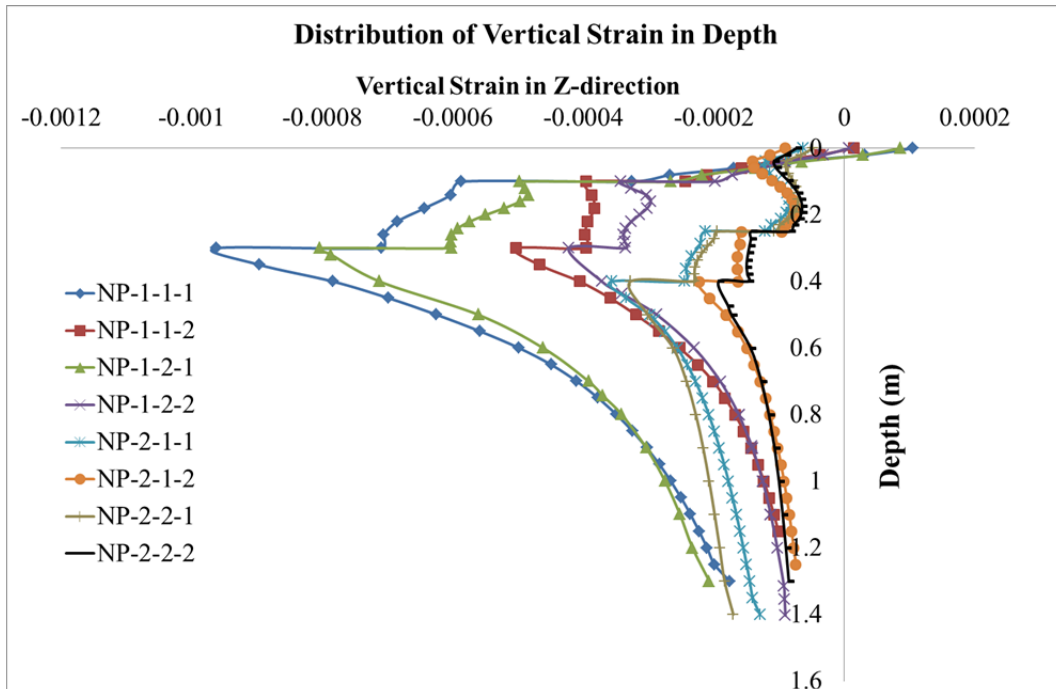


Figure 5.24- Distribution of Vertical Strain in Nonlinear Elastoplastic Analysis

The general mechanism of flexible pavement in different cases can be investigated by the distribution of strain in depth. Figure 5.23 and Figure 5.24 demonstrate the distribution of horizontal and vertical strain in depth respectively. The strain is computed beneath wheel number 2 (Figure 5.8). Travel direction is assumed to be Y-direction and depth is assumed to be in Z-direction.

As can be observed, the same trend of behaviour seen for linear elastoplastic materials has occurred here again. The strain distribution and mechanical response of the thin AC layer (10 cm) and thick AC layer (25 cm) demonstrate some important differences. The behaviour also varies from SADT to TADT loading.

Table 5.18 presents the four critical responses of all eight different cases of nonlinear elastic analysis.

Based on this table, increasing the asphalt thickness reduced the surface deflection and tensile strain at the bottom of the asphalt layer, which is the same trend that was observed in the linear elastic analysis. For example, a comparison of Case 1 and Case 5 reveals a decrease in surface deflection from 1.01 mm in Case 1 to 0.752 mm in Case 5 (26% reduction). Tensile strain at the bottom of the asphalt layer is reduced from 231 micro-strain in Case 1 to 62 micro-strain in Case 5 (73% reduction).

Due to TADT loading, an increase in surface deflection and strain at the asphalt and subgrade can be seen for thick layer asphalt. For example, comparing Case 5 and Case 7 shows an increase in surface deflection from 0.752 mm to 0.949 mm (25% increase).

Finally, the effect of material properties can be induced. The stronger materials (M2) caused less deflection and strain, but higher stress. In this case, a comparison between Case 1 and Case 2 indicates a decrease in surface deflection from 1.01 mm to 0.494 mm ( 51% reduction).

Table 5.18 - Responses of 8 Cases of Linear Elastoplastic Simulation

Case	Nonlinear Model	Vertical Deflection (Top of AC)	Horizontal Strain (X-Axis) (Bottom of AC)	Vertical Strain (Z-Axis) (Top of SG)	Vertical Stress (Top of SG)
1	<b>G1-L1-M1</b>	1.01 mm	-231E-6	-940E-6	-50709 Pa
2	<b>G1-L1-M2</b>	0.494 mm	-169E-6	-491E-6	-62705 Pa
3	<b>G1-L2-M1</b>	1.16 mm	-220E-6	-796E-6	-48992 Pa
4	<b>G1-L2-M2</b>	0.547 mm	-159E-6	-422E-6	-59687 Pa

5	<b>G2-L1-M1</b>	0.752 mm	-62E-6	-350E-6	-27736 Pa
6	<b>G2-L1-M2</b>	0.376 mm	-46E-6	-218E-6	-35579 Pa
7	<b>G2-L2-M1</b>	0.949 mm	-127E-6	-323E-6	-29211 Pa
8	<b>G2-L2-M2</b>	0.451 mm	-79E-6	-190E-6	-35308 Pa

The final section of this chapter contains general remarks and a discussion of the static analysis.

### 5.3 Remarks

In this chapter, a static analysis was conducted for four types of constitutive models. Eight different cases were numerically simulated to investigate the effects of layer thickness, materials properties and loading.

The results for the four critical responses of these eight cases are compared to each other in Figures 5–25 to 5–28. In these figures, LE indicates ‘Linear Elastic’, NE indicates ‘Nonlinear Elastic’, LP indicates ‘Linear Elastoplastic’ and NP indicates ‘Nonlinear Elastoplastic’.

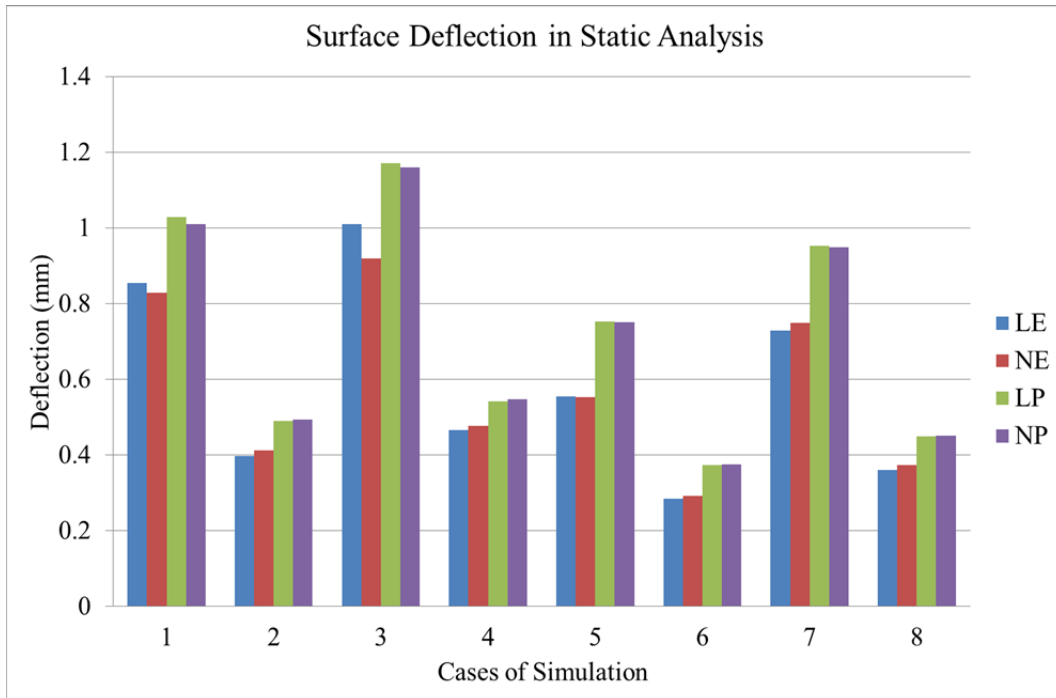


Figure 5.25 - Comparison of Surface Deflection in Static Analysis

In all four critical responses it can be seen that there is a tangible difference moving from elastic (either linear or nonlinear) to plastic (either linear or nonlinear) constitutive models. This change of materials constitutive model has a trend to increase the magnitude (absolute value) of all four critical responses.

The trend of change from linear (either elastic or plastic) to nonlinear (either elastic or plastic) depends on the case.

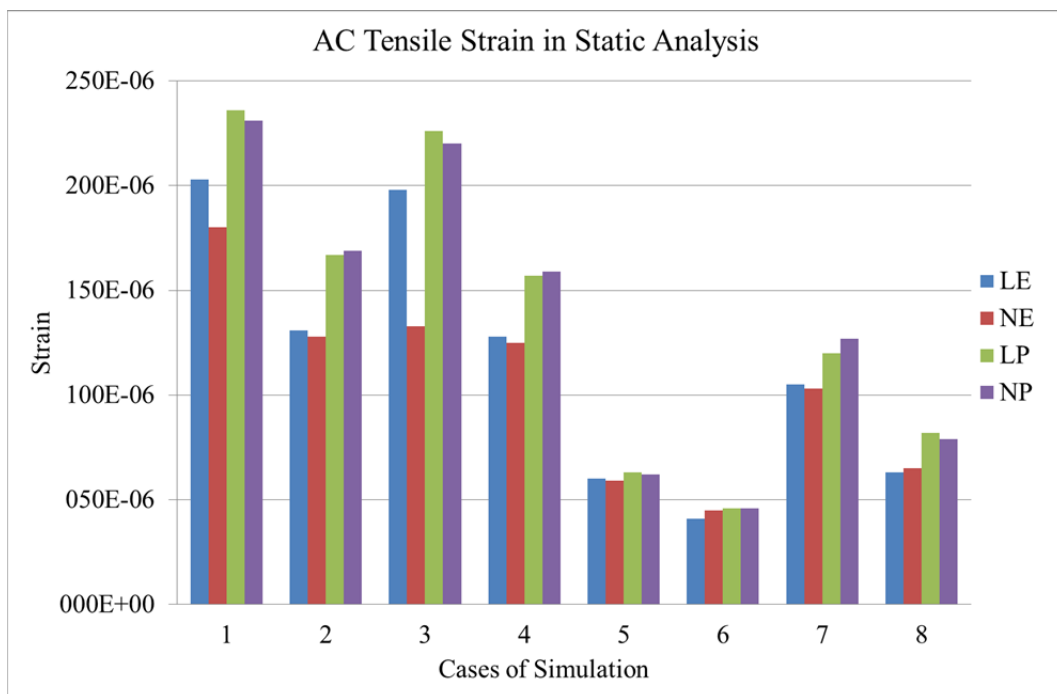


Figure 5.26-Comparison of AC Tensile Strain in Static Analysis

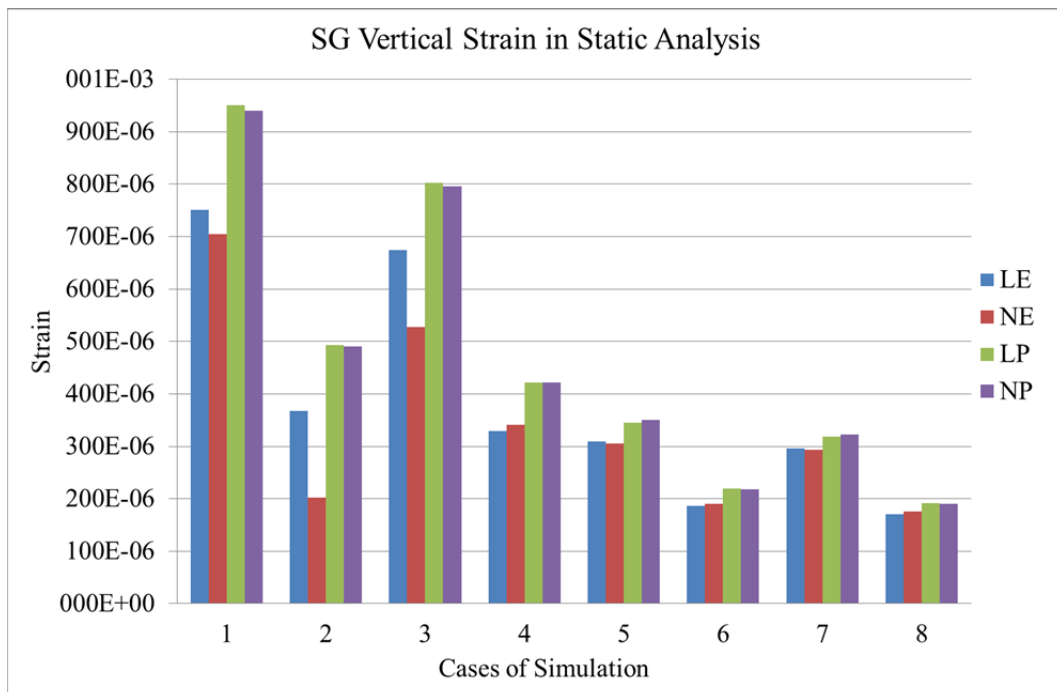


Figure 5.27-Comparison of SG Compressive Strain in Static Analysis

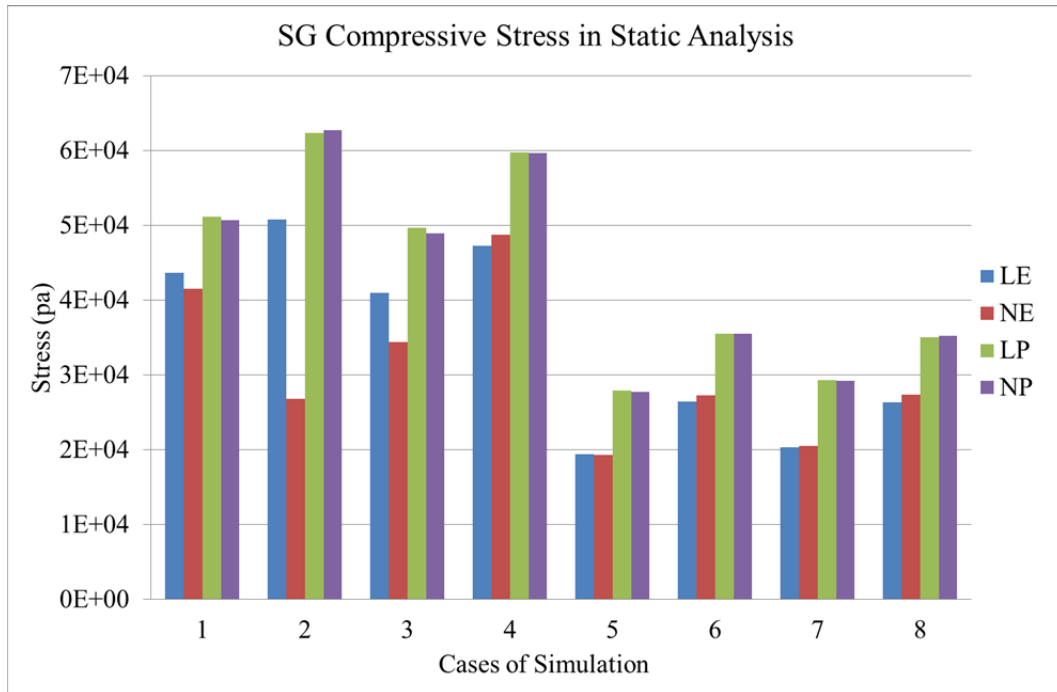


Figure 5.28-Comparison of SG Compressive stress in Static Analysis

For instance, comparison of tensile strain illustrates a decreasing trend from linear elastic to nonlinear elastic in cases 1, 2, 3, 4, 5 and 7, but an increasing trend for cases 6 and 8. This implies that the combination of load, layer thickness and material properties can define the general mechanical responses of the system. The effects of linearity or nonlinearity cannot be explicitly determined.

Finally, a comparison of linear elastic with nonlinear elastic shows a tangible change in results in some cases (for instance case 2 in Figure 5.27 and Figure 5.28), and insignificant change in others (for instance cases 5 and 7 in Figure 5.27). But just as for plastic analysis, there is always a slight difference between linear and nonlinear elastoplastic analysis. This implies that the effect of plastic behaviour override the effects of nonlinearity.

## CHAPTER 6

### 6: DYNAMIC SIMULATION OF LAYERED FLEXIBLE PAVEMENT

#### 6.1 Introduction

Chapter 6 discusses the details of model construction for the numerical simulation of layered flexible pavement under dynamic loading. Most attention was paid to the effects of different constitutive models used to represent granular layers, specifically the base layer.

The main objective of this chapter is to investigate the effects of shakedown and the soil-asphalt interaction to provide a basis for comparison between different dynamic simulations. The analyses started with a dynamic analysis considering simple Mohr-Coulomb nonlinear elastoplastic materials. The simulation then continued with a dynamic analysis of Mohr-Coulomb nonlinear elastoplastic materials taking into account the shakedown effects in the base layer. The final simulation was conducted on Mohr-Coulomb nonlinear elastoplastic materials taking into account the shakedown effects, while also examining the effect of the base-asphalt interaction.

In this chapter, all simulations were conducted using ABAQUS 6.10 (Hibbit and Sorenson, Inc. 2010). The main challenge in the dynamic simulation was the long computation time required, especially with a large number of cycles in the simulation. To overcome this problem, two solutions were considered: First of all, since a complete parameter study had been conducted in the previous chapter, the parameter study in the dynamic simulation could be omitted. As a matter of fact, the effects of the parameters would be the same for both static and dynamic

analysis. In other words, one would expect to see less deformation with an increase in AC thickness (as reported in Chapter 5). This trend does not change when considering dynamic forces in the simulation. The second solution was to apply a scale of 1/1000 in the constitutive models (Mohr-Coulomb and shakedown), so that each cycle of loading would represent 1000 cycles in the field. Although some approximation of calculations would be forced by this assumption, the results of verification proved that the approximations were within an acceptable range.

Although the two solutions greatly decreased the computation time, each dynamic analysis still took approximately 10 days (full computation is conducted by Dell XPS core i7 2860QM @2.5 GHz 16GB Ram) for an equivalent of 100,000 cycles. The results of this chapter will hopefully be of use for future research.

## 6.2 Dynamic Analysis

This chapter firstly explains the details of model construction. This consists of mesh construction and refinement, boundary conditions, loading and finally material characteristics.

The next section presents the results of the dynamic analysis considering simple Mohr-Coulomb nonlinear elastoplastic materials. Surface deformation in both transverse and vertical directions is presented. The time history of displacement under the loading tyre and the time history of strain (total and plastic) on the base layers are discussed. Then, stress-strain hysteresis loops are investigated to provide more in-depth knowledge of actual material behaviour. Finally, a table of critical results is presented.

Section 6.2.3 conducts an analysis of the dynamic Mohr-Coulomb nonlinear elastoplastic materials taking shakedown effects into account. Mesh deformed in transverse directions is presented. The time histories of displacement under the loading tyre are studied, along with the time history of total and plastic strain. Stress-strain hysteresis loops are presented, and finally the critical results are presented in a table.

Section 6.2.4 conducts the final dynamic analysis of Mohr-Coulomb nonlinear elastoplastic materials taking shakedown into account as well as the effects of soil-asphalt interaction. This phase is considered the most complete analysis in this research. The results of deformation, strains, and hysteresis loops are presented and discussed in the same way as in previous sections.

The final section of this chapter compares and remarks upon the results of the three different dynamic analyses and discusses the effects of dynamic analysis in respect to static analysis is provided.

### **6.2.1 Model Construction**

This section describes the details of the constructed model. The major components of model construction include the elements, mesh, boundary conditions, loading and material properties.

The dynamic analysis takes into account the recommended ratio which was used for static analysis in order to minimize the effects of boundary conditions (see Chapter 5). However the number and order of elements are optimized to reduce the computation time as much as possible. During the dynamic analysis it was found that optimized mesh could significantly affect the computation time. The

concern is greater when three-dimensional analysis is involved. In this case, the effect of refinements on the model will increase the total number of elements by an order of three. For example, resizing the mesh to half size will increase the total number of elements by eight times. According to this a well distributed mesh refinement should be attained. In the current mesh construction, fine mesh distribution was selected close to the loading tyre, but coarser mesh further from the loading area. Figure 6.1 illustrates the constructed mesh used in the dynamic analysis.

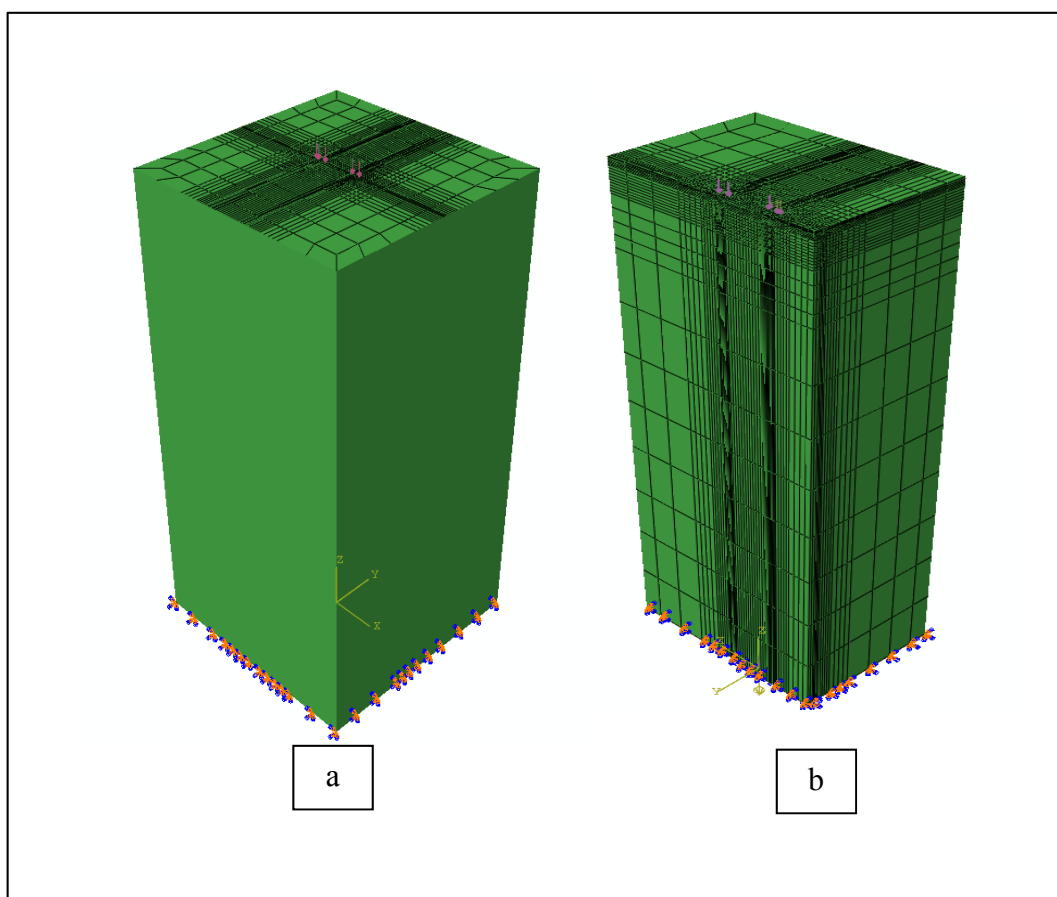


Figure 6.1- Constructed Mesh for Dynamic Analysis

Overview (a) and View-Cut (b)

As can be seen in Figure 6.1, the fine mesh is distributed close to the loading axle. The distribution of the mesh in depth is also finer close to the surface and gradually gets coarser in the vertical direction. After a trial and error process of optimizing the mesh distribution, the final model consisted of 59,392 elements and 64,185 nodes. Two types of element were selected to represent the body of soil (C3D8R) and the infinite boundary of the model (CIN3D8).

In the dynamic analysis, a standard single axle dual tyre was used to represent loading. Figure 6.2 demonstrates the details of the loading axle modelled in this simulation.

Dynamic loading was assumed to be a periodic vertical pressure applied to the same spot. In this regard, it should be noticed that the effect of a moving tyre was neglected in this research. Instead the focus was on the impact of repeated loading cycles on the same spot. This approach is the same as that taken by previous researchers (Bodhinayake 2008; Saad, Mitri and Poorooshasb 2005; Al-Qadi, Wang and Tutumluer 2010).

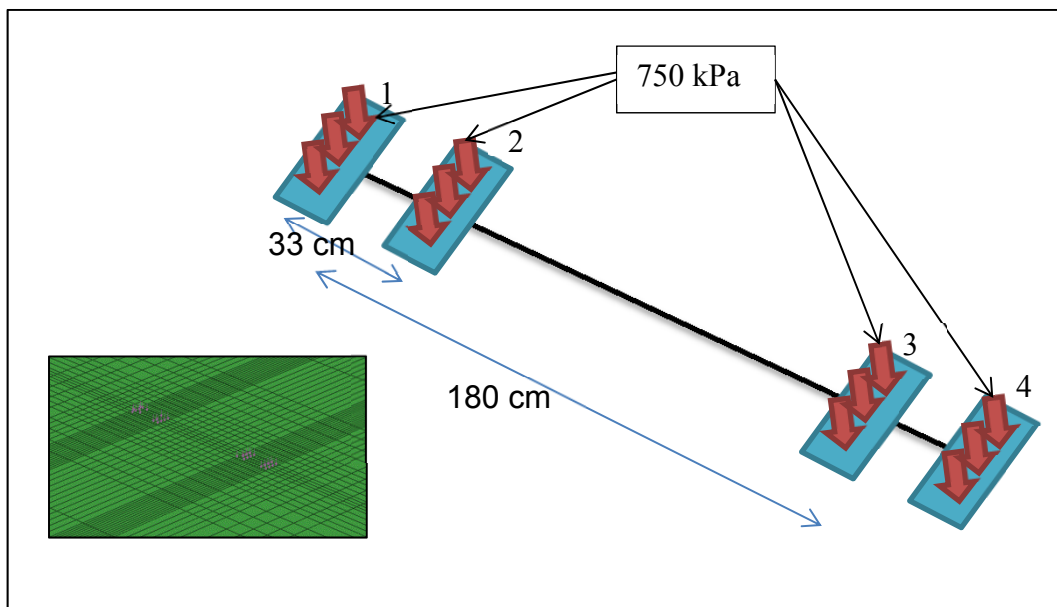


Figure 6.2 - Loading in Dynamic Analysis

The loading was simulated at 0.1 s followed by a 0.9 s rest period. Based on previous studies (Barksdale 1971; Bodhinayake 2008; Saad, Mitri and Poorooshagh 2005), this represents a vehicle travelling at a speed of approximately 100 km/hr (Figure 6.3). This specific type of loading has been used to simulate cyclic loading in repeated triaxial cells to simulate shakedown behaviour (Allou, Chazallon and Horny 2007; Chazallon, Horny and Mouhoubi 2006; Chazallon, Koval and Mouhoubi 2011; Siripun, Nikraz and Jitsangiam 2011). It should be remembered that the constitutive model of shakedown depends on the experimental relationship between UGM plastic strain and the number of loading cycles. The implementation of this specific type of loading therefore satisfies the loading conditions enforced by the experiments. As explained in Chapter 4, loading cycles are assumed to be haversine curves (Figure 6.3).

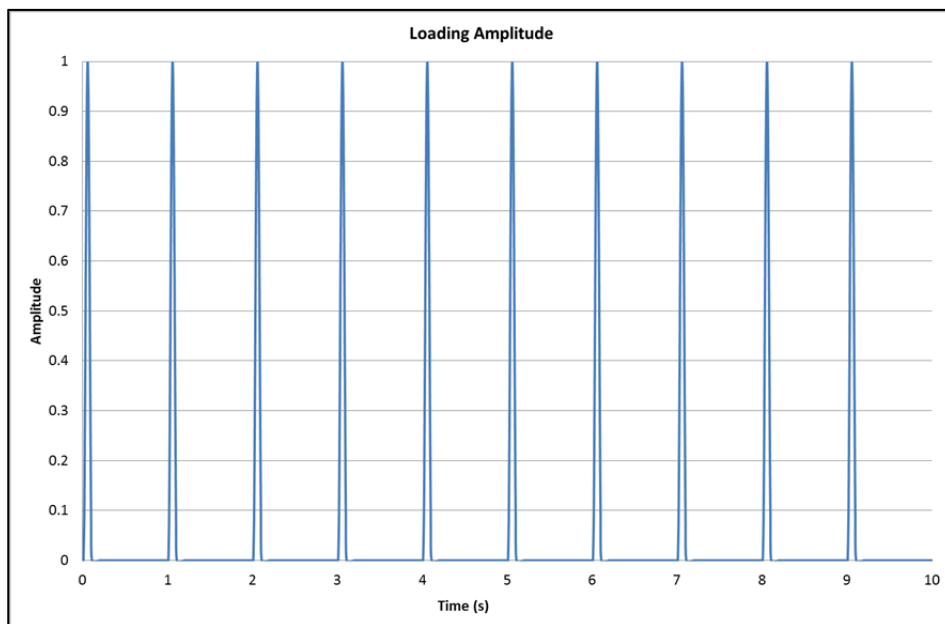


Figure 6.3- Amplitude of Loading in Dynamic Analysis

The implementation of the rest period also provides enough time for the damping properties of materials to diminish the induced motion. The advantage of this is that it can reduce the chance of undesirable resonance during the simulation.

Finally it should be noted that the pressure distribution on the tyre was supposed to be uniform (as in the static analyses).

The boundary conditions in dynamic analysis can have a great influence on the results. As well as the known effects of reflection from the boundaries, they can also produce undesirable resonance effects in the model. It should be stated here that the induction of resonance is expected in this specific type of simulation where loading is applied constantly at the same amplitude and period. Having a sufficient vertical depth of soil mass with proper  $\alpha$ -damping parameters can solve the problem. However, to resolve problem for horizontal boundaries, the

preferable solution would be the usage of infinite elements (Kouroussis, Verlinden and Conti 2009, 2010; Motamed et al. 2009; Pan and Selby 2002; Al-Qadi, Wang and Tutumluer 2010). Based on this, the encastré condition was applied to the bottom of the model while infinite elements were implemented around the horizontal boundaries.

ABAQUS provides the user with a specific type of infinite element that can model infinite half-space. In a dynamic simulation, the response of the infinite elements is calculated based on the assumption of the perpendicular passage of plane body waves through the boundaries. It is assumed that the response has a small amplitude far from the boundaries, which provides linear elastic conditions in the medium. Assuming isotropic linear elastic materials, a proper damping ratio is applied to represent infinity. The concepts relating to and details of this method were described in Chapter 3.

In this simulation, CIN3D8 elements were selected to represent brick infinite elements on the boundaries of the model (Figure 6.4).

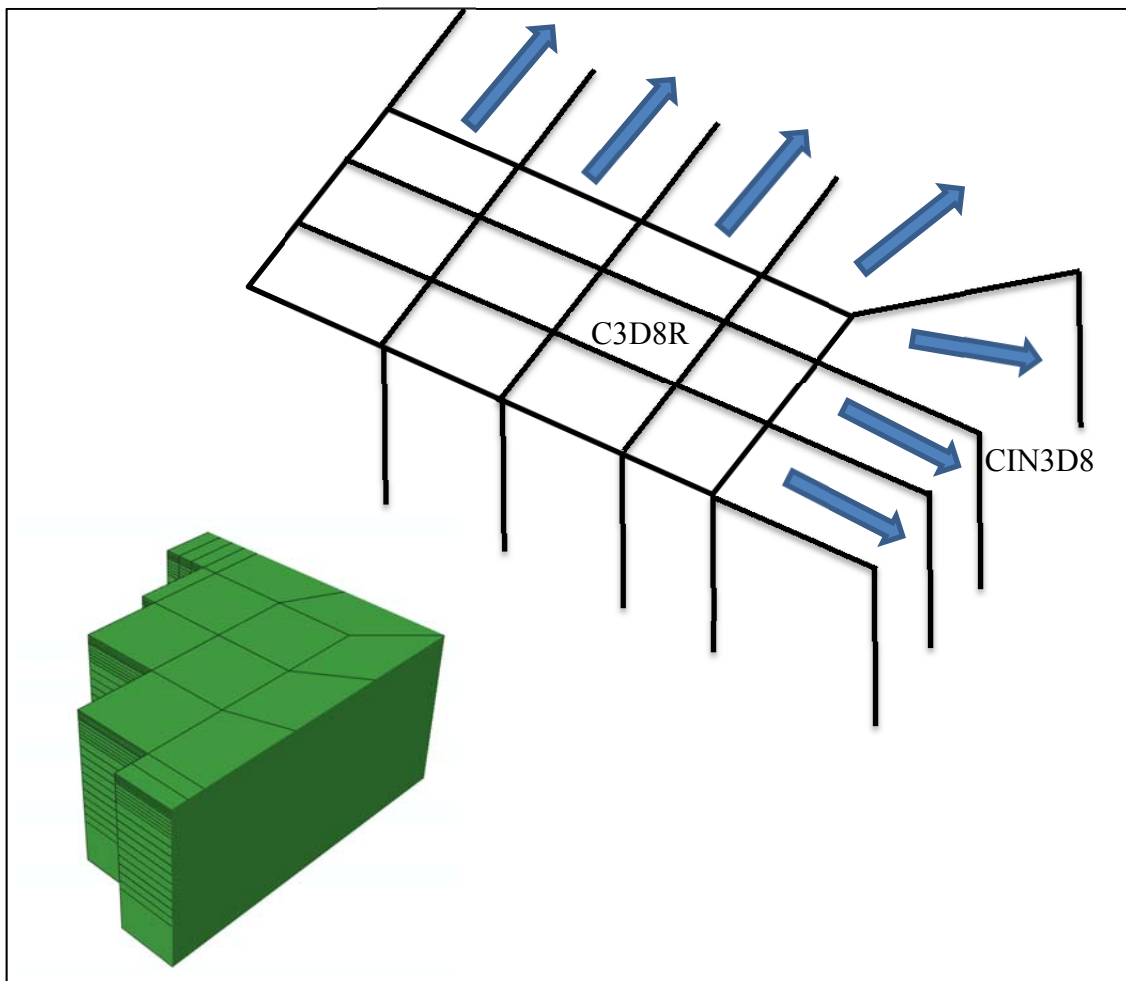


Figure 6.4 - Implementation of Infinite Elements in Dynamic Analysis

There are three different dynamic analyses covered in this chapter. The first analysis assumes Mohr-Coulomb material behaviour for subgrade and nonlinear elastic Mohr-Coulomb behaviour for the base layer, while asphalt is assumed to be linear elastic. In the second analysis, nonlinear elastic Mohr-Coulomb behaviour taking the effect of shakedown into account is considered for the base materials, while Mohr-Coulomb material behaviour is assumed for the subgrade layer and the asphalt is assumed to be linear elastic. The final analysis assumes shakedown nonlinear elastic Mohr-Coulomb behaviour for the base layer, while

the interaction of base and asphalt layers is taken into account. The subgrade materials are assumed to be Mohr-Coulomb and the asphalt layer is assumed to behave linear elastically.

In all of these three analyses the Rayleigh damping coefficients (as described in Chapter 3) are assumed to be 10%. The behaviour of the asphalt-base interaction is assumed to be frictional in a tangential direction and hard contact in a normal direction. Therefore, the asphalt layer is not permitted to penetrate the base layer.

Chapters 3 and 4 laid out the details of the constitutive models and their coding algorithms. The constitutive models are modified in such a way that each cycle of loading simulates 1000 cycles (based on the plastic strain developed). This will reduce the total number of cycles required for the simulation, while enforcing approximation of the analysis. Since the main objective of this chapter was to consider the development of plastic strain and permanent deformation, such assumptions are appropriate in this analysis.

Two previously published shakedown curves were selected to verify the newly developed constitutive model of shakedown model. One of these curves was then used to simulate shakedown in this research. It should be remembered that any type of material has its own specific shakedown curve; however, the curve can easily be implemented in the presented approach.

ABAQUS provides the ability to introduce the new constitutive model through coding of the UMAT subroutine. Therefore the algorithms described in Chapter 4 were incorporated in UMAT coding and integrated into the model. The following subsection presents the results of three different models. Model 1 represents the dynamic responses of a simple Mohr-Coulomb constitutive model, Model 2

represents the dynamic responses of Mohr-Coulomb taking shakedown effects into account, and finally Model 3 represents the results of dynamic shakedown taking into account the effects of soil-base interactions.

### **6.2.2 Nonlinear Elastoplastic assuming Mohr-Coulomb Plasticity**

In Model 1, the first dynamic analysis was run in order to gain an understanding of the dynamic behaviour of the layered structure of flexible pavement. In this analysis, the constitutive equation for the materials is the same as that stated in Figure 4.9 displays the properties of the materials used for the different layers in the dynamic analysis.

Table 6.1- Materials Properties in Dynamic Analysis Model 1

<b>Properties</b>	<b>Layer</b>		
	Asphalt (AC)	Base	Subgrade
Elastic Modulus (MPa)	2800	K1= 332(MPa), k2 = 0.08, k3 = 0.2	50
Poisson's Ratio	0.35	0.4	0.45
Friction angle (degrees)	0	30	20
Cohesion (kPa)	0	10	10
Dilation angle (degrees)	0	15	10
Density (Kg/M <sup>3</sup> )	2400	1800	1700
Rayleigh Damping	10%	10%	10%

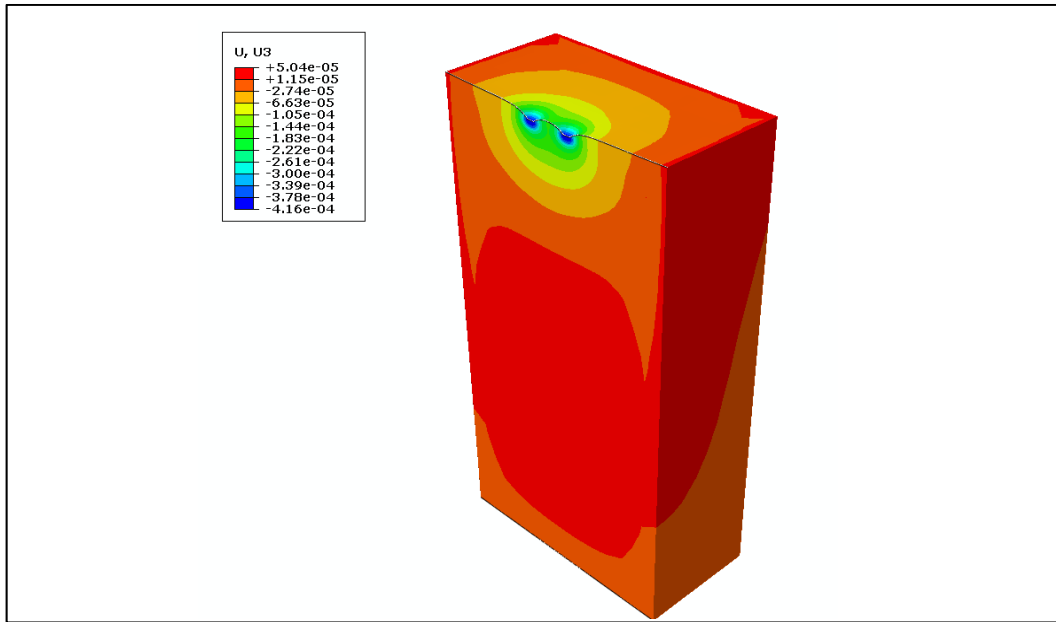


Figure 6.5 - Deformed Mesh in Dynamic Analysis (Model 1)

As stated previously, dynamic analysis required the values for the damping of materials in order to prevent resonance. In this analysis, 10% damping was applied and was found to properly diminish undesirable resonance effects. It is important to note that the value of damping applied should work together with the boundary conditions. The values for the density of the materials are selected according to the typical values of these materials as stated by AUSTROADS (2004).

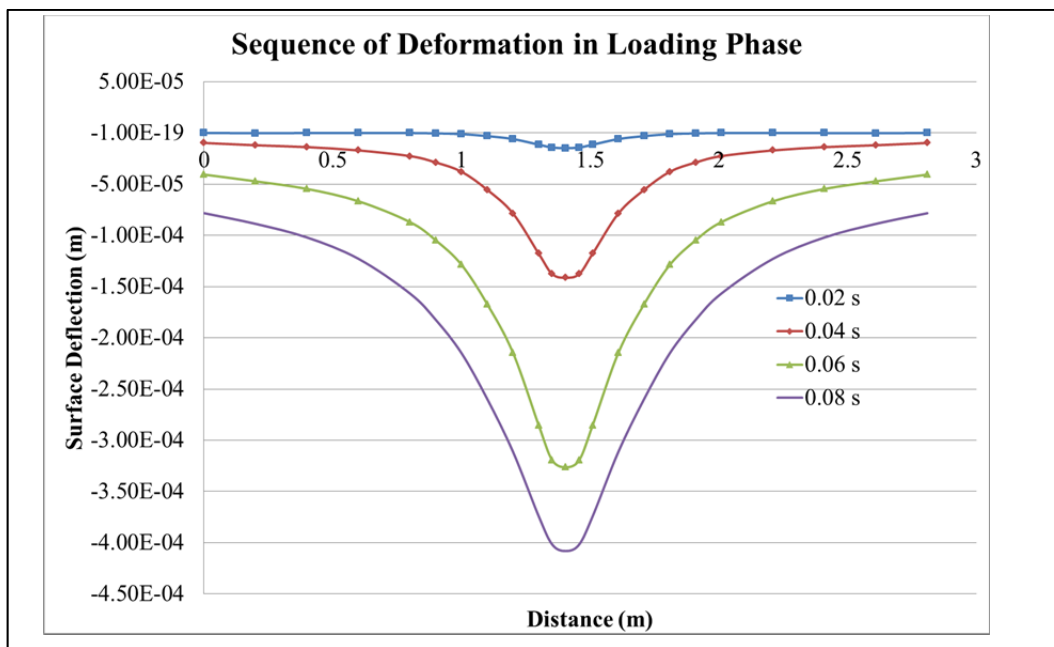


Figure 6.6 – Sequence of Dynamic Longitudinal Deformation: Loading (Model 1)

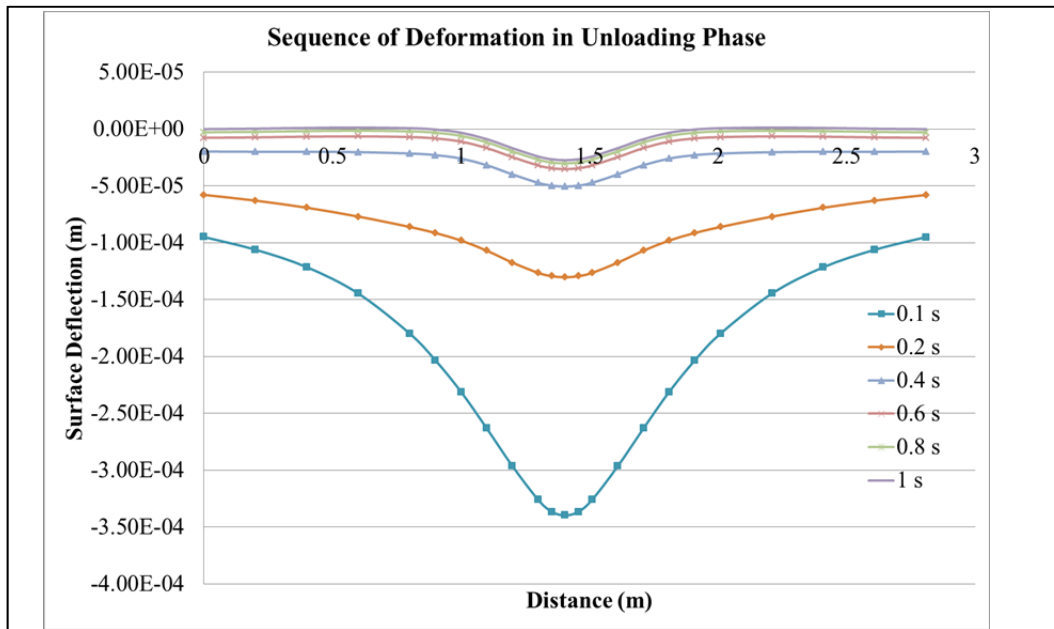


Figure 6.7 – Sequence of Dynamic Longitudinal Deformation: Unloading  
(Model 1)

Figure 6.5 demonstrates the deformed mesh for the first dynamic cycle in Model 1. The model has been cut in transverse axis, passing through the middle of the tyre axle. The schematic contours of the vertical deformation here are similar to those of the static analysis but with lower values of deflection.

To have a closer look at the actual dynamic behaviour of the materials, the sequence of loading and unloading in the first dynamic cycle under tyre pressure in a longitudinal direction are illustrated in Figure 6.6 and Figure 6.7.

Here the term ‘longitudinal direction’ refers to the direction of travel, where it is perpendicular to the tyre axle. In the ABAQUS model, this direction was represented by axis number 2 (y-direction). Here the selected node for deflection is the node in the middle of tyre number 1 (see Figure 6.2).

As can be seen from these two figures, in the loading phase the vertical deflection below the tyre progressively grew until it reached a value of 4E-4 m (.4 mm) in 0.1s, which was the loading time span. After that, the deflection was gradually retrieved during the 0.9 s resting time until it reached 1.5E-5 m. This final amount is the residual deformation produced in this cycle, and can be accumulated with the residual deflection caused from subsequent loading.

Similar to the longitudinal direction, the results of the induced vertical deflection on the middle of tyre number 1 in the transverse direction are illustrated in Figure 6.8 and Figure 6.9.

In this direction, the effect of the particular loading tyre can be observed. According to the results, the maximum deflection occurred under loading tyre

number 2. This was also observed in the static analysis for the same tyre (Chapter 5).

The values of deflection in the transverse direction are close to the values of deflection in the longitudinal direction. However, there is a minor difference in the shape of the deflection for the loading and unloading phase.

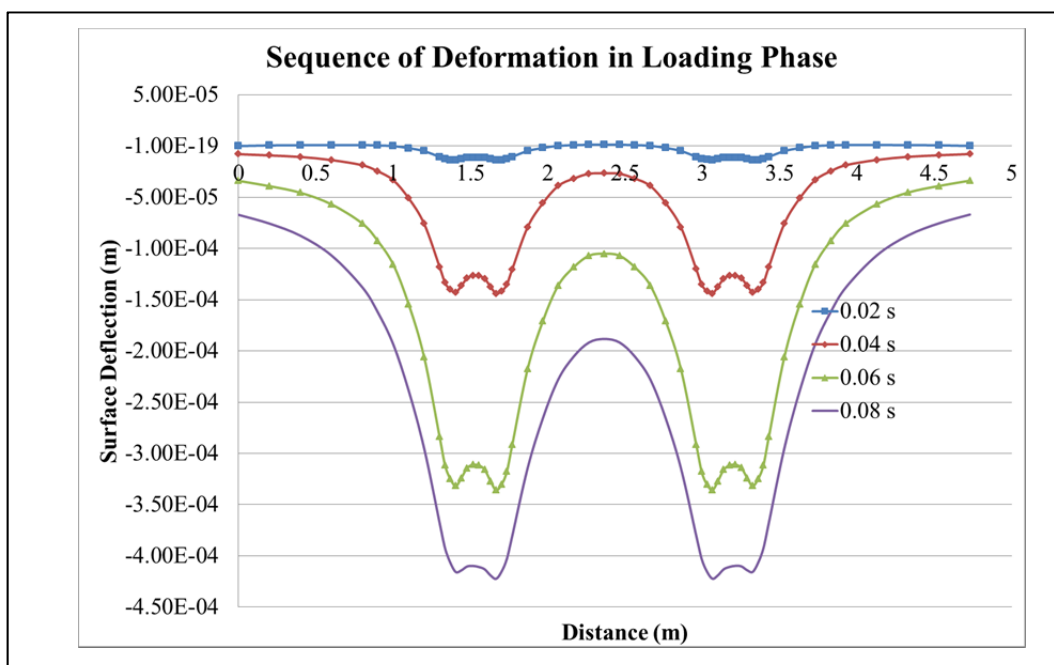


Figure 6.8 – Sequence of Dynamic Transverse Deformation: Loading (Model 1)

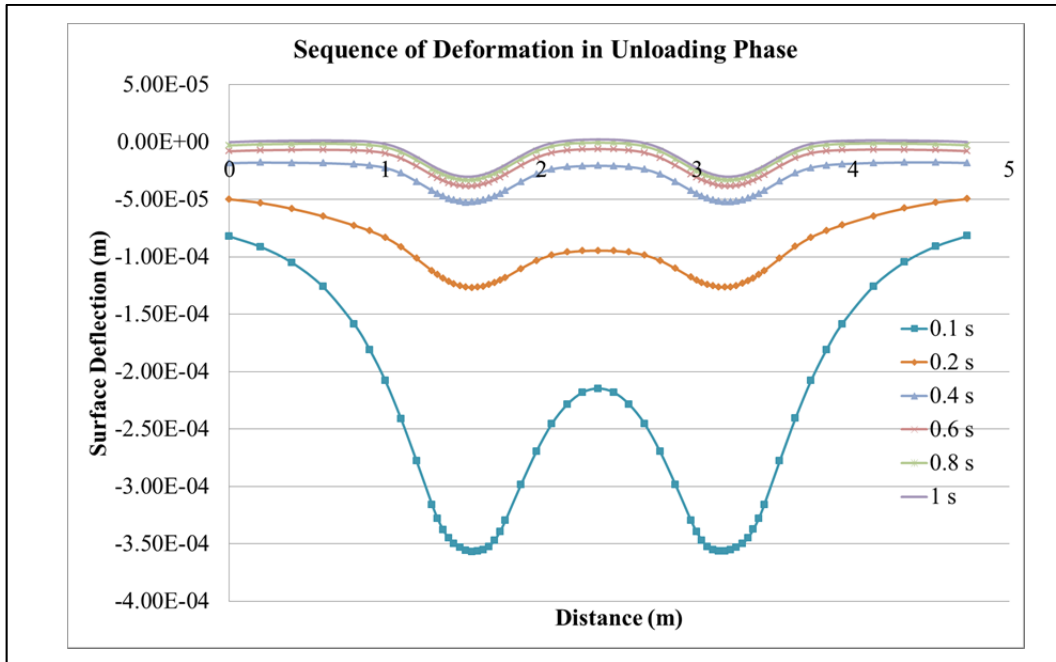


Figure 6.9 – Sequence of Dynamic Transverse Deformation: Unloading (Model 1)

In the loading phase, the effect of the tyres is clear, while in the unloading phase the shape of the deflection has formed a more uniform curve induced by the effects of both loading tyres.

One of the most important findings of this research is the representation of the history of deflection with regard to the loading cycles. This is displayed in Figure 6.10. It is clear that due to the accumulation of residual deflection, the deflection under the loading wheel increased with each step. The results of the vertical deflections are presented for the node in the middle of tyre number 1.

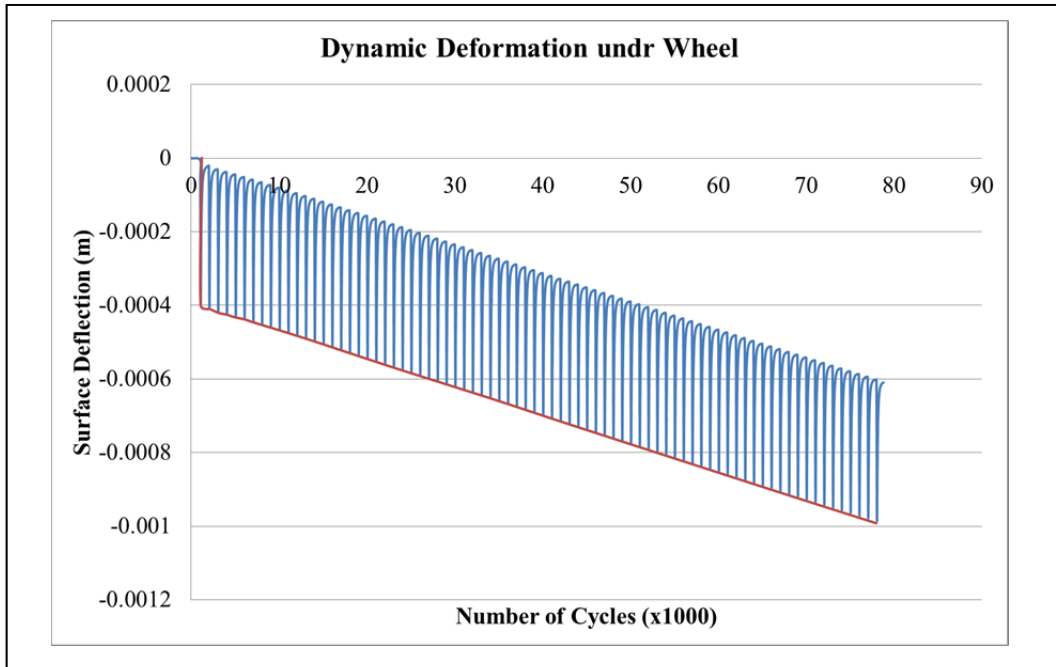


Figure 6.10 – Time History of Deformation under the Wheel (Model 1)

Here the vertical deflection below the loading tyre increased from an initial value of 4E-4 m to 10E-4 at the end of loading.

The trend of increase is fairly close to a straight line. This is expected since the simple Mohr-Coulomb constitutive model does not consider the effects of material modification during each cycle of loading. Therefore, if the same loading stress is applied, almost the same permanent deformation will be generated. The obvious trend here confirms this.

It should be noted that while Model 1 was set to run to an equivalent of 100,000 cycles, it stopped close to 80,000 due to excessive plastic strain induced during the dynamic analysis. This further explained in the following paragraphs.

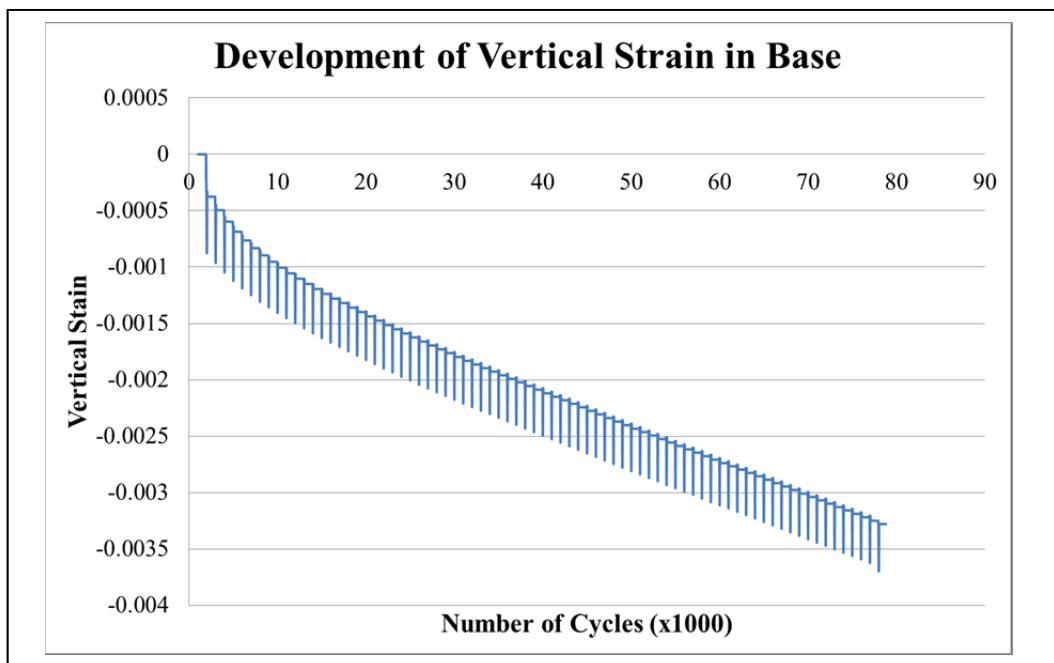


Figure 6.11 – Development of Total Vertical Strain (Model 1)

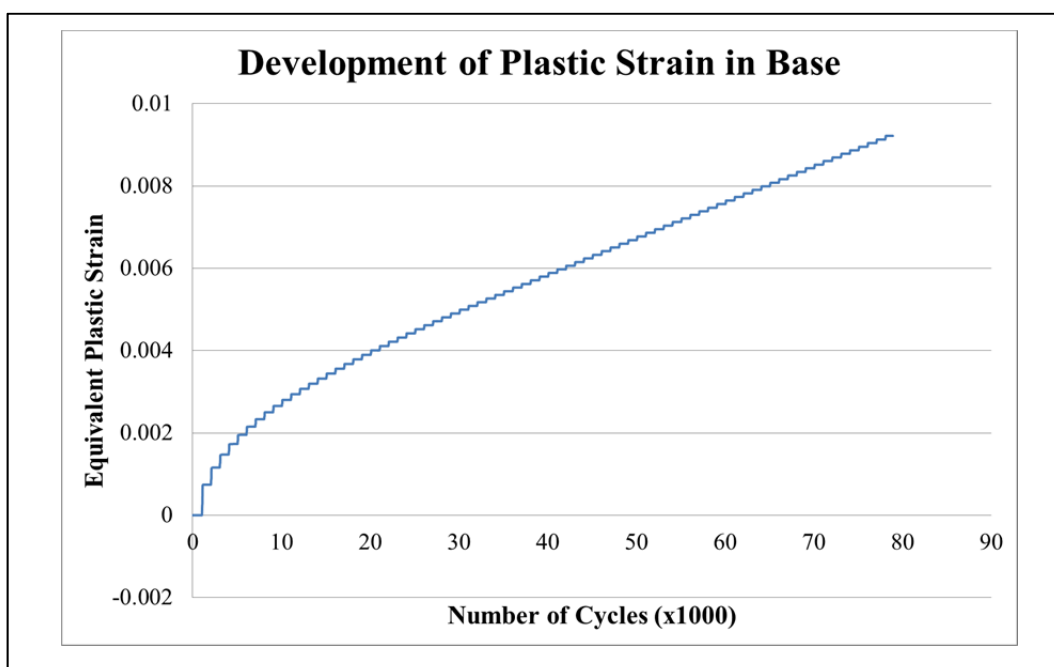


Figure 6.12 – Development of Equivalent Plastic Strain (Model 1)

Figure 6.11 represents the development of vertical strain at the element on top of the base layer exactly beneath the middle of loading tyre number 1. The initial strain here started at -0.000876 and gradually increased to -0.0037. The trend was almost linear after a few cycles and it can be deduced that the permanent deformation trend was governed by a trend of accumulative vertical strain.

Figure 6.12 displays the development of equivalent plastic strain in the same element of the base layer. The value of the plastic strain grows to an amount that cannot be considered a small strain (which is the assumption of this analysis). When the amount of strain hits the maximum permitted, the analysis stops and it is considered a failure in the material. Therefore, according to the dynamic analysis using the simple Mohr-Coulomb constitutive model, the structural layers of flexible pavement can only stand 80,000 cycles of loading. This implication becomes more interesting when compared to the results calculated for the same model but taking shakedown effects into account. This will be presented in the next section.

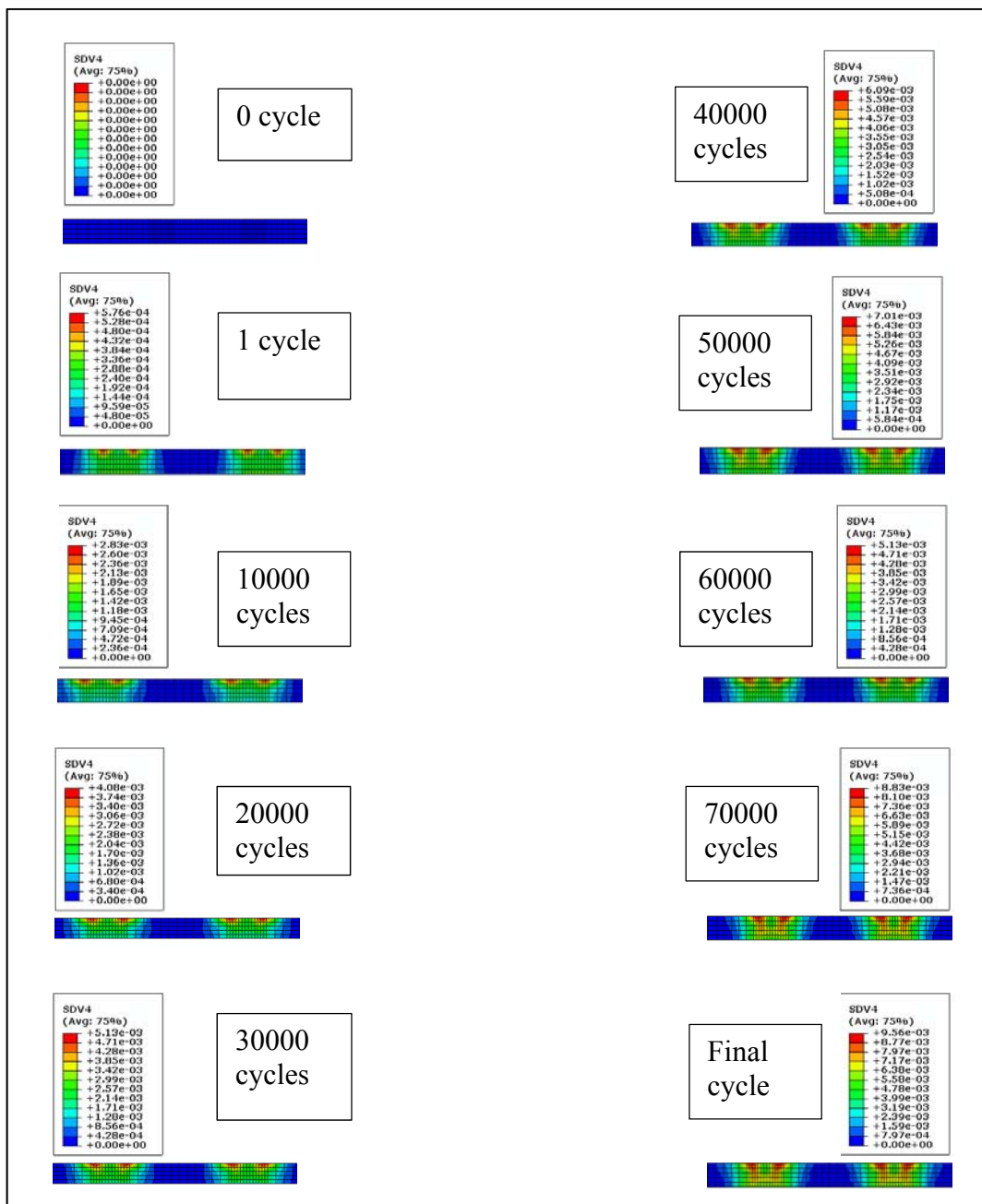


Figure 6.13- Development of Equivalent Plastic Strain in Base (Model 1)

In a progressive trend, Figure 6.13 demonstrates the development of equivalent plastic strain in the base layer in a transverse direction at the middle of the wheel axle.

The plastic strain is demonstrated from the initial stage of the dynamic analysis until the last cycle. As can be seen from the figure, the plastic strain increased below the wheels, gradually forming a column-like plastic area in the base layer. Then from cycle 50,000, an area with severe plasticity grew particularly beneath the point of contact of the two wheels.

The contours presented in this graph provide the reader with a clearer understanding of the plastic mechanism developed in the base as a result of the loading cycle.

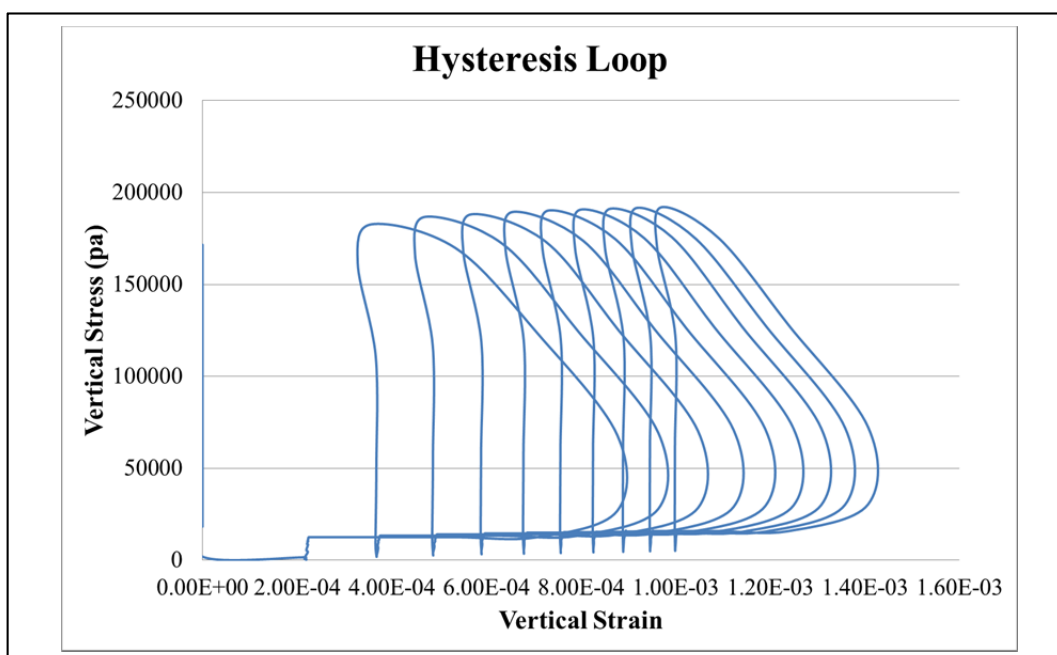


Figure 6.14 – Hysteresis Loops of Initial Cycles (Model 1)

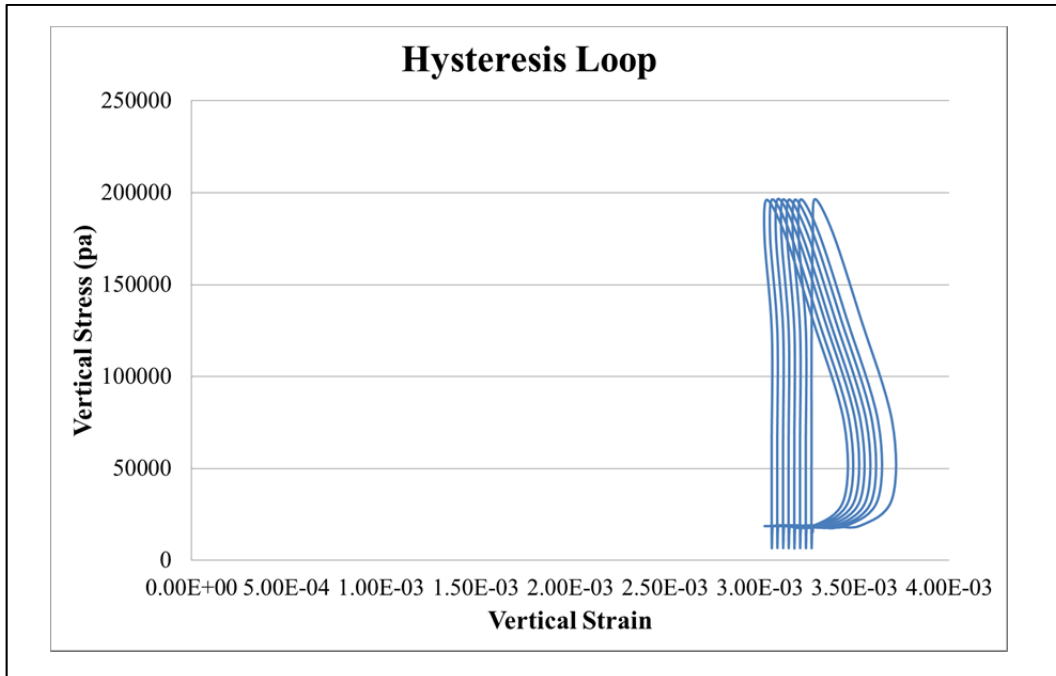


Figure 6.15 – Hysteresis Loops of Final Cycles (Model 1)

To gain a more comprehensive understanding of material behaviour under dynamic loading, hysteresis loops for the same element in the base layers are displayed in Figure 6.14 and Figure 6.15 (the absolute values of stress and strain are graphed).

It can be seen that in the hysteresis loops for the initial stage of the analysis, the materials show a slow trend of compaction (Figure 6.14). This compaction is purely imposed by the geometrical criteria of the adjacent elements, not by modifications to the material properties. The effect has almost vanished in the final cycles where the hysteresis loops have the same area for each cycle (Figure 6.15). It can therefore be deduced that the same amount of energy is accumulated as plastic deformation in each cycle, which can cause the failure of material.

Finally, to provide grounds for comparison, Table 6.2 **Error! Not a valid bookmark self-reference.** indicates the results for four critical responses of the flexible layer in the dynamic analysis, at the initiation of the analysis and at the final cycle.

In order to be consistent with the results of the static analysis, all of the values are indicated for the element in the middle of loading tyre number 2. As can be seen from the values, there is a huge increase from the initial cycles to the final cycles. For instance, the vertical strain of the subgrade increased from -217E-6 to -870E-6 (400%). Such a severe increase can be related to the behaviour of the constitutive model in response to the large number of repeated loadings.

The next section presents the results of the dynamic loading assuming shakedown effects.

Table 6.3 - Responses of Flexible Layer in Dynamic Analysis (Model 1)

Time	Vertical Deflection (Top of AC)	Horizontal Strain (X-Axis) (Bottom of AC)	Vertical Strain (Z-Axis) (Top of SG)	Vertical Stress (Top of SG)
Initial	0.4 mm	-150E-6	-217E-6	-19109 Pa
Final	1.0 mm	-1050E-6	-870E-6	-57703.2 Pa

### **6.2.3 Nonlinear Elastoplastic assuming Mohr-Coulomb Plasticity considering Shakedown Effects**

This section presents the results of the dynamic simulation of granular materials in the base layer under shakedown effects. The basics of the concept have previously been discussed in Chapter 3 and 4.

In the first part of this stage, two verification analyses were conducted to ensure that the coding of the new constitutive model was working in agreement with laboratory observations.

The model created for the verification simulated the standard triaxial cylinder to represent the same geometrical conditions as the experiments in the laboratory. The model was created under axisymmetric conditions. Figure 6.16 represents the model constructed for the purpose of verification.

The first laboratory results selected for the verification are those generated in a laboratory at Curtin University by the Pavement Research Group. These results were published in 2010 (Siripun, Jitsangiam and Nikraz 2010). The confining and deviator stresses were applied as stated in the paper. Material properties as stated in Table 1 by Siripun, Jitsangiam, and Nikraz (2010) were adhered to, including a cohesion of 32 kPa, friction angle of  $59^\circ$  and dilation angle of  $30^\circ$ . The constitutive modelling discussed in Chapter 3 and Chapter 4 was coded to represent the shakedown behaviour of this material under Mohr-Coulomb plasticity criteria. The simulation was run for the equivalent of 600,000 cycles.

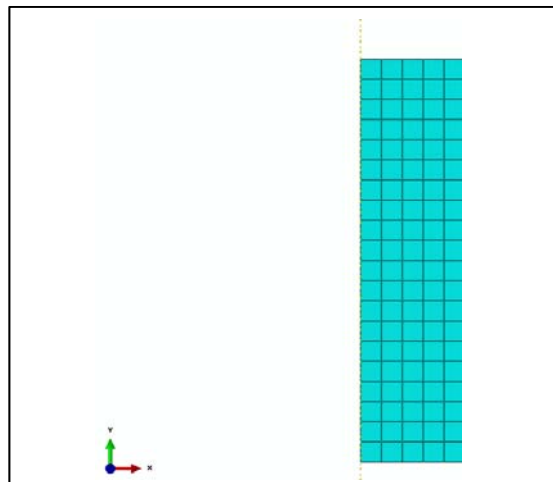


Figure 6.16 - Constructed Mesh for Verification Purpose in Shakedown Simulation

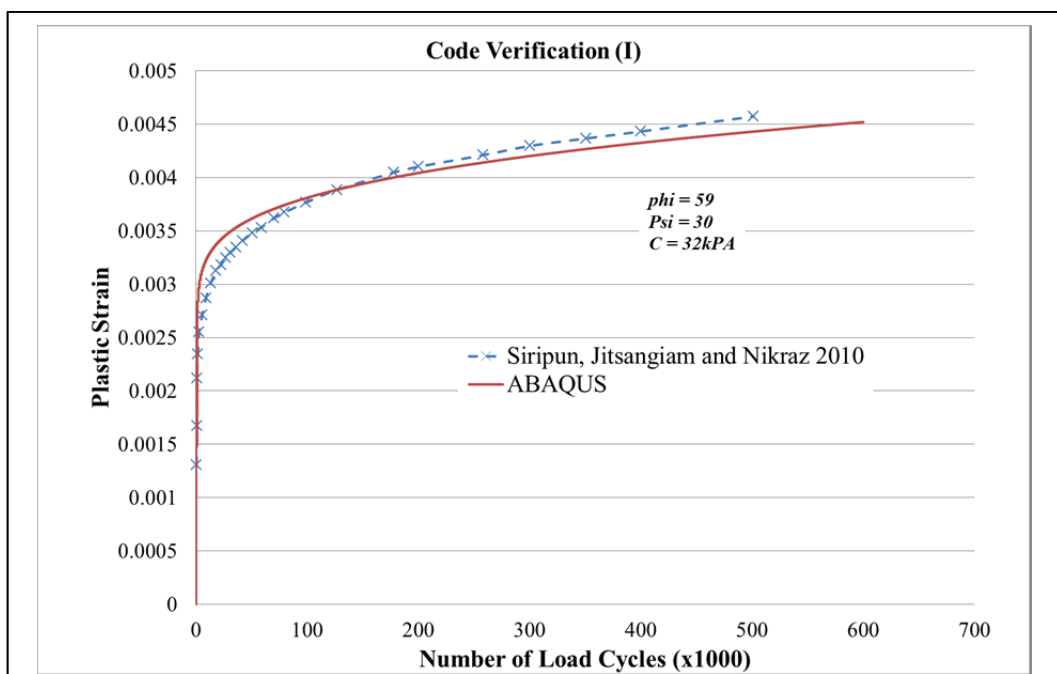


Figure 6.17- Shakedown Code Verification (I)

The plastic strain developed from the simulation is plotted against the plastic strain developed in the laboratory experiment. As can be observed in Figure 6.17, a similar result is generated. Small differences can be related to the natural idealization inherited in finite element simulation, while actual material behaviour can have more complex traits. However, the maximum difference was found to be less than 3%.

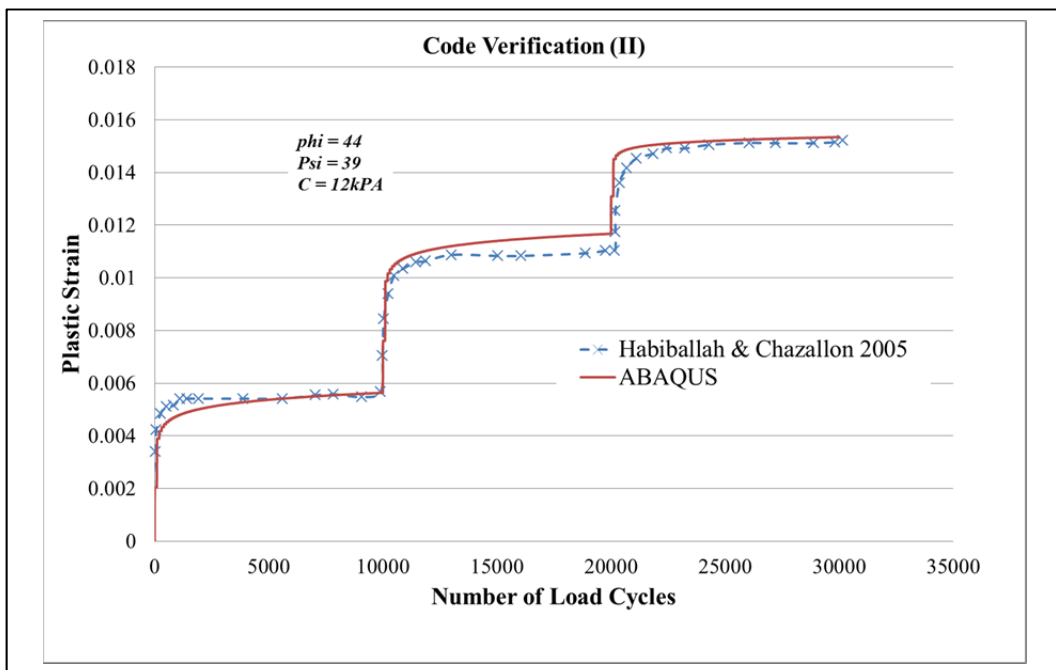


Figure 6.18-Shakedown Code Verification (II)

The second verification simulation was selected from laboratory results published in the literature (Habiballah and Chazallon 2005). The same material properties stated in Table III of the paper were implemented in the ABAQUS model, including a cohesion of 12.26 kPa, friction angle of  $44^\circ$  and dilation angle of  $15^\circ$ .

This simulation was run for three stages of confining pressure and deviator stress ( $q/p = 3$ ) as detailed by Habiballah and Chazallon (2005). The results of the induced plastic strain with regard to the loading cycle were then graphed.

Figure 6.18 demonstrates the results of the simulation against the reported results from the laboratory. Here again a close trend can be identified, although there were still differences. The major difference occurred in cycle 20,000 where there was a maximum of 5% variation between the simulation and laboratory results.

After the two verification analyses it was decided that the embedded code could closely reflect the shakedown behaviour of unbound granular materials under a large number of cycles of loading.

The second dynamic analysis was conducted in Model 2 to investigate the effect of shakedown behaviour on the layered structure of flexible pavement. The constitutive equation implemented in this model is the one described in Figure 4.10. To provide grounds for comparison, the material properties used in this analysis were the same as for Model 1,

In Model 1, the first dynamic analysis was run in order to gain an understanding of the dynamic behaviour of the layered structure of flexible pavement. In this analysis, the constitutive equation for the materials is the same as that stated in Figure 4.9 displays the properties of the materials used for the different layers in the dynamic analysis.

Table 6.1. The UGM used in the base layer is assumed to have a decay function like the one indicated by Siripun, Jitsangiam, and Nikraz (2010b) in the Curtin University laboratory. This is stated in Equation 6-1.

$$\varepsilon^p = 2.1989 \left[ \frac{N}{1000} \right]^{0.1175} \quad \text{Equation 6-1}$$

Where

$\varepsilon^p$  = plastic strain

N = number of loading cycle

Equation 6-1 plays the role of decay function  $f$  explained in Equation 3-42 and Equation 3-43.

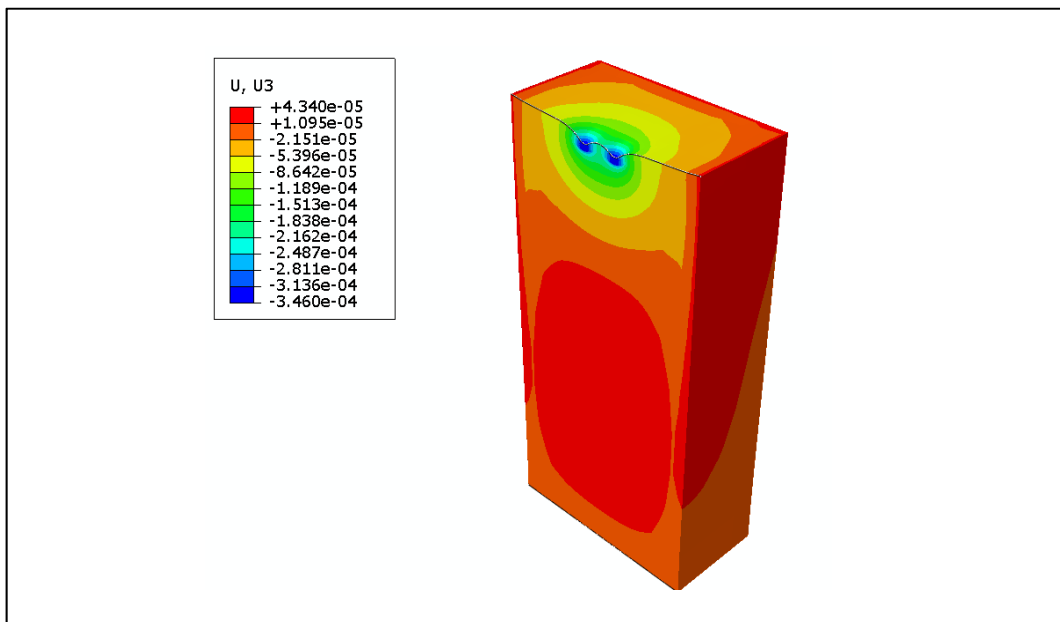


Figure 6.19-Deformed Mesh in Dynamic Analysis (Model 2)

The Rayleigh damping values selected were the same as the values for Model 1 of the dynamic analysis. Figure 6.19 illustrates the deformed mesh of the first loading cycle in the Model 2 simulation. A section has been cut through the

transverse axis passing through the middle of the tyre axle. The contours of deformation in the first cycle are fairly similar to those of Model 1.

Figure 6.20 and Figure 6.21 demonstrate the dynamic response of the layered structure to sequences of loading and unloading for the first dynamic cycle under tyre pressure in a longitudinal direction. The vertical deflection increased to a value of 4E-4 m (0.4 mm) and then gradually returned to 1.5E-5 m. The values are close to those obtained for the first loading cycle for Model 1. This is to be expected since the difference between Model 1 and Model 2 should be due to the change in materials during the loading cycles, and in the first round of loading this should not be too different for the two models (that is, the degree of variation is small).

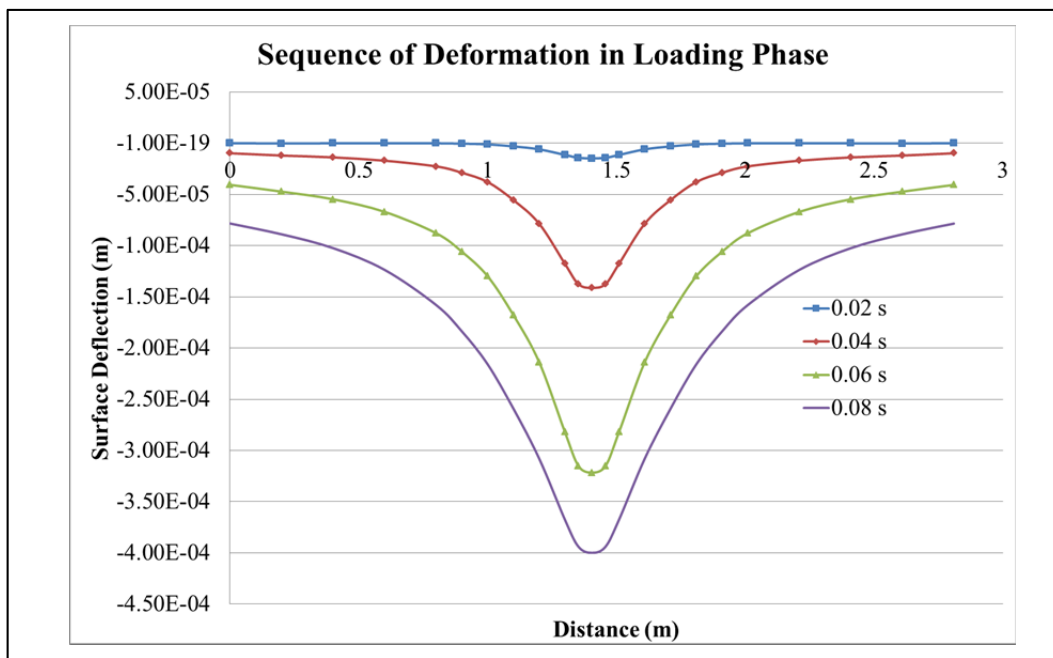


Figure 6.20- Sequence of Dynamic Longitudinal Deformation: Loading (Model 1)

In the same as for the longitudinal direction, the responses in terms of vertical deflection on the middle of the axle in a transverse direction are presented in Figure 6.22 and Figure 6.23.

Based on these results, the maximum deflection occurred under loading tyre number 2. As for Model 1, similar responses are observable for both transverse and longitudinal directions. The same shape of response for loading and unloading phases was obtained.

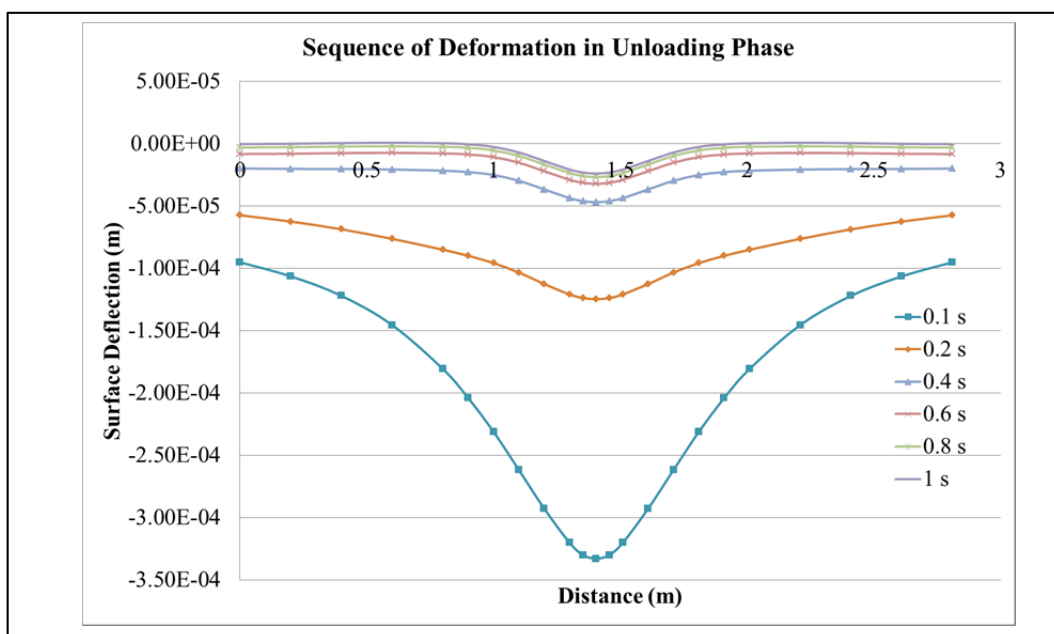


Figure 6.21 – Sequence of Dynamic Longitudinal Deformation: Unloading (Model 2)

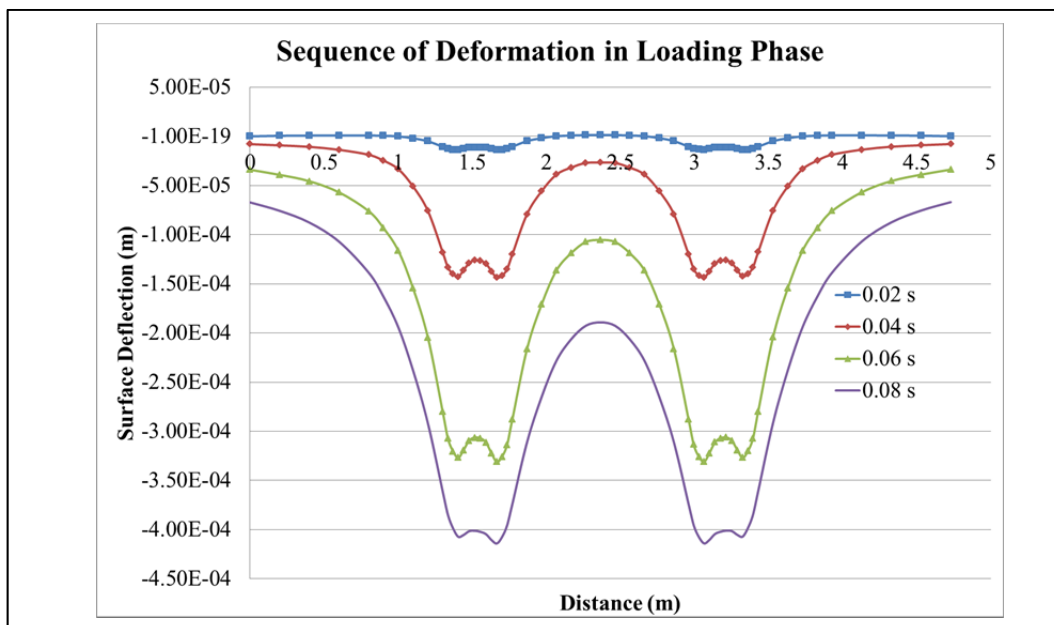


Figure 6.22 – Sequence of Dynamic Transverse Deformation: Loading (Model 2)

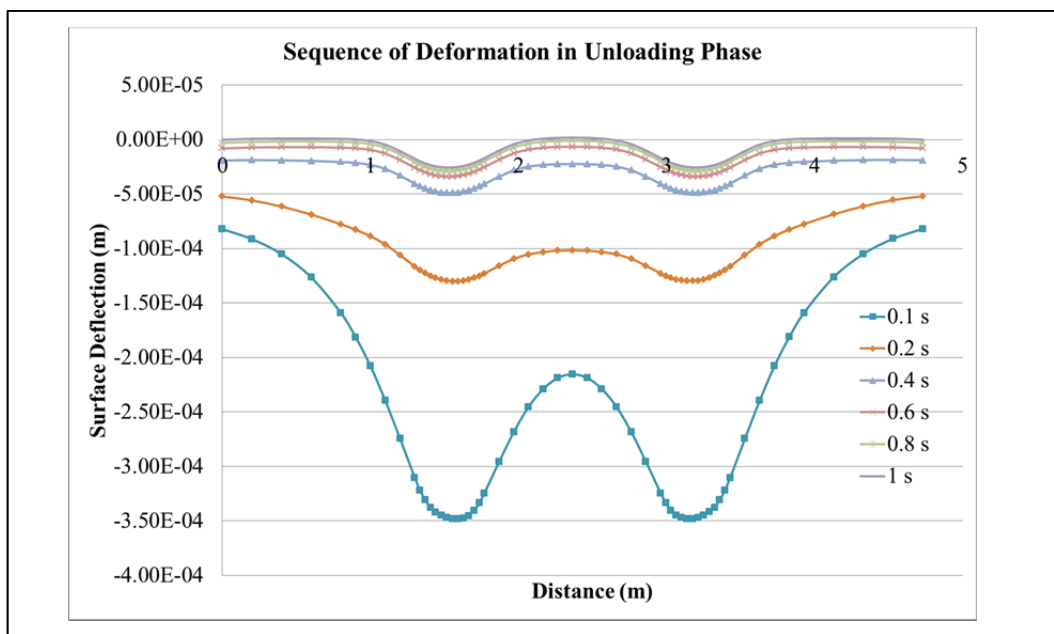


Figure 6.23 – Sequence of Dynamic Transverse Deformation: Unloading (Model 2)

The time history of the development of displacement under the loading tyre during the loading cycles is represented in Figure 6.24. While the accumulation of residual deformation is observable, the trend of deflection under the loading wheel is different from that in Model 1. While in Model 1 the increasing trend was close to a straight line, here the increase in deflection gradually decreased. It should be noted that the results apply to the same node as those for Model 1.

In this model, the vertical deflection below the loading tyre increased from 4E-4 m for the initial cycle to 5.8E-4 m at the end of the analysis. This value is comparable to the 10E-4 m obtained from Model 1 at the end of the analysis. There is a meaningful decrease in the deflection obtained from Model 2 compared to Model 1.

This change in surface deflection can be attributed to the change in the mechanical behaviour of materials induced by the introduction of the new constitutive model which accounts for shakedown effects.

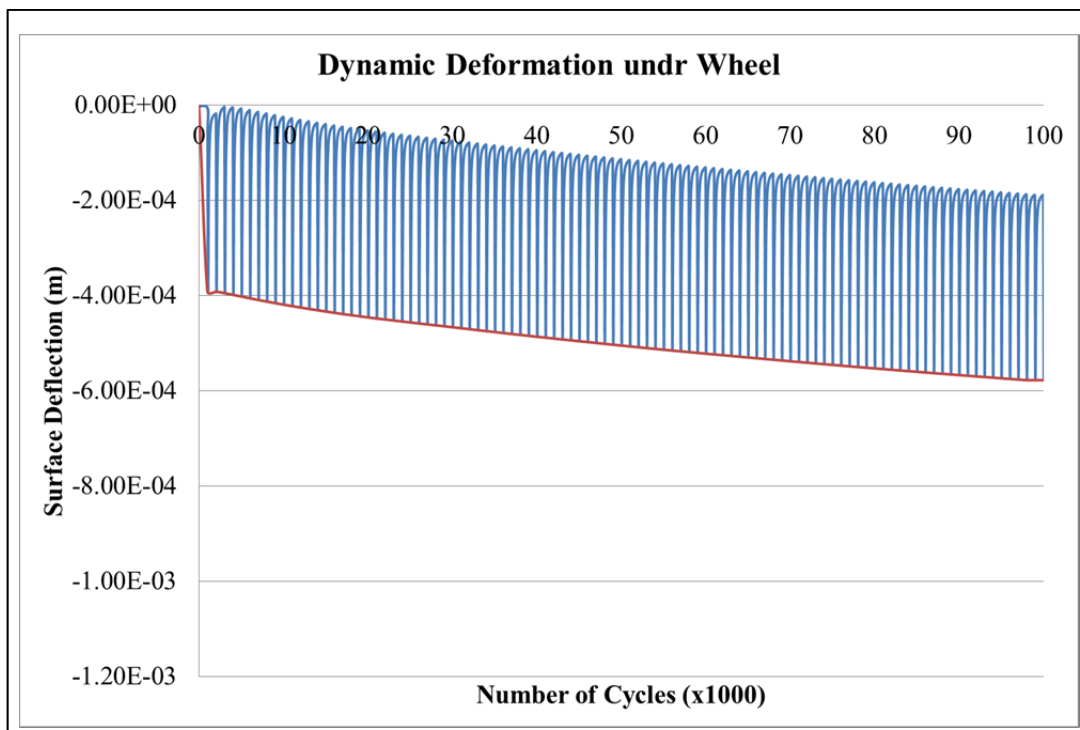


Figure 6.24 – Time History of Deformation under the Wheel (Model 2)

Figure 6.25 demonstrates the gradual growth in vertical strain at the element on top of the base layer exactly beneath the middle of loading tyre number 1 (the same element used for Figure 6.11). The vertical strain here has a value of -0.000582 (compared to -0.000876 in Model 1) and gradually increases to -0.000682 (compared to -0.00037 in Model 1). An interesting trend is that after a few initial cycles the growth in vertical strain is almost constant, which can be attributed to the effect of material change due to the incorporation of shakedown. It should be noted that the material change associated with the shakedown model is almost complex, since the occurrence of shakedown depends on the stress state in the element.

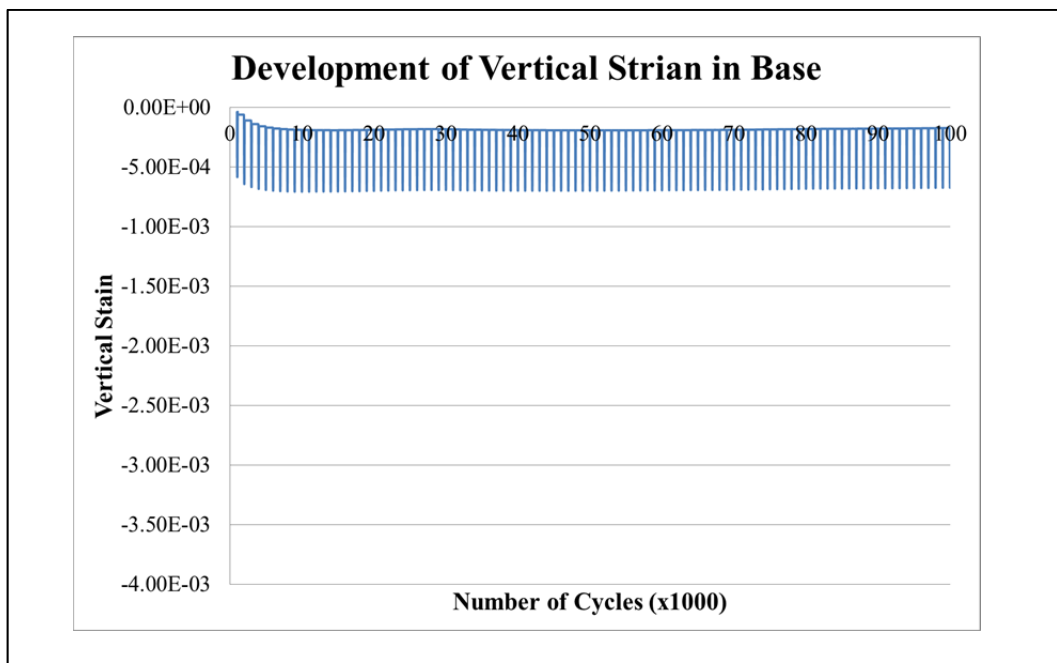


Figure 6.25 – Development of Total Vertical Strain (Model 2)

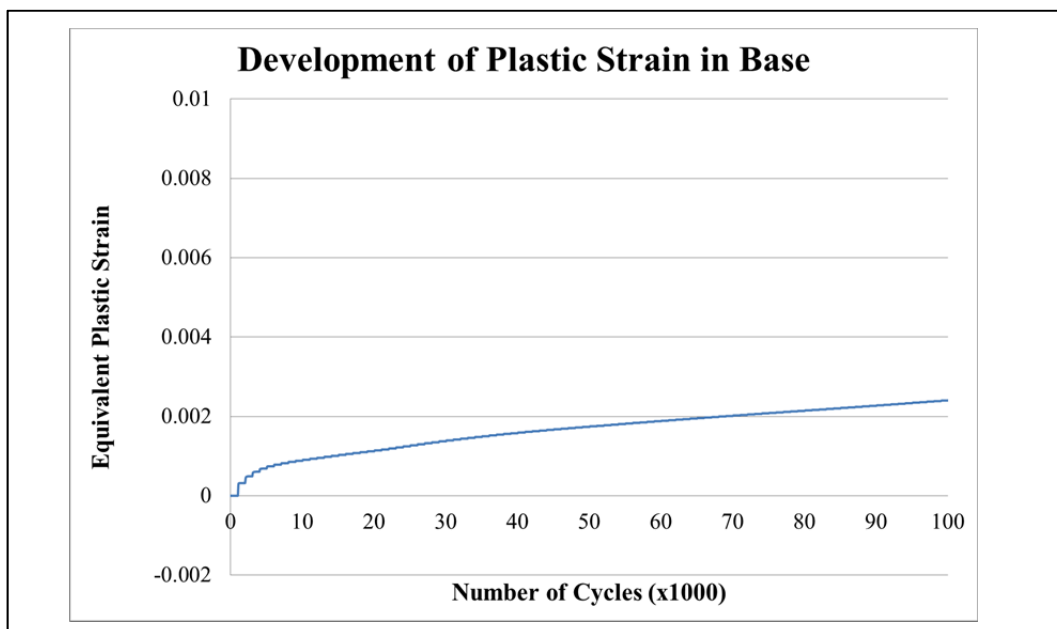


Figure 6.26 – Development of Equivalent Plastic Strain (Model2)

In addition it should be kept in mind that the elastic behaviour of materials is not linear and is also a function of the stress state. Therefore, it is quite possible for a single element to show shakedown behaviour in some of the cycles while not in some of the others, depending on the stress state induced in the specific cycle. Another important indication of Figure 6.25 is that the material behaviour in the vertical direction did not vary significantly after 20,000 cycles. This implies that 100,000 cycles can approximately represent the behaviour of the materials in the long term.

Figure 6.26 presents the development of the equivalent plastic strain in the same element of the base layer in Model 2. Here an interesting comparison can be made between this figure and Figure 6.13. While in Model 1 the increase in plastic strain indicated actual failure in the model, here it can be seen that the model remained less than 0.003 plastic strains after 100,000 cycles. This gives a strong indication regarding the design procedure for flexible pavement design. Section 6.3 will provide a complete discussion regarding the comparison of the results. The influence of the results on the design method will also be discussed in detail in Chapter 7.

Figure 6.27 illustrates the development of equivalent plastic strain in the base layer in a transverse direction at the middle of the wheel axle.

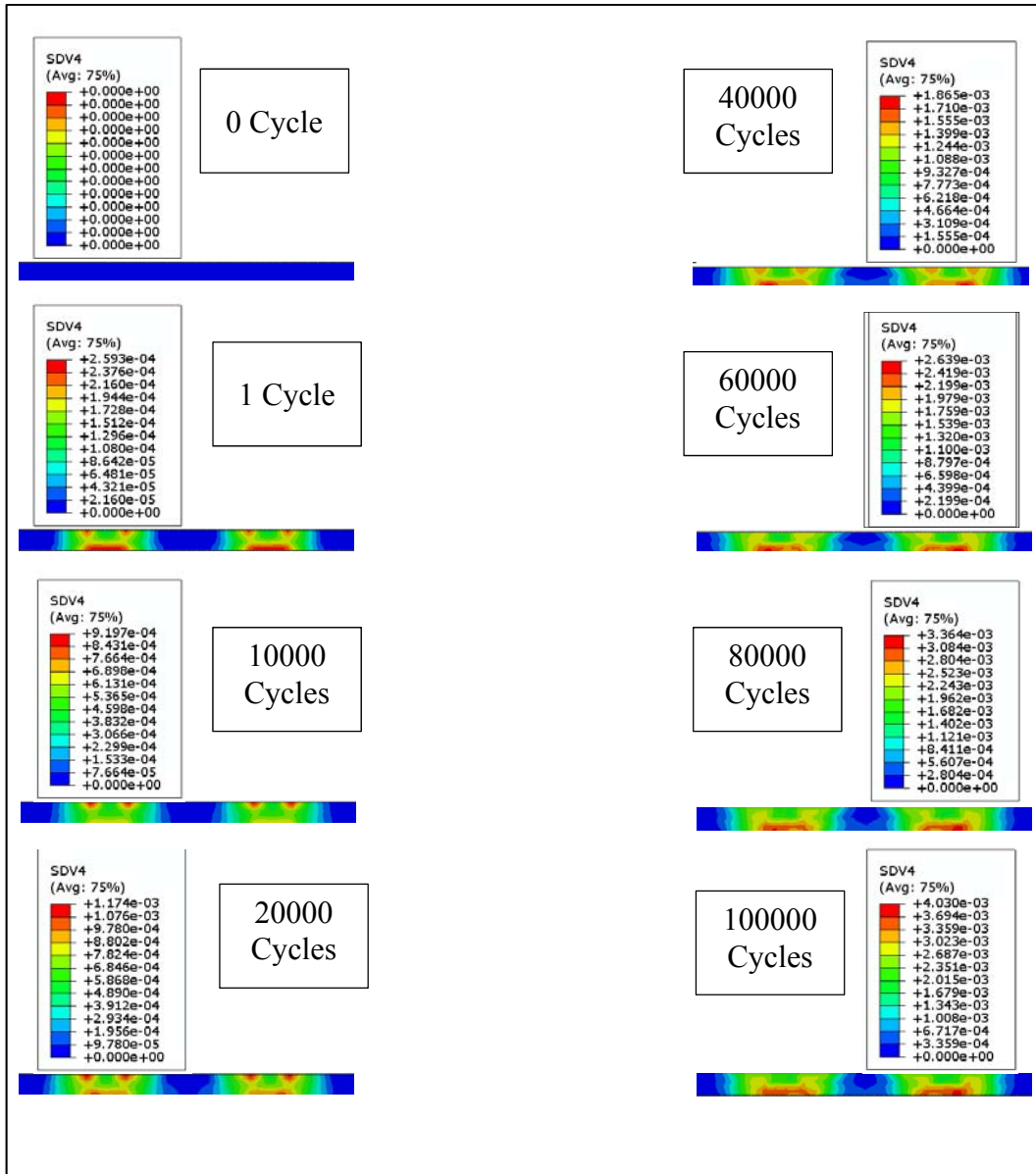


Figure 6.27- Development of Equivalent Plastic Strain in Base (Model 2)

The plastic strain is illustrated for the initial stage of the dynamic analysis, followed by the first loading cycle and the 10,000<sup>th</sup>, 20,000<sup>th</sup>, 40,000<sup>th</sup>, 60,000<sup>th</sup>,

80,000<sup>th</sup> and finally the 100,000<sup>th</sup> cycle, which was the final stage in the dynamic analysis of Model 2. It can be seen that the growth in plastic strain started from the top of the base layer and then passed to the bottom of this layer. This is different from the trend observed in Figure 6.13 for Model 1 when the base material showed a high plastic strain on top of the base layer till the failure of the model. It is interesting to observe in Figure 6.27 that the material first became compacted at the top of the layer and then when it reached a sort of consistent behaviour, the material at the bottom of the layer started to experience the same trend.

Interesting results can be found by studying the hysteresis loops for the same element in the base layers. This is shown in Figure 6.28 and Figure 6.29, where the absolute values of stress and strain are graphed.

From these two figures it can be seen that at the initial stage of analysis, the hysteresis loops for the materials were inclined to move from a wider range to a closer loop (Figure 6.28). However, these loops formed a uniform shape in the final stages of the analysis (Figure 6.29). If these figures are compared to those of the same element for model 1 (Figure 6.14 and Figure 6.15), a completely different type of behaviour is recognizable.

There is also an interesting confirmation in Figure 6.28 and Figure 6.29 of what is described by Collins and Boulbibane (2000). Referring to Figure 2.7 in Chapter 2, the reader can see that the base materials in Model 2 behaved very similarly to what is described as plastic shakedown.

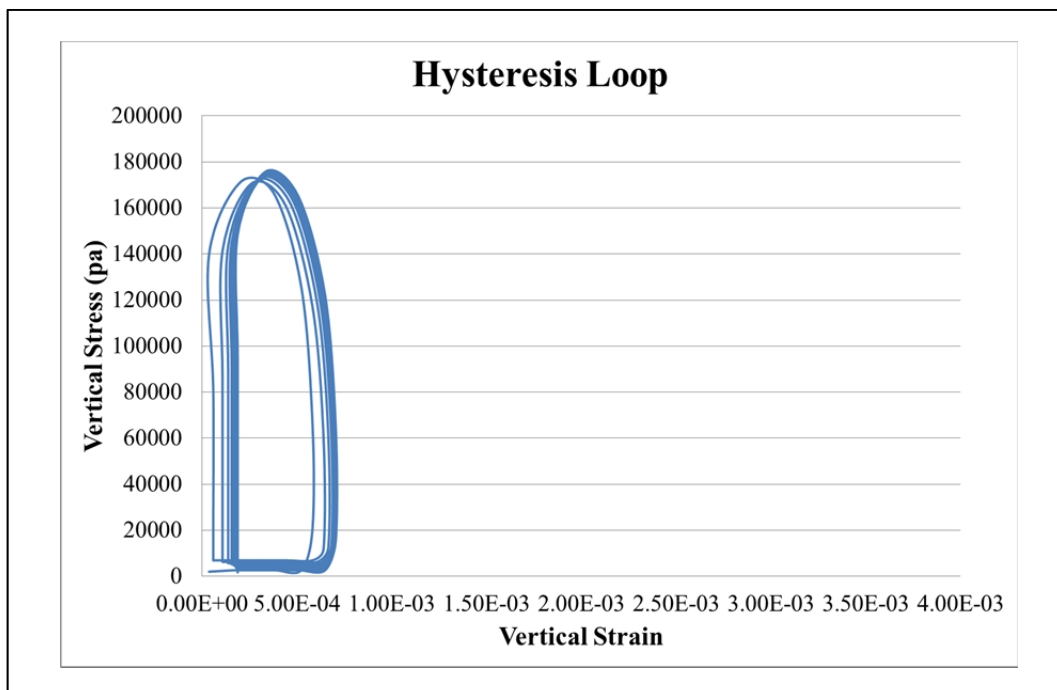


Figure 6.28 – Hysteresis Loops of Initial Cycles (Model 2)

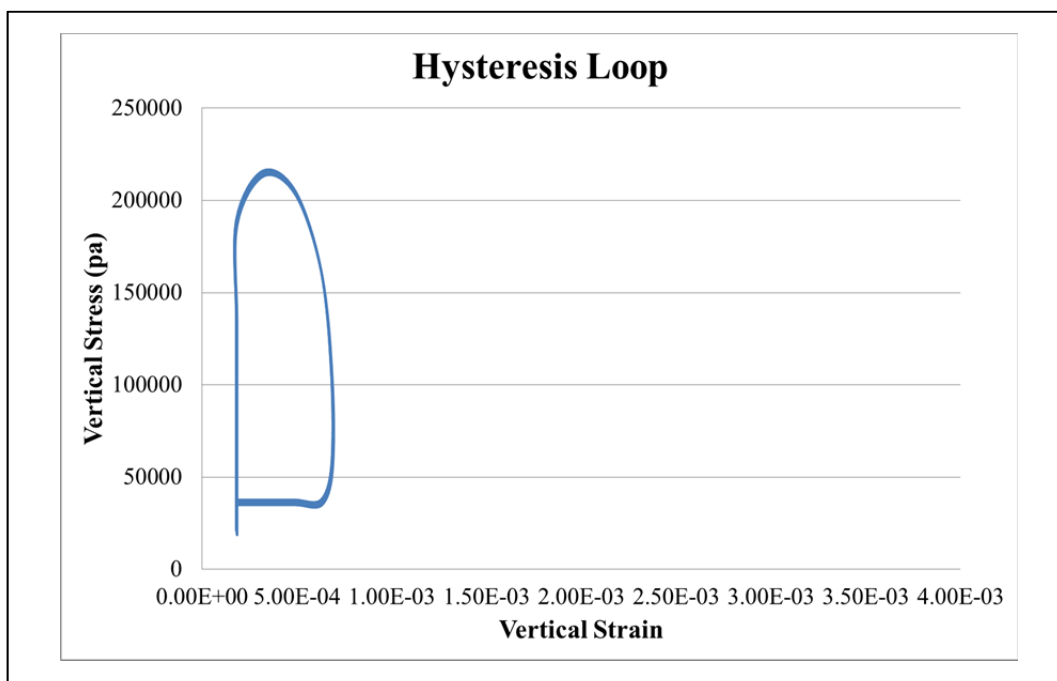


Figure 6.29 – Hysteresis Loops of Final Cycles (Model 2)

Table 6.4 - Responses of Flexible Layer in Dynamic Analysis (Model 2)

Time	Vertical Deflection (Top of AC)	Horizontal Strain (X-Axis) (Bottom of AC)	Vertical Strain (Z-Axis) (Top of SG)	Vertical Stress (Top of SG)
<b>Initial</b>	0.4 mm	-168E-6	-440E-6	-30849.5 Pa
<b>Final</b>	0.58 mm	-114E-6	-480E-6	-18832.5

The final part of this section presents the results of four critical responses in Model 2 in

Table 6.4.

As in the previous section, all of the values concern the element in the middle of loading tyre number 2. An increase can be reported from the initial to the final cycles. For example, the vertical strain of the subgrade increased from -440E-6 to -489E-6 (10%). The increase is quite small if compared to the calculated increase in Model 1 (400%). This can be attributed to the effect of accounting for shakedown in the base materials.

The next section of this chapter describes the effect of considering the dynamic interaction between the asphalt and base layer.

#### **6.2.4 Final Dynamic Analysis Considering Mohr-Coulomb Plasticity, Shakedown effects and Base-Asphalt Interaction**

The final dynamic analysis was conducted to investigate the effects of dynamic soil-structure interaction. The basic concept of such effects and their implementation in the dynamic analysis of finite elements was studied by Wolf (1985). In Model 3, the material behaviour is the same as for Model 2, but the interaction of soil and asphalt is taken into account. Here it is assumed that asphalt has a structural role (because of its higher elastic moduli and linear elastic behaviour), while base material represents soil. The interaction effects were taken into account through the implementation of interface elements. The details of the mathematical formulation of these elements were explained in Chapter 3. The interface elements are assumed to be hard contact in a normal direction and frictional in a tangential direction with the same frictional properties as base materials.

Figure 6.30 represents the general deformed mesh for the first loading cycle in Model 3. Compared to Model 1 and Model 2, some inconsistency can be observed in Model 3 which is due to interactional forces.

Figure 6.31 and Figure 6.32 illustrate the sequence of the dynamic deformation of the layered structure under loading and unloading for the first dynamic cycle under tyre pressure in a longitudinal direction. The vertical deflection increases to a value of 3.75E-4 m (0.4 mm) and then gradually returns to 1.4E-5 m. The values are close to the results obtained for the first loading cycle for Model 1 and Model 2 (albeit slightly lower).

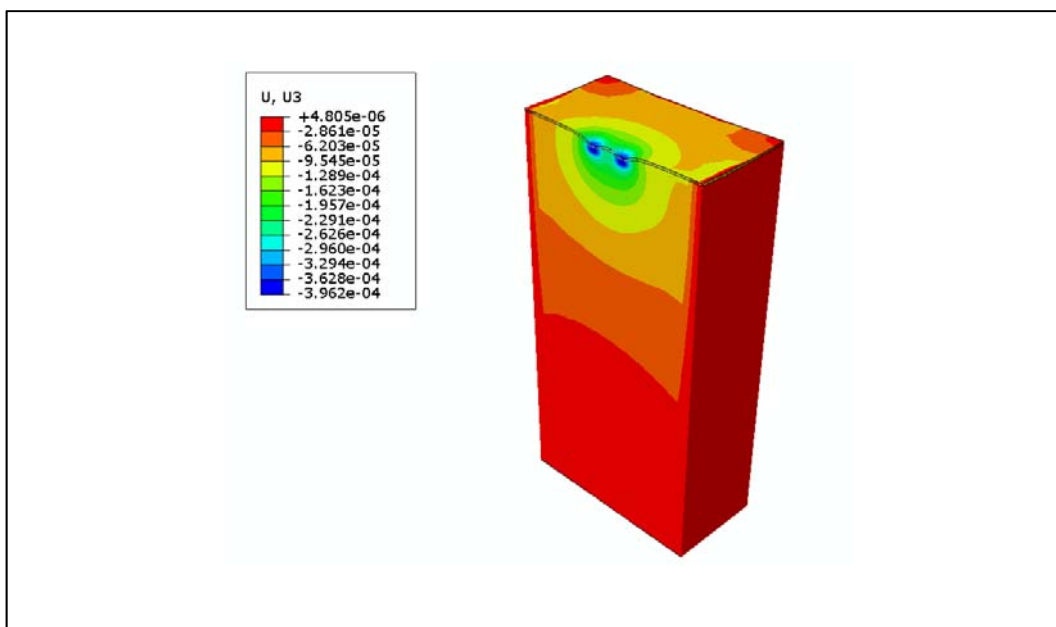


Figure 6.30 - Deformed Mesh in Dynamic Analysis (Model 3)

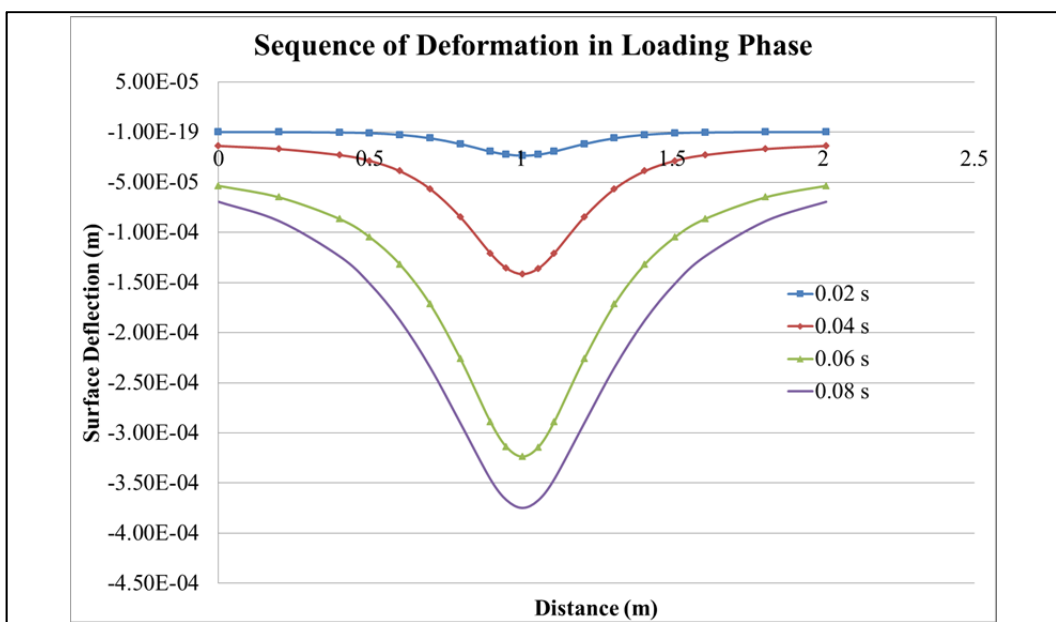


Figure 6.31 – Sequence of Dynamic Longitudinal Deformation: Loading (Model 3)

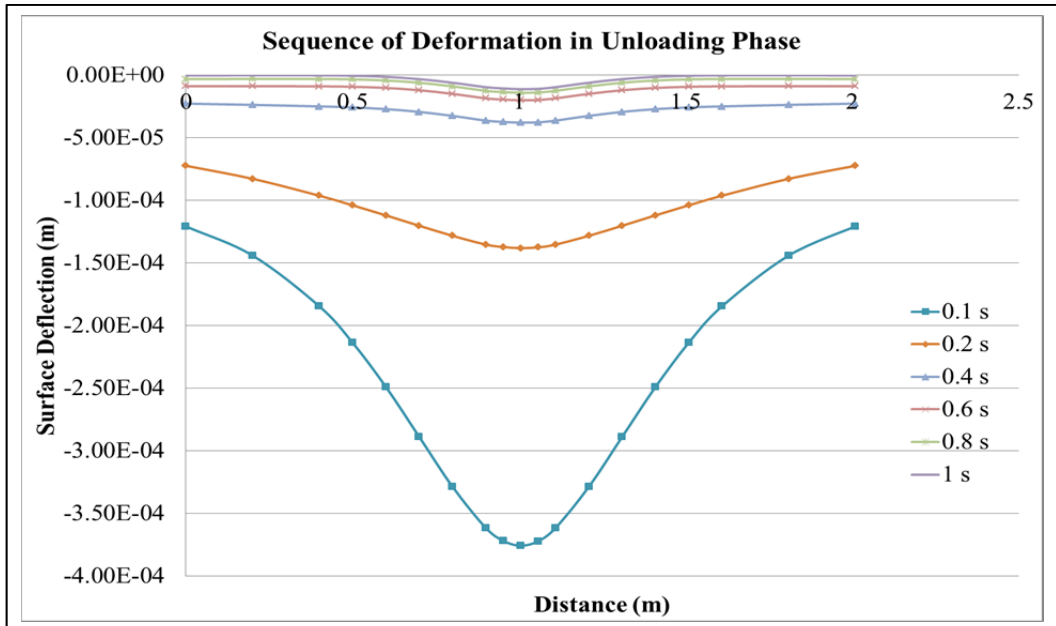


Figure 6.32 – Sequence of Dynamic Longitudinal Deformation: Unloading  
(Model 3)

As in the previous sections (Model 1 and Model 2), the responses of the vertical deflection on the middle of the axle in a transverse direction are presented in Figure 6.33 and Figure 6.34 .

Again, the maximum deflection is calculated under loading tyre number 2. Here, based on these three dynamic analyses, one of the outputs of the research can be stated as follows: in the dynamic analysis of a single axle dual tyre loading on flexible pavement, the maximum surface deflection occurs at the middle of the inner tyre. The calculated values are close to those for Model 1 and Model 2 but slightly lower.

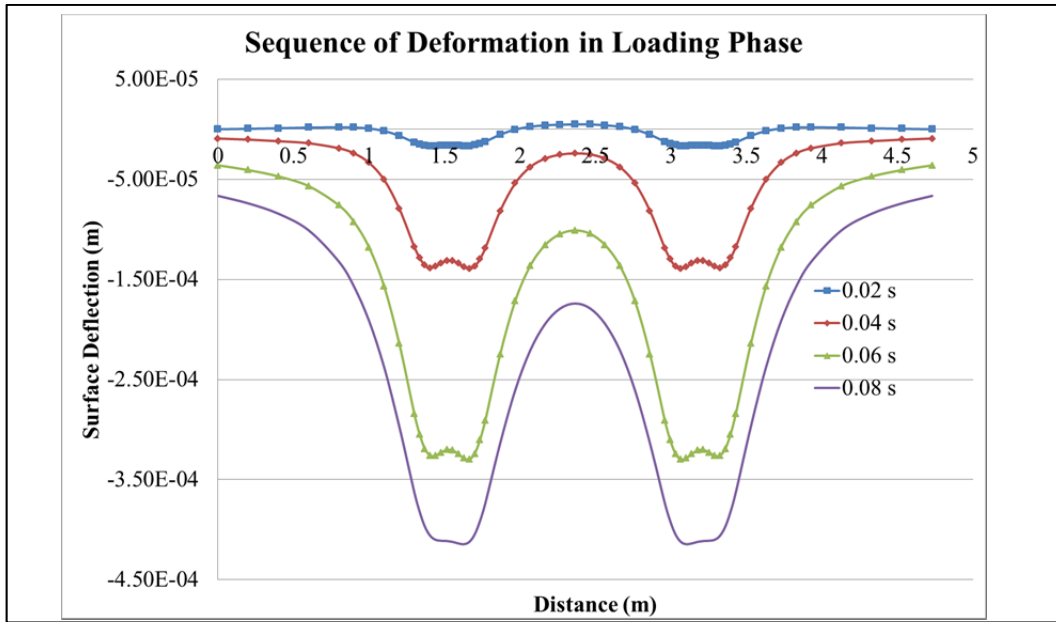


Figure 6.33 – Sequence of Dynamic Transverse Deformation: Loading (Model 3)

Figure 6.35 displays time history of the progress of displacement under the loading tyre during the loading cycles. The trend in accumulation of residual deflection is similar to that observed for Model 2, but the growth rate is smaller in each step. It should be noted that the results are for the same node as in Model 2.

In this simulation, vertical deflection of the loading tyre increases from 3.75E-4 m at the initial cycle to 5.0E-4 m at the end of the analysis. This value can be compared to the 5.8E-4 m calculated from Model 2 at the end of the analysis. There is therefore slight reduction observable in the final analysis.

The lesser deflection seen in Model 3 compared to Model 2 can be ascribed to the dissipation of energy through the interaction between soil and asphalt. Since a portion of forces should pass through layers with different properties, this results in the additional damping of energy through layers and therefore less deflection.

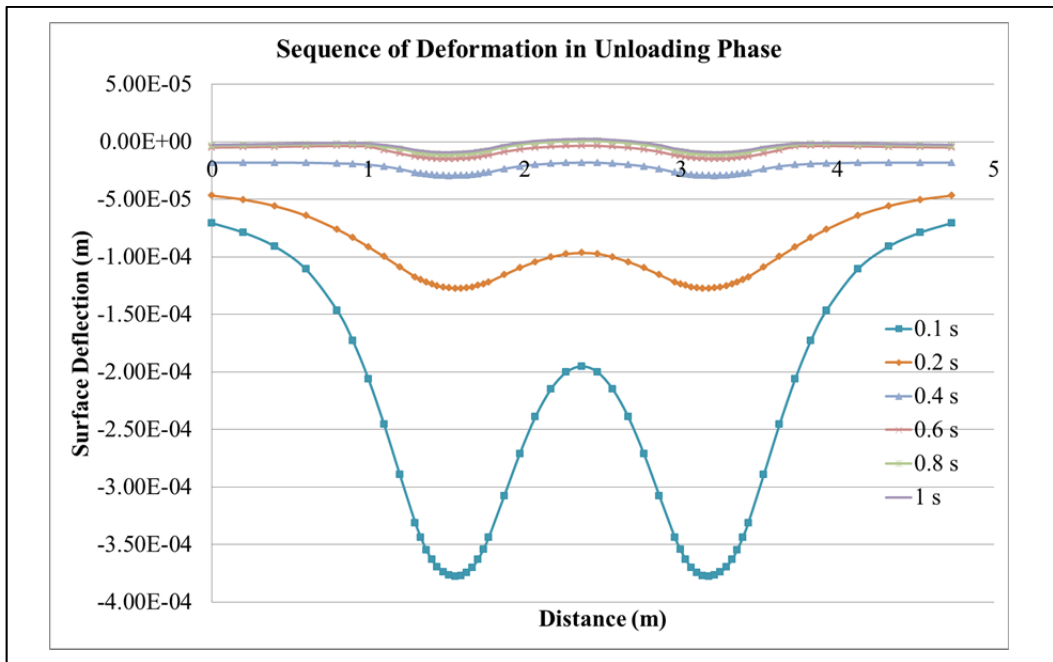


Figure 6.34 – Sequence of Dynamic Transverse Deformation: Unloading  
(Model 3)

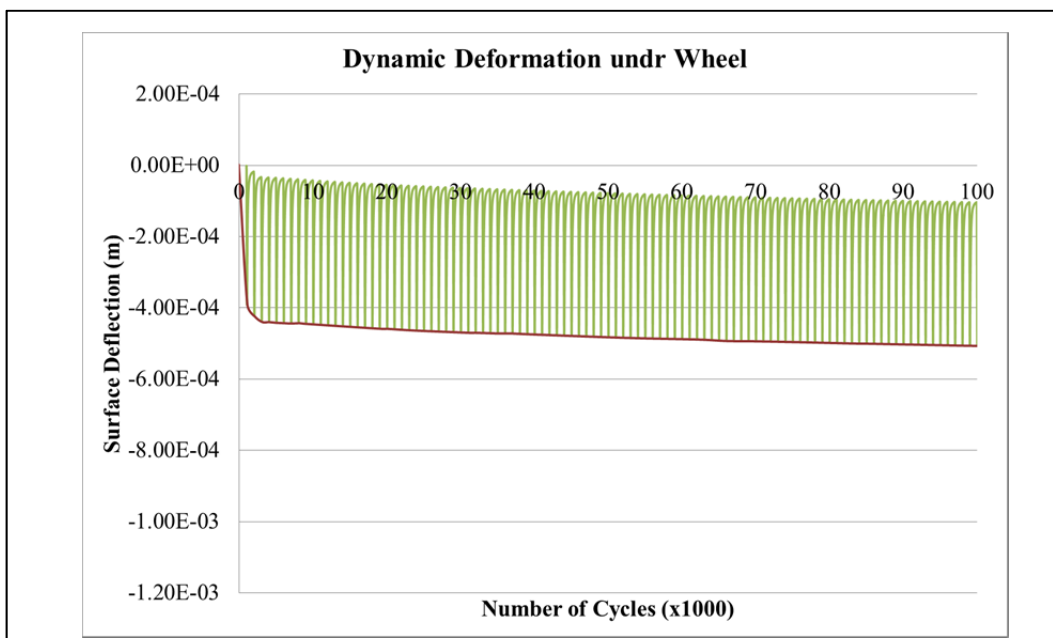


Figure 6.35 – Time History of Deformation under the Wheel (Model 3)

Figure 6.36 portrays the gradual increase in vertical strain at the element on top of the base layer exactly beneath the middle of loading tyre number 1 (the same element used in Figure 6.25). The vertical strain was -0.000265 (compared to -0.000582 in Model 2) and increased to -0.000310 (compared to -0.000682 in Model 2). It should be mentioned that unlike the other models here, the increasing trend is not uniform. The graph of vertical strain also shows some inconsistency compared to those for Model 1 and Model 2. There are several factors contributing to this effect, among which is the interactional forces between layers.

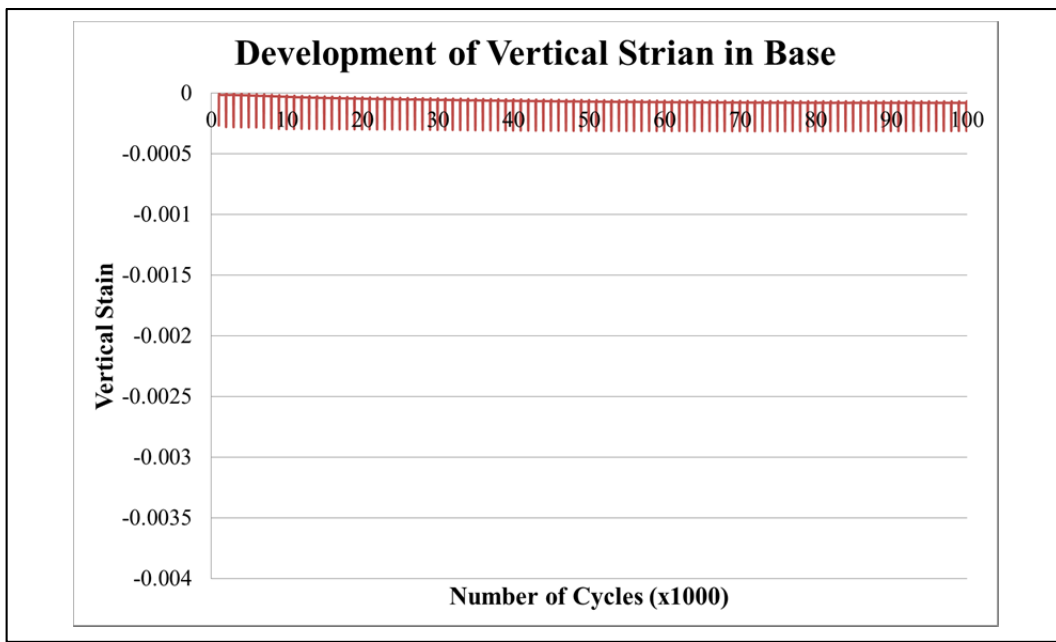


Figure 6.36 – Development of Total Vertical Strain (Model 3)

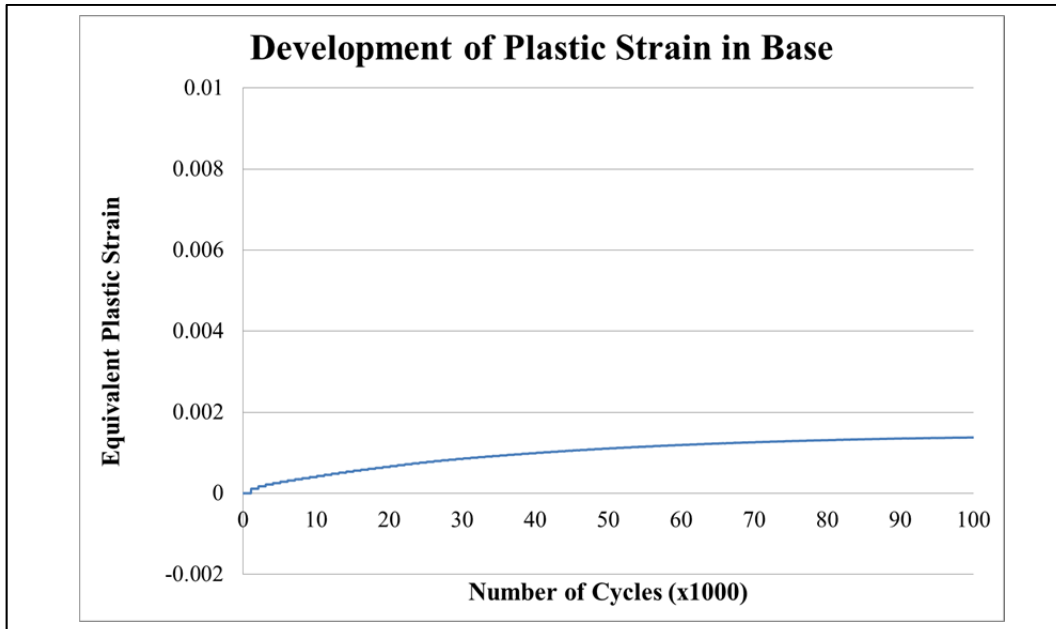


Figure 6.37 – Development of Equivalent Plastic Strain (Model 3)

The interactional forces can also influence the shakedown phenomenon through induced stress in the base layer. However, a general conclusion can be made as follows: accounting for the interactional force between the soil and asphalt layer reduced the induced vertical strain on top of the base layer at the final stage of analysis.

The material behaviour remained almost constant after the equivalent of 40,000 cycles, which can be attributed to shakedown behaviour.

The progressive increase in equivalent plastic strain is demonstrated in Figure 6.37 in the same element of base layer. As in Model 2, the shakedown behaviour governed the development of plastic strain. The final calculated value was smaller than those calculated for Model 2 and Model 3. This can be explained by the diminishing of forces through the layers according to the interaction which leads to less distributed force (stress) in the field. A comprehensive explanation

with comparisons of this phenomenon is provided in the next section of this chapter.

Figure 6.38 portrays the progressive increase in equivalent plastic strain in the base layer in a transverse direction at the middle of the wheel axle.

The sequences were selected as for Model 2 in the first loading cycle, the 10,000<sup>th</sup>, 20,000<sup>th</sup>, 40,000<sup>th</sup>, 60,000<sup>th</sup>, 80,000<sup>th</sup> and the final stage of dynamic loading. The same trend in behaviour as reported for Model 2 can be seen here again. The growth in plastic strain started at the top of the base layer and then travelled towards the bottom of this layer. The rate of growth decreased after 40,000 cycles and the contours shape of the plastic strain remained almost unchanged in the loading cycles after that. Therefore it is expected that the materials showed shakedown behaviour in those cycles.

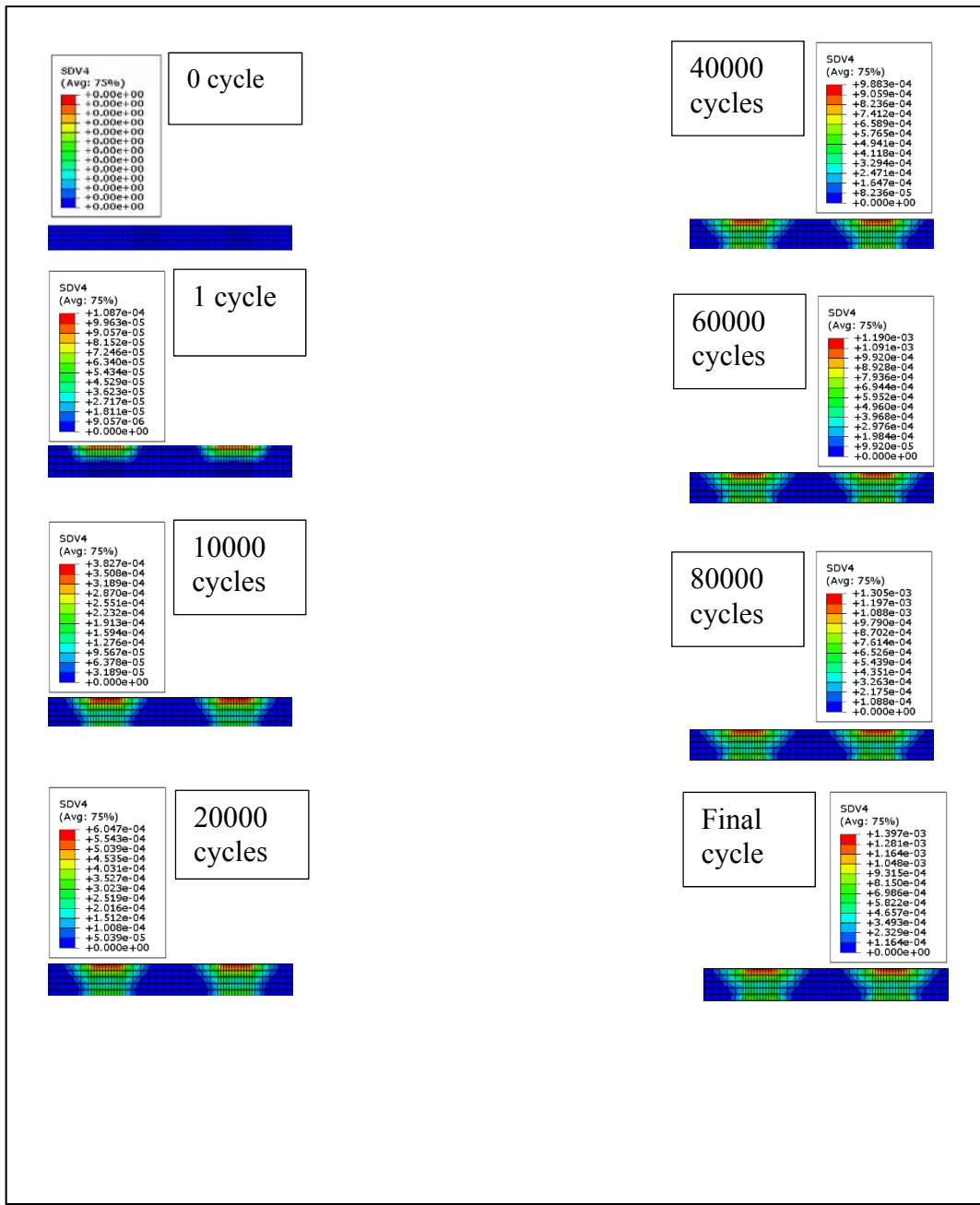


Figure 6.38- Development of Equivalent Plastic Strain in Base (Model 3)

A significant finding from this stage can be observed from the hysteresis loops of the same elements of the base layers. Figure 6.39 and Figure 6.40 present the initial and final loops, with the absolute values of stress and strain being graphed.

Compared to the hysteresis loops calculated from Model 2 (Figure 6.28 and Figure 6.29), there are two major differences to be addressed. First of all the shape of the loops has a tendency to enclose less area. Considering the explanation provided by Collins and Boulbibane (2000), the materials in Model 3 behaved very closely to elastic shakedown (see Figure 2.7 in Chapter 2). The second difference is that there was a very sharp inconsistency in the hysteresis loops compared to Model 2, which clearly demonstrates the effects of transferring interactional force between layers. This effect is close to a slow impact (high values of stress in a short duration of time).

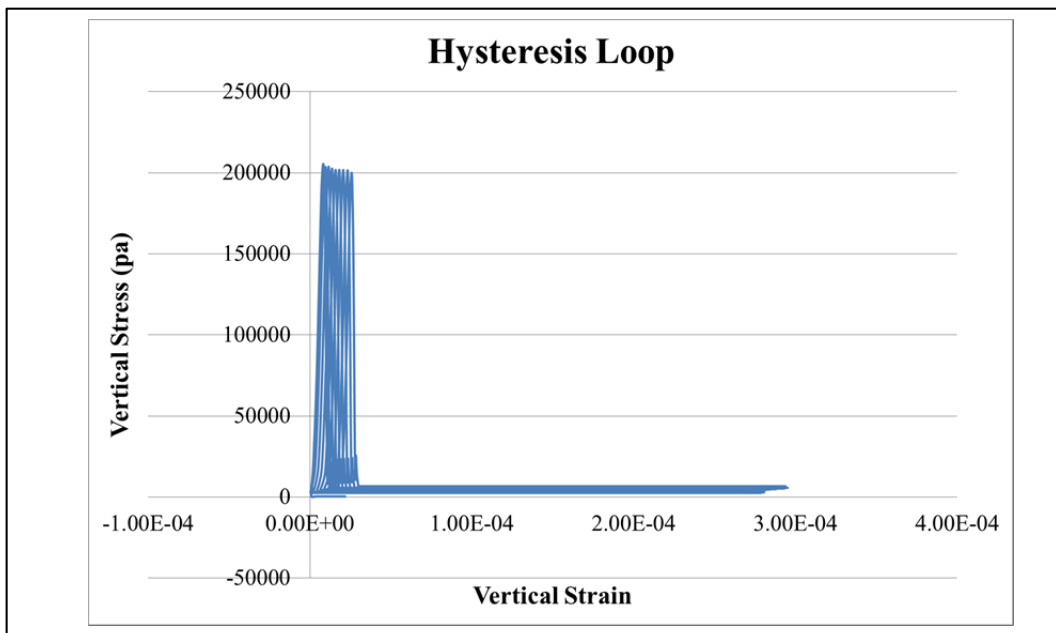


Figure 6.39 – Hysteresis Loops of Initial Cycles (Model 3)

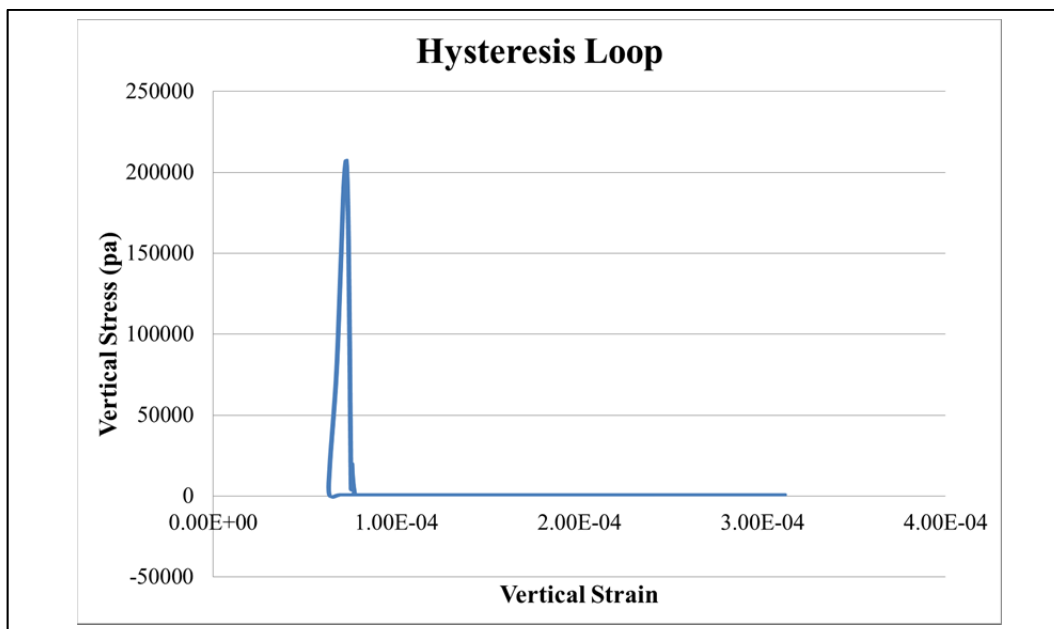


Figure 6.40 – Hysteresis Loops of Final Cycles (Model 3)

Finally, the results for four critical responses in Model 3 are reported in Table 6.5**Error! Not a valid bookmark self-reference.**.

Table 6.6 - Responses of Flexible Layer in Dynamic Analysis (Model 3)

Time	Vertical Deflection (Top of AC)	Horizontal Strain (X-Axis) (Bottom of AC)	Vertical Strain (Z-Axis) (Top of SG)	Vertical Stress (Top of SG)
Initial	0.14 mm	-192E-6	-230E-6	-26970 Pa
Final	0.49 mm	-201E-6	-360E-6	-15457 Pa

The values are reported for the element in the middle of loading tyre number 2. An increase can be seen from the initial cycles to the final cycles. For instance, the

vertical strain of the subgrade increased from -230E-6 to -360E-6 (36%). The increase is larger compared to that in Model 2 (10%). However, the values are lower than those calculated in Model 2.

The final section of this chapter provides general remarks on the dynamic analyses.

### 6.3 Remarks

This chapter presented the results of the dynamic analyses conducted for three different models. The material properties, geometrical structure, loads and boundary conditions remained the same for all three models. In Model 1, the materials were assumed to behave nonlinear elastoplastically based on Mohr-Coulomb criteria. In Model 2, nonlinear elastoplastic Mohr-Coulomb behaviour was modified to consider shakedown due to cycles of loading. In Model 3, the shakedown of nonlinear elastoplastic materials was considered along with the effects of soil and asphalt interaction.

This section compares the major results of the three analyses to extract the general outcomes of this chapter.

First of all, let us consider the developed curve of deformation beneath the loading tyre calculated for these models. As illustrated in Figure 6.42, the accumulated displacement reached 1 mm in Model 1, while it was restricted to 0.58 and 0.49 mm for Model 2 and Model 3, respectively. Based on this it can be stated that taking shakedown into account reduced the amount of surface displacement in

long-term loading. Moreover, the effects of soil-asphalt interaction also caused a slight reduction in the surface displacement.

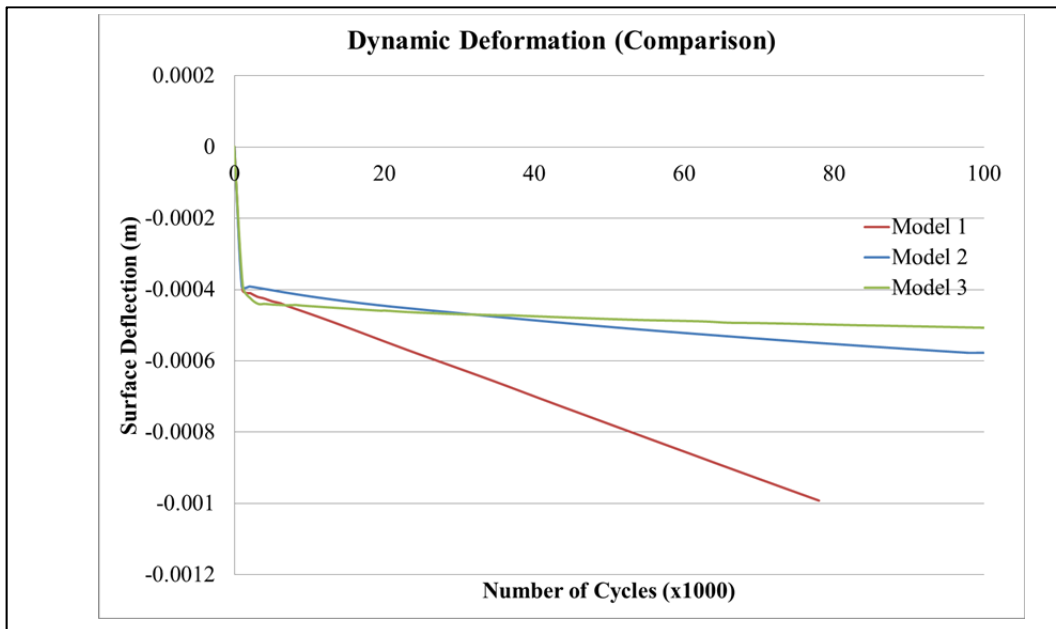


Figure 6.41-Comparison of Surface Deformation

Figure 6.42 and Figure 6.43 compare the induced strain in the base layer. It can be observed that the trend of accumulative strain (plastic and total) is almost linear (after few initial cycles) for Model 1 where Mohr-Coulomb material is used. However, this trend is different in Model 2 and Model 3. Based on these results, the final total vertical strain calculated from Model 2 and Model 3 (-0.000310 and -0.000682) is significantly less than that calculated from Model 1 (-0.0035). This clearly shows how the shakedown behaviour can affect the results in term of strain.

The behaviour of materials in shakedown has been categorized by Collins and Boulbibile (2000) and reviewed in Chapter 2. Material can respond in four ways to cyclic loading: purely elastic, elastic shakedown, plastic shakedown or ratchetting (increasing plastic strain without limitation).

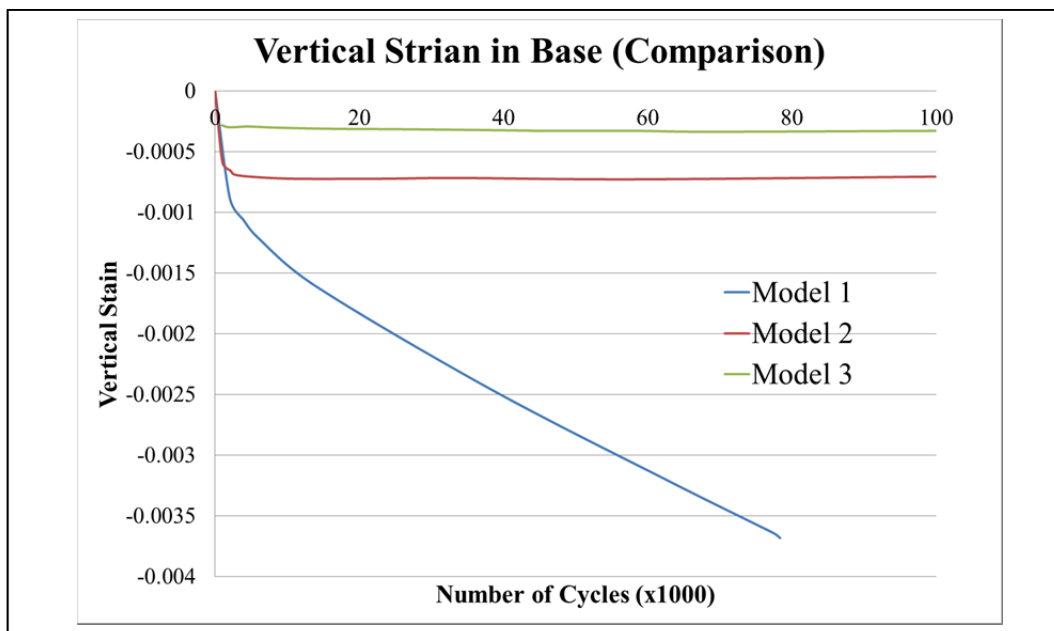


Figure 6.42-Comparison of Vertical Total strain in Base

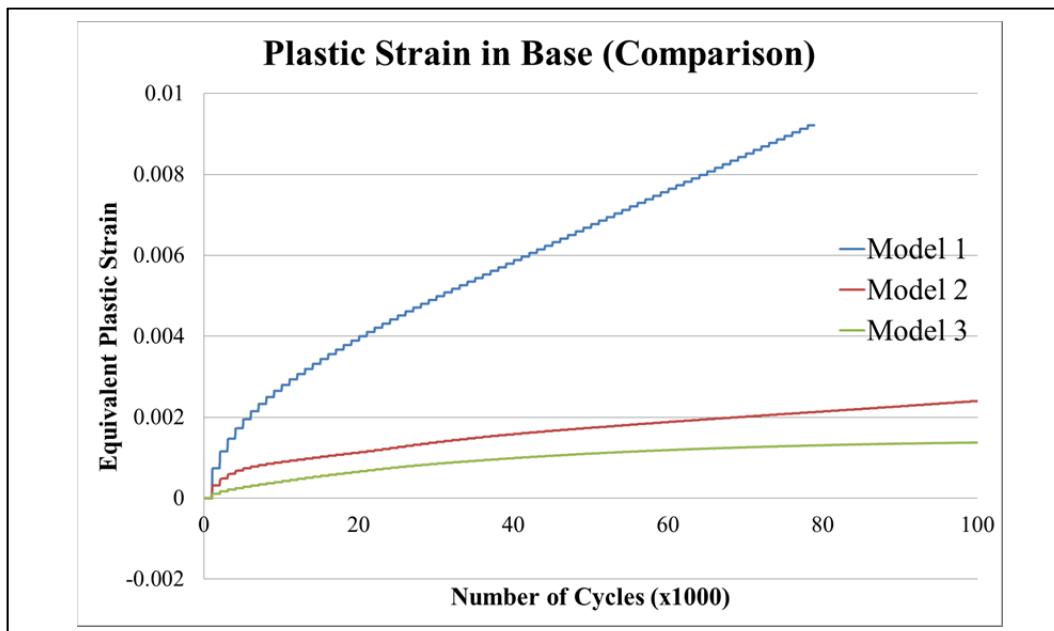


Figure 6.43-Comparison of Plastic Strain in Base

The type of response of a sample to cyclic loading is dependent on the loading magnitude and material properties. In this regard, Figure 6.44 displays the

hysteresis loops for the final cycles calculated from Model 1, Model 2 and Model 3.

Comparing the schematic graphs provided by Collins and Boulbibane (2000), it can be stated that the behaviour of base materials in Model 1 shows ratchetting, in Model 2 something close to plastic shakedown, and in Model 3 something close to elastic shakedown. Therefore, the mechanical response of materials can change significantly based on consideration of shakedown behaviour and the effects of the soil-asphalt interaction.

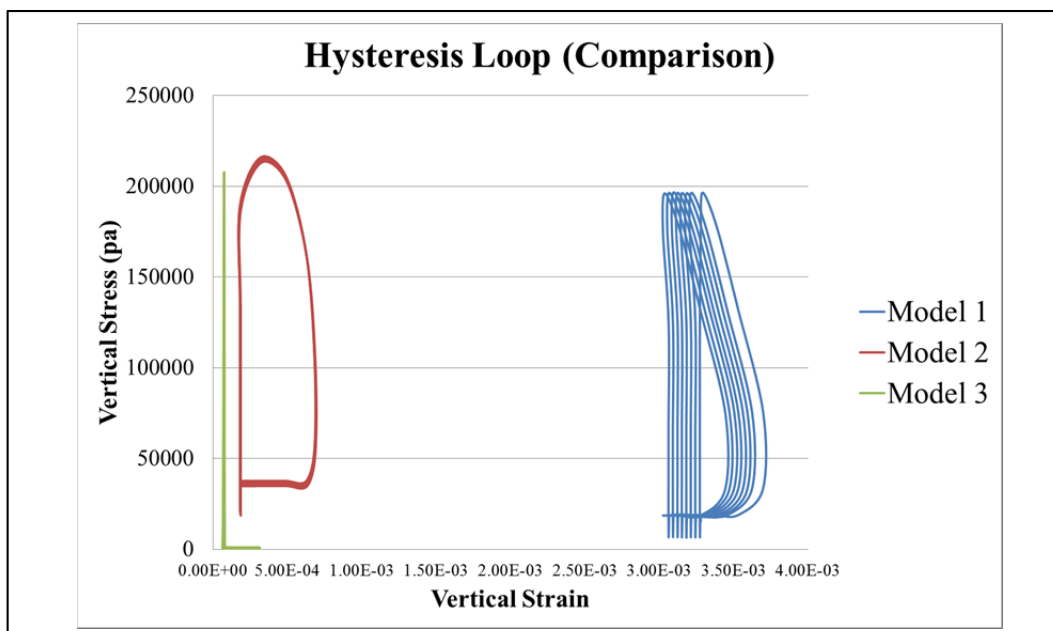


Figure 6.44-Comparison of Final Hysteresis Loops in Base

Finally, in order to obtain an engineering estimation for the effects of each model on critical design parameters, Figure 6.45 and Figure 6.46 present the normalized values of critical parameters.

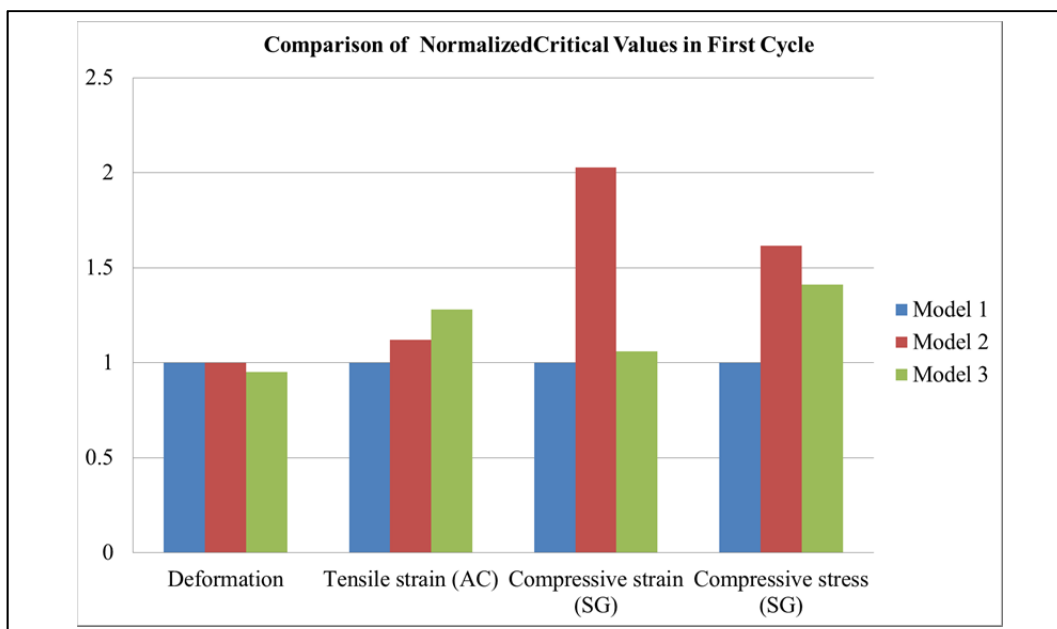


Figure 6.45-Comparison of Critical Values in First Cycle

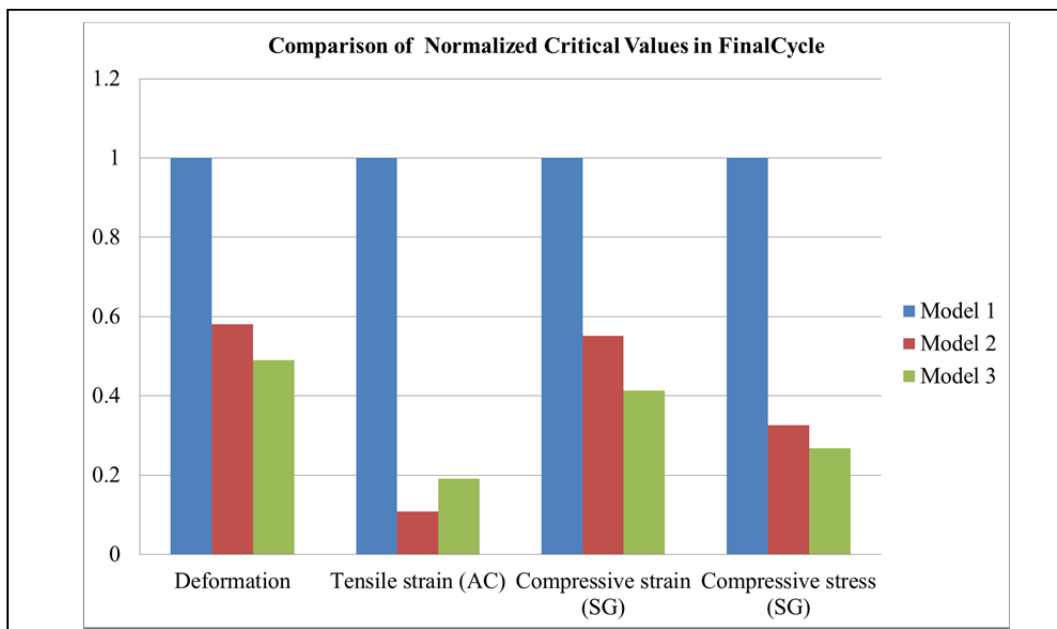


Figure 6.46-Comparison of Critical Values in Final Cycle

The values in this figure are divided by the values calculated from Model 1 (Mohr-Coulomb). Figure 6.45 displays the values at the first cycle while Figure 6.46 displays the values at the final stage of the dynamic analysis. While in the first cycle of analysis Model 1 resulted in values close to or less than the other two models, in the long term there is a significant difference between the results of the three models. It can be stated that in the long term, taking shakedown into account leads to a lower critical value (therefore, ignoring this effect results in conservative design). The effect of soil-asphalt interaction can be unfavourable for the asphalt layer (more tensile strains) while favourable for the granular layer (less strains and stresses).

## **CHAPTER 7**

### **7: COMPARISON, REMARKS AND DISCUSSION**

#### **7.1 Introduction**

This chapter compares the results of the analyses with each other from various points of view, and points out the correlation of the results with other available technical sources such as design codes, scientific papers and publications. An attempt is also made to identify the technical difficulties experienced during this research and shed light on possible solutions.

In this research the main focus has been on developing and introducing new constitutive models to simulate the behaviour of the unbound granular materials used in the base and subgrade of flexible pavement structures. There were two categories of analyses conducted: static analysis and dynamic analysis. In each of them, the relevant constitutive models were developed and then coded in numerical simulations.

With respect to static analysis, two general types of material constitutive models can be cited: elastic and elastoplastic. Various constitutive models have been presented for each of them in the literature and practice of pavement engineering. In elastic models it is only the loading path which is considered representative of material behaviour, and the unloading path is assumed to be the same as the loading path. However, in the case of elastoplastic material behaviour, the difference between the loading and unloading paths can be determined through the defining of a plastic cap.

Based on the abovementioned points, the results gathered in this research are compared from different perspectives to exclude the influence of the material constitutive models in the two types of analyses (static and dynamic).

## 7.2 Comparison of Results of Elastic Analysis

This section compares and discusses the simulation of granular material as an elastic layer (either linear or nonlinear elastic).

In numerical simulation, it is important for a 2-D model representation to properly answer the actual structure. To investigate this, a series of linear elastic analyses were conducted (see Chapter 5). Three models were examined, including plane strain, axisymmetric and 3-D models. The results showed that the plane strain assumption leads to unacceptable values and should be used with caution. This is in strong agreement with the work of Cho, McCullough, and Weissmann (1996).

The results of the 3-D and axisymmetric models were close but the axisymmetric model is unable to address different axle loading configurations. There is a strong trend among researchers to use the axisymmetric model in their numerical simulations (Holanda et al. 2006; Kim and Tutumluer 2006b; Myers, Roque and Birgisson 2001). This is because axisymmetric conditions provide great efficiency with regard to computation time. However, it should be noted that axisymmetric modelling cannot be selected for a complete simulation. This is important especially when material behaviour is not just dependent on the material characteristics but also on the stress state presented in the field. The materials would then behave differently under different types of loading in the field.

If a two-dimensional analysis was selected, it would probably need other modifications to reach a better approximation. This is the same approach applied by Myers, Roque, and Birgisson (2001).

Based on this, the use of 3-D analysis is recommended to correctly research a variety of mechanical responses of flexible pavement. However, there are some difficulties that should be mentioned. The selection of the 3-D model usually compels a restriction on the tyre contact area. Since it is usual to use brick elements in 3-D models (to achieve a quicker computation time and better mesh distribution), the tyre contact should be mapped to a rectangle shape. This will enforce some approximation to the results.

The boundary conditions for the 3-D model should also be selected with caution, with especial attention to the boundary conditions on the sides of the modelling area.

Chapter 5 presented the effects of the implementation of different nonlinear elastic models on the behaviour of granular materials, as well as their influence on the final mechanical responses of the pavement structure. The nonlinear constitutive models used here were selected from those frequently cited in literature, and were used to simulate the behaviour of granular materials used in the base, subbase and subgrade of flexible pavement (Araya et al. 2011; Cho, McCullough and Weissmann 1996; González, Saleh and Ali 2007; Taciroglu and Hjelmstad 2002; Tutumluer 1995; Tutumluer, Little and Kim 2003). Different UMATs were developed in order to include different nonlinear constitutive models in the simulation. The UMAT was first verified against the results presented by Kim and Tutumluer (2006b). The results indicated that the selection of a constitutive model

equation could hugely influence the final results and behaviour of granular materials. Therefore, the selection should be made based on the nature of the granular materials and available test data. Among researchers, the Uzan-Witczak model is more popular for simulating the granular layer used as base (Bodhinayake 2008; Cho, McCullough and Weissmann 1996; Kim 2007; Kim and Tutumluer 2006b; Kim, Tutumluer and Kwon 2009; González, Saleh and Ali 2007). The reason is that the Uzan-Witczak model can consider the effects of deviator and confining stress simultaneously. Moreover, when the base materials are selected from good quality granular resources, the use of the Uzan-Witczak model leads to appropriate results (Cho, McCullough and Weissmann 1996; González, Saleh and Ali 2007; Kim 2007; Kim and Lee 2011; Kim and Tutumluer 2006a; Kim and Tutumluer 2010; Kim, Tutumluer and Kwon 2009). Based on the comparison presented in Chapter 5, the Uzan-Witczak model provided stiffer behaviour than linear elastic. This is under the condition that the asphalt and subgrade layers are assumed to behave linear elastically, and is in agreement with the conclusions of Kim and Tutumluer (2006a).

The mechanical response of the flexible pavement structure is a function of layer geometry, load characteristics and material behaviour. Complexity arises when material behaviour is also a function of loading and geometry. Researchers have therefore always investigated constitutive models with different combinations of loading and geometries. The results here are in firm agreement with those reported previously by Cho, McCullough, and Weissmann (1996). The same approach was taken in this research. Two different types of layer composition, two different types of material characteristics and two different axles of loading were selected in order to simulate a total of eight combinations of loading, geometry and materials.

The results indicated that increasing the asphalt thickness significantly decreases the contribution of granular layers to the final responses. This phenomenon especially has an impact on the behaviour of granular materials which is a function of induced stress in the field. A comparison between Table 5-5 and Table 5-12 demonstrates that the effects of nonlinearity decrease a great deal when the thickness of asphalt is increased. On the other hand, an increase in load can lead to an increase in the influence of the nonlinear behaviour of materials on the final responses.

Finally in this section, it should be mentioned that the results of the elastic analysis are those that will be used by the usual pavement design codes (AASHTO 2002; AUSTROADS 2004), and therefore the influence of the linear or nonlinear elasticity of the materials can make a difference in the final design.

### **7.3 Comparison of Results of Elastoplastic Analysis**

Another series of analyses was conducted to examine the effects of the elastoplastic behaviour of materials. The effects of elastoplastic material behaviour are greater when the reloading path is taken into account. Therefore, these effects are more significant for the simulation of a dynamic loading (where a series of loading and unloading paths is modelled). While there are several studies that have considered Drucker-Prager elastoplastic behaviour for granular materials (Allou, Chazallon and Hornyph 2007; Allou et al. 2009; Chazallon, Hornyph and Mouhoubi 2006; Chazallon, Koval and Mouhoubi 2011; Saad, Mitri and Poorooshshab 2005; Zaghloul and White 1993), this research selected the Mohr-Coulomb criterion to represent the plastic behaviour of materials. In support of this choice, it should be noted that the Mohr-Coulomb criterion is a model specially developed to simulate granular behaviour. The only difficulty with this

model is that it has undifferentiable corners in stress space, which produces numerical difficulties. However, as stated in Chapter 4, a new method based on the piecewise function used in this thesis (Clausen, Damkilde and Andersen 2007) made the application of Mohr-Coulomb criterion more feasible.

Two different types of behaviour were considered in this dissertation, being linear elastoplastic behaviour and nonlinear elastoplastic behaviour. In nonlinear elastoplastic behaviour, the elastic part is modelled as stress-dependent materials based on the Uzan-Witczak equation.

The results of the simulation illustrated that including the elastoplastic behaviour of materials leads to greater deformation and strain in the layers. In all simulation cases the same trends were obvious. There is little variation between the nonlinear elastoplastic results and linear elastoplastic results. It should be noted that the effects of elastoplasticity have more importance in the case of a thin asphalt layer, where the asphalt thickness in the model is 10 cm.

Another important point is that the results of the elastoplastic simulation cannot directly be applied to the current design codes. In the design codes (AASHTO 2002; AUSTROADS 2004), the effects of elastoplasticity have been considered through the concept of transfer functions. In this case, a designer needs to calculate the elastic responses of a given pavement structure and then put those values into an experimental transfer function to calculate the final responses. However, in order to calculate the exact mechanical response of a given pavement, a full dynamic numerical simulation must be conducted. In the simulation, the effects of elastoplasticity need to be considered in the correct way.

Taking account of elastoplasticity increases the complexity of the numerical simulation due to the presence of failure criteria. In this regard, there are cases where the modelled pavement cannot resist the induced strain in the layers (considered to be large strain), and the simulation will be aborted. In this instance, the mechanical failure should be reported.

In conclusion, it is recommended that an elastoplastic static analysis to be conducted for any flexible pavement design. In this way, a case of instant failure (due to large loads and insufficient structural resistance) will be prevented.

#### **7.4 Effect of Dynamic Loading**

Another class of simulation belongs to dynamic analysis. In this class, instead of simplifying the actual problem on the pavement, an attempt will be made to consider the effects of loading in a way that is closer to reality. Correspondingly, this will increase the computation time of the simulation and its complexity.

Chapter 6 of this dissertation presented the results of three cases of dynamic simulation. In dynamic analysis, three major changes should be considered in comparison with static analysis. The first change is the nature of loading, which is dynamic and therefore time dependent. In this regard, various types of loading can be selected (these were reviewed in Chapter 2). Here, haversine loading with a rest period was selected to represent dynamic loading. The other change is material characteristics, where damping and inertia can have an influence on the results. In this regard, material damping is considered to be Rayleigh damping and the effects of inertial force are considered through the definition of mass density. The final change relates to boundary conditions. The nature of dynamic analysis produces waves of stresses in the modelled medium. These stress waves can be

reflected towards the model if the boundary conditions are not properly selected. To avoid such an effect, infinite elements are implemented as boundary conditions around the model. Infinite elements have a formulation that assumes linear elastic behaviour at a distance far from the studied area (here, this area is the tyre contact area). Three different simulations were conducted using these three general changes in modelling. The first simulation assumed simple Mohr-Coulomb behaviour without shakedown effects. In the second simulation, the effects of shakedown were taken into account. Finally, the interaction between the asphalt and base layers was simulated. In all three dynamic analysis models, material behaviour was assumed to be nonlinear elastoplastic as discussed in the previous section.

Generally, the results obtained from the dynamic analysis for the first cycle of loading were less than those calculated from the static analysis. This is in firm agreement with trends previously reported in the literature (Saad, Mitri and Poorooshagh 2005; Uddin, Zhang and Fernandez 1994; Zaghloul and White 1993). The contribution of damping and inertial forces could be the main reason for such a decrease. This will intensify the need for dynamic analysis to apply a better understanding of the mechanical behaviour of flexible pavement. The reduction is more notable when the effect of interaction between the layers is also considered.

Inclusion of elastoplastic behaviour in dynamic analysis has a critical effect. This is especially important if more than one round of loading is going to be simulated. In this case, elastoplastic criteria can define the loading-unloading behaviour of materials. If the behaviour is assumed to be elastic, then the effects of internal energy dissipation cannot be considered. The energy dissipation can be demonstrated through the hysteresis loops of stress-strain in the elements.

However, considering the Mohr-Coulomb criterion as the only representative of material behaviour can produce difficulties in the dynamic analysis. The reason is that if a large number of repetitions of the same load is applied over the flexible pavement, the growth of plastic strain can be limitless and cause the final failure of the layered structure. This may be the main reason for the simulation of just one cycle of loading (or a few) in previously published literature (Al-Qadi, Wang and Tutumluer 2010; Mallela and George 1994; Pan, Okada and Atluri 1994; Saad, Mitri and Poorooshashb 2005; Uddin, Zhang and Fernandez 1994; Zaghloul and White 1993). The same problem was observed in this research when the dynamic analysis was aborted due to the large value of plastic deformation in Model 1.

The effects of shakedown behaviour have been known in the field of structural fatigue especially for metals (Zarka and Casier 1979), however, it is also useful for investigating the simulated behaviour of complex layered structures (i.e. flexible asphalt pavement). The idea has recently been applied in the pavement engineering field (Boulbibane and Weichert 1997; Brett 1987; Brown, Juspi and Yu 2008; Chazallon, Koval and Mouhoubi 2011; Collins and Boulbibane 2000; Ghadimi, Nega and Nikraz 2014; Habiballah and Chazallon 2005; Hossain and Yu 1996; Maier et al. 2003; Ravindra and Small 2008; Sharp 1985; Sharp and Booker 1984; Sun et al. 2012), and the effects of this phenomenon are taken into account in current research. As seen from the simulation, taking shakedown effects into account can meaningfully reduce the produced plastic strain, especially if a large number of loading repetitions is considered. The effects can particularly be understood if the hysteresis loops of stress-strain in plastic materials are considered. Applying shakedown behaviour resulted in a constant quantity of dissipated energy for all cycles. This refers to the energy trapped inside a plastic element. In the other words, granular layers can resist some stress

without failure occurring. The effects of shakedown can be meaningful in the calculation of rutting in flexible pavement, especially if a relatively thin layer of asphalt is placed over the granular layers. In this case, ignoring shakedown effects may result in a relatively conservative design (thicker asphalt layer or lower traffic allowance).

### **7.5 Effect of Interaction of Soil-Asphalt layers**

Finally in this research, an attempt has been made to investigate the effects of interaction between the layers in the numerical simulation of flexible pavement structure. There are few studies in the literature regarding the dynamic interaction of asphalt and soil (Pan, Okada and Atluri 1994; Wolf 1985), and in those studies, the nonlinearity of the granular layers is usually ignored. Through advances in computer technology, ABAQUS software now enables the user to introduce a variety of interface elements that can correctly simulate the interactional behaviour. When the interactional forces between the asphalt and base layers are considered, there is a complex trend of transferring forces between the layers. However, it was generally observed that considering the interactions between layers may cause a reduction in critical values. This can be attributed to the dissipation of energy through the layers. It was observed that simulation of the interactional forces was simulated, led to a decrease in the value of the stresses experienced by the base layer and the hysteresis loops in the base layers were therefore inclined to show elastic behaviour after sufficient repetitions of loading. This phenomenon can be considered elastic shakedown, where after some initial plastic strain, material behaviour tends toward elastic behaviour (Collins and Boulbibane 2000).

### **7.6 Discussion**

In this research a step-by-step approach was taken to achieve the numerical simulation of flexible pavement structure. In each of these steps, more factors were considered in the simulations and the numerical simulation therefore improved progressively through the stages of research. In addition, numerical modelling was also evaluated and the impact of each factor on the calculated mechanical behaviour of layered structures was pointed out. The simulation started with a geometrical investigation where 2-D and 3-D models were studied and the effects of each model on the calculated numerical responses were noted. Then two categories of simulation (static and dynamic) were conducted to examine the impact of the nature of loading on the mechanical responses of flexible pavements.

The static simulation considered the effects of different loading axles and layer thicknesses. Two sets of material strength were also incorporated in the numerical simulation. Four different constitutive models were then implemented and the effects of each constitutive model were investigated. This procedure made it possible to gain a general knowledge of the effects of different factors of modelling on numerical simulation. It was found that the mechanical behaviour of pavement structure is determined through a combination of these factors.

Dynamic simulation is similar to static simulation except that the effects of inertial forces, damping and dynamic loading are taken into account. Therefore, the effects of layer thickness, material strength and loading magnitude are assumed to be the same as those calculated from static analysis. However, two particular factors can affect the results and can only be investigated in dynamic analysis. The first factor is the change in material behaviour due to loading cycles. This factor can only be examined if the repetition of loading is taken into account, which is obviously not applicable in static analysis. Another factor is the dynamic

interaction between layers where the dynamic forces are transferred from the structural layer to granular layers. This second effect is also negligible in static analysis.

The results of the simulation were verified at different stages using results published in the literature. The finite element simulation of linear elastic analysis and the investigation of model dimensions were verified and compared with the calculated results of the closed form solution and the literature (Cho, McCullough and Weissmann 1996; Wardle 1977). The results of the nonlinear stress dependent behaviour of granular materials in an elastic domain were verified with the published research of Kim and Tutumluer (2006b). Finally, the verification of shakedown constitutive models was presented with the published results in this area (Habiballah and Chazallon 2005; Siripun, Jitsangiam and Nikraz 2010).

The results of this research could potentially have an important impact on future design methods. First of all, it should be mentioned that material nonlinearity can have an important impact on the evaluation of the critical responses of flexible pavement. In some cases, the stress dependency of granular material can help the pavement structure to resist traffic loading, and ignoring this effect may result in conservative design.

Moving from empirical to mechanistic design methods requires consideration of the plastic behaviour of materials. In this case, plastic strain has an important role in identifying the mechanical behaviour of layered systems. Particularly in the case of dynamic loading, attention should be paid to the material changes due to loading. If the material changes are ignored, large virtual strains may be calculated which are not close to what has been reported from practice. Therefore, it is necessary for a designer to be aware of the fact that granular material will be

compacted and will show better resistance in some cases (where shakedown occurs).

In this research an attempt has been made to calculate the simulated response of layered flexible pavement under a large number of loading cycles (100,000). However, the repetition of loading in the numerical simulation was restricted by computation time. For each of the three different models studied in this research, an average of 10 days computation time was required. If computer technology advances, it may be possible to include more cycles with a shorter computation time. In that case, a full mechanical design may be possible.

## **CHAPTER 8**

### **8: Conclusion and Recommendation**

#### **8.1 Conclusion of the research**

This chapter presents the final conclusions for the study, along with recommendations for the future development of research along the same lines. Firstly, the whole thesis is briefly reviewed and then mention is made of the objectives achieved by the research and their contribution to knowledge and practice.

This dissertation consists of eight chapters. Chapter 1 provided the scope of work of the research and the introduction, and Chapter 2 reviewed the literature in the field of pavement modelling. Approaches to modelling were categorized, and this was followed by an in-depth review of numerical modelling, especially the finite element approach. Chapter 3 explained the basic concepts of the finite element method and the contribution of constitutive modelling to the simulation. This was followed by a discussion of the the formulation of the new constitutive models developed or used in this research. This chapter also provided a specific description of the numerical simulation of static and dynamic loading. Chapter 4 outlined the modelling approach and the coding algorithms, as well as indicating the trends in the evaluation of constitutive models. Chapter 5 of this dissertation presented a series of static analyses investigating the different factors of modelling, including model dimensions, boundary conditions, layer thickness, loading axles and material properties. The constitutive models, including linear elastic, nonlinear elastic, linear plastic and nonlinear elastoplastic behaviour, were incorporated in the simulations and the mechanical responses of the layered flexible pavement were calculated in terms of deformation, strain and stress.

Chapter 6 of this research presented the results of the dynamic analyses. In this simulation, three different models were constructed and the effects of shakedown behaviour and soil-asphalt interaction were studied. The results of the simulations were verified using published results of laboratory tests. Specific discussion was provided regarding the resulting hysteresis loops of loading and unloading on layers, and their contribution to energy dissipation in materials. Chapter 7 compared, analyzed and discussed all of the results of the different simulations from different points of view. The relationship between the results of this research and other outcomes published in the literature was noted, along with the possible effects of this research on design methods and practices. Chapter 8 is devoted to the conclusion and recommendations for future research.

Based on the results of this dissertation, the following major conclusions can be drawn:

- I. This research presented the mechanical response of layered flexible pavement in terms of stress, strain and deflection, and investigated the effects of different types of materials used as granular layers (base and subgrade). It was found that in the elastic domain, considering the nonlinearity of the materials and the effect of stress dependency can significantly affect the critical responses of the pavement structure. The effects can be favourable or unfavourable to the asphalt layer depending on the layer geometry, material properties and loading combination.
- II. When dynamic analysis was conducted, the results of the hysteresis loops demonstrated the mechanical behaviour of elastoplastic materials in the loading and unloading cycles. It was found that accounting for material changes due to loading cycles can significantly influence the results. In the investigation of the effects of material modification due to loading cycles,

the concept of the shakedown behaviour of granular materials was manipulated. It was found that taking shakedown behaviour into account in a simulation can result in lower levels of plastic strain, especially under large cycles of loading.

- III. The investigation into the shakedown behaviour of the granular layer also demonstrated that the energy dissipation of the granular layer can decrease if the shakedown phenomenon occurs. In this case, materials tend to behave elastically when sufficient compaction is applied through the loading cycles.
- IV. This research examined different constitutive models to simulate nonlinear elasticity. Coding was also verified with results published in the literature, after which a new constitutive model was developed based on the Mohr-Coulomb criterion and taking shakedown effects into account. The results of verification illustrated that the coding can simulate the nonlinear elastoplastic behaviour of materials in repeated loading cycles.
- V. The effects of model dimensions were investigated by comparing different numerical simulations. It was found that the plane-strain simulation should be used with caution, while axisymmetric and three-dimensional modelling can be suitable for simulation purposes. The effects of dynamic loading were also considered and it was found that dynamic simulation resulted in less deformation and strain in the asphalt layer when compared to static loading. The effect can be combined with shakedown behaviour to provide a more realistic simulation, accordingly a more cost effective design can be achieved.

- VI. There are few studies regarding the effects of soil-structure interaction in flexible pavement simulation, so this area was investigated in this research. Interface elements were implemented to simulate frictional behaviour between the asphalt and base layers. It was found that the effects of the soil-asphalt interaction resulted in more dissipation of energy through transferring the load. However, it may also intensify tensile strain on the asphalt layer. This effect is therefore favourable for rutting criteria but unfavourable for fatigue failure criteria.

## **8.2 Recommendation for Future Studies**

Based on the research presented in this thesis, the following recommendations can be made to facilitate future studies in the same field:

- I. In this research, tyre loading was simulated by the application of cyclic vertical pressure over a rectangular area. While this is one of the most commonly used methods of simulation, the effects of different simulation methods could still be beneficial. In this regard, the following studies are suggested:
  - a. Effect of loading as a combination of horizontal and vertical pressure;
  - b. Loading of different contact areas including circular, elliptical, etc.;
  - c. Effect of different pressure distributions on the tyre, including semicircle, uniform, etc.;
  - d. Effect of different loading velocities.
- II. In this research, dynamic analysis was conducted for the equivalent of 100,000 cycles of loading. This number was defined by the computation time required for the dynamic simulation. However, advancements in computer technology may enable shorter computation times for higher

loading cycles. If this happens, then simulations undertaking  $10^6$  loading cycles would be achievable. This can achieve complete mechanical design where the actual loading on flexible pavement structure is modelled. Therefore, a future line of study could be an attempt to simulate more cycles of loading. Especial consideration is recommended regarding the inclusion of shakedown effects (or any other material modification due to loading cycle) and soil-asphalt interaction.

- III. In this research, the calculation of shakedown limits relied on results gathered from the published literature, however, a completely analytical approach could also be integrated in the simulation. There are different methods for calculating shakedown limits based on limit analysis. It is recommended that shakedown limit be included as a part of numerical analysis.
- IV. The effects of soil-asphalt interaction are considered in this research through the implementation of interface elements. However, the behaviour of interface elements was assumed to be frictional. To further study the effects of soil-asphalt interaction following recommendations are made:
  - a. Investigation of the different behaviours of interface elements, including frictionless, sliding and completely attached;
  - b. Studying the effects of different elastic moduli of asphalt/base layers and the thickness of the asphalt layer;
  - c. Studying the effects on the interactional layer of different loadings of tyre pressure at higher speeds.

## References

- American Association of State Highways and Transportation Officials  
(AASHTO). 1986. *Guide for the Design of Pavement Structures*.  
Washington D.C.: American Association of State Highways and  
Transportation Officials.
- 2002. *Guide for Mechanistic Empirical Design of New and Rehabilitated Pavement Structure*. Washington D.C.: American Association of State Highways and Transportation Officials.
- Adu-Osei, A., D. N. Little, and R. L. Lytton. 2001. Cross-anisotropic Characterization of Unbound Granular Materials. *Transportation Research Record: Journal of the Transportation Research Board* 1757 (1): 82-91.
- Ahmed, S. B., and H. G. Larew. 1962. *A Study of the Repeated Load Strength Moduli of Soils*. 1962, *International Conference on the Structural Design of Asphalt Pavements*. 203(1).
- Al-Khateeb, G., and A. Shenoy. 2004. A Distinctive Fatigue Failure Criterion. *Journal of the Association of Asphalt Paving Technologists* 73: 585-622.
- Al-Qadi, I. L., M. A. Elseifi, and P. J. Yoo. 2004. In-situ Validation of Mechanistic Pavement Finite Element Modeling. In *Proc. 2nd Int. Conf. on Accelerated Pavement Testing, 2004*.
- Al-Qadi, I. L., H. Wang, and E. Tutumluer. 2010. Dynamic Analysis of Thin Asphalt Pavements by Using Cross-Anisotropic Stress-Dependent Properties for Granular Layer. *Transportation Research Record: Journal of the Transportation Research Board* 2154 (1): 156-163.

- Allou, F., C. Chazallon, and P. Hornych. 2007. A Numerical Model for Flexible Pavements Rut Depth Evolution with Time. *International Journal for Numerical and Analytical Methods in Geomechanics* 31 (1): 1-22.
- Allou, F., C. Petit, C. Chazallon, and P. Hornych. 2009. *Influence Of The Macroscopic Cohesion On The 3D FE Modeling Of A Flexible Pavement Rut Depth*. Bearing Capacity of Roads, Railways and Airfields. 8th International Conference (BCR2A'09).
- Araya, A. A., M. Huirman, L. J. Houben, and A. A. Molenaar. 2011., *Characterizing Mechanical Behavior of Unbound Granular Materials for Pavements*. Transportation Research Board 90th Annual Meeting. No. 11-0407.
- Araya, A. A., M. Huirman, A. A. Molenaar, and L. J. Houben. 2012. Investigation of the Resilient Behavior of Granular Base Materials with Simple Test Apparatus. *Materials and Structures* 45 (5): 695-705.
- Arnold, G., D. Alabaster, and B. Steven. 2001. *Prediction of Pavement Performance from Repeat Load Tri-axial (RLT) Tests on Granular Materials*. PLACE OF PUBLICATION: PUBLISHER.
- Attia, M., and M. Abdelrahman. 2011. Effect of State of Stress on the Resilient Modulus of Base Layer Containing Reclaimed Asphalt Pavement. *Road Materials and Pavement Design* 12 (1): 79-97.
- Austroads. 2004. *Pavement Design – A Guide to the Structural Design of Road Pavements*. Sydney, Australia: Austroads.

- Baek, J., H. Ozer, H. Wang, and I. L. Al-Qadi. 2010. Effects of Interface Conditions on Reflective Cracking Development in Hot-mix Asphalt Overlays. *Road Materials and Pavement Design* 11 (2): 307-334.
- Barksdale, R. D. 1971. Compressive Stress Pulse Times in Flexible Pavements for Use in Dynamic Testing. *Highway Research Record* 345: 32-44
- Barksdale, R. D. 1972. Laboratory Evaluation of Rutting in Base Course Materials. *3rd International Conference on the Structural Design of Asphalt Pavements, London, Grosvenor House, Park Lane, London, England, Sept. 11-15, 1972.. Vol. 1*
- Beskou, N. D., and D. D. Theodorakopoulos. 2011. Dynamic Effects of Moving Loads on Road Pavements: A Review. *Soil Dynamics and Earthquake Engineering* 31 (4): 547-567.
- Bohdinayake, B. C. 2008. A Study on Nonlinear Behaviour of Subgrades Under Cyclic Loading for the Development of a Design Chart for Flexible Pavements. Thesis, University of Wollongong.
- Boulbibane, M., and D. Weichert. 1997. Application of Shakedown Theory to Soils with Non-associated Flow Rules. *Mechanics Research Communications* 24 (5): 513-519.
- Boussinesq, J. 1885. *Application des potentiels à l'étude de l'équilibre et du mouvement des solides élastiques: principalement au calcul des déformations et des pressions que produisent, dans ces solides, des efforts quelconques exercés sur une petite partie de leur surface ou de leur intérieur: mémoire suivi de notes étendues sur divers points de physique, mathématique et d'analyse*. Gauthier-Villars.

- Boyce, J., S. Brown, and P. Pell. 1976. The resilient behaviour of a granular material under repeated loading. *Australian Road Research Board Conference Proc., Vol. 8. No. 1. 1976.*
- Brett, J. 1987. *Stability and Shakedown in Pavement Roughness Change with Age. New Zealand Roading Symposium, 1987, Wellington, New Zealand (volume 4).* 1987.
- Brown, S., S. Juspi, and H. Yu. 2008. *Experimental Observations and Theoretical Predictions of Shakedown in Soils under Wheel Loading. Advances in Transportation Geotechnics: Proceedings of the 1st International Conference on Transportation Geotechnics, Nottingham, UK.* 2008.
- Brown, S., and P. Pell. 1974. *Repeated Loading of Bituminous Materials. Proceedings of the Second International Conference on Asphalt Pavements for Southern Africa.* 1974.
- Burmister, D. M. 1945. The General Theory of Stresses and Displacements in Layered Systems. I. *Journal of Applied Physics* 16 (2): 89-94.
- Burmister, D. M., L. Palmer, E. Barber, A. D. Casagrande, and T. Middlebrooks. 1943. The Theory of Stress and Displacements in Layered Systems and Applications to the Design of Airport Runways. *Highway Research Board Proceedings, Vol. 23.* 1944.
- Cerni, G., F. Cardone, A. Virgili, and S. Camilli. 2012. Characterisation of Permanent Deformation Behaviour of Unbound Granular Materials under Repeated Triaxial Loading. *Construction and Building Materials* 28 (1): 79-87.

- Chazallon, C., F. Allou, P. Hornych, and S. Mouhoubi. 2009. Finite Elements Modelling of the Long-term Behaviour of a Full-scale Flexible Pavement with the Shakedown Theory. *International Journal for Numerical and Analytical Methods in Geomechanics* 33 (1): 45-70.
- Chazallon, C., P. Hornych, and S. Mouhoubi. 2006. Elastoplastic Model for the Long-Term Behavior Modeling of Unbound Granular Materials in Flexible Pavements. *International Journal of Geomechanics* 6: 279.
- Chazallon, C., G. Koval, and S. Mouhoubi. 2011. A Two-mechanism Elastoplastic Model for Shakedown of Unbound Granular Materials and DEM Simulations. *International Journal for Numerical and Analytical Methods in Geomechanics* 36.17 (2012): 1847-1868.
- Chen, J., T. Pan, and X. Huang. 2011. Numerical Investigation into the Stiffness Anisotropy of Asphalt Concrete from a Microstructural Perspective. *Construction and Building Materials* 25 (7): 3059-3065.
- Cho, Y. H., B. F. McCullough, and J. Weissmann. 1996. Considerations on Finite-element Method Application in Pavement Structural Analysis. *Transportation Research Record: Journal of the Transportation Research Board* 1539 (-1): 96-101.
- Clausen, J., L. Damkilde, and L. Andersen. 2007. An Efficient Return Algorithm for Non-associated Plasticity with Linear Yield Criteria in Principal Stress Space. *Computers & Structures* 85 (23): 1795-1807.
- Collins, I., and M. Boulbibane. 1998. The Application of Shakedown Theory to Pavement Design. *Metals and Materials* 4 (4): 832-837.

- Collins, I., and M. Boulbibane. 2000. Geomechanical Analysis of Unbound Pavements Based on Shakedown Theory. *Journal of Geotechnical and Geoenvironmental Engineering* 126 (1): 50-59.
- Cortes, D., H. Shin, and J. Santamarina. 2012. Numerical Simulation of Inverted Pavement Systems. *Journal of Transportation Engineering* 138 (12): 1507-1519.
- Dassault Systemes Simulia Corp. 2010. *Abaqus 6.10*. Providence, USA.
- De Jong, D., M. Peatz, and A. Korswagen. 1973. *Computer Program Bisar: Layered Systems Under Normal and Tangential loads. External Report AMSR 6*. Amsterdam: Koninklijke Shell-Laboratorium.
- Desai, C. S. 2007. Unified DSC Constitutive Model for Pavement Materials with Numerical Implementation. *International Journal of Geomechanics* 7 (2): 83-101.
- Desai, C. S., and R. Whitenack. 2001. Review of Models and the Disturbed State Concept for Thermomechanical Analysis in Electronic Packaging. *Journal of Electronic Packaging* 123: 19.
- Duncan, J. M., and C.-Y. Chang. 1970. Nonlinear Analysis of Stress and Strain in Soils. *Journal of the Soil Mechanics and Foundations Division* 96 (5): 1629-1653.
- Duncan, J. M., C. L. Monismith, and E. L. Wilson. 1968. Finite Element Analyses of Pavements. *Highway Research Record* 228: 18-33.
- Dunne, F., and N. Petrinic. 2005. *Introduction to Computational Plasticity*. New York: Oxford University Press.

- Elliott, J., and F. Moavenzadeh. 1971. Analysis of Stresses and Displacements in Three-layer Viscoelastic Systems. *Highway Research Record* 345 : 45-57
- Fahey, M., and J. P. Carter. 1993. A Finite Element Study of the Pressuremeter Test in Sand Using a Nonlinear Elastic Plastic Model. *Canadian Geotechnical Journal* 30 (2): 348-362.
- Fang, H., J. E. Haddock, T. D. White, and A. J. Hand. 2004. On the Characterization of Flexible Pavement Rutting Using Creep Model-based Finite Element Analysis. *Finite Elements in Analysis and design* 41 (1): 49-73.
- Foster, C. R., and R. G. Ahlvin. 1958. *Development of Multiple-wheel CBR Design Criteria*. American Society of Civil Engineers.
- François, S., C. Karg, W. Haegeman, and G. Degrande. 2010. A Numerical Model for Foundation Settlements Due to Deformation Accumulation in Granular Soils Under Repeated Small Amplitude Dynamic Loading. *International Journal for Numerical and Analytical Methods in Geomechanics* 34 (3): 273-296.
- Gedafa, D. S. 2006. *Comparison of Flexible Pavement Performance Using Kenlayer and HDM-4*. Ames, Iowa, U.S.A.: Midwest Transportation Consortium.
- Ghadimi, B., H. Asadi, H. Nikraz, and C. Leek. 2013. Effects of Geometrical Parameters on Numerical Modeling of Pavement Granular Material. Paper presented at *2013 Airfield and Highway Pavement Conference: Sustainable and Efficient Pavements, Los Angeles, 9-12 June 2013*.

- Ghadimi, B., A. Nega, and H. Nikraz. 2014. Simulation of Shakedown Behavior in Pavement's Granular Layer. *International Journal of Engineering and Technology* 7 (3): 6.
- Ghadimi, B., H. Nikraz, and C. Leek. 2013. Effects of Asphalt Layer Thickness on the Dynamic Analysis of Flexible Pavement: A Numerical Study. In *15th AAPA International Flexible Pavements Conference, Brisbane, Australia*. Brisbane: AAPA.
- Ghadimi, B., H. Nikraz, C. Leek, and A. Nega. 2013a. A Comparison between Austroads Pavement Structural Design and AASHTO Design in Flexible Pavement. *Advanced Materials Research* 723: 3-11.
- 2013b. A Comparison between Effects of Linear and Non-Linear Mechanistic Behaviour of Materials on the Layered Flexible Pavement Response. *Advanced Materials Research* 723: 12-21.
- Ghuzlan, K. A., and S. H. Carpenter. 2000. Energy-derived, Damage-based Failure Criterion for Fatigue Testing. *Transportation Research Record: Journal of the Transportation Research Board* 1723 (-1): 141-149.
- González, A., M. Saleh, and A. Ali. 2007. Evaluating Nonlinear Elastic Models for Unbound Granular Materials in Accelerated Testing Facility. *Transportation Research Record: Journal of the Transportation Research Board* 1990 (1): 141-149.
- Habiballah, T., and C. Chazallon. 2005. An Elastoplastic Model Based on the Shakedown Concept for Flexible Pavements Unbound Granular Materials. *International Journal for Numerical and Analytical Methods in Geomechanics* 29 (6): 577-596.

- Hadi, M., and M. Symons. 1996. Computing Stresses in Road Pavements using CIRCLY, MSC/NASTRAN and STRAND6. *Transactions of the Institution of Engineers, Australia. Civil Engineering* 38 (2-4): 89-93.
- Hadi, M. N., and B. Bodhinayake. 2003. Non-linear Finite Element Analysis of Flexible Pavements. *Advances in Engineering Software* 34 (11): 657-662.
- Harichandran, R., M. Yeh, and G. Baladi. 1990. MICH-PAVE: A Nonlinear Finite Element Program for Analysis of Flexible Pavements. *Transportation Research Record* (1286): 1286: 123-131
- Helwany, S. 2006. *Applied Soil Mechanics*. PLACE OF PUBLICATION: Wiley Online Library.
- Helwany, S., J. Dyer, and J. Leidy. 1998. Finite-element Analyses of Flexible Pavements. *Journal of Transportation Engineering* 124 (5): 491-499.
- Hibbit, K., and Sorenson, Inc. 2010. *ABAQUS User's Manual. V. 6.10*. Providence, RI.
- Hicks, R. G., and C. L. Monismith. 1971. Factors Influencing the Resilient Response of Granular Materials. *Highway Research Record*, 345: 15-31
- Hjelmstad, K., and E. Taciroglu. 2000. Analysis and Implementation of Resilient Modulus Models for Granular Solids. *Journal of Engineering Mechanics* 126 (8): 821-830.
- Holanda, Á. S., E. Parente Junior, T. D. P. Araújo, L. T. B. Melo, F. Evangelista Junior, and J. B. Soares. 2006. *Finite Element Modeling of Flexible Pavements*. Iberian Latin American Congress on Computational Methods in Engineering.

- Hossain, M., and H. Yu. 1996. *Shakedown Analysis of Multi-layer Pavements Using Finite Elements and Linear Programming*. Australia: Institution of Engineers.
- Howard, I. L., and K. A. Warren. 2009. Finite-element Modeling of Instrumented Flexible Pavements under Stationary Transient Loading. *Journal of Transportation Engineering* 135 (2): 53-61.
- HRB, N. R. C. H. R. B. 1962. *The AASHO Road Test: Proceedings of a Conference Held May 16-18, 1962, St. Louis, Mo.* National Academy of Sciences – National Research Council.
- Huang, Y. 1969. Finite Element Analysis of Nonlinear Soil Media. *Proceedings, Symposium on Application of Finite Element Methods in Civil Engineering*. Nashville, Tennessee: Vanderbilt University.
- Huang, Y. H. 1993. *Pavement Analysis and Design*. New Jersey, USA: Prentice-Hall Inc.
- , 2004. *Pavement Analysis and Design*. U.S.A.: Pearson Prentice Hall, Pearson Education Inc.
- Huurman, M. 1997. Permanent Deformation in Concrete Block Pavements. PhD Thesis, Delft University of Technology.
- Kim, M. 2007. Three-dimensional Finite Element Analysis of Flexible Pavements Considering Nonlinear Pavement Foundation Behavior. Thesis, University of Illinois.
- Kim, M., and J. H. Lee. 2011. Study on Nonlinear Pavement Responses of Low Volume Roadways Subject to Multiple Wheel Loads. *Journal of Civil Engineering and Management* 17 (1): 45-54.

- Kim, M., and E. Tutumluer. 2006. Modeling Nonlinear, Stress-Dependent Pavement Foundation Behavior Using A General-Purpose Finite Element Program. *Geotechnical Special Publication* 154: 29.
- Kim, M., and E. Tutumluer. 2010. Validation of a Three-Dimensional Finite Element Model using Airfield Pavement Multiple Wheel Load Responses. *Road Materials and Pavement Design* 11 (2): 387-408.
- Kim, M., E. Tutumluer, and J. Kwon. 2009. Nonlinear Pavement Foundation Modeling for Three-dimensional Finite-element Analysis of Flexible Pavements. *International Journal of Geomechanics* 9: 195.
- Kim, Y. R., H. J. Lee, and D. N. Little. 1997. Fatigue Characterization of Asphalt Concrete Using Viscoelasticity and Continuum Damage Theory (with Discussion). *Journal of the Association of Asphalt Paving Technologists* 66: 520-569
- Koiter, W. T. 1960. *General Theorems for Elastic-plastic Solids*. Amsterdam: PUBLISHER.
- Korkiala-Tanttu, L., R. Laaksonen, and J. Törnqvist. 2003. Effect of Spring and Overload to the Rutting of a Low-volume Road. *HVS-Nordic—research, Finnra Reports* 22
- Kouroussis, G., O. Verlinden, and C. Conti. 2009. Ground Propagation of Vibrations from Railway Vehicles using a Finite/Infinite-element Model of the Soil. *Proceedings of the Institution of Mechanical Engineers, Part F: Journal of Rail and Rapid Transit* 223 (4): 405-413.

- , 2010. On the Interest of Integrating Vehicle Dynamics for the Ground Propagation of Vibrations: The Case of Urban Railway Traffic. *Vehicle System Dynamics* 48 (12): 1553-1571.
- Lade, P. V., and R. B. Nelson. 1987. Modelling the Elastic Behaviour of Granular Materials. *International Journal for Numerical and Analytical Methods in Geomechanics* 11 (5): 521-542.
- Lee, J., J. Kim, and B. Kang. 2009. Normalized Resilient Modulus Model for Subbase and Subgrade Based on Stress-dependent Modulus Degradation. *Journal of Transportation Engineering* 135 (9): 600-610.
- Lekarp, F., U. Isacsson, and A. R. Dawson. 2000. State of the Art. II: Permanent Strain Response of Unbound Aggregates. *Transportation Engineering* 126 (1): 76-84.
- Li, H., and H. Yu. 2006. A Nonlinear Programming Approach to Kinematic Shakedown Analysis of Frictional Materials. *International Journal of Solids and Structures* 43 (21): 6594-6614.
- Ling, H. I., and H. Liu. 2003. Finite Element Studies of Asphalt Concrete Pavement Reinforced with Geogrid. *Journal of Engineering Mechanics* 129 (7): 801-811.
- Little, P. H. 1993. The Design of Unsurfaced Roads Using Geosynthetics. PhD Thesis, University of Nottingham.
- Liu, Y., Z. You, and Y. Zhao. 2012. Three-dimensional Discrete Element Modeling of Asphalt Concrete: Size Effects of Elements. *Construction and Building Materials* 37: 775-782.

- Maier, G., J. Pastor, A. Ponter, and D. Weichert. 2003. Direct Methods of Limit and Shakedown Analysis. *Comprehensive Structural Integrity*, Elsevier-Pergamon, Amsterdam (2003)
- Mallela, J., and K. George. 1994. Three-dimensional Dynamic Response Model for Rigid Pavements. *Transportation Research Record* (1448): 92-99.
- Mashrei, M. A., R. Seracino, and M. Rahman. 2013. Application of Artificial Neural Networks to Predict the Bond Strength of FRP-to-concrete Joints. *Construction and Building Materials* 40: 812-821.
- Melan, E. 1938. Zur plastizität des räumlichen kontinuums. *Archive of Applied Mechanics* 9 (2): 116-126.
- Mishra, D., and E. Tutumluer. 2012. Aggregate Physical Properties Affecting Modulus and Deformation Characteristics of Unsurfaced Pavements. *Journal of Materials in Civil Engineering* 24 (9): 1144-1152.
- Motamed, R., K. Itoh, S. Hirose, A. Takahashi, and O. Kusakabe. 2009. Evaluation of wave barriers on ground vibration reduction through numerical modeling in ABAQUS. *Proceedings of the SIMULIA Customer Conference 2009*. 402-41
- Myers, L. A., R. Roque, and B. Birgisson. 2001. Use of Two-dimensional Finite Element Analysis to Represent Bending Response of Asphalt Pavement Structures. *International Journal of Pavement Engineering* 2 (3): 201-214.
- Nega, A., H. Nikraz, C. Leek, and B. Ghadimi. 2013a. Evaluation and Validation of Characterization Methods for Fatigue Performance of Asphalt Mixes for Western Australia. *Advanced Materials Research* 723: 75-85.

- , 2013b. Pavement Materials Characterization of Hot-Mix Asphalt Mixes in Western Australia. *Advanced Materials Research* 723: 434-443.
- Ozer, H., I. L. Al-Qadi, and C. A. Duarte. 2011. A Three-dimensional Generalised Finite Element Analysis for the Near-surface Cracking Problem in Flexible Pavements. *International Journal of Pavement Engineering* 12 (4): 407-419.
- Ozer, H., I. L. Al-Qadi, H. Wang, and Z. Leng. 2012. Characterisation of Interface Bonding Between Hot-mix Asphalt Overlay and Concrete Pavements: Modelling and In-situ Response to Accelerated Loading. *International Journal of Pavement Engineering* 13 (2): 181-196.
- Pan, G., H. Okada, and S. Atluri. 1994. Nonlinear Transient Dynamic Analysis of Soil-Pavement Interaction Under Moving Load: A Coupled BEM-FEM Approach. *Engineering Analysis with Boundary Elements* 14 (1): 99-112.
- Pan, J., and A. Selby. 2002. Simulation of Dynamic Compaction of Loose Granular Soils. *Advances in Engineering Software* 33 (7): 631-640.
- Paute, J. L., P. Horny, and J. P. Benaben. 1996. Repeated load triaxial testing of granular materials in the French Network of Laboratories des Ponts et Chaussées. *European Symposium on Flexible Pavements*. Rotterdam: Balkema.
- Pelgröm, L. 2000. *Engineering Mechanical Properties Densiasphalt. Report prepared for Densit a/s by KOAC-WMD*. Aalborg, Denmark.
- Pell, P., and K. Cooper. 1975. The Effect of Testing and Mix Variables on the Fatigue Performance of Bituminous Materials. *Journal of the Association of Asphalt Paving Technologists* 44: 1-37.

- Perloff, W., and F. Moavenzadeh. 1967. *Deflection of Viscoelastic Medium Due to a Moving Load*. *Intl Conf Struct Design Asphalt Pvmts.* 1967.
- Pidwerbesky, B. D. 1996. Fundamental Behaviour of Unbound Granular Pavements Subjected to Various Loading Conditions and Accelerated Trafficking, Ph.D. thesis, Univ. of Canterbury, Christchurch, New Zealand.
- Raad, L., and J. L. Figueroa. 1980. Load Response of Transportation Support Systems. *Journal of Transportation Engineering* 106 (1): 111-128
- Rao Tangella, S., J. Craus, J. Deacon, and C. Monismith. 1990. *Summary Report on Fatigue Response of Asphalt Mixtures. SHRP Project A-003-A*. U.S.A.: University of California, Berkeley.
- Ravindra, P., and J. Small. 2008. *Shakedown Analysis of Road Pavements*. In the *12th International Conference of International Association for Computer Methods and Advances in Geomechanics (IACMAG)*, Goa, India. 2008.
- Rowe, G. 1993. Performance of Asphalt Mixtures in the Trapezoidal Fatigue Test. *Asphalt Paving Technology* 62: 344-344.
- Rowshanzamir, M. A. 1997. *Resilient Cross-anisotropic Behaviour of Granular Base Materials Under Repetitive Loading*. Sydney, Australia: University of New South Wales.
- Saad, B., H. Mitri, and H. Poorooshahb. 2005. Three-dimensional Dynamic Analysis of Flexible Conventional Pavement Foundation. *Journal of Transportation Engineering* 131 (6): 460-469.

- Sadd, M. H. 2009. *Elasticity: Theory, Applications, and Numerics*. Academic Press, 2014.
- Saltan, M., and H. Sezgin. 2007. Hybrid Neural Network and Finite Element Modeling of Sub-base Layer Material Properties in Flexible Pavements. *Materials & Design* 28 (5): 1725-1730.
- Schofield, A. N., and P. Wroth. 1968. *Critical State Soil Mechanics*. London: McGraw-Hill.
- Seed, H. B., C. Chan, and C. Lee. 1962. *Resilience Characteristics of Subgrade Soils and their Relation to Fatigue Failures in Asphalt Pavements*. *International Conference on the Structural Design of Asphalt Pavements. Supplement*. 1962.
- Selig, E. 1987. Tensile Zone Effects on Performance of Layered Systems. *Geotechnique* 37 (3): 247-254.
- Seyhan, U., and E. Tutumluer. 2000. *Advanced Characterization of Granular Materials for Mechanistic Based Pavement Design*. No. GSP No. 98. 2000.
- Sharp, R. 1985. Pavement Design Based on Shakedown Analysis. *Transportation Research Record* (1022): 99-107
- Sharp, R. W., and J. R. Booker. 1984. Shakedown of Pavements Under Moving Surface Loads. *Journal of Transportation Engineering* 110: 1.
- Shen, W., and D. J. Kirkner. 2001. Non-linear Finite-element Analysis to Predict Permanent Deformations in Pavement Structures Under Moving Loads. *International Journal of Pavement Engineering* 2 (3): 187-199.

Shook, J., F. Finn, M. Witczak, and C. Monismith. 1982. *Thickness Design of Asphalt Pavements—The Asphalt Institute Method. Proc., 5th Int. Conf. on the Structural Design of Asphalt Pavements*, Delft Univ. of Technology, Delft, The Netherlands, I, 17–44.

Siripun, K. 2010. Characterisations of Base Course Materials in Western Australian Pavements. PhD Thesis, Department of Civil Engineering, Faculty of Engineering and Computing, 2010, Curtin University: Perth.

Siripun, K., P. Jitsangiam, and H. Nikraz. 2010. Permanent deformation behaviour and model of crushed rock base. *Australian Journal of Civil Engineering* 8 (1): 41.

Siripun, K., H. Nikraz, and P. Jitsangiam. 2011. Mechanical Behavior of Unbound Granular Road Base Materials Under Repeated Cyclic Loads. *International Journal of Pavement Research and Technology* 4 (1): 56-66.

Starovoitov, É., and F. Nağıyev. 2012. *Foundations of the Theory of Elasticity, Plasticity, and Viscoelasticity*. CRC Press, 2012.

Sukumaran, B., M. Willis, and N. Chamala. 2004. Three dimensional finite element modeling of flexible pavements. *FAA Worldwide Airport Technology Transfer Conference, Atlantic City, New Jersey*,

Sun, Y., S.-L. Shen, X.-H. Xia, and Z.-L. Xu. 2012. A Numerical Approach for Predicting Shakedown Limit in Ratcheting Behavior of Materials. *Materials & Design*: 47 (2013): 106-114

- Sweere, G. T. H. 1990. Unbound Granular Bases for Roads. PhD Thesis, Delft University of Technology.
- Taciroglu, E., and K. Hjelmstad. 2002. Simple Nonlinear Model for Elastic Response of Cohesionless Granular Materials. *Journal of Engineering Mechanics* 128 (9): 969-978.
- Tayebali, A. A., G. M. Rowe, and J. B. Sousa. 1992. Fatigue Response of Asphalt-aggregate Mixtures (with Discussion). *Journal of the Association of Asphalt Paving Technologists* 61: 333-360
- Thompson, M., and R. Elliott. 1985. ILLI-PAVE-based Response Algorithms for Design of Conventional Flexible Pavements. *Transportation Research Record* (1043): 50-57
- Thompson, M. R., and Q. L. Robnett. 1979. Resilient Properties of Subgrade Soils. *Transportation Engineering Journal* 105 (1): 71-89.
- Tutumluer, E. 1995. Predicting Behavior of Flexible Pavements with Granular Bases. PhD thesis, Georgia Institute of Technology, Atlanta.
- Tutumluer, E., D. N. Little, and S. H. Kim. 2003. Validated Model for Predicting Field Performance of Aggregate Base Courses. *Transportation Research Record: Journal of the Transportation Research Board* 1837 (-1): 41-49.
- Uddin, W., and Z. Pan. 1995. Finite-Element Analysis of Flexible Pavements with Discontinuities. *Transportation Congress, Volumes 1 and 2@ Civil Engineers—Key to the World's Infrastructure*. VI, ASCE, New York, N. Y., U. S. A., 410-423.

- Uddin, W., D. Zhang, and F. Fernandez. 1994. Finite Element Simulation of Pavement Discontinuities and Dynamic Load Response. *Transportation Research Record* (1448): 100-106.
- Ullidtz, P. 2002. Keynote Address. In *Proceedings of the 9th International Conference on Asphalt Pavements: Analytical Tools for Design of Flexible pavements*. Copenhagen: PUBLISHER.
- Uzan, J. 1985. Characterization of Granular Material. *Transportation Research Record* (1022): 52-59
- Vale, C. 2008. Influence of Vertical Load Models on Flexible Pavement Response—an Investigation. *International Journal of Pavement Engineering* 9 (4): 247-255.
- Vermeer, P. 1982. *A Five-constant Model Unifying Well-established Concepts. Constitutive Relation for Soils*, Balkema, Rotterdam (1984), 175–197
- Wang, H., and I. L. Al-Qadi. 2012. Importance of Nonlinear Anisotropic Modeling of Granular Base for Predicting Maximum Viscoelastic Pavement Responses under Moving Vehicular Loading. *Journal of Engineering Mechanics* 139 (1): 29-38.
- Wardle, L. 1977. *Program CIRCLY: A Computer Program for the Analysis of Multiple Complex Circular Loads on Layered Anisotropic Media. User's Manual*. Australia: Division of Applied Geomechanics, Commonwealth Scientific and Industrial Research Organization.
- Wardle, L., G. Youdale, and B. Rodway. 2003. Current Issues for Mechanistic Pavement Design. *21st ARRB and 11th REAAA Conference, Cairns, Australia*: ARRB Transport Research.

- Werkmeister, S., A. Dawson, and F. Wellner. 2004. Pavement Design Model for Unbound Granular Materials. *Journal of Transportation Engineering* 130 (5): 665-674.
- Witczak, M. W., and J. Uzan. 1988. *The Universal Airport Pavement Design System Rep. I Granular Material Characterization*. College Park, MD, USA: Department of Civil Engineering, University of Maryland.
- Wolf, J. P. 1985. *Dynamic Soil-structure Interaction*. Prentice Hall.
- Wolff, H., and A. Visser. 1994. Incorporating Elasto-plasticity in Granular Layer Pavement Design. *Proceedings of the ICE-Transport* 105 (4): 259-272.
- Burland, J. B., and Hai-Sui Yu. *Plasticity and geotechnics*. Vol. 13. Springer, 2007.
- Yu, H.-S., and M. Z. Hossain. 1998a. Lower Bound Shakedown Analysis of Layered Pavements Using Discontinuous Stress Fields. *Computer Methods in Applied Mechanics and Engineering* 167: 209-222.
- Yu, H., and M. Hossain. 1998b. Lower Bound Shakedown Analysis of Layered Pavements Using Discontinuous Stress Fields. *Computer Methods in Applied Mechanics and Engineering* 167 (3): 209-222.
- Zaghoul, S., and T. White. 1993. Use of a Three-dimensional, Dynamic Finite Element Program for Analysis of Flexible Pavement. *Transportation Research Record* (1388): 60-69.
- Zarka, J., and J. Casier. 1979. Elastic Plastic Response of Structure to Cyclic Loading: Practical Rules. *Mechanics Today* 6: 93-198.

*Every reasonable effort has been made to acknowledge the owners of copyright material. I would be pleased to hear from any copyright owner who has been omitted or incorrectly acknowledged.*